Oscillatory motor discharges by brainstem neurons: functional mechanisms and consequences for cell survival

Thesis submitted for the degree of "Doctor Philosophiae"

S.I.S.S.A. – Neurobiology Sector

Candidate:

Dr. Elina Sharifullina

Supervisor

Prof. Andrea Nistri

TABLE OF CONTENTS

NOTE

Part of the data reported in this thesis has been published in the articles, listed below. In all cases, the candidate personally performed the experimental work, data analysis and contributed to the paper writing.

Sharifullina E, Ostroumov K, Nistri A (2004). Activation of group I metabotropic glutamate receptors enhances efficacy of glutamatergic inputs to neonatal rat hypoglossal motoneurons in vitro.
Eur J Neurosci **20**, 1245-1254.

Sharifullina E, Ostroumov K, Nistri A (2005). Metabotropic glutamate receptor activity induces a novel oscillatory pattern in neonatal rat hypoglossal motoneurones. *J Physiol* **563,** 139-159

Sharifullina E & Nistri A (2006). Glutamate uptake block triggers deadly rhythmic bursting of neonatal rat hypoglossal motoneurons. *J Physiol* **572,** 407-423.

Nistri A, Ostroumov K, **Sharifullina E**, Taccola G (2006). Tuning and playing a motor rhythm: how metabotropic glutamate receptors orchestrate generation of motor patterns in the mammalian central nervous system. *J Physiol* **572,** 323-334.

The work on metabotropic glutamate receptors has been done in collaboration with Konstantin Ostroumov.

ABSTRACT

Brainstem hypoglossal motoneurons (HMs) supply the exclusive motor innervation to tongue muscles and thus play a fundamental role in functions like mastication, suckling, swallowing, and maintenance of airway patency during respiration. Because of HM motor commands are often expressed as rhythmic oscillations driven by brainstem nuclei, it is important to understand the interaction between the oscillatory networks termed central pattern generators and their target motoneurons, and to clarify the contribution by motoneuron intrinsic properties to patterned discharges. The present thesis is based on a study of the electrophysiological properties of HMs using whole cell patch clamp recording from transverse brainstem slices obtained from neonatal rats. A number of studies, including those carried out in our lab, have shown that distinct subclasses of metabotropic glutamate receptors (mGluRs) can induce oscillatory activity (via subtype 1 and 5 of group I of mGluRs) in brain and spinal networks. The first issue examined by the present investigation was whether brainstem networks, comprising HMs, could generate sustained electrical oscillations, supported by mGluRs. Normally mGluRs do not participate in synaptic transmission, because their localization is seemingly remote from synapses. Hence, the selective agonist of group I mGluRs DHPG was applied to enhance the efficacy of glutamatergic inputs to HMs. In about sixty percent HMs, the DHPG-elicited enhancement of excitatory transmission was associated with persistent, regular electrical oscillations (4–8 Hz), dependent on network glutamatergic transmission (via AMPA receptors) and independent from synaptic inhibition. Simultaneous recording from pairs of HMs demonstrated that oscillations were due to HM electrical coupling and were suppressed by the gap junction blocker carbenoxolone. Pacing of slow oscillations apparently depended on the operation of K_{ATP} conductances. Under current clamp conditions, oscillations transformed irregular at high rate firing into a regular, lower frequency spike firing of motoneurones.

The second question the present study addressed was whether by blocking glutamate uptake (with TBOA), it would be possible to build up enough extracellular glutamate to produce rhythmic bursting. TBOA-induced bursting was characterized by large, irregular and long-lasting events, whose occurrence was facilitated by inhibitory transmission block. These bursts depended on synergic activation of distinct classes of glutamatergic receptors (AMPA,

NMDA and mGluRs) and were supported by gap junctions amongst HMs. Intracellular Ca^{2+} imaging demonstrated strong bursting synchrony in HMs. Prolonged glutamate uptake block led to cell damage in a population of neurons. Neuronal death was prevented by the same antagonists, which arrested HM bursting.

The present study shows that even a thin slice preparation of the brainstem displays the ability to generate different types of bursting once suitable pharmacological tools are employed. In particular, the present data indicate an important modulatory role of mGluRs on synaptic transmission, and their ability to generate rhythmic theta-frequency bursting. Furthermore, the model of impaired glutamate uptake suggests a strong correlation between large bursting and HM death, outlining a possible mechanism for early motoneuron damage in certain neurodegenerative diseases.

INTRODUCTION

1. NUCLEUS HYPOGLOSSUS AND XII CRANIAL NERVE

1.1 ANATOMY

The hypoglossal nerve is the XII cranial nerve, which exclusively innervates the muscles of the tongue. The XII cranial nerve arises from the axons of the long column of multipolar motorneurons in the hypoglossal nucleus. The hypoglossal nucleus is situated in the medulla oblongata close to the midline immediately beneath the floor of the fourth ventricle. Exiting as separate rootlets from the anteroventral surface of the medulla oblongata, each rootlet pierces the *dura mater* and coalesces to form the hypoglossal nerve in the hypoglossal canal. The nerve then runs downward and forward in the neck into the floor of the mouth, where its fibers are distributed to the hypoglossus, styloglossus, geniohyoid and genioglossus muscles and all the intrinsic muscles of the tongue (see Figure 1). The intrinsic muscles of the tongue alter the shape of the tongue, while the extrinsic muscles alter its shape and position. The genioglossus muscle protrudes the tongue and dilates the upper airway.

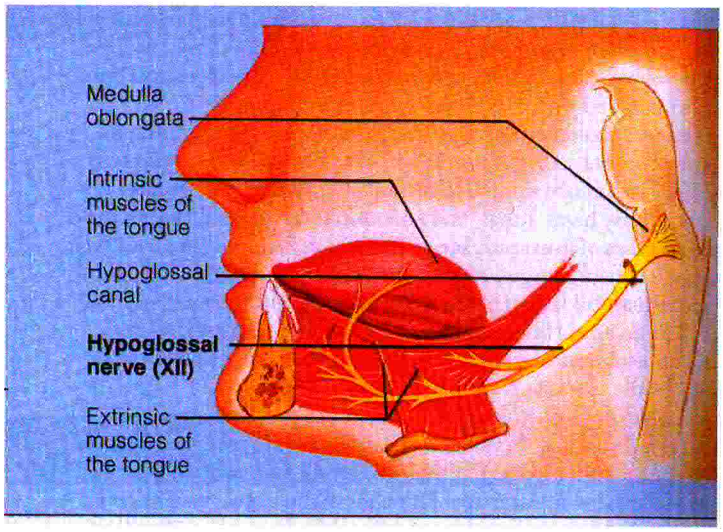

Fig 1. Origin and course of the hypoglossal nerve (XII).

In the neonatal as well as in the adult rat (Nunez-Abades & Cameron, 1995) hypoglossal motoneurons (HMs) comprise the largest population (about 90%; Viana *et al*, 1990) of neurons within the hypoglossal nucleus. They are large (25-50 μm) multipolar cells, whereas

interneurons (10-18 μm somatic diameter) are round to oval-shaped neurons and are much less numerous (Boone & Aldes, 1984). The functional organization of movement of the tongue is best defined by the myotopically organized neurons of the hypoglossal nucleus. In the rat, HMs innervating the tongue protractor muscles are located in the ventrolateral subdivision of XII nuclei (Aldes, 1995), HMs responsible for retraction are mainly in the dorsal part (McClung & Goldberg, 1999; 2000), and HMs, which control the tongue intrinsic muscle are found in the middle third of the hypoglossal nucleus (Sokoloff, 2000). The HM organization represents the level of anatomical order available to the afferents that control the various tongue movements used during mastication, sucking, swallowing and other oral behaviors. All these functions require rhythmic contractions with appropriate muscle coordination to avoid, for example, obstruction of upper airways by the tongue or tongue-biting during feeding. Understanding the mechanisms underlying the rhythmicity and regularity of motor commands to the tongue is an interesting goal for studies of sensory-motor integration in the brain.

The primary source of inputs to the XII nucleus arises from an extended region of the caudal reticular formation immediately ventral to the nucleus of the solitary tract (NTS), termed dorsal medullary reticular column (DMRC; Cunningham & Sawchenko, 2000, see Figure 2). Projections from the DMRC are largely bilateral and distributed to both the dorsal and the ventral subdivisions of nucleus hypoglossus, which allows simultaneous activation of both tongue retraction and protractions during initiation of swallowing. In this regard, Dobbins & Feldman (1995) and Fay & Norgren (1997c) demonstrated overlapping, yet, partially segregated, inputs from DMRC to protractor *vs*. retractor HMs. This anatomical arrangement may reflect a capacity for independent, yet coordinated, activation of the two motoneuron pools. Sparse connections were shown between HMs and NTS, although retrograde labeling from XII nucleus never demonstrated labeled cells in the central subnucleus of the NTS. Finally, unlike humans, whose hypoglossal nucleus receives cortico-nuclear fibers from the pre-central gyrus of both cerebral hemispheres, no direct cortical connections to orofacial nuclei, including the XII, have been demonstrated in rats (Travers & Norgren, 1983).

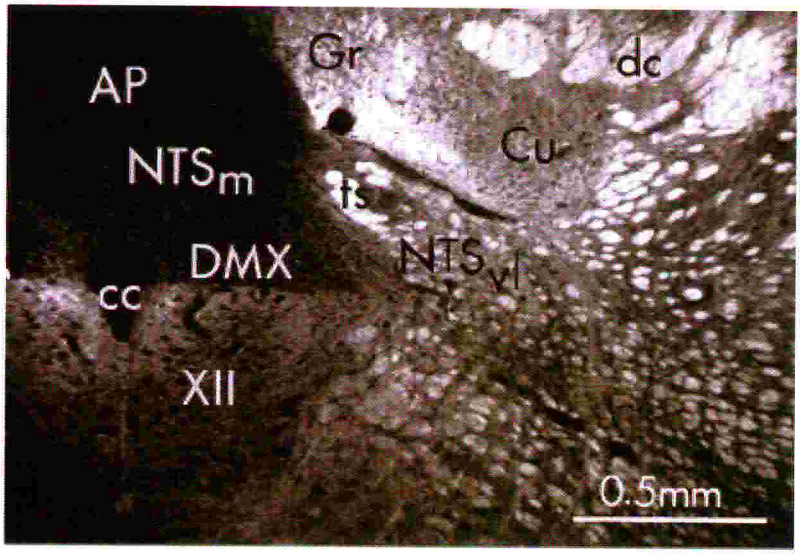

Fig 2. The inputs to the XII nucleus. **AP** area postrema; cc central canal; **Cu** cuneate nucleus; **dc** dorsal column nucleus; **DMX** dorsal motor nucleus of the vagus nerve; **Gr** gracile nucleus; **NTSm** nucleus of the solitary tract, medial subdivision; **NTSvl** nucleus of the solitary tract, ventrolateral subdivision; **XII** hypoglossal nucleus (from Cunningham & Sawchenko, 2000, ***J Comp Neurol***).

On HMs the main excitatory neurotransmitter glutamate mediates fast component of synaptic transmission via AMPA ionotropic receptors. The presence of GluR2 subunits on AMPA receptors confers minimal Ca^{2+} permeability (for review see Dingledine *et al*, 1999). A certain degree of expression of $GluR_2$ subunits has been previously reported in native AMPA receptors of neonatal rat HMs (Essin *et al*, 2002). Expression of the $GluR_2$ subunit is down-regulated selectively by ischaemia (Pellegrini-Giampietro *et al*, 1997) and epilepsy (Friedman, 1998), or up-regulated by intense synaptic activity (Liu & Cull-Candy, 2000) or even modulated according to the level of spontaneous activity (Liu & Cull-Candy, 2002). For HM even a small decrease in their $GluR_2$ expression might lead to the appearance of a significant pool of Ca^{2+} permeable AMPA receptors and might therefore contribute, together with the low endogenous Ca^{2+} buffer capacity of HM (Lips & Keller, 1998) and the relatively high AMPA receptor current density typical for motoneurons (Vandenberghe *et al*, 2000), to strong Ca^{2+} influx and to the selective vulnerability of such cells to Ca^{2+}-dependent glutamate toxicity (Krieger *et al*, 1994; Reiner *et al*, 1995).

NMDA receptors mediate comparatively slow synaptic responses at many synapses in the brain (Collingridge & Lester, 1989). However, their contribution to synaptic transmission in mature spinal motoneurons is controversial (Jahr & Yoshioka, 1986; Walmsley & Bolton,

1994). In neonatal rat brainstem slices trigeminal and hypoglossal motoneurons apparently express both NMDA and non-NMDA receptors at synaptic sites (Trueblood *et al*, 1996; O'Brien *et al*, 1997), but recordings obtained in vivo from adult rat abducens motoneurons (Ouardouz & Durand, 1994) together with results obtained from embryonic organotypic cultured hypoglossal motoneurons (Launey *et al*, 1999), suggest that NMDA receptors are located either at extrasynaptic sites or at silent synapses, and are not directly involved in synaptic transmission on motoneurons. The major inhibitory neurotransmitters on motoneurons are thought to be GABA and glycine, which operate via activation of distinct postsynaptic receptors gating Cl^- channels (for review see Rekling *et al*, 2000). These GABA receptors mainly belong to the $GABA_A$ class and are reversibly blocked by bicuculline, while glycine receptors are antagonized by strychnine (Barnard *et al*, 1993; Kuhse *et al*, 1995; Nistri 1983; Rajendra *et al*, 1997). Moreover, it has been reported that, on brainstem HMs, Cl^- mediated synaptic transmission is mainly due to glycine rather than GABA and that GABAergic and glycinergic events differ in terms of kinetics and pharmacological sensitivity to metabotropic glutamate receptor activation or TTX (Donato & Nistri, 2000).

1.2 BASIC INTRINSIC PROPERTIES OF HMs

To understand the basic properties controlling the firing behaviour of HMs, a detailed description of the various voltage-dependent currents of these cells is required. As shown in Table 1, available data are still incomplete. Particular attention is paid to voltage-dependent, persistent (i.e. non- or slowly inactivating) inward currents first activated in the voltage range below the threshold for spike initiation (Schwindt & Crill, 1982; Hounsgaard *et al*, 1984; Hounsgaard & Kiehn, 1989; Lee & Heckman, 1998a,b). Under voltage-clamp conditions, these persistent inward currents can lead to a region of negative slope conductance in the steady-state current-voltage (I-V) relation (Schwindt & Crill, 1982; Nishimura *et al*, 1989; Hsiao *et al*, 1998; Lee & Heckman, 1998a). Under current clamp conditions, these currents are thought to contribute to a number of behaviors, including an increase in the slope of the frequency-current relation (Schwindt & Crill, 1982; Bennett *et al*, 1998; Lee & Heckman, 1998a), firing rate acceleration (Hounsgaard *et al*, 1988; Lee & Heckman, 1998a), bistable discharge behavior (Hounsgaard *et al*, 1984, 1988; Lee & Heckman, 1998a), and

Table 1. Various voltage-dependent currents in HMs.

Current	Other name	Short description	References
Fast transient Na current	I_{Na}	fast inactivating, TTX-sensitive	Barrett & Crill, 1980; Sah & McLachlan, 1992; Takahashi, 1990; Lape & Nistri, 2001
Fast potassium current	A-current	action potential repolarization, 4-AP sensitive	Sah & McLachlan, 1992; Viana *et al*, 1993b; Lape & Nistri, 1999
Low-threshold calcium current	T-type Ca^{2+} channels	ADP, rebound responses, source of Ca^{2+} which activates K^+ channels responsible for AP repolarization, BK channels	Viana *et al*, 1993a; Umemiya & Berger, 1994
High-threshold calcium current	P-, N-, L-type Ca^{2+} conductance	ADP, full-size Ca^{2+} spikes (observed after strong reduction of outward K^+ currents), source of Ca^{2+} which activates K^+ channels responsible for AHP, SK-type	Viana *et al*, 1993a; Umemiya & Berger, 1994
Ca^{2+} - activated K^+ current	AHP conductance	mAHP apamine sensitive, important for spike frequency adaptation, SK-type potassium channels, BK and presumably SK-type K^+ channels	Viana *et al*, 1993b; Umemiya & Berger, 1994, Lape & Nistri, 2000
Potassium leak current	TASK-1, TASK-2	a widespread CNS mechanism by which transmitters induce slow excitation	Bayliss *et al*, 1994, Talley *et al*, 2000
Delayed rectifier potassium conductance	I_{KDR} DR-channels	action potential repolarization, TEA-sensitive	Viana *et al*, 1993b
h-current	I_h	hyperpolarization activated Na^+ and K^+ current ZD7288 sensitive	Bayliss *et al*, 1994
Persistent sodium conductance	I_{NaP}		Rekling & Laursen, 1989; Powers & Binder, 2003

amplification of synaptic currents (Lee & Heckman, 2000; Powers & Binder 2000; Prather *et al*, 2001). Persistent inward currents in spinal motoneurons are thought to be mediated by

membrane channels located primarily on the dendrites (Hounsgaard & Kiehn, 1993; Carlin *et al*, 2000). One indication of the dendritic location of these channels is a clockwise hysteresis in the whole-cell inward currents recorded in response to ascending and then descending voltage ramp commands, i.e., the deactivation of the inward current on the descending ramp occurs at a lower somatic voltage than activation on the ascending ramp (Svirskis & Hounsgaard, 1997; Lee & Heckman, 1998b; Carlin *et al*, 2000). This phenomenon is thought to arise because the voltage-dependent channels carrying the inward current are electrically distant from the soma and not under voltage-clamp control. As a result, the distal channels are activated at relatively high somatic depolarizations during the ascending voltage ramp command, but then continue to supply current to the soma during the descending ramp command (Booth *et al*, 1997; Lee & Heckman, 1998b; Carlin *et al*, 2000). In neonatal rat facial and hypoglossal motoneurons, the outward currents dominate the whole-cell voltage clamp records obtained from the somata of hypoglossal motoneurons. Persistent inward

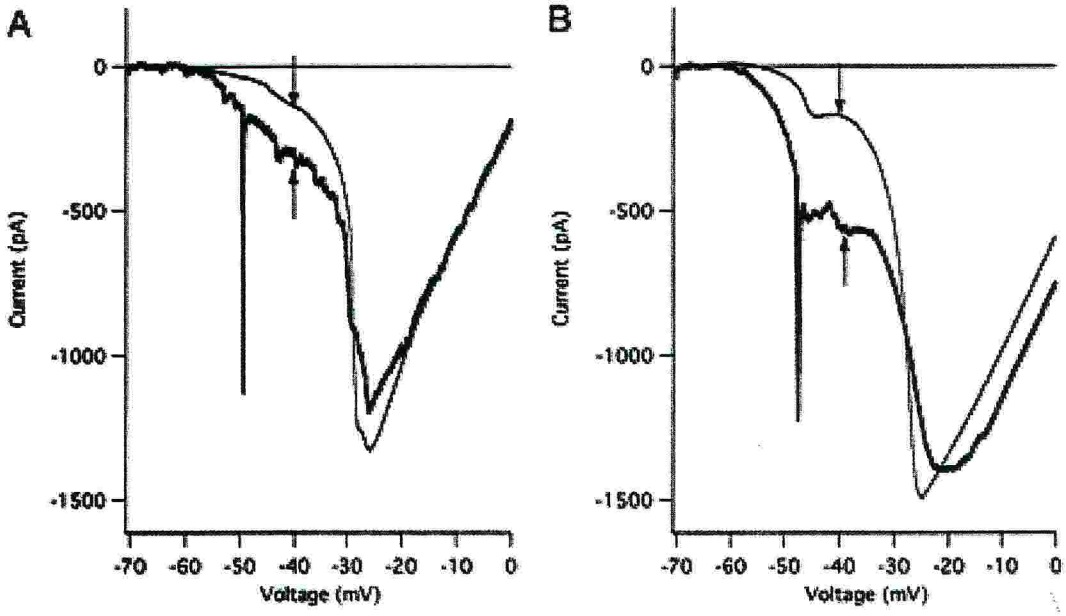

Fig 3. Persistent sodium currents in hypoglossal motoneuron in the presence of internal and external potassium channel blockers. Average, leak-subtracted currents during the ascending phase of a triangular voltage command plotted as a function of voltage for voltage ramp rates of 14 mV/s (A) and 70 mV/s (B). Responses obtained before TTX application are shown with thick lines; those after TTX application with thin lines. Arrows indicate the peak magnitude of the TTX-sensitive current, which is larger at the faster ramp rate (304 pA at 70 mV/s vs. 159 pA at 14 mV/s) (from Powers & Binder, 2003, ***J Neurophysiol***)

currents are mediated predominantly by Ca^{2+} channels, although L-type channels carry only about 5–7% of the total calcium current measured at the soma (Umemiya & Berger, 1994; Plant *et al*, 1998).

However, there is often a region of negative slope on the rising phase of the response to a slow, triangular voltage-clamp command, indicating the presence of TTX-sensitive (as demonstrated in the Figure 3) persistent inward currents.

When a HM is stimulated by a just suprathreshold current, it discharges at a minimum rate of steady firing (Mosfeldt Laursen & Rekling, 1989; Viana *et al*, 1995). A further increase in current intensity causes an increase in steady discharge rate with a linear frequency-current relation (Haddad et al, 1990; Nunez-Abades *et al*, 1993; Viana *et al*, 1993a,b, 1995). The motoneurons fire with high frequency only for a brief initial period just after the abrupt onset of stimulation. After that, there is a rapid decline in firing rate (initial adaptation, Granit *et al*, 1963; Kernell, 1965a,b). In contrast to adult HMs, which exhibit three adaptation phases (Sawczuk *et al*, 1995, 1997), neonatal HMs do not show strong spike frequency adaptation in response to current step injection (Viana *et al*, 1993b), and mostly have a potential to generate high frequency discharge (Viana *et al*, 1993b; Lape & Nistri, 2000). As proposed by Viana *et al*. (1995), Ca^{2+}-dependent afterhyperpolarization of medium duration (mAHP) controls adaptation of neonatal HMs. The data obtained after pharmacological block of mAHP in current and voltage clamp modes, confirmed its important role in controlling firing behavior (Lape & Nistri, 2000).

1.3 MOTOR PATTERN GENERATORS

Tongue muscles are engaged in motor activities (like suckling, mastication, etc.) where rapid, repeated contractions are required. These rapid activities need coordinated rhythmic oscillatory discharges from a group of functionally connected neurons that provide the timing of motoneuron discharge. Historically, there has been a lot of debate about the origin of rhythmic motor patterns among those who believed that rhythmic patterns result from chains and reflexes versus those who believed that they were generated by central neural oscillations (Hartline *et al*, 1988). This dilemma was resolved by studying rhythmic activities after removing all sensory inputs in *in vitro* preparations. Isolated regions of the central

nervous system were able to produce rhythmic motor patterns (Selverston, 1985; Marder & Calabrese, 1996). By analogy with invertebrates these functional circuits are termed central pattern generators (CPG), namely neurons wired together to supply the coherent motor output even in the absence of the commands from higher centers or from peripheral afferents. In the spinal cord the CPG for locomotion is further distinguished between rhythm generating interneurons (the "clock") which set the pace of locomotion, and the pattern-generating interneurons, whose task is to distribute motor commands (of excitatory or inhibitory nature) to various motor pools (a model obtained from the feline spinal cord by Lafreniere-Roula & McCrea, 2005). CPGs controlling locomotion are located in the spinal cord and are found in all vertebrates, including humans (for review see Kiehn, 2006). Likewise, respiratory activity may be produced by a distributed network of interacting clusters of neurons that may comprise oscillators. One recent theory says that distinct areas of the brainstem, like the pre-Bötzinger complex and the parafacial respiratory nucleus participate as rhythm generators for respiration via a complex interaction between local neurons releasing glutamate, GABA or glycine (Greer *et al*, 2006). In early postnatal life such an activity would represent a potent inspiratory drive to accelerate the rapid maturation of motoneurons involved in diaphragm muscle contractions, though motoneurons themselves are not rhythmogenic. Using fast Ca^{2+} imaging, Eugenin *et al*, (2006) have proposed that at least in a fetal mouse brain, the CPG for respiration is more distributed than hitherto supposed and does not depend on a single pacemaker.

It is now generally accepted that the motor command for the basic pattern of rhythmical oral-facial movements, as for respiration, is generated by a neuronal population in the brainstem. The CPG for mastication has been described by Nakamura & Katakura, (1995). Swallowing is preserved as long as the nervous structures located between the C_1 level and the trigeminal motor nuclei are intact (Doty *et al*, 1967), suggesting an extensive brainstem circuitry is involved in this motor pattern (for review see Jean, 2001).

1.4 NETWORKS SUBSERVING CPGs

The origin of motor rhythms in locomotor networks is disputed. According to the 'network theory', CPG activity was broadly assigned to interneuronal circuits (Grillner *et al*, 1998), while other studies have suggested that distinct spinal interneurons surrounding the central canal (Hochman *et al*, 1994) and even motoneurons themselves can generate oscillations dependent on NMDA receptors ('pacemaker theory') (Rioult-Pedotti, 1997; Guertin & Hounsgaard, 1998a; Schmidt *et al*, 1998) and propagated via gap junctions (Figure 6, 9) (Kiehn *et al*, 2000).

In the brainstem slices NMDA receptor-mediated intrinsic motoneuronal membrane oscillations are detected in rat abducens motoneurons (Durand, 1991) or in the trigeminal nucleus (Kim & Chandler, 1995). Slicing tissue inevitably excludes a lot of fibers and neurons, making recordings of spontaneous patterns restricted. As shown with transverse brainstem slices, respiratory activity can be recorded from the hypoglossal nerve provided the thickness of tissue, is sufficient to contain the pre-Bötzinger complex, (>350 μm; Smith *et al*, 1991). Recently, by using a thin brainstem (200 μm) slice preparation we confirmed the lack of spontaneous CPG activity recorded from HMs; however, application of NMDA (25 μM) activated the local network, bringing about HMs membrane oscillations (Figure 4). Previous studies of an isolated brain stem-spinal cord preparation from newborn rats reported rhythmical burst activity in response to NMDA application, recorded in XII nerve, distinct from and much faster than the respiratory rhythm (Katakura *et al*, 1995). However, based only on the brainstem hemisection study, without performing HMs recording, the authors suggested that HMs *per se* have no ability to generate rhythmical activity in response to NMDA application. By applying TTX we could demonstrate that NMDA evoked oscillations are still present in HMs (Figure 5), indicating the rhythmogenic potential of the brainstem slice preparation. Nevertheless, the interesting question of the contribution of HM's intrinsic conductances to a certain patterns is outside the scope of this thesis (because this work is still in progress).

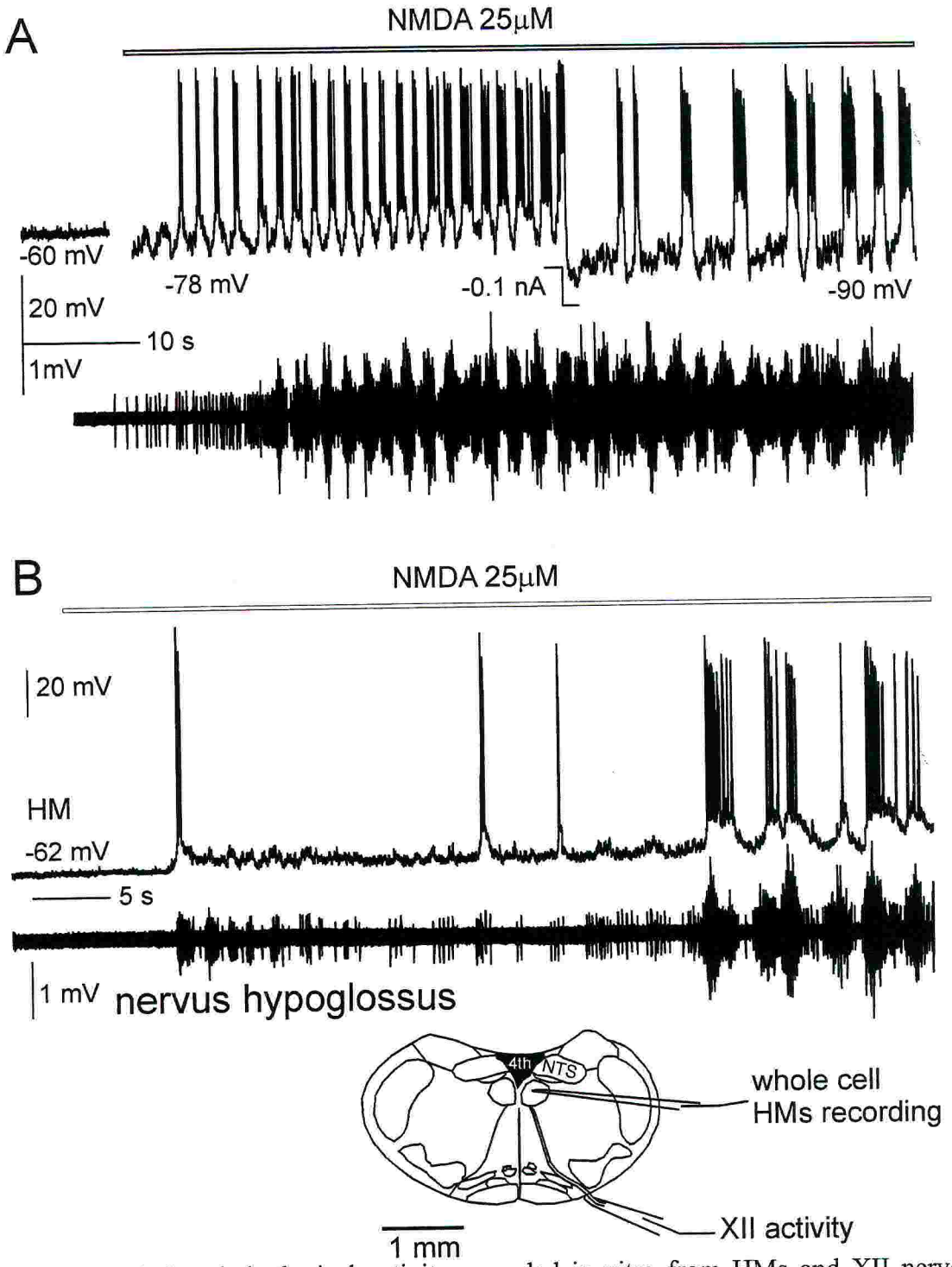

Fig 4. NMDA-induced rhythmical activity recorded in vitro from HMs and XII nerve of newborn rats. A. HM, that does not oscillate in control condition, after bath-aplication of NMDA exhibits rhythmic oscillations, better detected at hyperpolarized membrane potential. At -90 mV oscillations became rare and of longer duration (upper trace). XII nerve activity (different experiment) after bath application of NMDA demonstrates clustered synchronous activity, resembling that recorded from single HM (lower trace). B. Simultaneous recording from single HMs and nervus hypoglossus (the scheme of experiment is on the lower panel B) revealed synchronous oscillation in NMDA solution.

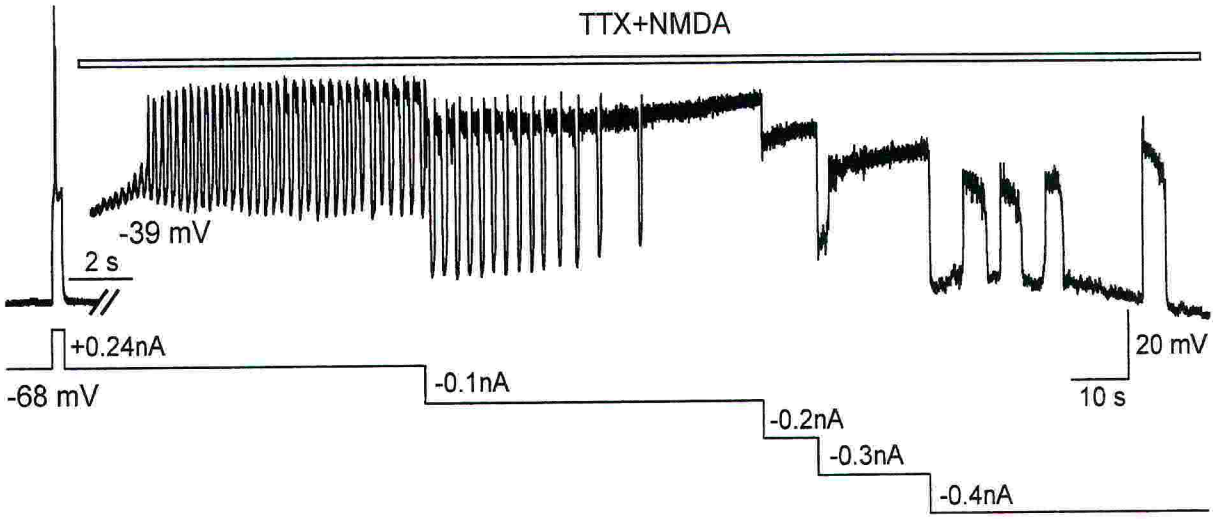

Fig 5. NMDA induces HM oscillatory activity. HM recorded in current clamp whole cell patch mode. Spike elicited by current step injection in standart Krebs solution, containing bicuculline and strychnine to block synaptic inhibition, is shown at the beginning of trace. NMDA (25 μM) induced membrane oscillations persist at different membrane potentials in the presence of TTX (1μM). Note the absence of fast sodium spikes in TTX solution. (Sharifullina E; unpublished data).

Although the brainstem neuronal wiring seems to include fewer motoneurons than in the spinal cord (Figure 6), understanding coordination between the anatomically-elusive oscillatory networks (CPG), responsible for the motor activity of swallowing, and their target motoneurons is complicated (Jean, 2001). Of note is that studies, performed in the rat by Ugolini *et al*, (1995), and by Fay & Norgren (1997a-c), have identified a column of cells in the dorsomedial medullary reticular formation and NTS (Cunningham & Sawchenko, 2000) that provides shared premotor input to motor regions of fifth (trigeminal), seventh (facial), eleventh (ambiguus) and XII cranial nerve nuclei, and is directly involved in the reflex control of oropharyngeal and esophageal phases of swallowing. Since the CPG for swallowing is not continuously active, the question arises as to whether the swallowing neurons may have other functions. It has been observed by Meyrand *et al*, (1991, 1994) that in invertebrates, swallowing depends on a pattern generator that is temporarily formed in anticipation of the production of motor activity. That is to say that, when a given stimulus is delivered, a pool of appropriate neurons is collectively activated and functionally forms the swallowing CPG, whereas these neurons are involved in other tasks when no swallowing activity is required. In keeping with the principles involving flexible circuits, recent

observations in mammals have suggested that, within the swallowing CPG, some neurons may participate in activities other than just swallowing-related ones (Jean, 2001) (Figure 7). It has been established that not only motoneurons, but also interneurons can be involved in at least two different tasks, such as swallowing and respiration, swallowing and mastication, or swallowing and vocalization.

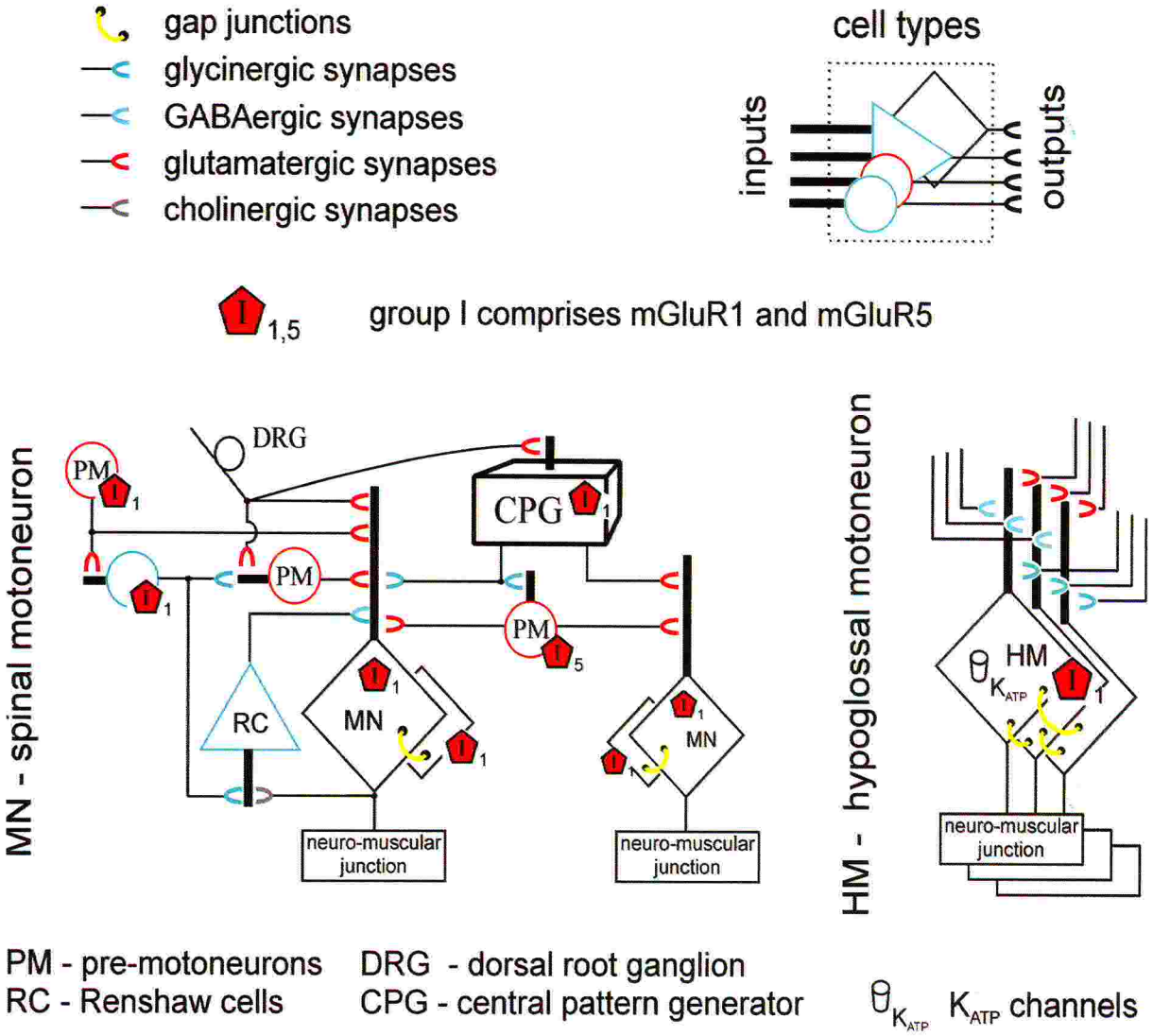

Fig 6. Idealized diagram of spinal and brainstem motor networks (Nistri *et al*, 2006, ***J Physiol***)

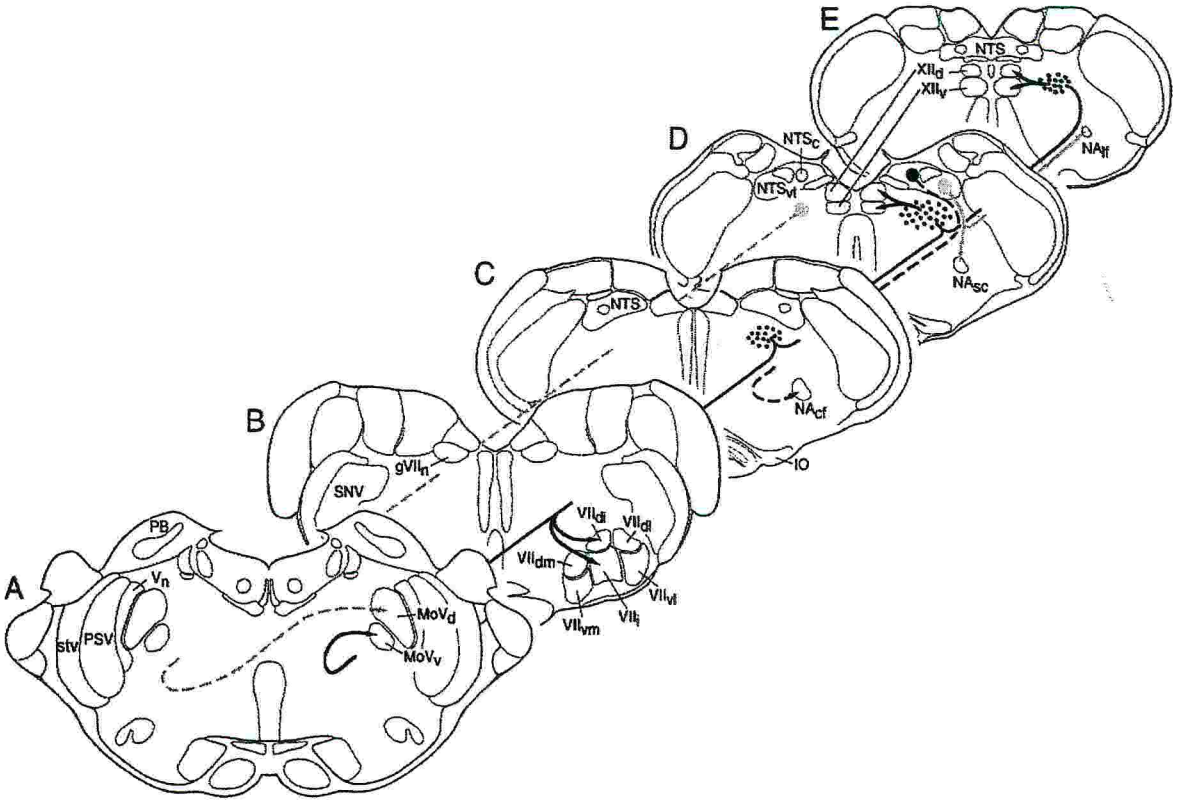

Fig 7. Schematic summary of dorsal medullary pathways projecting to the motor divisions of the fifth (MoV; A), seventh (VII; B), tenth (NA; C-E), and twelfth (XII; D, E) cranial nerve nuclei. Dorsal medullary inputs to MoV, VII, and XII arise primarily from DMRC. Projections from the DMRC are distributed preferentially to the ventral subdivision of MoV, to the dorsal and intermediate subdivisions of VII, and to both the dorsal and the ventral subdivisions of XII. Although not illustrated, these pathways are largely bilateral. In addition, a subpopulation of large multipolar neurons in the DMRC gives rise to a primarily crossed input to the dorsal subdivision of MoV. In contrast, dorsal medullary inputs to the NA arise from the NTS, are primarily uncrossed, and are organized such that the ventrolateral, intermediate, and interstitial subdivisions of the NTS project to the region of the loose and semicompact formations, whereas the central subdivision of the NTS provides input to the compact formation. Neither the NTS nor the DMRC gives rise to significant projections to the central subnucleus of the NTS. Together, these results provide evidence for discrete medullary pathways subserving sequential activation of reflexes active during the pharyngeal and esophageal phases of swallowing (from Cunningham & Sawchenko, 2000, ***J Comp Neurol***).

With regard to swallowing motoneurons, it has been reported that ambigual, trigeminal, and hypoglossal motoneurons can fire both in phase with respiration and during deglutition, as well as with swallowing and mastication, swallowing and vocalization, and even during swallowing, vocalization, and respiration (Amri & Car, 1988; Larson *et al*, 1994; Shiba *et al*, 1999; Sumi, 1963, 1969, 1970, 1977; Umezaki *et al*, 1998). These motoneurons presumably

receive a drive from separate CPGs, and their activity no doubt depends on synaptic interactions between networks. Although the mechanism of respiratory inhibition during the pharyngeal phase of swallowing is unknown, it may involve either direct projections from the NTS to respiratory centers in the ventrolateral medulla (Dobbins & Feldman, 1994), or indirect projections from the NTS to the ventrolateral medulla by way of the apneic site in the intertrigeminal region, located between the principal sensory and motor nuclei of the trigeminal nerve (Chamberlin & Saper, 1998).

Whether rhythmic motor discharges are due to either periodic patterns set by premotoneurons or intrinsic rhythmicity of motoneurons, or combination of both, the functional expression of these discharges is the appearance of electrical oscillations in motoneurons. As discussed below, motor oscillations are just one example of the wide class of electrical oscillations, a property often used for communicating certain information – coded signals in the brain.

2. NEURAL OSCILLATIONS

To quickly communicate and consolidate information within networks, neuronal electrical oscillations are generated in the thalamus and hippocampus (Kirk & Mackay, 2003; Steriade & Timofeev, 2003), inferior olivary complex (Marshall & Lang, 2004), cerebellum (Soteropoulos & Baker, 2006) and cortex (Traub *et al*, 1996; for review see Steriade, 2006). Electrical oscillations may differ in shape, frequency, regularity and phase distribution, reflecting certain modalities of neuron signaling. To date, network oscillations in vivo have been proposed to be important for sensory processing, for example in the olfactory system (Laurent *et al*, 1996; Freeman, 1972), in sensory and perceptual binding (Gray *et al*, 1989; Miltner *et al*, 1999; Rodriguez *et al*, 1999; Roelfsema *et al*, 1994; Singer & Gray, 1995), in motor programming (Murthy & Fetz, 1996), in associative learning (Larson & Lynch, 1988; Buzsáki, 2002), and in epileptogenesis (Grenier *et al*, 2001, 2003; Traub *et al*, 2001). One key proposal (Singer & Gray, 1995) has been that oscillations provide a temporal framework, so that neurons may fire in synchrony, and that the synchrony of firing carries coded information.

2.1 CLASSIFICATION OF BRAIN OSCILLATIONS

Although the description of neural oscillations is close to the original concept of brain waves, the latter usually refers to electroencephalogram (EEG) recordings and the former refer to more invasive recording techniques such as single-unit recordings with extracellular electrodes, intracellular recordings of neuronal potentials and recordings of local field potentials, using electrodes directly contacting the brain. Since the first EEG recording, obtained by Hans Berger in 1929, four major types of rhythmic brain activity are recognized (alpha, beta, delta and theta). There is no absolute borderline for the frequency ranges for each type.

Delta oscillations are in the frequency range up to 4 Hz, often associated with the very young and certain encephalopathies. They are normally found in stages 3 and 4 of sleep.

Theta oscillations are in the frequency range from 4 Hz to 8 Hz and are often associated with drowsiness and young age. This EEG frequency can sometimes be produced by hyperventilation. Theta waves can be seen during hypnagogic states such as trances, hypnosis, deep day dreams, lucid dreaming and light sleep and the preconscious state just upon waking, or before falling asleep.

Alpha (Berger's wave) oscillations are in the frequency range from 8 Hz to 12 Hz. They are characteristic of a relaxed, alert state of consciousness and are present from the age of two onwards. Alpha rhythms are best detected when the subject keeps his eyes closed, and most evident in the occipital (visual) cortex. An alpha-like normal variant called "μ" is sometimes seen over the motor cortex (central scalp) and decreases with movement, or rather with the intention to move.

Beta oscillations are in the frequency range above 12 Hz. Low amplitude beta waves with multiple and varying frequencies are often associated with active, busy or anxious thinking. Rhythmic beta waves with a dominant set of frequencies are associated with various pathologies and drug effects, especially benzodiazepines.

Gamma waves are in the frequency range of 26–80 Hz. Gamma rhythms appear to be involved in higher mental activity, including perception, problem solving, fear, and consciousness.

2.2 NEURONAL MECHANISMS OF OSCILLATIONS

Synchronized rhythmic activity is a general property of neuronal systems in mammals. However, the functional significance of such coherent states of activity and the degree to which these can be related to particular functions depends on the system under study (for review see Gray, 1994). Neuronal mechanisms of oscillations are complex. Both intrinsic neuronal properties (Llinas *et al*, 1991; Ramirez *et al*, 2004) and neural network properties are involved (Leinekugel *et al*, 2002; Sohal *et al*, 2006). Generation of rhythmic activity patterns in group of neurons can often arise from what otherwise seems to be a mechanism for maintaining stability. For instance, in many neural structures, abundant excitatory connections may lead to runaway excitation and instability, but are balanced by the ubiquitous presence of local inhibition. The basic configuration of short and long range excitation coupled with local inhibition readily leads to a pattern of synchronous oscillations (Freeman, 1968; Wilson & Bower, 1992; Steriade *et al*, 1993; Cope *et al*, 2005). Sustained excitation arising from afferent and intrinsic sources leads to transient and repeated inhibition with a periodic structure. The time delays inherent in the recurrent inhibitory circuit determine the frequency of oscillation.

At the cellular level there is an analogous interplay: depolarization produced by inward currents is balanced by outward currents to maintain stability. The voltage and time dependence of inward (excitatory) and outward (inhibitory) conductances confer a variety of intrinsic oscillatory behaviors to many different cell types (Llinas & Yarom, 1986; McMormick & Pape, 1990; Parri *et al*, 2001). Moreover, ion channels essential for generating pacemaker activity can be phosphorylated or dynamically modulated by intracellular Ca^{2+} signaling networks using intra- and extracellular Ca^{2+} sources (Ladewig *et al*, 2003; Levi *et al*, 2003; Pape *et al*, 2004). Recent work on thalamic neurons indicates that neuronal T-type of Ca^{2+} channels underlie membrane potential bistability, i.e. the existence of two resting membrane potentials, due to the *window current* ($I_{Twindow}$,, Williams *et al*. 1997; Toth *et al*, 1998) generated by these channels. This phenomenon is believed to be a key cellular mechanism (Crunelli *et al*, 2005; Figure 8) for the expression of the slow (<1 Hz) sleep oscillations, one of the fundamental EEG rhythms of non-REM sleep. By varying the conductances of only eight voltage-dependent ion channels, computational approaches yield 1.8 million single-compartment model neurons with different discharge properties,

including pacemaker activity ranging from irregular bursting, non-periodic bursting and one-spike bursting to regular bursting (Prinz *et al*, 2003). The modeling of eight ion channels in a single neuronal compartment is a simplification for practical purposes. Indeed, molecular cloning techniques have uncovered a large diversity of ion channel subtypes that are differentially distributed throughout the CNS and even within the dendritic and somatic compartments of the same neuron (Levi *et al*, 2003; Whittington & Traub, 2003; French *et al*, 2004).

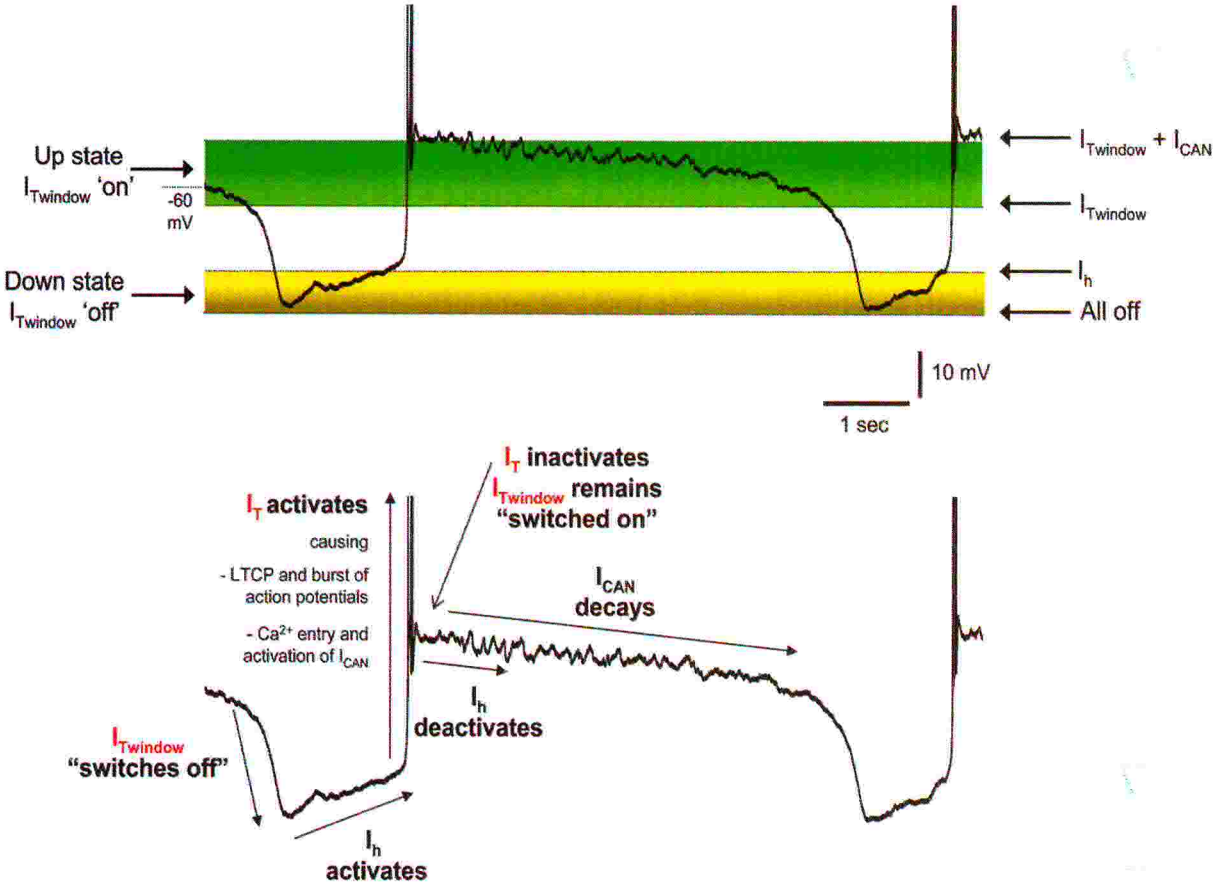

Fig 8. summarizes the cellular mechanism of the slow (< 1 Hz) sleep-like oscillations in thalamocortical neurones, in which (i) $I_{Twindow}$ plays the major role by setting the level of the up ($I_{Twindow}$ 'on') and down ($I_{Twindow}$ 'off') states of the oscillation, (ii) I_h is responsible for repolarizing the neurone from the down state and thus critically determines the duration of the down state, and (iii) I_{CAN} tightly controls the duration of the up state and is thus responsible for stabilizing the voltage region during slow oscillation. Low-threshold Ca^{2+} spike or potential is abbreviated LTCP. (from Crunelli *et al*, 2005, ***J Physiol***).

In spinal cord and brainstem the cyclic output of most motor circuits depends on the interplay between the excitation mediated by glutamate, GABA- and glycine-mediated

inhibition, and the activity of voltage-sensitive channels, including those permeable to Na^+, or Ca^{2+}, or with Ca^{2+} dependent K^+ permeability, as well as slow inward rectifiers (Grillner & Wallen, 2002; Alford *et al*, 2003; Kudo *et al,* 2004; Greer *et al*, 2006).

Amid the vast complexity of firing and subthreshold repertoires displayed by neurons, and the large ensemble of membrane currents responsible for this complexity, certain issues in neuronal intrinsic properties stand out for their relevance to oscillations. Included in these features (for review see Traub *et al*, 2004) are: 1. The conditions for spontaneous action potential generation. For example, in the hippocampus, low concentrations of kainate increase interneuron axonal excitability and can give rise to ectopic axonal spikes (Semyanov & Kullmann 2001) even in principal cells, important for gamma oscillations. 2. The processes, which allow metabotropic receptors to excite cells, by blocking selected K^+ currents and stimulating the emergence of oscillations in forebrain networks (Whittington *et al*, 1995; Beierlein *et al*, 2000; Cobb *et al*, 2000; Hughes *et al*, 2002). 3. The extent of dendritic electrogenesis present during oscillations. Thus, pyramidal cell dendritic Ca^{2+} spikes contribute to one type of in vitro theta-frequency oscillations in hippocampus (Gillies *et al*, 2002) and may also play a role in vivo (Kamondi *et al*, 1998, Penttonen *et al*, 1998). Na^+ dendritic electrogenesis may facilitate the gain of interneuron EPSPs and their tendency to fire doublets (Traub & Miles 1995; Martina *et al*, 2000). 4. The presence of gap junctions (Figure 9) and/or electrical synapses in the mammalian brain (for reviews see Bennett, 1977; Sotelo & Korn, 1978; Bennett & Zukin, 2004), which operate faster than chemical synapses, and therefore mediate reciprocal synchronous interactions between neurons (Kandel *et al*, 2000; Gibson *et al*, 1999). 5. Rapid intracellular Ca^{2+} mobilization might also facilitate oscillatory bursting in phasically firing cells in different brain regions (Deschenes *et al*, 1984; Leung & Yim, 1991; Li & Hatton, 1996). 6. The persistent sodium current (I_{NaP}) participates in burst generation and control of membrane excitability (Wu *et al*, 2005; Golomb *et al*, 2006).

In the rat spinal cord, electrical coupling of motoneurons is common in early development (Tresch & Kiehn, 2000) and decreases with maturation, but could reappear in axotomized neurons of the adult (Chang *et al*, 1999, 2000). In the brainstem electrical coupling is reported in the vestibular nucleus, the nucleus of trigeminal nerve and the inferior olivary nucleus. There has been some reports of weak neuron to glial cell coupling in the locus

coeruleus, and cerebellum (Alberts, 2002). Experimental data show strong gap junction expression in astrocytes (Altevogt & Paul, 2004; Schools *et al*, 2006).

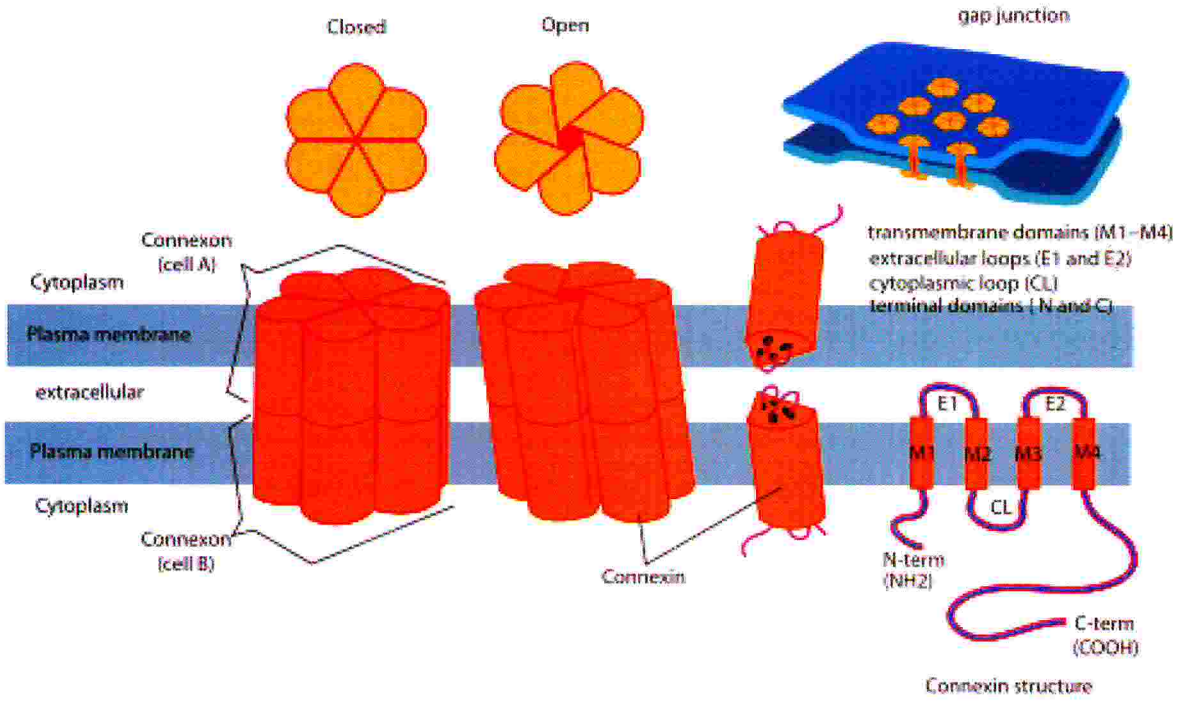

Fig 9. Schematic representation of the structure of gap junctions within the cell membrane. A connexon is an assembly of 6 proteins (connexins) that forms a bridge called a gap junction between the cytoplasm of two adjacent cells. The connexon is the hemichannel on one side of the junction; two connexons from opposing cells normally come together to form the complete intercellular gap junction channel. However, in some cells, the hemichannel itself is active as a conduit between the cytoplasm and the extracellular space.

Neuronal oscillations that synchronize activity of the neurons in a circuit appear to be an important encoding mechanism, involved in a particular neural computation. Nevertheless, by examining the activity of only one neuron in the visual cortex, it is very difficult to reconstruct the whole visual scene, especially because individual neurons are very noisy. This problem is solved by the brain expressing billions of neurons. Individual neurons may exhibit neuronal noise, but the population as a whole averages this noise out (Dragoi & Buzsaki, 2006). This view then questions the usefulness of *in vitro* models of neuronal oscillations. The analysis of various oscillatory types in neocortex and thalamus leads to the

conclusion that, in the intact brain, there are no "pure" rhythms, generated in simple circuits, but complex wave sequences (consisting of different, low and fast-frequency oscillations) that originate from synaptic interactions in cortico-cortical and cortico-thalamic neuronal loops (Steriade, 2001). Nevertheless, other types of rhythmic oscillations require more localized networks like the intrinsic spinal CPG that coordinate limb movements during locomotion even in the absence of descending commands from higher centers (Grillner, 1981; Kiehn & Kjaerulff, 1996). Likewise, rhythmical oro-facial motor activities in an isolated brain stem-spinal cord preparation can be monitored from the hypoglossal nerve of newborn rats (Katakura *et al*, 1995) or a spontaneous respiratory rhythm can be generated by thin (350-600 μm) medullary slices (Smith *et al*, 1991). All these observations suggest that, at least for some types of neuronal computation, the size of the local network is limited.

3. METABOTROPIC RECEPTORS MODULATE CENTRAL PATTERN GENERATORS

While glutamate plays a major role as a principal fast excitatory neurotransmitter in spinal cord and brainstem motor circuits (Rekling *et al*, 2000), it is conceivable that it might also modulate neuronal excitability by activating G-protein coupled metabotropic (mGlu) receptors that (unlike ionotropic glutamate receptors (iGluR)), mediate second messenger interactions. mGlu receptors, according to their distinctive amino acid sequences, pharmacology and signal transduction pathway, occur as eight molecularly distinct receptors, in addition to a number of splice variants (Sladeczek *et al*, 1985; Sugiyama *et al*, 1987; Tanabe *et al*, 1992), which have been divided into three groups (Table 2).

Group I mGluRs include mGluR1 and 5, and couple to Gq to stimulate phosphoinositide hydrolysis and phospholipase C. Group II (mGluR2 and 3) and Group III mGluRs (mGluR4, 6, 7, and 8) couple to Gi/Go to inhibit cAMP (Conn & Pin, 1997; Kew & Kemp, 2005). Through a growing number of studies, mGluRs have been shown to fulfill unique presynaptic and postsynaptic roles. In general, group I mGluRs are usually localized postsynaptically, are excitatory, acting to enhance neurotransmitter release, potentiate iGluR responses and modulate various depolarizing currents (Anwyl, 1999). Nevertheless, there is also evidence for presynaptic expression of group I mGluRs (Romano *et al*, 1995; Lujan *et*

Table 2. Classification, function and localization of metabotropic glutamate receptors. Adenyl cyclase (AC); phospholipase C (PLC). (from Moghaddam, 2004, ***Psychopharmacology***)

Subgroup	Subtype	G-protein coupling	Transduction mechanism	Primary localization
Group I	mGlu 1	Gq	↑ PLC	Postsynaptic to neurons, high density in forebrain and midbrain
	mGlu 5	Gq	↑ PLC	Glial cells, postsynaptic to neurons, high density in forebrain and midbrain
Group II	mGlu 2	G_i, G_o	↓ AC	Pre and postsynaptic in neurons, high density in forebrain
	mGlu 3	G_i, G_o	↓ AC	Glial cells, postsynaptic to neurons, high density in forebrain
Group III	mGlu 4	G_i, G_o	↓ AC	Pre and postsynaptic in neurons, high density in cerebellum
	mGlu 6	G_i, G_o	↓ AC	Postsynaptic, highly localized in retina
	mGlu 7	G_i, G_o	↓ AC	Pre and postsynaptic in neurons
	mGlu 8	G_i, G_o	↓ AC	Pre and postsynaptic in neurons, high density in spinal cord

al, 1996; Wittmann *et al*, 2001), which are reported to modulate glutamate release (Gereau & Conn, 1995; Rodriguez-Moreno *et al*, 1998; Reid *et al*, 1999; Mannaioni *et al*, 2001).

In several systems, group II and III mGluRs are predominantly localized to presynaptic terminals, where they inhibit transmitter release (for reviews see Anwyl, 1999; Schoepp, 2001). At the axon terminal, G-protein-mediated effects may include inhibition of high threshold calcium channels, activation of potassium channels and direct inhibition of transmitter release machinery (Scanziani *et al*, 1995; Takahashi *et al*, 1996; Cochilla & Alford, 1998). All mGluRs are expressed by neurons, while mGluR3 and 5 are additionally expressed by glial cells (Ohishi *et al*, 1993; Petralia *et al*, 1996; van den Pol *et al*, 1995).

Modulation of rhythmic motor pattern generator activity mediated by metabotropic receptors for glutamate has been reported in invertebrates (Takahashi & Alford, 2002), reptiles (Douse & Mitchell, 1990; Guertin & Hounsgaard, 1998b; Delgado-Lezama *et al*, 1999) and in the mammalian spinal cord (Krieger *et al*, 1998; El Manira *et al*, 2002; Marchetti 2003, 2005; Taccola *et al*, 2003, 2004), indicating that such receptors are a potential target for pharmacological up- or downregulation of spinal rhythmicity. Specifically, in the rat spinal cord, application of the group I mGluR agonist DHPG evokes motoneuron depolarization at network level and generates sustained network-dependent oscillations (Marchetti *et al*, 2003). Activation of group II mGluRs blocks disinhibited bursting, a phenomenon, representing the inherent ability of spinal networks to generate rhythmic patterns (Bracci *et al*, 1996), which appear after blocking spinal GABA- and glycine-mediated synaptic inhibition. The group III mGluRs agonist L-AP4 largely depresses cumulative depolarization, windup and associated oscillations (Taccola *et al*, 2004).

In the rat brainstem trigeminal nucleus mGluRs can be recruited by glutamatergic premotoneurons, producing depression of excitatory transmission, combined with increased postsynaptic excitability, which enhances the signal-to-noise ratio of oral-related synaptic input to trigeminal motoneurons during rhythmical jaw movements (Del Negro & Chandler, 1998). Distinct subtypes of metabotropic glutamate receptors mediate differential actions on excitability of spinal respiratory motoneurons, innervating the diaphragm (Dong & Feldman, 1999). Pre and postsynaptic effects of metabotropic glutamate receptor activation on neonatal rat hypoglossal motoneurons have also been reported (Donato *et al*, 2003). In particular, at the presynaptic level, activation of mGluRs by the broad spectrum agonist *trans*-ACPD (*t*-ACPD) depresses evoked glutamatergic currents, while at postsynaptic level *t*-ACPD enhanced motoneuron excitability. Finally, glycinergic (but not GABA) inhibitory transmission is facilitated by *t*-ACPD (Donato & Nistri, 2000). However, these results have been obtained using a broad-spectrum agonist of all three groups of mGluRs. Hence, the effects of selective activation of different groups of mGluRs in HMs have not been reported so far. Previous studies have shown how metabotropic receptors for acetylcholine (ACh) (Pagnotta *et al*, 2005) or serotonin (5-HT) (Berger & Huynh, 2002) can modulate inputs to HMs.

3.1 TOPOGRAPHY OF METABOTROPIC GLUTAMATE RECEPTORS IN THE BRAINSTEM

Detailed mapping of the distribution of mGluR subtypes within the dorsal and ventral medullary regions of the rat brain has been performed by Hay *et al*, (1999) and Pamidimukkala *et al*, (2002). Fusiform and multipolar (Figure 10A) mGluR1 containing cells within the hypoglossal nucleus are intensely stained. This labeling is observed throughout the rostral-caudal extent of the nucleus. No mGluR2/3, mGluR5, or mGluR7 labeling is found in the hypoglossal nucleus. mGluR8 labeling is also observed in HMs. At a higher magnification, labeling appears to be restricted to the cytoplasm and the cell membrane. Sparse labeling for mGluR subtypes 1, 2, 3, 5, 7, 8 is found in NTS and its subdivisions, lateral reticular nucleus, ventrolateral medulla and nucleus ambiguous (Figure 10B).

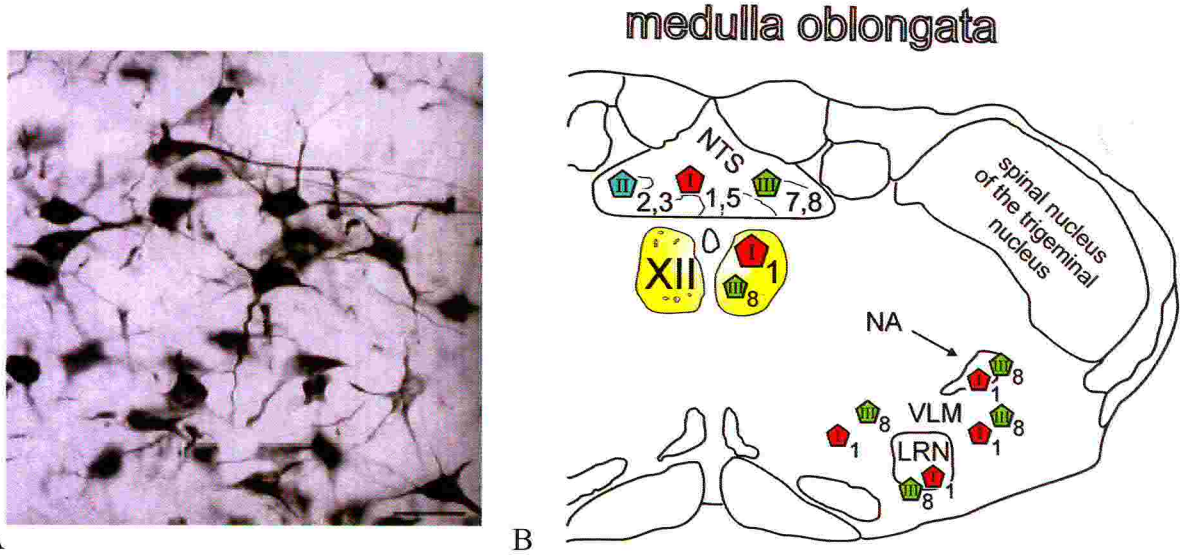

Fig 10. A. mGluR1 immunoreactive cell bodies and processes within the hypoglossal nucleus. Scale bar is 50 µm. (from Hay *et al*, 1999, ***J Comp Neurol***) B. Topography of mGluRs in the brainstem. Pentagons indicate different types of mGluRs. Group I (mGluR1/5), group II (mGluR2/3) and group III (mGluR7/8) mGluRs show different distribution throughout subnuclei of NTS and of the ventrolateral medulla. Only mGluR1 and mGluR8 subtypes are expressed by hypoglossal motoneurons (XII) (from Nistri *et al*, 2006, ***J Physiol***)

3.2 METABOTROPIC GLUTAMATE RECEPTOR ACTIVITY

Unlike ionotropic glutamate receptors, mGlu receptors are not responsible for transmitting fast synaptic responses and are usually inactive during single synaptic release events (Conn, 2003). The rapid clearance system restricts the spread of the neurotransmitter (at least at physiological temperature, Kullmann *et al*, 1999) and it ensures that synaptic transmission occurs in a point-to-point fashion. Excessive activation of glutamate receptors is harmful, and glutamate is thereby toxic in high extracellular concentrations. mGluRs are often extrasynaptic (Baude *et al*, 1993; Yokoi *et al*, 1996), so that they can bind the transmitter only under high neuronal activity conditions (Scanziani *et al*, 1997; Shigemoto *et al*, 1997; Cartmell & Schoepp, 2000) or after blocking glutamate uptake (Maki et al, 1994; Fitzsimonds & Dichter, 1996; see also section 'Discussion' in my paper "Glutamate uptake block triggers deadly rhythmic bursting of neonatal rat hypoglossal motoneurons", J Physiol 572, 2006, p.420 below). This strategic location of mGluRs confers them a role in

pathophysiological conditions (Figure 11). In fact, in brainstem respiratory system, it seems likely that mGluRs are involved in excitoxicity or ischaemia (Cartmell & Schoepp, 2000) under conditions of massive glutamate release and impaired uptake (Nicholls & Attwell, 1990). Selective group I antagonists do not normally change the inspiratory current drive (Bocchiaro & Feldman, 2004) from respiratory centres to HMs (for review, see Ballanyi *et al*, 1999), implying that, at least during the standard respiratory rhythm, there is insufficient ambient glutamate to activate mGluRs.

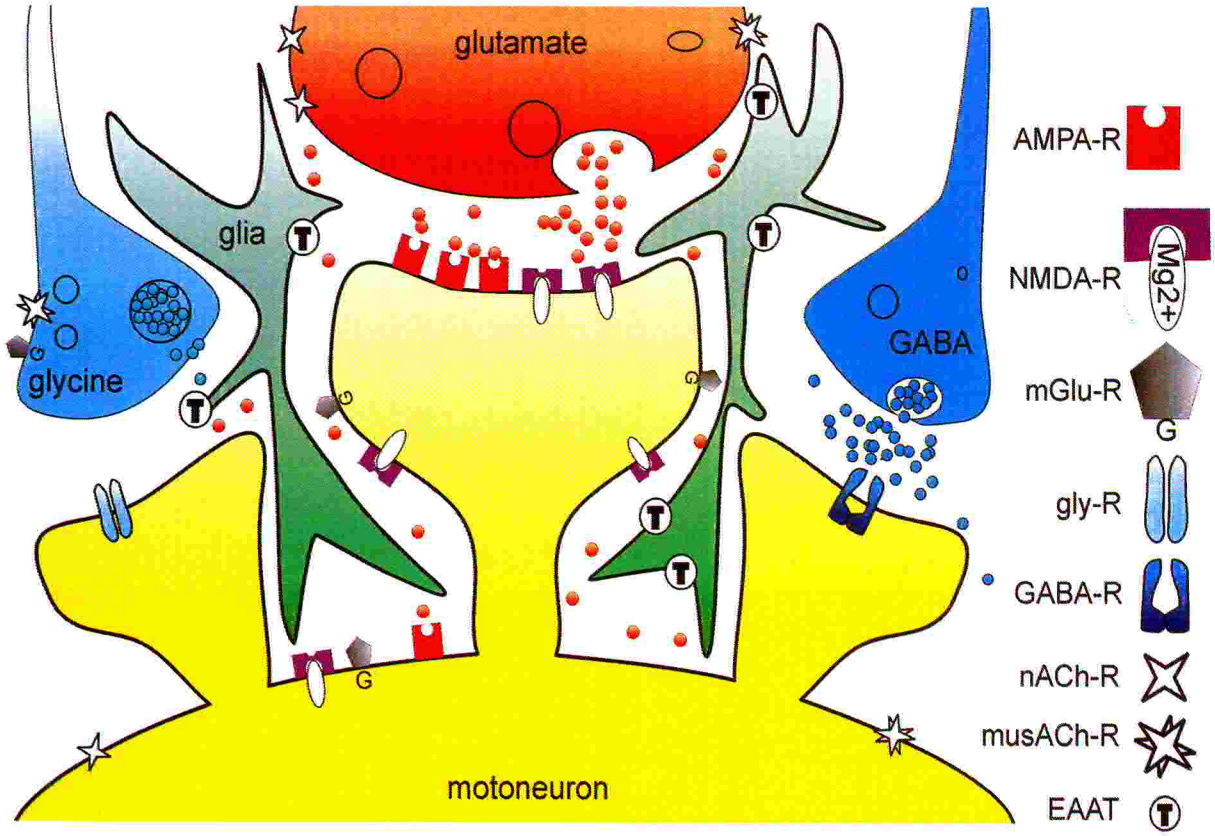

Fig 11. Idealized scheme of synapse. The excitatory amino acid transporter is abbreviated EAAT (redrawn from Huang & Bergles, 2004, ***Curr Opin Neurobiol***).

4. TIGHT CONTROL OF EXTRACELLULAR GLUTAMATE CONCENTRATION

Since there is no fast enzymatic metabolism of glutamate in the extracellular space, the only rapid way to remove glutamate is by cellular uptake (Balcar & Johnston, 1972; Logan & Snyder, 1972; Johnston, 1981; Danbolt, 2001). Although simple diffusion appears to be an important mechanism for glutamate removal from the synaptic clefts on the submillisecond timescale, at least at small synapses (e.g. hippocampal Schaffer collateral to pyramidal cell synapses (Spacek, 1985; Harris & Sultan, 1995; Lehre & Danbolt, 1998; Ventura & Harris, 1999) and parallel fiber synapses on dendritic shafts of interneurons (basket, stellate and Golgi cells) in the cerebellum (Palay & Chan-Palay, 1974), where diffusion of glutamate is limited partly by the glial covering and partly by binding to glutamate transporters). Diffusion can only work effectively for very short distances (a few hundred nanometers) and it can only be an efficient removal mechanism as long as the glutamate concentration in the extracellular fluid is not very high. At large complex synapses, like e.g. hippocampal mossy fiber to CA3 pyramidal cell synapses (Blackstad & Kjaerheim, 1961; Amaral & Dent, 1981; Chicurel & Harris, 1992) and cerebellar mossy fiber to unipolar brush cell synapse (Rossi *et al*, 1995; Mugnaini *et al*, 1997), diffusion out of the synaptic cleft is limited by tortuosity (Danbolt, 2001). It follows that, at many synapses, the leak of glutamate out of the brain tissue into the cerebrospinal fluid is a process too slow to maintain low extracellular levels of this transmitter.

The ability of extrasynaptic iGlu and mGlu receptors to participate in signaling is tightly regulated by EAAT activity (Huang & Bergles, 2004; Figure 11). Astrocytes express the highest density of EAATs and dominate the process of clearance away from these receptors. Synapses that are not associated with astrocyte processes, experience greater mGluR activation and can be exposed to glutamate released by adjacent synapses (Brasnjo & Otis, 2001; Huang & Bergles, 2004).

Five sodium and potassium coupled EAATs have been cloned so far (for review, see Saier, 1999; Slotboom *et al*, 1999): GLAST (EAAT1) (Storck *et al*, 1992; Tanaka, 1993), GLT (EAAT2) (Pines *et al*, 1992), EAAC (EAAT3) (Kanai & Hediger, 1992), EAAT4 (Fairman *et al*, 1995) and EAAT5 (Arriza *et al*, 1997). (The human homologues of the three more

ubiquitous subtypes are shown in brackets). All five proteins catalyze transport of L-glutamate as well as L- and D-aspartate (Danbolt, 2001). Because of the high rates of glutamate release, inhibition of glutamate uptake leads to high extracellular levels of glutamate within seconds (Jabaudon *et al*, 1999).

GLT (EAAT2) and GLAST (EAAT1) are responsible for most of the glutamate uptake activity. This notion is probably applicable to all regions of the mammalian CNS and emphasizes the major role of astroglia (Bergles & Jahr, 1998; Takayasu *et al*, 2005, 2006) in glutamate removal because GLT and GLAST proteins have only been found in astroglial cells in CNS with strong labeling in cerebellar Bergmann glia and more diffuse labeling in the forebrain. GLT-1 is almost exclusively expressed in glia and is widespread and abundant throughout the forebrain, cerebellum, and spinal cord. EAAC is found predominantly in a variety of different neurons (glutamatergic, GABAergic and cholinergic) of the spinal cord and brain. EAAT4 has properties of a ligand-gated Cl-channel and is localized mainly to cerebellar Purkinje cells. EAAT5 is retina-specific.

While neurons contain GLT mRNA, they do not normally express GLT protein. There is, however, evidence for the existence of a glutamate transporter in glutamatergic nerve endings as well. This evidence stems from immunocytochemical studies of D-aspartate immunoreactivity (Gundersen *et al*, 1993, 1996). It is still unknown how quantitatively and functionally important neuronal glutamate uptake is when compared to the glial.

5. ROLE OF GLUTAMATE TRANSPORTERS IN AMYOTROPHIC LATERAL SCLEROSIS

The term motor neuron disease is used to designate a chronic progressive disorder characterized by the selective degeneration of motor neurons in the cerebral cortex, brainstem and spinal cord. It is manifested clinically by muscular weakness, atrophy, and spasticity with exaggeration of tendon reflexes in varying combinations. The most frequent form is called amyotrophic lateral sclerosis (ALS or 'Lou Gehrig's disease'). The literature on ALS is extensive and a large number of pathological changes have been reported in these patients. Several pathogenic factors have been proposed, including glutamate excitotoxicity (Couratier *et al*, 1993; Rothstein, 1995; Heath & Shaw, 2002), production of reactive oxygen

species (ROS) (Agar & Durham, 2003), Ca^{2+}-dependent formation of protein aggregates (Tateno *et al*, 2004), defective axonal transport (Jablonka *et al*, 2004), mitochondrial dysfunction, deregulation of Ca^{2+} homeostasis with increased glutamate receptor mediated calcium influx and autoimmune reactions (e.g. autoantibodies to calcium channels causing increased calcium influx), and induction of pro-apoptotic pathways (Przedborski, 2004). There is a body of circumstantial evidence implicating excitotoxicity as a contributing factor to motor neuron injury either as a primary or as a secondary mechanism (Ludolph & Műnch, 1999; Shaw, 1999; Spencer, 1999). Harmful overstimulation of glutamate receptors (excitotoxicity) has been suggested to be important in motoneuron disease via: (a) increased glutamate levels (e.g. due to reduced uptake) or (b) increased sensitivity to endogenous excitatory amino acids (e.g. because of changed glutamate receptors, defective energy production or free radical defence) or (c) intake of exogenous (dietary) excitotoxins (Whiting, 1964; Ross *et al*, 1989; Perl *et al*, 1990; Stewart *et al*, 1990; Teitelbaum *et al*, 1990; Staton & Bristow, 1997). Cerebrospinal fluid (CSF) from patients with ALS is toxic to cultured neurons as compared to control CSF and the neurotoxic effect is suggested to be mediated via AMPA receptors (Couratier *et al*, 1993; Kawahara *et al*, 2004). Reduced uptake of glutamate (Trotti *et al*, 2001) as measured by uptake in synaptosomes (Rothstein *et al*, 1992) has been observed in autopsy material from patients with amyotrophic lateral sclerosis. Apparently, the brainstem HMs are among the most vulnerable, giving early symptoms like slurred speech and dysphagia in the bulbar form of ALS (Krieger *et al*, 1994; Lips & Keller, 1999; Laslo *et al*, 2001). While the early damage of hypoglossal motoneurons (HMs) may be related to their characteristic intracellular Ca^{2+} homeostasis (Donato *et al*, 2003; Ladewig *et al*, 2003) and expression of Ca^{2+}-permeable AMPA receptors (Del Cano *et al*, 1999; Laslo *et al*, 2001; Essin *et al*, 2002), it is also suggested that vulnerable motor nuclei possess distinctive properties of glutamate uptake to protect them against the risk factor of excitoxocity (Medina *et al*, 1996). Despite these findings, there is no information about HM function and survival after glutamate uptake block.

6. AIMS OF THE STUDY

The main goal of this study was to investigate the properties of hypoglossal motoneurons, especially those related to their rhythmic activity. For this purposes, we studied the modulatory role that group I mGlu receptors may have in shaping motor output and HM responsiveness.

The questions we tried to answer during this thesis were the following ones:

1. What are the consequences of activating group I mGlu receptors within the nucleus hypoglossus network?

This question leads to studying:

- functional localization of mGluRs within brainstem network and their participation to normal excitatory synaptic transmission (after pharmacological block of GABA and glycine mediated inhibition)
- their action on HMs,
- their ability to produce oscillatory activity of HMs

2. What are the characteristics of oscillatory activity in HMs and their functional consequences?

This question should shed the light on:

- the topographic arrangement of oscillating neurons,
- mechanisms of self-regulation, network propagation and protection from excitotoxicity,
- the role of oscillations in determining the firing properties of HMs,

3. The possible role of endogenous glutamate in activating of mGluRs within the local brainstem network, especially following block of the glutamate uptake system?

4. Hypoglossal motoneuron survival in the face of extracellular build-up of glutamate after uptake block.

European Journal of Neuroscience, Vol. 20, pp. 1245–1254, 2004

Activation of group I metabotropic glutamate receptors enhances efficacy of glutamatergic inputs to neonatal rat hypoglossal motoneurons *in vitro*

Elina Sharifullina, Konstantin Ostroumov and Andrea Nistri
Neurobiology Section and INFM Unit, International School for Advanced Studies (SISSA), Via Beirut 4, 34014 Trieste, Italy

Keywords: brainstem, DHPG, hypoglossus nucleus, respiration, swallowing

Abstract

Group I metabotropic glutamate receptors (mGluRs) are the main class of metabotropic receptors expressed in the hypoglossus nucleus. Their role in glutamatergic transmission was investigated using patch-clamp recording from motoneurons in a neonatal rat brainstem slice preparation. After pharmacological block of γ-aminobutyric acid and glycine-mediated inhibition, under voltage-clamp, the selective group I agonist (RS)-3,5-dihydroxyphenylglycine (DHPG) induced a motoneuron inward current by depressing a leak conductance, and strongly facilitated spontaneous glutamatergic synaptic currents. This effect was blocked by 7-(hydroxyimino)cyclopropa[b]chromen-1a-carboxylate ethyl ester (CPCCOEt) and unaffected by 2-methyl-6-(phenylethynyl)pyridine hydrochloride (MPEP), indicating a role for subtype 1 mGluRs. The frequency but not the amplitude of miniature glutamatergic currents was also enhanced by DHPG. Currents elicited by puffer application of (RS)-α-amino-3-hydroxy-5-methyl-4-isoxazolepropionic acid (AMPA) in the presence of tetrodotoxin were also unchanged, suggesting that DHPG facilitated release of glutamate. Glutamatergic currents evoked by electrically stimulating the dorsomedullary reticular column premotoneurons were, however, depressed by DHPG in a CPCCOEt-sensitive fashion. Neither CPCCOEt nor MPEP *per se* changed glutamatergic transmission. Under current-clamp, even if DHPG depressed excitatory postsynaptic potentials, motoneuron spike threshold and time to peak were reduced so that facilitation of synaptic potential/spike coupling became apparent. We propose a wiring diagram to account for the differential action by DHPG on spontaneous and evoked transmission, based on the discrete distribution of subtype 1 mGluRs on glutamatergic afferents. Although under standard recording conditions there was insufficient ambient glutamate to activate mGluRs, such receptors were a powerful target to upregulate excitatory synaptic transmission and enhance signalling by hypoglossal motoneurons to tongue muscles.

Introduction

The brainstem hypoglossus nucleus supplies the principal motor innervation (via the XII cranial nerve) to the tongue muscles and therefore plays a fundamental role in functions like respiration, swallowing and mastication (Sawczuk & Mosier, 2001). Hypoglossal motoneurons (HMs) receive excitatory glutamatergic, and inhibitory γ-aminobutyric acid (GABA) and glycinergic inputs (Rekling *et al.*, 2000), whose finely balanced actions underlie the complex firing patterns of such cells (Sawczuk *et al.*, 1995) and are regulated by neuromodulators (Bayliss *et al.*, 1997).

Glutamatergic transmission on HMs is predominantly mediated by (RS)-α-amino-3-hydroxy-5-methyl-4-isoxazolepropionic acid (AMPA)-sensitive receptors (Paarmann *et al.*, 2000; Essin *et al.*, 2002). Nevertheless, glutamate may also exert complex actions via metabotropic glutamate receptors (mGluRs), which are G-protein coupled receptors operating via several intracellular second messengers (Conn & Pin, 1997; Cartmell & Schoepp, 2000).

In the hypoglossus nucleus, the large majority of mGluRs belong to the group I (Hay *et al.*, 1999) usually linked to phospholipase C activation and production of inositol-1,4,5-trisphosphate (Conn & Pin, 1997; Cartmell & Schoepp, 2000). The precise cellular distribution of such receptors is, however, unclear. In other brain areas immunohistochemical studies indicate a mainly postsynaptic location for group I mGluRs (Martin *et al.*, 1992; Shigemoto *et al.*, 1997; Katayama *et al.*, 2003), which induce strong increase in neuronal excitability (Anwyl, 1999). Nevertheless, there is also evidence for presynaptic expression of group I mGluRs (Romano *et al.*, 1995; Lujan *et al.*, 1996; Wittmann *et al.*, 2001), which are reported to modulate glutamate release (Gereau & Conn, 1995; Rodriguez-Moreno *et al.*, 1998; Reid *et al.*, 1999; Mannaioni *et al.*, 2001).

In the hypoglossus nucleus, the role of mGluRs is poorly understood. In fact, a previous report found that the agonist (±)-1-aminocyclopentane-*trans*-1,3-dicarboxylic acid (*trans*-ACPD) depressed evoked glutamatergic currents, yet it did not impair their paired-pulse facilitation (Donato *et al.*, 2003) in analogy to inhibition by *trans*-ACPD of evoked and miniature excitatory currents on trigeminal motoneurons (Del Negro & Chandler, 1998). Because *trans*-ACPD is a broad spectrum agonist acting on all major classes of mGluRs (Schoepp *et al.*, 1999), it is difficult to discern a distinct role for group I mGluRs. Group I selective antagonists do not change the inspiratory current drive (Bocchiaro & Feldman, 2004) from respiratory centres to HMs (for review, see Ballanyi *et al.*, 1999), implying that, at least during the standard respiratory rhythm, there is insufficient ambient glutamate to activate mGluRs. Because HMs are

Correspondence: Professor A. Nistri, as above.
E-mail: nistri@sissa.it

Received 20 April 2004, revised 14 June 2004, accepted 1 July 2004

doi:10.1111/j.1460-9568.2004.03590.x

also involved in oromotor reflexes (Sawczuk & Mosier, 2001), it is, however, possible that under conditions of phasic, intense excitation, mGluRs play a modulatory role. In fact, during repeated network activity mGluRs can be activated by endogenous glutamate (Scanziani *et al.*, 1997), a phenomenon apparently also occurring on trigeminal motoneurons (Del Negro & Chandler, 1998).

Our goal was to investigate whether, on HMs of a neonatal rat brainstem slice preparation (when synaptic inhibition was pharmacologically blocked), group I mGluRs could modulate glutamatergic transmission, whether their effect was direct or network-mediated, and whether they modulated HM firing activity.

Materials and methods

Slice preparation

Experiments were performed on brainstem transverse slices obtained from neonatal Wistar rats (0–5 days old) under urethane anaesthesia, as described previously (Donato & Nistri, 2000), in accordance with the regulations of the Italian Animal Welfare Act and approved by the local authority veterinary service. Thin (200 μm) brainstem slices were prepared following the procedure described by Viana *et al.* (1994), Donato & Nistri (2000) and Marchetti *et al.* (2002).

Electrophysiological recording

HMs were identified within the nucleus hypoglossus with an infrared video-camera. All cell recordings were obtained, at ambient temperature, under whole-cell patch-clamp conditions by using either an L/M PCA patch-clamp amplifier (List Medical, Darmstadt, Germany, voltage-clamp experiments) or an Axoclamp 2B (Axon Instruments, Foster City, CA, USA, current-clamp experiments). For voltage-clamp experiments, patch electrodes had 3–5 MΩ resistance, whereas those pulled for current-clamp experiments had 8–12 MΩ resistance. Cells were clamped at values between −60 and −70 mV holding potential (V_h), so that V_h was as close as possible to resting potential. Cells were chosen for analysis if series resistance (R_S) increases did not exceed 10% (no decrease was routinely observed). In current-clamp mode the bridge was routinely balanced throughout the experiment. Voltage and current pulse generation and data acquisition were performed with a PC using pClamp 9.0 software. All recorded currents were filtered at 3 kHz and sampled at 5–10 kHz.

For extracellular stimulation of afferent premotoneurons within the reticular formation, a single bipolar tungsten electrode was placed in the lateral reticular formation under direct visual inspection. The stimulation area that gave most consistent glutamatergic evoked currents was located in a dorsolateral position with respect to the edge of the hypoglossal nucleus (about 200 ± 100 μm from it; see also scheme in Fig. 3A) to activate premotoneurons of the dorsomedullary reticular column (DMRC; Cunningham & Sawchenko, 2000). Even modest shifts in the electrode position led to loss of evoked synaptic responses, suggesting that the stimulus was affecting a restricted population of local interneurons. Electrically evoked glutamatergic responses were elicited at 15-s intervals by delivering stimuli of intensity adjusted to obtain 25–50% failures for 10 consecutive stimuli (so-called 'minimal stimulation'). These responses were judged to be monosynaptic, as indicated by their high failure rate and small latency jitter (Doyle & Andresen, 2001). In other experiments, excitatory glutamatergic currents were elicited by applying a train of five pulses (2 Hz; 0.1 ms; 10–100 V intensity). This five-pulse protocol was repeated at ≥1min interval for ≥3 times. All responses (including failures) were stored as individual files and averaged with pClamp software over different trials after discarding failed events.

Solutions and drugs

For slice preparation and subsequent incubation, the solution was (in mM): NaCl, 130; KCl, 3; $NaHCO_3$, 25; Na_2HPO_4, 1.5; $CaCl_2$, 1; $MgCl_2$, 5; glucose, 15 (310–320 mOsm). For electrophysiological recordings, the extracellular control solution containing (in mM): NaCl, 130; KCl, 3; $NaHCO_3$, 25; Na_2HPO_4, 1.5; $CaCl_2$, 1.5; $MgCl_2$, 1; glucose, 15 (pH 7.4, 310–320 mOsm) was continuously oxygenated. In all experiments, bicuculline (10 μM) and strychnine (0.4 μM) were used as pharmacological tools to block GABAergic and glycinergic transmission (see Donato & Nistri, 2000; Marchetti *et al.*, 2002). The patch pipette solution was (in mM): KCl, 130; NaCl, 5; $MgCl_2$, 2; $CaCl_2$, 0.1; HEPES, 10; EGTA, 5; ATP-Mg, 2; GTP-Na, 1 (pH 7.2 with KOH, 280–300 mOsm). Drugs were applied in two different ways: either bath-applied via the extracellular solution superfused at 2–5 mL/min (for a minimum of 5–10 min to reach apparent equilibrium conditions) or applied by means of pressure pulses. For the latter method, a thin-walled glass micropipette was pulled by a two-stage puller (3P-A, List Medical, Germany) to obtain a DC resistance of 6–10 MΩ. The pipette, visually positioned about 50 μm from the HM soma of superficial motoneurons, was filled with the drug solution (diluted to the final concentration in the external recording solution), and connected to a Pneumatic Picopump (WPI, Sarasota, FL, USA) for delivering brief pulses (30 ms) of 6–8 p.s.i. pressure. Whenever the effects of an mGluR antagonist were examined, the blocker was applied at least 10 min prior to the agonist application and maintained throughout the agonist superfusion period.

The following mGluR agonist and antagonists were purchased from Tocris (Bristol, UK); data concerning their pharmacological selectivity on rat motoneurons were taken from Schoepp *et al.* (1999), Marchetti *et al.* (2003) and Taccola *et al.* (2004): 7-(hydroxyimino)cycloprop-a[b]chromen-1a-carboxylate ethyl ester (CPCCOEt; selective antagonist for mGlu1Rs), (RS)-3,5-dihydroxyphenylglycine (DHPG; selective agonist for group I receptors and equipotent on mGlu1 and mGlu5 subtypes), 2-methyl-6-(phenylethynyl)pyridine hydrochloride (MPEP; selective antagonist for mGlu5Rs; used at 40 μM concentration to retain its subtype receptor selectivity; Gasparini *et al.*, 1999).

Other drugs were: AMPA, 6-cyano-7-nitroquinoxaline-2,3-dione (CNQX), D-amino-phosphonovaleriate (APV) also purchased from Tocris, while bicuculline methiodide and strychnine hydrochloride were from Sigma, Milan, Italy; tetrodotoxin (TTX) was purchased from Latoxan, France.

Data analysis

Cell input resistance (R_{in}) was calculated by measuring the current response to 10 mV hyperpolarizing pulses from V_h, or from the slope of the linear part of the current/voltage (I/V) relation obtained by applying a slowly rising voltage signal (ramp test). Single postsynaptic currents were detected using AxoGraph 4.6 (Axon Instruments) software, while Sigma Plot (Jandel Scientific, San Rafael, CA, USA), Clampfit (Axon Instruments) and Origin 6.1 (Microcal Software) software packages were used for linear regression analysis of experimental data. Results were quantified as means ± SE, with n = number of cells. Statistical significance was assessed with the Student's paired or unpaired t-test applied to raw data with parametric distribution; $P < 0.05$ was considered as the acceptable level of statistical significance.

Results

The database of the present study comprises 140 motoneurons with average resting potential of −67 ± 4 mV and 260 ± 30 MΩ input resistance.

Effects of the mGluR I agonist DHPG on HMs

Bath-application of DHPG (5 μM) evoked a slowly rising, persistent inward current (−58 ± 6 pA, $n = 27$; see example in Fig. 1A), accompanied by increased input resistance (on average 27 ± 3%; $P < 0.005$) and largely enhanced synaptic activity in terms of frequency and amplitude (Table 1), as exemplified by superimposed average traces in Fig. 1B. Such a synaptic activity (in the presence of 10 μM bicuculline and 0.4 μM strychnine) consisted of glutamatergic spontaneous postsynaptic currents (sPSCs). In approximately 33% of cells the mGluR I group agonist also elicited oscillatory activity (similar to that noted after application of the broad spectrum agonist *trans*-ACPD; Donato *et al.*, 2003), which will be the subject of a separate report. All the effects of DHPG were reversibly washed out within 5–10 min.

DHPG was ineffective at < 1 μM concentration, while at 50 μM it produced a robust inward current with very strong oscillatory and spontaneous activities, which could not be readily resolved. Unless otherwise indicated, DHPG was subsequently applied at the concentration of 5 μM in line with data reported in previous studies (see review by Schoepp *et al.*, 1999). To investigate if the effect of mGluR I activation could be network-mediated rather than due to a direct action on the HM membrane, some experiments were carried out in the presence of TTX (1 μM). In TTX solution the inward current produced by DHPG (5 μM) was smaller (−29 ± 5 pA) than in control,

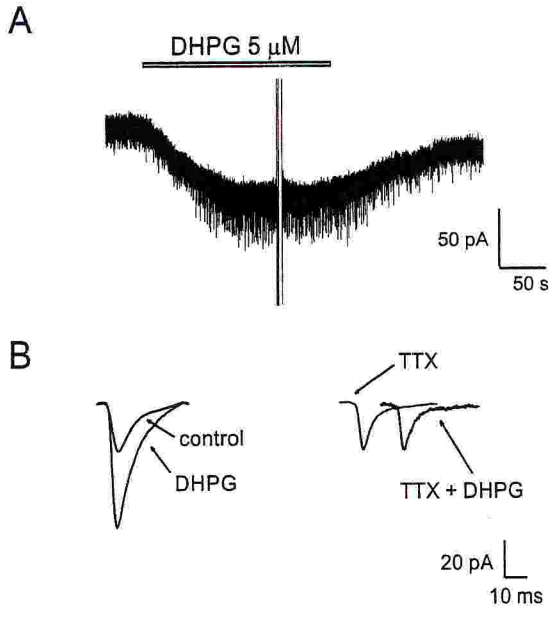

FIG. 1. Bath-application of (RS)-3,5-dihydroxyphenylglycine (DHPG) (5 μM) evokes an inward current and increases the amplitude and frequency of glutamatergic sPSCs. (A) Example of recording from HM, patch-clamped at −62 mV, in the presence of bicuculline and strychnine. Large deflection near the end of DHPG application is due to the ramp test for the voltage–current relation. (B) Left, average sPSCs recorded from the same cell in control and DHPG solution; right, average miniature glutamatergic currents before and after applying DHPG in the presence of 1 μM tetrodotoxin (TTX); $V_h = -62$ mV.

TABLE 1. Amplitude and frequency of spontaneous glutamatergic currents

	Amplitude (pA)	Frequency (Hz)	*n*
Control	−14 ± 1.0	0.20 ± 0.04	19
DHPG (5 μM)	−21 ± 2.0**	0.98 ± 0.20**	27
TTX (1 μM)	−12 ± 0.5	0.10 ± 0.01	16
TTX (1 μM) + DHPG (5 μM)	−12 ± 0.8	0.22 ± 0.04*	13
CPCCOEt (100 μM)	−12 ± 0.9	0.24 ± 0.04	7
CPCCOEt (100 μM) + DHPG (5 μM)	−12 ± 0.5	0.42 ± 0.06*	7
MPEP (40 μM)	−13 ± 1.0	0.18 ± 0.04	9
MPEP (40 μM) + DHPG (5 μM)	−16 ± 1.0	0.83 ± 0.20**	9

*$P < 0.05$; **$P < 0.005$ vs. control.

yet associated with a significant rise (15 ± 4%, $n = 13$; $P < 0.05$) in input resistance. There was, however, no detectable change in the mean amplitude of miniature postsynaptic currents (mPSCs; Fig. 1B, right panel). Despite lack of any amplitude change, DHPG still increased the frequency of mPSCs very strongly (215 ± 39%, $n = 13$; $P < 0.05$), as summarized in Table 1. The amplitude of the inward current evoked by DHPG in the presence of CNQX (10 μM) and APV (30 μM) was similar (−44 ± 9; $n = 6$) to that in the control solution, while there was no detectable spontaneous synaptic activity.

Is the postsynaptic action of DHPG voltage dependent?

The voltage dependence of the postsynaptic action by DHPG was investigated with a protocol as shown in Fig. 2. First, we applied slow voltage ramps (6 s) from −80 to +20 mV and recorded the total membrane current (see example in Fig. 2A) initially in control solution and then in the presence of DHPG. The membrane potential region comprised between −40 and −80 mV had a linear *I/V* relation reflecting chiefly the passive or 'leak' conductance of the cell (comprised between the two arrows in Fig. 2A). Systematic analysis of 19 neurons confirmed response linearity within this voltage range. Note that, although the plots remained linear after adding DHPG, the slope of the plot became shallower (open squares), as shown in Fig. 2B (average slopes were 4.23 and 3.43 pA/mV in control and DHPG solution, respectively; $n = 10$). Extrapolation of the two lines in Fig. 2B shows an estimated reversal potential of −98 mV ($n = 10$), which is very close to the calculated equilibrium potential for K^+ (−97 mV) on the basis of the Nernst equation.

We next investigated whether DHPG could modulate voltage-activated conductances. To explore this issue we first subtracted the leak current response from control as well as from DHPG *I/V* plots to reveal the voltage-sensitive components. The latter in the presence of DHPG was subtracted from control, as shown in the inset to Fig. 2B. It is apparent that DHPG could only generate a small outward current observed at potential positive to −25 mV.

Further confirmation that the main action by DHPG was a change in leak conductance and that this phenomenon was primarily responsible for the inward current generation was obtained by plotting the dynamics of membrane current and leak resistance changes during continuous superfusion with 5 μM DHPG (Fig. 2C).

Action of DHPG on electrically evoked glutamatergic transmission

To clarify the presynaptic action of DHPG within the brainstem slice network, it seemed advantageous to explore a restricted presynaptic circuitry with monosynaptic connections to motoneurons. For this

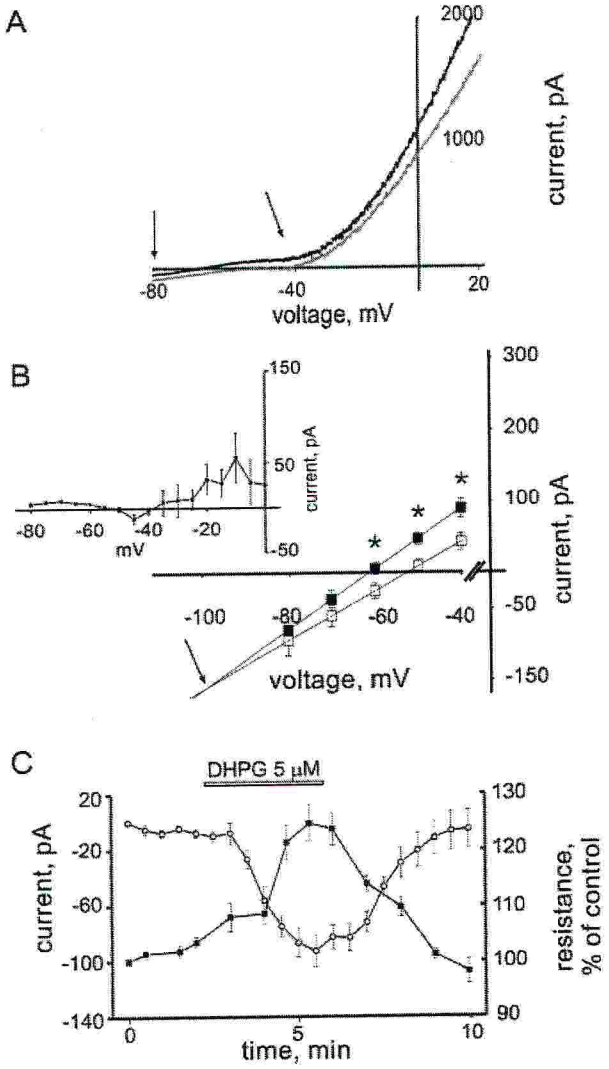

FIG. 2. Current–voltage relation in the presence of (RS)-3,5-dihydroxyphenylglycine (DHPG, 5 μM). (A) Total membrane current in response to voltage ramp (from −80 to 20 mV) in control (black, upper line) and DHPG (grey, lower line) solution. The linear part of the *I/V* relation between −40 and −80 mV (shown by arrows) reflects mainly passive membrane conductance (leak). (B) Average *I/V* curves display linearity (ohmic behaviour) with decrease in the slope during application of DHPG (open squares, $n = 19$). The data points significantly different between the two plots are indicated by asterisks; the intercept of each plot represents the extrapolated reversal potential (−98 mV, pointed by arrow); the inset shows *I/V* relation for net (leak subtracted) response evoked by DHPG. (C) Time course of membrane current (open circles) and leak resistance (filled squares) variations indicates their mirror-like change before, during and after DHPG superfusion ($n = 6$).

purpose we studied the effect of DHPG on excitatory postsynaptic currents (EPSCs) elicited by electrical stimuli applied to premotoneurons in the DMRC (see scheme in Fig. 3A), which represents one important monosynaptic input to HMs (Cunningham & Sawchenko, 2000). First, we investigated synaptic responses to 'minimal stimulation' that should have activated very few or perhaps even just one cell. Figure 3B shows a representative example of such synaptic responses (after excluding failures) in control or in the presence of DHPG (5 μM). Note depression of peak amplitude (on average to 78 ± 5% of control; $n = 9$) without apparent change in latency. Neither the synaptic current rise time (2.85 ± 0.04 ms in control and 3.14 ± 0.08 ms in DHPG solution) nor its decay time (26.9 ± 3.0 ms and 22.9 ± 1.7 ms, respectively; $n = 9$) was significantly altered. There was, however, substantial increase in the number of failures, which grew from 24 ± 9% in control condition to 48 ± 7% ($n = 6$, $P < 0.05$) with 5 μM DHPG.

Some studies have demonstrated that mGluRs do not contribute to fast synaptic transmission because of their localization to membrane areas remote from the active zones of synaptic release (Baude *et al.*, 1993; Nusser *et al.*, 1994; Lujan *et al.*, 1996, 1997; Cartmell & Schoepp, 2000). However, with repeated stimulation the concentration of released glutamate might exceed its rapid clearance (by uptake processes) to reach presynaptic metabotropic glutamate receptors, thereby providing autoregulation of excitatory transmitter release (Scanziani *et al.*, 1997). To check the applicability of this phenomenon to HMs, we recorded EPSCs evoked by a train of stimuli (2 Hz). With this protocol in control solution, there was large, short-term facilitation of evoked responses, as demonstrated when the first and fifth events are compared (Fig. 3C; $n = 8$). In the presence of DHPG the first response was already depressed, indicating that the inhibition of synaptic transmission was not use-dependent. Nevertheless, synaptic facilitation (ratio between fifth and first response) developed in the same fashion in control (234 ± 9%; $n = 8$) or in DHPG (240 ± 12%; $n = 8$) solution.

Finally, it seemed interesting to see how dynamic changes in evoked transmission were paralleled by alterations in the frequency of sPSCs on the same HMs. For this purpose, we compared sPSCs recorded in the interval between the first two pulses with those recorded between the last two pulses. In control solution sPSC frequency did not significantly change between these two time frames (2.3 ± 0.5 Hz and 3.7 ± 0.6 Hz, respectively; $n = 17$; $P > 0.05$). Conversely, in DHPG solution the sPSC frequency went from 1.8 ± 0.5 Hz to 4.8 ± 0.6 Hz ($n = 9$; $P < 0.005$).

Subtype receptor selectivity of DHPG-induced response

We tested the sensitivity of DHPG-induced effects to the subtype 1 antagonist CPCCOEt and the subtype 5 antagonist MPEP. As summarized in Table 1, neither CPCCOEt (100 μM) nor MPEP (40 μM) *per se* affected the amplitude and frequency of glutamatergic SPSCs. When co-applied with DHPG, MPEP prevented the sPSC amplitude enhancement by DHPG (Table 1), partially blocked the DHPG inward current (−32 ± 4 pA vs. −58 ± 6 pA; $n = 9$; $P < 0.05$), but it did not prevent the increase in frequency of sPSCs (Table 1). CPCCOEt (100 μM) strongly antagonized the DHPG-induced inward current (−10 ± 4 pA; $n = 7$; $P < 0.05$), prevented the increase in sPSC amplitude and attenuated the rise in frequency of sPSCs (Table 1). When CPCCOEt and MPEP were co-applied, all effects by DHPG were fully blocked ($n = 4$; not shown).

We then tested if either antagonist was effective in blocking the depressant action by DHPG on EPSCs. Figure 3D shows that CPCCOEt (100 μM) antagonized the depressant effect by DHPG, while in the presence of MPEP (40 μM) DHPG could still significantly inhibit EPSCs. Neither antagonist *per se* had a significant effect on the EPSCs (95 ± 9% for CPCCOEt and 108 ± 8% for MPEP, $n = 7$).

Responses to focal application of AMPA are potentiated by DHPG

The multifarious effects of DHPG on sPSCs and EPSCs suggested that this dissimilarity was perhaps due to a variable combination of

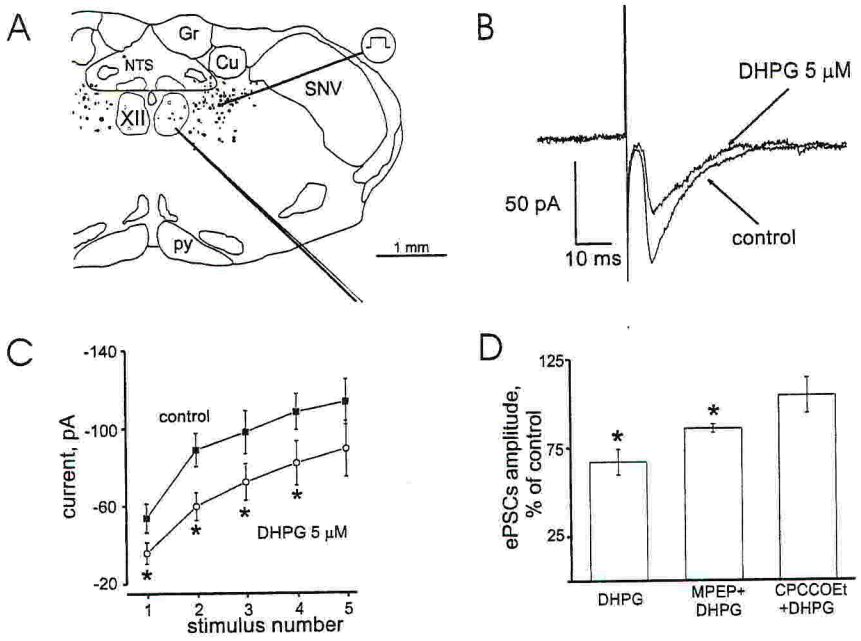

FIG. 3. (RS)-3,5-Dihydroxyphenylglycine (DHPG) inhibits electrically evoked glutamatergic transmission. (A) Schematic sketch of XII nucleus localization within brainstem slice with patch pipette approaching the right-hand side HM region. The stimulating electrode is placed laterally in the DMRC, depicted as a cluster of cells immediately ventral and lateral to the nucleus of the tract solitarius (NTS). Cu, cuneate nucleus; Gr, gracile nucleus; py, pyramidal tract; SNV, spinal nucleus of the trigeminal nucleus. The scheme is a modification from Cunningham & Sawchenko (2000) reprinted by permission of Wiley-Liss Inc©. (B) Average superimposed responses (after excluding failures) of single HM to minimal stimulation in control or DHPG solution. DHPG depresses excitatory postsynaptic currents (EPSC) amplitude without changing the latency. (C) EPSCs induced by pulse train (2 Hz). Note similar short-term facilitation in control and DHPG solution. The first response to the train in DHPG solution is already depressed ($n = 8$, $^*P < 0.05$ vs. control). (D) DHPG-induced inhibition of EPSCs is antagonized by the subtype 1 selective antagonist 7-(hydroxyimino)cyclopropa[b]chromen-1a-carboxylate ethyl ester (CPCCOEt, 100 μM; $n = 7$, $P < 0,05$). 2-Methyl-6-(phenylethynyl)pyridine hydrochloride (MPEP, 40 μM) does not prevent the DHPG-induced inhibition of EPSCs ($n = 7$).

presynaptic depression and postsynaptic potentiation. As a first approach it seemed feasible to test if postsynaptic glutamatergic currents mediated by the main class of ionotropic glutamate receptors, namely those sensitive to AMPA, were modulated by mGluR activation with DHPG. Previous studies have shown that on rat brainstem motoneurons mGluR activation by *trans*-ACPD potentiates AMPA receptor-mediated currents without affecting those sensitive to *N*-methyl-D-aspartate (Del Negro & Chandler, 1998). Brief (30 ms) pressure pulses of AMPA (100 μM) applied every 45 s from a puffer pipette to the soma of motoneurons induced monophasic currents of −430 ± 50 pA mean amplitude ($n = 5$). The example in Fig. 4A shows that 5 μM DHPG (while producing an inward current as shown by the baseline shift) increased the AMPA evoked current (on average by 21 ± 6%; $n = 5$). During the AMPA-mediated inward currents there were no sPSCs, as shown by consecutive records in Fig. 4C. The AMPA current potentiation was reversible on washout of DHPG (Fig. 4C) and completely prevented when experiments were performed in the presence of TTX (1 μM; Fig. 4B).

Current-clamp experiments

The complexity of effects originating from group I mGluR activation begs the question of the consequences of this phenomenon to the functional activity of motoneurons. To this end, a series of experiments was performed under current-clamp conditions. One example of this approach is provided in Fig. 5A in which a motoneuron fired action potentials in response to injection of small current pulses (0.12 nA, 5 s, resting potential = −66 mV). DHPG (5 μM) evoked cell depolarization that, on average, was 15 ± 4 mV ($n = 24$) and was opposed by repolarizing the cell to its resting potential level via intracellular current injection. The action of DHPG was accompanied by increased input resistance (by 40 ± 9%, $n = 6$, $P < 0.05$) and intense firing of action potentials followed by a larger afterhyperpolarization (AHP, the right panel of Fig. 5A; recovery was attained on washout, not shown) plus enhanced frequency of excitatory postsynaptic potentials (EPSPs; not shown). Figure 5B plots the peak amplitude of the spike AHP measured after the end of the current pulse vs. the number of spikes for each cell before (open squares) and after (filled squares) application of DHPG. It is apparent that the augmented firing was accompanied by a larger AHP at equivalent membrane potential. Figure 5C shows that high probability of firing was observed when EPSPs were generated by DMRC stimulation (0.1 Hz). In control solution an action potential appeared in 1 out of 10 EPSPs, while in the presence of DHPG each EPSP was accompanied by one or more spikes.

While these phenomena confirmed the enhanced excitability detected with intracellular depolarizing pulses (Fig. 5A), it seemed necessary to analyse in more detail the changes in EPSPs, especially because in voltage-clamp conditions DHPG actually depressed EPSCs.

Under current-clamp conditions, DHPG also depressed the amplitude of electrically evoked EPSPs in analogy with data under voltage-clamp conditions (see example in Fig. 6A). On average this reduction, albeit small (13 ± 4%), was significant ($P < 0.05$) in seven cells, while in four cells there was no significant change. The example of Fig. 6B shows that the cell generated an action potential in the

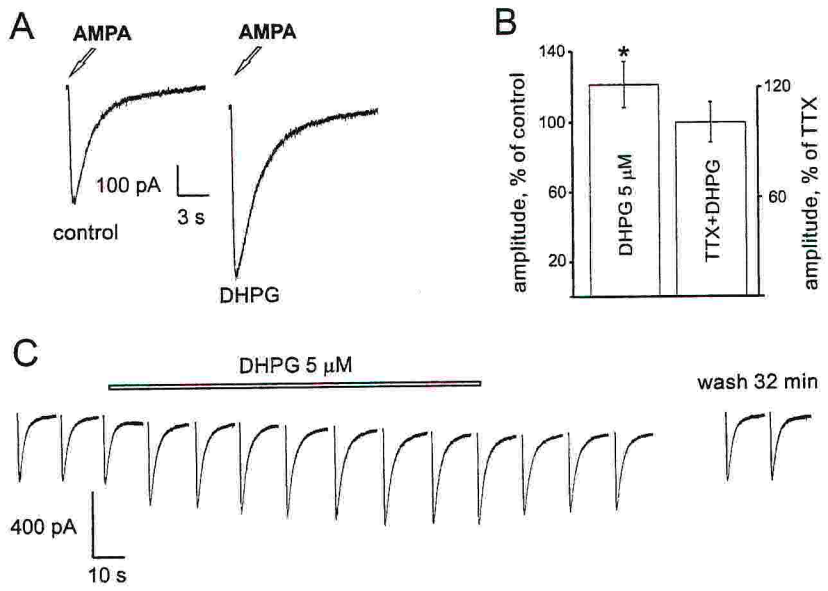

FIG. 4. (RS)-3,5-Dihydroxyphenylglycine (DHPG, 5 μM) enhances postsynaptic currents in response to local puffs (30 ms) of (RS)-α-amino-3-hydroxy-5-methyl-4-isoxazolepropionic acid (AMPA, 100 μM). (A) AMPA-evoked response in control or DHPG solution. Note the baseline shift due to inward current induced by DHPG. (B) Histograms of AMPA current amplitude in the presence of DHPG as percentage of those in control solution. $*P < 0.05$ ($n = 5$). Tetrodotoxin (TTX) blocks the enhancing effect of DHPG on AMPA responses ($n = 5$). (C) The increase in AMPA current amplitude and baseline shift due to DHPG are reversible after washout. Note the lack of spontaneous PSCs.

presence of DHPG. In fact, the threshold for action potential generation was -51 ± 2 mV in control and became -56 ± 2 mV in the presence of DHPG ($n = 11$; $P < 0.05$). Hence, the coupling between EPSP and action potential was improved. In the presence of DHPG the spike latency (measured from the stimulus artefact to the peak of the spike) was smaller (see example in Fig. 6C). On average the fall in latency was $40 \pm 7\%$ ($n = 11$).

Discussion

The principal finding of the present study is that group I mGluR activation generated complex actions comprising direct increase in HM excitability associated with an inward current (caused by leak conductance block) plus facilitation of spontaneous glutamatergic transmission. Electrically evoked glutamatergic transmission was paradoxically attenuated, but it could still elicit motoneuron spikes more efficiently than in control conditions. These results may be interpreted with a unitary hypothesis based on similar mGluRs coupled to distinct cellular effectors.

Direct effect of mGluR I activation on HMs

DHPG generated an inward current (and membrane depolarization in current-clamp), which developed slowly (as expected in the case of mGluR activation), was partly attenuated by TTX and insensitive to blockers of ionotropic glutamate receptors. These data indicate that DHPG could directly act on motoneurons via subtype 1 mGluRs in view of the antagonism by CPCCOEt. This result is consistent with the action of DHPG on rat spinal motoneurons (Dong & Feldman, 1999; Marchetti *et al.*, 2003). In the present experiments, the action of DHPG was associated with a significant reduction in the leak current. The tight relation between the time course of the slow inward current generation and the increase in cell resistance confirms that the inward current recorded from HMs was apparently due to the conductance block. Thus, it is proposed that subtype 1 mGluR activity led to suppression of a background K^+ conductance as suggested by the value of the estimated reversal potential. There are at least two K^+ channels potentially targeted by the activation of group I mGluRs. One of them, namely TASK-1, is believed to be a major contributor to the leak conductance of HMs and can be modulated by various transmitters (Talley *et al.*, 2000). The other one is Kir2.4, also expressed by HMs, responsible for dampening excitability of such cells and blocked by protein kinase C (Topert *et al.*, 1998), which is activated by group I mGluRs (Conn & Pin, 1997; Cartmell & Schoepp, 2000).

At membrane potentials positive to −25 mV, DHPG additionally produced a small net outward current, a phenomenon similar to the rapid upregulation of a transient K^+ current by mGluR activation in lamprey interneurons (Cochilla & Alford, 1998).

Because in TTX solution DHPG did not change either the responses to brief pulses of AMPA or the amplitude of miniature glutamatergic currents, it seems likely that, on HMs, intracellular messengers activated by subtype 1 mGluRs could not modulate AMPA receptors (at least within the time frame of the present experiments), perhaps because mGluRs were remotely located from them.

Presynaptic and network actions of group I mGluRs

The very large enhancement in the frequency of sPSCs suggests that DHPG depolarized network neurons (in analogy with its action on HMs) and therefore augmented their release of glutamate. Furthermore, the strong (about 100%) increase in glutamate release in the presence of TTX indicates that presynaptic terminals contacting HMs bear mGluRs sensitive to DHPG. Because MPEP had modest antagonism of DHPG effects while CPCCOEt was a potent blocker, it appears that the subtype 1 mGluRs were the principal receptor class involved. This observation accords with studies of the distribution and

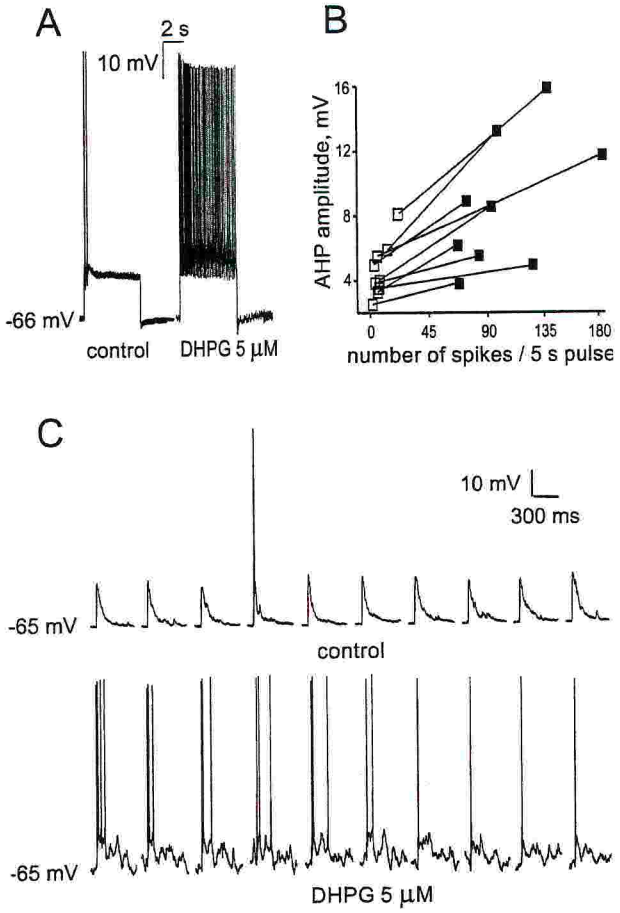

FIG. 5. (RS)-3,5-Dihydroxyphenylglycine (DHPG) augments firing probability of motoneurons under current-clamp conditions. (A) 5 μM DHPG solution strongly enhances firing of single HM in response to injection of 0.12 nA current pulse (5 s). (B) DHPG increases the number of spikes in parallel with increase in the afterhyperpolarization (AHP) amplitude following injection of intracellular current pulses (5 s). For each HM, the open square refers to control and the filled square to DHPG application. (C) The probability of spiking during single EPSPs is increased by DHPG. Top trace depicts data in control solution while the bottom one shows the same cell in the presence of DHPG. Note that in all records the depolarization generated by DHPG is nullified by injecting opposite steady DC current into the recorded cell. In all traces the cell membrane potential is shown on the left alongside the electrophysiological record.

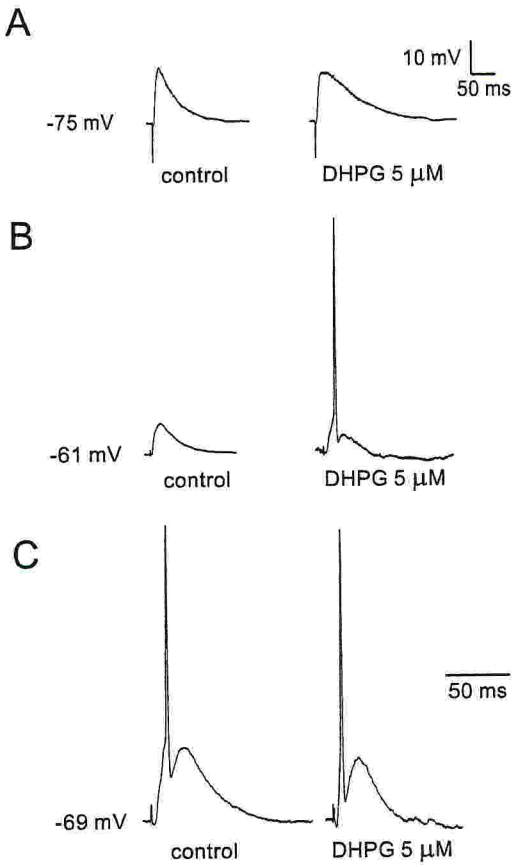

FIG. 6. (RS)-3,5-Dihydroxyphenylglycine (DHPG) depresses the amplitude of EPSPs in current-clamp conditions. Values on the left of each trace represent membrane potential. (A) Example of average EPSP from single HM with resting membrane potential of −75 mV (control, left), and in the presence of DHPG (right). Note smaller peak and larger area in DHPG solution. (B) HM with resting potential of −61 mV (different cell from A). EPSP in control solution is subthreshold for firing (left). In DHPG solution (right) the amplitude of EPSPs is smaller, but the cell generates an action potential. (C) EPSP with action potential in control (left) and in the presence of DHPG. Note that spike starts from lower threshold (right). In each example the DHPG effect is studied after repolarizing the membrane potential to the resting value. The voltage calibration is the same for all traces, while the time calibration in (A) applies to (B) also. Note larger time bar in (C).

prevalence of subtype 1 mGluRs in the rat hypoglossus (Hay *et al.*, 1999). Neither antagonist *per se* could significantly change glutamatergic transmission, hinting that ambient level glutamate was insufficient to activate group I mGluRs and modulate fast synaptic transmission. The question of the functional role of such receptors remains therefore unclear: it seems likely that they may play a role in excitoxicity or ischaemia (Cartmell & Schoepp, 2000) under conditions of massive glutamate release and impaired uptake (Nicholls & Attwell, 1990).

Effect of DHPG on electrically evoked transmission

Monosynaptic glutamatergic responses were elicited by electrical pulses applied to a discrete locus in the reticular formation termed DMRC. Previous studies have shown that DMRC premotoneurons directly project to HMs (Cunningham & Sawchenko, 2000) to provide a robust excitatory glutamatergic input (Bellingham & Berger, 1994). Such responses are fully blocked by ionotropic glutamate receptor antagonists and reverse at 0 mV (Donato *et al.*, 2003), confirming they are mediated by glutamate channels permeable to cations. In contrast to data on spontaneous transmission, EPSCs were reversibly depressed by DHPG without change in their kinetics. This inhibition of synaptic transmission was, however, limited (about 22%) and did not preclude the strong facilitation of postsynaptic responses during repeated stimulation of glutamatergic inputs. Because Cl^--mediated inhibition was routinely blocked by bicuculline and strychnine (Donato & Nistri, 2000; Marchetti *et al.*, 2002), it is unlikely that any mGluR-dependent facilitation of inhibitory transmission (Donato & Nistri, 2000) could be the reason for the depression of evoked glutamatergic currents. Similar data have been reported by Cirone *et al.* (2002) working on rat collicular neurons in which DHPG depressed evoked glutamatergic

inputs by about 30% even when GABAergic transmission was blocked. Likewise, presynaptic group I mGluRs are believed to be responsible for blocking evoked glutamatergic transmission in rat mesencephalic neurons (Bonci *et al.*, 1997).

The discrepancy between spontaneous and evoked transmission data is reminiscent of the observations at the glutamatergic synapses between parallel fibres and Purkinje cells in the rat cerebellum (Levenes *et al.*, 2001). In such a case subtype 1 mGluRs are thought to be exclusively located postsynaptically where they generate an increase in intracellular Ca^{2+} to promote postsynaptic glutamate release, which then acts presynaptically via AMPA receptors to enhance spontaneous release and then to depress electrically evoked release. Although immunoelectron microscopy data on the pre- and postsynaptic localization of group I mGluRs in the hypoglossus nucleus are lacking, it seems that such an explanation is not readily applicable to HMs. First, HMs were dialysed with the Ca^{2+} chelator EGTA, which should have minimized any postsynaptic release of glutamate; and second, puffer application of AMPA, which should mimic the action of retrogradely released glutamate, failed to enhance spontaneous glutamate release. Third, in the presence of DHPG, depression was probably not caused by transmitter vesicular depletion as suggested for cerebellar neurons (Levenes *et al.*, 2001) because we observed concurrent potentiation of spontaneous release. It is noteworthy that enhancement of spontaneous transmission with concomitant block of electrically evoked one by mGluR activation has also been found for GABAergic synapses in slices of the rat ventral tegmental area (Zheng & Johnson, 2003), in which there is no retrograde release of glutamate. Finally, the DHPG-induced depression of evoked glutamatergic currents in substantia nigra neurons is clearly due to activation of presynaptically located subtype 1 mGluRs, as demonstrated with electrophysiological and electron microscopy methods (Wittmann *et al.*, 2001).

Group I antagonists *per se* failed to change EPSCs, indicating that there was insufficient ambient glutamate to activate mGluRs and control evoked synaptic transmission. The depressant action by DHPG was readily antagonized by CPCCOEt and insensitive to MPEP, suggesting that subtype 1 mGluRs were mainly involved in mediating the action of DHPG like in the case of enhancement of spontaneous synaptic transmission.

Functional consequences of group I mGluR activation

Despite depression of EPSCs, it was clear that, under current-clamp, DHPG depolarized HMs and facilitated their spike firing induced by intracellular current pulses or by electrically evoked EPSPs. Even if the average amplitude of such EPSPs was significantly reduced by DHPG, EPSPs displayed slower decay presumably because of the concomitant increase in input resistance. This phenomenon was accompanied by a large increase in HM excitability with spike threshold and latency decrease. Hence, the efficiency of coupling between the EPSP and the spike was improved. Previous observations have shown that, on HMs, mGluR activation did not change the intrinsic properties of the spike (Donato *et al.*, 2003), as confirmed in the present report by the persistence of the spike AHP following DHPG application. The small outward current recorded in voltage-clamp experiments during application of DHPG could not evidently prevent the strong enhancement in HM excitability, presumably due to the higher input resistance. This effect is similar to the leak current block typically observed with neuropeptides like thyrotropin-releasing hormone (Bayliss *et al.*, 1992; Fisher & Nistri, 1993) and substance P (Ptak *et al.*, 2000; Yasuda *et al.*, 2001), and accompanied by a sustained rise in cell excitability. If this phenomenon was replicated at network level, it might have accounted for the strong augmentation of spontaneous glutamatergic transmission.

A scheme to interpret the action of DHPG on glutamatergic transmission

Figure 7 presents an idealized scheme to summarize the effects observed after application of DHPG. Subtype 1 receptors of group I mGluRs (shaded pentagons; Hay *et al.*, 1999) as much as AMPA receptors (AMPA-R) for synaptically released glutamate (Simon *et al.*, 1985; Paarmann *et al.*, 2000; Essin *et al.*, 2002) are present on HMs. Because mGluR activation did not affect the amplitude of AMPA receptor currents or miniature glutamatergic events, it seems likely that mGluRs are remotely located from the ionotropic glutamate receptors (Paarmann *et al.*, 2000) involved in fast synaptic transmission on HMs (Bellingham & Berger, 1994; Essin *et al.*, 2002; Donato *et al.*, 2003). The role of mGluRs on HMs would probably be to amplify incoming signals via leak conductance reduction. At network level group I mGluRs might facilitate firing as they do on HMs, thereby boosting spontaneous glutamate release. Their presence on presynaptic terminals would also promote miniature glutamate release. These effects may be produced by suppression of a K^+ leak conductance and/or enhancement of Ca^{2+} influx at presynaptic level (for reviews, see Anwyl, 1999; Fagni *et al.*, 2000).

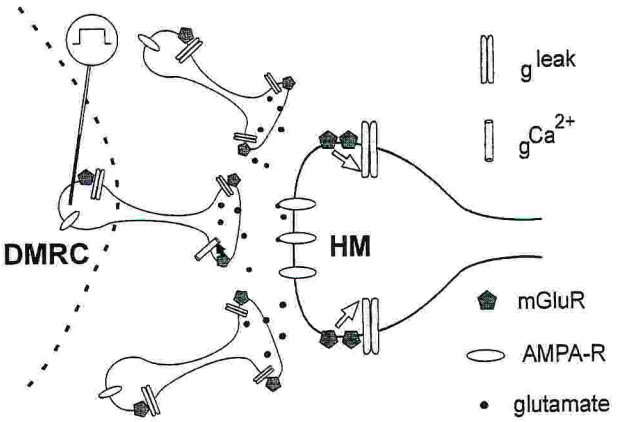

FIG. 7. Idealized diagram to account for the action of group I metabotropic glutamate receptors (mGluRs). The hypoglossal motoneuron (HM) possesses mGluRs (shaded pentagons) which, once activated, block a background current (gLeak; see large open arrows) and increase excitability without modulating (RS)-α-amino-3-hydroxy-5-methyl-4-isoxazolepropionic acid (AMPA) receptors (AMPA-R) directly. Such mGluRs are also present on various neurons establishing synaptic contacts with the HM and are not normally accessible to endogenous glutamate because selective mGluR antagonists do not change excitability or synaptic transmission. Network located mGluRs activated by DHPG can facilitate spontaneous glutamate release in a spike-dependent as well as independent fashion, presumably because the diffuse block of gLeak might stimulate transmitter release from multiple inputs. Dorsomedullary reticular column (DMRC) premotoneurons might bear mGluRs coupled to gLeak inhibition, but the main coupling of their mGluRs is supposed to be to depression of presynaptic Ca^{2+} influx (see small filled arrow) with consequent reduction in electrically evoked transmitter release. The concomitant facilitation of spontaneous release and depression of evoked one is an important argument to imply the existence of separate glutamatergic inputs with differential coupling of group I mGluRs. Despite decreased glutamate liberation by electrical pulses, the heightened excitability of the HM is transduced into more efficient coupling between the glutamatergic synaptic potential and the generation of the HM spike.

In order to explain the depression of electrically evoked release from DMRC cells, it is proposed that, on such neurons, some mGluRs are coupled to a distinct effector system, which can cause partial inhibition of presynaptic Ca^{2+} currents responsible for transmitter release (for a review, see Meir *et al.*, 1999). The input from DMRC to HMs is reputed to be quantitatively less extensive than inputs from other brainstem structures, so its downregulation by mGluRs may be overshadowed by the concomitant upregulation of the other inputs, thus yielding a global increase in spontaneous transmission. However, when DMRC cells are directly stimulated, the inhibition by mGluRs negatively coupled to glutamate release becomes apparent, though inadequate to cancel the spike facilitation caused by leak conductance block plus enhanced spontaneous glutamate release by other reticular neurons. Thus, activation of group I mGluRs may be seen as a complementary system to serotoninergic receptors to control HM excitability (Ladewig *et al.*, 2004). Of course, it is also possible that certain reticular interneurons possess group I mGluRs coupled to inhibition of Ca^{2+} influx and that, had we electrically stimulated these cells, we would have demonstrated depression by DHPG of their evoked transmitter release. This hypothesis is, however, difficult to be tested experimentally because the precise location of such reticular cells within the reticular formation is currently unknown. In any case, the presence of additional mGluRs associated with reduced Ca^{2+} influx would not alter the general characteristics of the scheme in Fig. 7.

It should be noted that the present scheme was obtained from an experimental model in which synaptic inhibition was pharmacologically blocked. Although activation of mGluRs facilitates GABA and glycine-mediated transmission (Donato & Nistri, 2000), in the functionally intact brainstem network the overall consequence of mGluR activation is enhanced HM excitability (Donato *et al.*, 2003), presumably because the increase in excitation outweighs the one in inhibition.

A further issue to be considered is the fact that the present scheme was obtained using neonatal rat slices and might not be wholly applicable to the mature brain. Because the density of group I mGluRs strongly increases throughout the rat brain postnatally (Shigemoto *et al.*, 1992; Catania *et al.*, 1994), it seems likely that the role of such receptors in upregulating HM excitability would be amplified, even though their molecular profile remains unchanged (Laslo *et al.*, 2001).

In summary, it seems likely that the process of mGluR activation can produce fine tuning of the output signals from HMs to tongue muscles and can therefore represent an interesting target to modify the oromotor reflexes subserving the neural control of swallowing (Cunningham & Sawchenko, 2000). This would be a desirable goal to help to control dysphagia in a variety of brain disorders like Parkinsons's disease (Fuh *et al.*, 1997), stroke (Ramsey *et al.*, 2003), amyotrophic lateral sclerosis (Ertekin *et al.*, 2000) and cervical spinal injury (Wolf & Meiners, 2003).

Acknowledgement

This work was supported by a FIRB grant from MIUR.

Abbreviations

AHP, afterhyperpolarization; AMPA, (RS)-α-amino-3-hydroxy-5-methyl-4-isoxazolepropionic acid; APV, D-amino-phosphonovaleriate; CNQX, 6-cyano-7-nitroquinoxaline-2,3-dione; CPCCOEt, 7-(hydroxyimino)cyclopropa[b]chromen-1a-carboxylate ethyl ester; DHPG, (RS)-3,5-dihydroxyphenylglycine; DMRC, dorsomedullary reticular column; EPSCs, excitatory postsynaptic currents; EPSPs, excitatory postsynaptic potentials; GABA, γ-aminobutyric acid; HM, hypoglossal motoneuron; mGluRs, metabotropic glutamatergic receptors; MPEP, 2-methyl-6-(phenylethynyl)pyridine hydrochloride; mPSCs, miniature postsynaptic currents; sPSCs, spontaneous postsynaptic currents; *trans*-ACPD, (±)-1-aminocyclopentane-*trans*-1,3-dicarboxylic acid; TTX, tetrodotoxin.

References

Anwyl, R. (1999) Metabotropic glutamate receptors: electrophysiological properties and role in plasticity. *Brain Res. Rev.*, **29**, 83–120.

Ballanyi, K., Onimaru, H. & Homma, I. (1999) Respiratory network function in the isolated brainstem-spinal cord of newborn rats. *Prog. Neurobiol.*, **59**, 583–634.

Baude, A., Nusser, Z., Roberts, J.D., Mulvihill, E., McIlhinney, R.A. & Somogyi, P. (1993) The metabotropic glutamate receptor (mGluR1 alpha) is concentrated at perisynaptic membrane of neuronal subpopulations as detected by immunogold reaction. *Neuron*, **11**, 771–787.

Bayliss, D.A., Viana, F. & Berger, A.J. (1992) Mechanisms underlying excitatory effects of thyrotropin-releasing hormone on rat hypoglossal motoneurons in vitro. *J. Neurophysiol.*, **68**, 1733–1745.

Bayliss, D.A., Viana, F., Talley, E.M. & Berger, A.J. (1997) Neuromodulation of hypoglossal motoneurons: cellular and developmental mechanisms. *Respir. Physiol.*, **110**, 139–150.

Bellingham, M.C. & Berger, A.J. (1994) Adenosine suppresses excitatory glutamatergic inputs to rat hypoglossal motoneurons in vitro. *Neurosci. Lett.*, **177**, 143–146.

Bocchiaro, C.M. & Feldman, J.L. (2004) Synaptic activity-independent persistent plasticity in endogenously active mammalian motoneurons. *Proc. Natl. Acad. Sci. USA*, **101**, 4292–4295.

Bonci, A., Grillner, P., Siniscalchi, A., Mercuri, N.B. & Bernardi, G. (1997) Glutamate metabotropic receptor agonists depress excitatory and inhibitory transmission on rat mesencephalic principal neurons. *Eur. J. Neurosci.*, **9**, 2359–2369.

Cartmell, J. & Schoepp, D.D. (2000) Regulation of neurotransmitter release by metabotropic glutamate receptors. *J. Neurochem.*, **75**, 889–907.

Catania, M.V., Landwehrmeyer, G.B., Testa, C.M., Standaert, D.G., Penney, J.B. Jr & Young, A.B. (1994) Metabotropic glutamate receptors are differentially regulated during development. *Neuroscience*, **61**, 481–495.

Cirone, J., Sharp, C., Jeffery, G. & Salt, T.E. (2002) Distribution of metabotropic glutamate receptors in the superior colliculus of the adult rat, ferret and cat. *Neuroscience*, **109**, 779–786.

Cochilla, A.J. & Alford, S. (1998) Metabotropic glutamate receptor-mediated control of neurotransmitter release. *Neuron*, **20**, 1007–1016.

Conn, P.J. & Pin, J.P. (1997) Pharmacology and functions of metabotropic glutamate receptors. *Annu. Rev. Pharmacol. Toxicol.*, **37**, 205–237.

Cunningham, E.T. Jr & Sawchenko, P.E. (2000) Dorsal medullary pathways subserving oromotor reflexes in the rat: implications for the central neural control of swallowing. *J. Comp. Neurol.*, **417**, 448–466.

Del Negro, C.A. & Chandler, S.H. (1998) Regulation of intrinsic and synaptic properties of neonatal rat trigeminal motoneurons by metabotropic glutamate receptors. *J. Neurosci.*, **18**, 9216–9226.

Donato, R., Lape, R. & Nistri, A. (2003) Pre and postsynaptic effects of metabotropic glutamate receptor activation on neonatal rat hypoglossal motoneurons. *Neurosci. Lett.*, **338**, 9–12.

Donato, R. & Nistri, A. (2000) Relative contribution by GABA or glycine to Cl^--mediated synaptic transmission on rat hypoglossal motoneurons in vitro. *J. Neurophysiol.*, **84**, 2715–2724.

Dong, X.W. & Feldman, J.L. (1999) Distinct subtypes of metabotropic glutamate receptors mediate differential actions on excitability of spinal respiratory motoneurons. *J. Neurosci.*, **19**, 5173–5184.

Doyle, M.W. & Andresen, M.C. (2001) Reliability of monosynaptic sensory transmission in brain stem neurons in vitro. *J. Neurophysiol.*, **85**, 2213–2223.

Ertekin, C., Aydogdu, I., Yuceyar, N., Kiylioglu, N., Tarlaci, S. & Uludag, B. (2000) Pathophysiological mechanisms of oropharyngeal dysphagia in amyotrophic lateral sclerosis. *Brain*, **123**, 125–140.

Essin, K., Nistri, A. & Magazanik, L. (2002) Evaluation of GluR2 subunit involvement in AMPA receptor function of neonatal rat hypoglossal motoneurons. *Eur. J. Neurosci.*, **15**, 1899–1906.

Fagni, L., Chavis, P., Ango, F. & Bockaert, J. (2000) Complex interactions between mGluRs, intracellular Ca^{2+} stores and ion channels in neurons. *Trends Neurosci.*, **23**, 80–88.

Fisher, N.D. & Nistri, A. (1993) A study of the barium-sensitive and -insensitive components of the action of thyrotropin-releasing hormone on lumbar motoneurons of the rat isolated spinal cord. *Eur. J. Neurosci.*, **5**, 1360–1369.

Fuh, J.L., Lee, R.C., Wang, S.J., Lin, C.H., Wang, P.N., Chiang, J.H. & Liu, H.C. (1997) Swallowing difficulty in Parkinson's disease. *Clin. Neurol. Neurosurg.*, **99**, 106–112.

Gasparini, F., Lingenhohl, K., Stoehr, N., Flor, P.J., Heinrich, M., Vranesic, I., Biollaz, M., Allgeier, H., Heckendorn, R., Urwyler, S., Varney, M.A., Johnson, E.C., Hess, S.D., Rao, S.P., Sacaan, A.I., Santori, E.M., Velicelebi, G. & Kuhn, R. (1999) 2-Methyl-6-(phenylethynyl)-pyridine (MPEP), a potent, selective and systemically active mGlu5 receptor antagonist. *Neuropharmacology*, **38**, 1493–1503.

Gereau, R.W. & Conn, P.J. (1995) Multiple presynaptic metabotropic glutamate receptors modulate excitatory and inhibitory synaptic transmission in hippocampal area CA1. *J. Neurosci.*, **15**, 6879–6889.

Hay, M., McKenzie, H., Lindsley, K., Dietz, N., Bradley, S.R., Conn, P.J. & Hasser, E.M. (1999) Heterogeneity of metabotropic glutamate receptors in autonomic cell groups of the medulla oblongata of the rat. *J. Comp. Neurol.*, **403**, 486–501.

Katayama, J., Akaike, N. & Nabekura, J. (2003) Characterization of pre- and post-synaptic metabotropic glutamate receptor-mediated inhibitory responses in substantia nigra dopamine neurons. *Neurosci. Res.*, **45**, 101–115.

Ladewig, T., Lalley, P.M. & Keller, B.U. (2004) Serotonergic modulation of intracellular calcium dynamics in neonatal hypoglossal motoneurons from mouse. *Brain Res.*, **1001**, 1–12.

Laslo, P., Lipski, J. & Funk, G.D. (2001) Differential expression of Group I metabotropic glutamate receptors in motoneurons at low and high risk for degeneration in ALS. *Neuroreport*, **12**, 1903–1908.

Levenes, C., Daniel, H. & Crepel, F. (2001) Retrograde modulation of transmitter release by postsynaptic subtype 1 metabotropic glutamate receptors in the rat cerebellum. *J. Physiol. (Lond.)*, **537**, 125–140.

Lujan, R., Nusser, Z., Roberts, J.D., Shigemoto, R. & Somogyi, P. (1996) Perisynaptic location of metabotropic glutamate receptors mGluR1 and mGluR5 on dendrites and dendritic spines in the rat hippocampus. *Eur. J. Neurosci.*, **8**, 1488–1500.

Lujan, R., Roberts, J.D., Shigemoto, R., Ohishi, H. & Somogyi, P. (1997) Differential plasma membrane distribution of metabotropic glutamate receptors mGluR1 alpha, mGluR2 and mGluR5, relative to neurotransmitter release sites. *J. Chem. Neuroanat.*, **13**, 219–241.

Mannaioni, G., Marino, M.J., Valenti, O., Traynelis, S.F. & Conn, P.J. (2001) Metabotropic glutamate receptors 1 and 5 differentially regulate CA1 pyramidal cell function. *J. Neurosci.*, **21**, 5925–5934.

Marchetti, C., Pagnotta, S., Donato, R. & Nistri, A. (2002) Inhibition of spinal or hypoglossal motoneurons of the newborn rat by glycine or GABA. *Eur. J. Neurosci.*, **15**, 975–983.

Marchetti, C., Taccola, G. & Nistri, A. (2003) Distinct subtypes of group I metabotropic glutamate receptors on rat spinal neurons mediate complex facilitatory and inhibitory effects. *Eur. J. Neurosci.*, **18**, 1873–1883.

Martin, L.J., Blackstone, C.D., Huganir, R.L. & Price, D.L. (1992) Cellular localization of a metabotropic glutamate receptor in rat brain. *Neuron*, **9**, 259–270.

Meir, A., Ginsburg, S., Butkevich, A., Kachalsky, S.G., Kaiserman, I., Ahdut, R., Demirgoren, S. & Rahamimoff, R. (1999) Ion channels in presynaptic nerve terminals and control of transmitter release. *Physiol. Rev.*, **79**, 1019–1088.

Nicholls, D. & Attwell, D. (1990) The release and uptake of excitatory amino acids. *Trends Pharmacol. Sci.*, **11**, 462–468.

Nusser, Z., Mulvihill, E., Streit, P. & Somogyi, P. (1994) Subsynaptic segregation of metabotropic and ionotropic glutamate receptors as revealed by immunogold localization. *Neuroscience*, **61**, 421–427.

Paarmann, I., Frermann, D., Keller, B.U. & Hollmann, M. (2000) Expression of 15 glutamate receptor subunits and various splice variants in tissue slices and single neurons of brainstem nuclei and potential functional implications. *J. Neurochem.*, **74**, 1335–1345.

Ptak, K., Konrad, M., Di Pasquale, E., Tell, F., Hilaire, G. & Monteau, R. (2000) Cellular and synaptic effect of substance P on neonatal phrenic motoneurons. *Eur. J. Neurosci.*, **12**, 126–138.

Ramsey, D.J., Smithard, D.G. & Kalra, L. (2003) Early assessments of dysphagia and aspiration risk in acute stroke patients. *Stroke*, **34**, 1252–1257.

Reid, M.E., Toms, N.J., Bedingfield, J.S. & Roberts, P.J. (1999) Group I mGlu receptors potentiate synaptosomal [3H]glutamate release independently of exogenously applied arachidonic acid. *Neuropharmacology*, **38**, 477–485.

Rekling, J.C., Funk, G.D., Bayliss, D.A., Dong, X.W. & Feldman, J.L. (2000) Synaptic control of motoneuronal excitability. *Physiol. Rev.*, **80**, 767–852.

Rodriguez-Moreno, A., Sistiaga, A., Lerma, J. & Sanchez-Prieto, J. (1998) Switch from facilitation to inhibition of excitatory synaptic transmission by group I mGluR desensitization. *Neuron*, **21**, 1477–1486.

Romano, C., Sesma, M.A., McDonald, C.T., O'Malley, K., Van den Pol, A.N. & Olney, J.W. (1995) Distribution of metabotropic glutamate receptor mGluR5 immunoreactivity in rat brain. *J. Comp. Neurol.*, **355**, 455–469.

Sawczuk, A. & Mosier, K.M. (2001) Neural control of tongue movement with respect to respiration and swallowing. *Crit. Rev. Oral Biol. Med.*, **12**, 18–37.

Sawczuk, A., Powers, R.K. & Binder, M.D. (1995) Spike frequency adaptation studied in hypoglossal motoneurons of the rat. *J. Neurophysiol.*, **73**, 1799–1810.

Scanziani, M., Salin, P.A., Vogt, K.E., Malenka, R.C. & Nicoll, R.A. (1997) Use-dependent increases in glutamate concentration activate presynaptic metabotropic glutamate receptors. *Nature*, **385**, 630–634.

Schoepp, D.D., Jane, D.E. & Monn, J.A. (1999) Pharmacological agents acting at subtypes of metabotropic glutamate receptors. *Neuropharmacology*, **38**, 1431–1476.

Shigemoto, R., Kinoshita, A., Wada, E., Nomura, S., Ohishi, H., Takada, M., Flor, P.J., Neki, A., Abe, T., Nakanishi, S. & Mizuno, N. (1997) Differential presynaptic localization of metabotropic glutamate receptor subtypes in the rat hippocampus. *J. Neurosci.*, **17**, 7503–7522.

Shigemoto, R., Nakanishi, S. & Mizuno, N. (1992) Distribution of the mRNA for a metabotropic glutamate receptor (mGluR1) in the central nervous system: an in situ hybridization study in adult and developing rat. *J. Comp. Neurol.*, **322**, 121–135.

Simon, J.R., DiMicco, S.K. & Aprison, M.H. (1985) Neurochemical studies of the nucleus of the solitary tract, dorsal motor nucleus of the vagus and the hypoglossal nucleus in rat: topographical distribution of glutamate uptake, GABA uptake and glutamic acid decarboxylase activity. *Brain Res. Bull.*, **14**, 49–53.

Taccola, G., Marchetti, C. & Nistri, A. (2004) Modulation of rhythmic patterns and cumulative depolarization by group I metabotropic glutamate receptors in the neonatal rat spinal cord in vitro. *Eur. J. Neurosci.*, **19**, 533–541.

Talley, E.M., Lei, Q., Sirois, J.E. & Bayliss, D.A. (2000) TASK-1, a two-pore domain K^+ channel, is modulated by multiple neurotransmitters in motoneurons. *Neuron*, **25**, 399–410.

Topert, C., Doring, F., Wischmeyer, E., Karschin, C., Brockhaus, J., Ballanyi, K., Derst, C. & Karschin, A. (1998) Kir2.4: a novel K+ inward rectifier channel associated with motoneurons of cranial nerve nuclei. *J. Neurosci.*, **18**, 4096–4105.

Viana, F., Bayliss, D.A. & Berger, A.J. (1994) Postnatal changes in rat hypoglossal motoneuron membrane properties. *Neuroscience*, **59**, 131–148.

Wittmann, M., Hubert, G.W., Smith, Y. & Conn, P.J. (2001) Activation of metabotropic glutamate receptor 1 inhibits glutamatergic transmission in the substantia nigra pars reticulata. *Neuroscience*, **105**, 881–889.

Wolf, C. & Meiners, T.H. (2003) Dysphagia in patients with acute cervical spinal cord injury. *Spinal Cord*, **41**, 347–353.

Yasuda, K., Robinson, D.M., Selvaratnam, S.R., Walsh, C.W., McMorland, A.J. & Funk, G.D. (2001) Modulation of hypoglossal motoneuron excitability by NK1 receptor activation in neonatal mice in vitro. *J. Physiol. (Lond.)*, **534**, 447–464.

Zheng, F. & Johnson, S.W. (2003) Dual modulation of gabaergic transmission by metabotropic glutamate receptors in rat ventral tegmental area. *Neuroscience*, **119**, 453–460.

J Physiol 563.1 (2005) pp 139–159

Metabotropic glutamate receptor activity induces a novel oscillatory pattern in neonatal rat hypoglossal motoneurones

Elina Sharifullina, Konstantin Ostroumov and Andrea Nistri

Neurobiology Sector and INFM Unit, International School for Advanced Studies (SISSA), Trieste, Italy

Tongue muscles innervated by the hypoglossal nerves play a crucial role to ensure airway patency and milk suckling in the neonate. Using a slice preparation of the neonatal rat brain, we investigated the electrophysiological characteristics of hypoglossal motoneurones in the attempt to identify certain properties potentially capable of synchronizing motor commands to the tongue. Bath-applied DHPG, a selective agonist of group I metabotropic glutamate receptors (mGluRs), generated persistent, regular electrical oscillations (4–8 Hz) recorded from patch-clamped motoneurones. Under voltage clamp, oscillations were biphasic events, comprising large outward slow currents alternated with fast, repeated inward currents. Electrical oscillations had amplitude and period insensitive to cell membrane potential, and required intact glutamatergic transmission via AMPA receptors. Oscillations were mediated by subtype 1 receptors of group I mGluRs (mGluR1s), and were routinely observed during pharmacological block of glycinergic and GABAergic inhibition, although they could also be recorded in standard saline. Simultaneous recordings from pairs of motoneurones within the same hypoglossal nucleus demonstrated that oscillations were due to their strong electrical coupling and were blocked by the gap junction blocker carbenoxolone. Pacing of slow oscillations apparently depended on the operation of K_{ATP} channels in view of the block by tolbutamide or glibenclamide. Under current clamp, oscillations generated more regular spike firing of motoneurones and facilitated glutamatergic excitatory inputs. These data suggest that neonatal motoneurones of the nucleus hypoglossus possess a formerly undisclosed ability to express synchronous electrical oscillations, unveiled by activation of mGluR1s.

(Resubmitted 18 November 2004; accepted after revision 15 December 2004; first published online 20 December 2004)
Corresponding author A Nistri: Neurobiology Sector and INFM Unit, International School for Advanced Studies (SISSA), Trieste, Italy. Email: nistri@sissa.it

In brain areas like the thalamus or the hippocampus, neuronal electrical oscillations represent a signalling process important to communicate and consolidate information within networks (Kirk & Mackay, 2003; Steriade & Timofeev, 2003). Since oscillations may differ in shape, frequency, regularity and phase distribution, it seems likely that distinct oscillatory activities reflect specific modalities of network signalling. Studying their origin and function therefore represents a useful approach to understand the computational properties of certain neuronal networks.

As far as motor systems are concerned, rhythmic activities are typically expressed by locomotor networks. The origin of motor rhythms is traditionally assigned to interneuronal circuits (Grillner *et al.* 1998), although further studies have reported that spinal motoneurones themselves can generate oscillations dependent on NMDA receptors (Schmidt *et al.* 1998) and propagated via gap junctions (Kiehn *et al.* 2000). Rhythmic activities are also expressed by brainstem neurones (Oyamada *et al.* 1999; Wu *et al.* 2001; Leznik *et al.* 2002; Rybak *et al.* 2003) and can be investigated using as a model hypoglossal motoneurones (HMs) which convey the sole motor output to tongue muscles. Thus, HMs express rhythmic motor commands in conjunction with functions like respiration, swallowing, mastication and vocalization (Jean, 2001). It is, however, uncertain whether HMs can generate intrinsic oscillations and if they do so, the functional impact of oscillations on motor output.

We have recently observed how selective activation of subtype 1 receptors belonging to group I metabotropic glutamate receptors (mGluR1s) facilitates glutamatergic excitatory inputs onto HMs of the neonatal rat brainstem (Sharifullina *et al.* 2004). Because this receptor

DOI: 10.1113/jphysiol.2004.079509

subtype is largely expressed in the developing hypoglossal nucleus (Hay *et al.* 1999), it seems likely that it could play an important role in HM-dependent activities like respiration and milk suckling that are vital for the neonate. Because mGluR1s can stimulate the emergence of oscillations in forebrain networks (Whittington *et al.* 1995; Beierlein *et al.* 2000; Cobb *et al.* 2000; Hughes *et al.* 2002*b*), we wondered whether mGluR1-mediated rhythmic oscillations could be a strategy employed by the hypoglossal nucleus network to optimize its motor output.

The present study reports how mGluR1 activation can trigger HMs to generate intrinsic, persistent oscillations propagated amongst these cells via electrical coupling and paced by rhythmic activation of K_{ATP} channels. These oscillations made spike firing coherent and regular, thus suggesting they could represent an important process to express rhythmic, synchronized motor commands to the tongue.

Methods

Slice preparation

All experiments were done in accordance with the regulations of the Italian Animal Welfare act (DL 27/1/92 n. 116) following the European Community directives no. 86/609 and 93/88 (Italian Ministry of Health authorization for the local animal care facility in Trieste: D. 69/98-B), and approved by the local authority veterinary service.

Under deep urethane anaesthesia (2 g (kg body wt)$^{-1}$), I.P. injection) neonatal (1- to 6-day-old; P1–6) Wistar rats were decapitated, their brainstems dissected out and fixed to an agar block (Donato & Nistri, 2000). Transverse slices 200 μm thick were cut in ice-cold Krebs solution. After 1 h recovery at 32°C, slices were kept for at least 1 h at room temperature before recording.

Whole-cell patch recording

HMs were visualized within nucleus hypoglossus with an infrared video-camera, patched and recorded under voltage and current clamp mode. A few cells were also injected with neurobiotin through patch pipette (0.2% in intracellular solution) and processed for histology (Lape & Nistri, 2001). All electrophysiological recordings (in voltage or current clamp mode) were carried out as described before in detail (Sharifullina *et al.* 2004). For voltage clamp experiments HMs were clamped within the range of −60 to −70 mV holding potential to minimize the leak current at rest. For current clamping, cells were initially kept at their resting level of membrane potential without injecting intracellular current which was applied for certain tests only.

Analysis of a sample of cells voltage clamped with a Cs^+-filled pipette gave an average holding potential of -62 ± 1 mV (input resistance $= 148 \pm 8$ MΩ; $n = 62$), while for a pool of cells recorded with intracellular K^+ solution the corresponding holding potential was -67 ± 2 mV (input resistance $= 163 \pm 13$ MΩ; $n = 26$; $P = 0.35$ between cell groups). For double-patch recordings two neighbour cells were simultaneously patch clamped (average distance ≤ 30 μm). To elicit synaptic glutamatergic responses we electrically stimulated premotoneurones in dorsomedullary reticular column (DMRC; Cunningham & Sawchenko, 2000) as detailed earlier (Sharifullina *et al.* 2004). Single stimuli were applied at 10 s interval (0.1 ms, 10–100 V intensity). All electrophysiological responses were filtered at 3 kHz, sampled at 5–10 kHz, acquired and analysed with pCLAMP 9.0 software (Axon Instruments).

Solutions and drugs

The external solution for cutting and maintaining slices contained (mM): NaCl, 130; KCl, 3; $NaHPO_4$, 1.5; CaCl, 1; $MgCl_2$, 5; glucose 15 (315–320 mosm), and was continuously oxygenated with O_2 95%–CO_2 5%. In the recording chamber slices were superfused with gassed solution containing (mM): NaCl, 130; KCl, 3; $NaHPO_4$, 1.5; $CaCl_2$, 1.5; $MgCl_2$, 1; glucose 15 (315–320 mosmol l^{-1}), pH 7.4. Unless otherwise stated, all experiments were done in the continuous presence of bicuculline (10 μM) and strychnine (0.4 μM) to block GABA and glycine-mediated transmission (Donato & Nistri, 2000; Marchetti *et al.* 2002) so that glutamatergic effects could be observed in isolation. Patch pipettes contained (mM): KCl, 130; NaCl, 5; $MgCl_2$, 2; $CaCl_2$ 0.1; Hepes, 10; EGTA, 5; ATP-Mg, 2; GTP-Na, 1 (pH 7.2 with KOH, 280–300 mosmol l^{-1}). In about 50% of recordings K^+ was replaced with equimolar Cs^+. The pipette solution used for voltage clamp experiments often also contained QX-314 (300 μM) to block voltage-activated Na^+ currents and slow inward rectifier (I_h) (Marchetti *et al.* 2003) as indicated in the Results. In a group of experiments 20 mM BAPTA was added to patch pipette to buffer intracellular Ca^{2+}.

Drugs were applied via the recording saline (2–3 ml min^{-1} superfusion rate) with the exception of AMPA, which was applied by pressure pulses (10–50 ms; 6 p.s.i. pressure; 100 μM solution; once every 45 s to minimize desensitization) via a closely positioned puffer pipette as described before (Sharifullina *et al.* 2004). General reagents were of analytical grade. The following drugs were purchased from Tocris (Bristol, UK): 7-(hydroxyimino)cyclopropa[b]chromen-1a-carboxylate ethyl ester (CPCCOEt; selective antagonist for mGlu1 receptors), (*RS*)-3,5-dihydroxyphenylglycine (DHPG; selective agonist for group I receptors and equipotent on mGlu1 and mGlu5 subtypes), 2-methyl-6-(phenylethynyl)pyridine hydrochloride (MPEP; selective

antagonist for mGlu5 receptors); (*RS*)-α-amino-3-hydroxy-5-methyl-4-isoxazolepropionic acid (AMPA), 6-cyano-7-nitroquinoxaline-2,3-dione (CNQX), D-amino-phosphonovalerate (APV), *N*-(2,6-dimethylphenylcarbamoylmethyl) triethylammonium bromide (QX-314), 4-ethylphenylamino-1,2-dimethyl-6-methylaminopyrimidinium chloride (ZD 7288), glibencl-amide, apamin, (*aS*)-*a*-amino-3-[(4-carboxyphenyl)methyl]-3,4-dihydro-5-iodo-2,4-dioxo-1(2H)-pyrimid-inepropanoic acid (UBP 301; selective antagonist for kainate receptors), (+/−)-4-(4-aminophenyl)-1,2-dihydro-1-methyl-2-propylcarbamoyl-6,7-methylenedio-xyphthalazine (SYM 2206; selective antagonist for AMPA receptors), (2*S*)-3-[[(1*S*)-1-(3,4-dichlorophenyl)ethyl]amino-2-hydroxypropyl](phenyl-methyl)phosphinic acid (CGP 55845; selective antagonist for $GABA_B$ receptors).

Bicuculline methiodide, 4-hydroxyquinoline-2-carboxylic acid (kynurenic acid), dihydro-β-erythroidine hydrobromide, atropine sulphate, 1,2-bis(2-aminophenoxy)ethane-*N*,*N*,*N*′,*N*′-tetraacetic acid tetrapotassium salt (BAPTA), tolbutamide, strychnine hydrochloride, and carbenoxolone (disodium salt) were purchased from Sigma; tetrodotoxin (TTX) was purchased from Latoxan, and caesium chloride from Calbiochem. Full details about receptor specificity and concentrations of DHPG and antagonists on mGluR1s are given by Schoepp *et al.* (1999).

Data analysis

Cell input resistance (R_{in}) was measured as mentioned previously (Sharifullina *et al.* 2004) while cell capacitance was monitored on-line using pCLAMP 9.0 software. To estimate the strength of electrical coupling between cell pairs, rectangular pulses (±0.3 nA, 1000 ms) were applied to one cell under current clamp and responses recorded simultaneously from both cells: the coupling coefficient was then estimated from the ratio between the response of the stimulated cell and the one of its coupled neighbour (Long *et al.* 2004).

Each oscillatory cycle comprised a cluster of fast inward currents followed by a slow outward component. To quantify the oscillatory period we measured the time between the first fast discharge in each cycle and the first discharge in the following cycle. For each cell at least 50 cycles were measured and averaged. Analysis of all current responses (synaptic as well as oscillatory ones) was carried out using a template search protocol (pCLAMP 9.0) applied to at least 5-min-long consecutive records. For each cell, templates of various events (synaptic, oscillatory components, etc.) were obtained from electrophysiological records and checked for adequacy when compared with actual responses. Coefficient of variation (standard deviation/mean; CV) was expressed as a percentage value. Data for response rise and decay times were obtained from the 10–90% time interval of the response peak. To fit slow oscillatory outward currents we used the sum of two exponents with pCLAMP 9.0 software. To quantify oscillation periods from current clamp traces when oscillations were associated with intermittent firing, we used their fast Fourier transform obtained with pCLAMP 9.0 software. Whenever current clamp oscillations were accompanied by spikes or devoid of any spike activity, we instead used the standard template constructing protocol reported above to obtain period values.

To check cross correlation between two simultaneously recorded cells, standard cross-correlation analysis was performed using pCLAMP 9.0 for 1 s epochs. Linear regression analysis was carried out with Origin 6.1 (OriginLab Corporation, Northampton, MA, USA). Data are given as mean ± S.E.M. and *n* is the number of cells, unless otherwise indicated. Statistical significance was assessed with Student's paired or unpaired *t* test, applied only to raw data with parametric distribution; $P < 0.05$ was considered as significant.

Results

To optimize detection of oscillations, the present investigation employed maximally effective concentrations (25–50 μM) of DHPG (Sharifullina *et al.* 2004). The database of the present study comprises 274 visually identified HMs (an example of a neurobiotin-filled cell is in Fig. 1*A*), 139 of which were recorded with intracellular Cs^+ solution and 135 with intracellular K^+.

Repertoire of oscillatory activity evoked by DHPG

Under voltage clamp conditions, DHPG (25–50 μM) induced a slowly developing inward current (see Fig. 1*B*), which peaked at 2.2 ± 0.1 min ($n = 49$) from the start of the application. On average, on cells recorded with intracellular Cs^+ the DHPG current amplitude was −101 ± 5 pA ($n = 44$) regardless of the presence of oscillations. On cells recorded with intracellular K^+ solution, the DHPG current amplitude differed depending on the presence (−125 ± 11 pA; $n = 28$) or the absence (−73 ± 9 pA; $n = 12$; $P = 0.008$) of oscillations.

As the inward current developed, a complex series of electrical events appeared as exemplified in Fig. 1*B*. First, the DHPG inward current was accompanied by a series of fast discharges made up by rapid, inward deflections of stereotypic nature (see their expanded time course in Fig. 1*C* where the record segment indicated by the open horizontal bar in Fig. 1*B* is shown on a 10 times faster scale). This response component was transient and, after 5.6 ± 0.9 s, was replaced by a distinctive, persistent oscillatory pattern, with repetitive events of considerably larger amplitude. The transition from fast discharges to

slow oscillations is shown in Fig. 1*C*. To better separate the characteristics of fast discharges and slow oscillations, such responses are compared in Fig. 1*D* and *E*, respectively, on a much faster time base. Each slow oscillation cycle was biphasic (Fig. 1*E*) with an outward current (with respect to the steady-state level reached in the presence of DHPG; see dashed line) and an inward component predominantly inclusive of fast oscillations.

Slow oscillations were present in 60% of cells recorded with intracellular Cs^+ and in 58% of those recorded with intracellular K^+, indicating they were not due to the choice of the main intracellular cation. Hence, because we found no difference in the incidence of cells generating oscillations in relation to the intracellular electrode solution, data were pooled together. Eighty-six per cent of cells which developed slow oscillations also generated early fast discharges such as those of Fig. 1*D*. The frequency of their electrical oscillations was in the 4–8 Hz range. Fast Fourier transform of the slow outward component of these oscillations revealed a single peak corresponding to 6.5 ± 0.6 Hz ($n = 12$).

Temporal characteristics of oscillatory activity

Figure 2*A* and *B* shows examples of further analysis of the inward and outward components of slow oscillations (same cell as in Fig. 1). A typical outward component (Fig. 2*A*) had a bi-exponential time course as indicated in the inset to the top of Fig. 2*A* in which the average ($n = 216$ events) as well as the bi-exponentially fitted outward currents are compared. Note that the initial fast deflection was followed by a slower phase gradually waning and turning inward, thus leading to the onset of the next event.

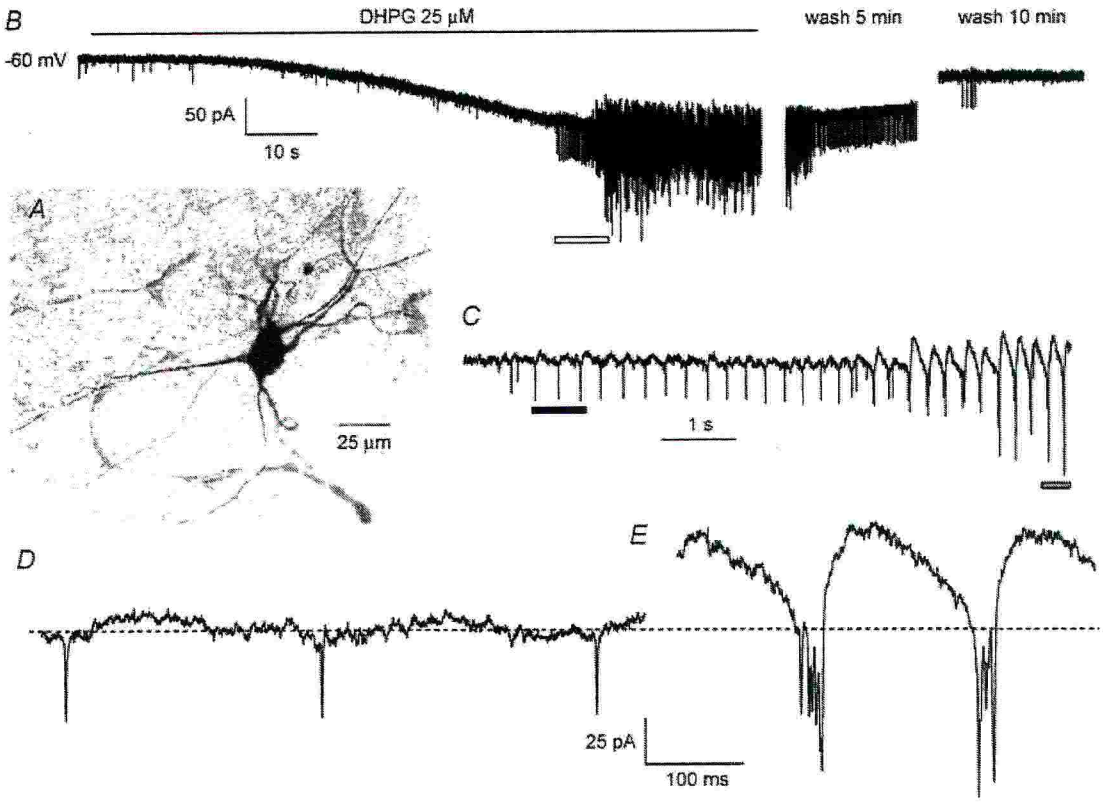

Figure 1. Oscillatory activity induced by DHPG on HMs
A, microphotograph of neurobiotin-filled neurone within the nucleus hypoglossus. Morphological features and size correspond to those of a HM. *B*, application of DHPG induces inward current and delayed appearance of oscillatory activity which gradually wanes after washout. *C*, faster time base records of trace indicated by open horizontal bar in *A* to show that the start of oscillatory activity comprises fast discharges and slow biphasic oscillations. Vertical calibration as in *B*. *D* and *E*, fast time base records of fast discharges and slow oscillations indicated in *C* by filled and shaded bars, respectively. Dashed line shows that slow oscillations include a large outward current (with superimposed synaptic currents) with respect to baseline attained between fast discharges. All data are from the same HM held at −60 mV.

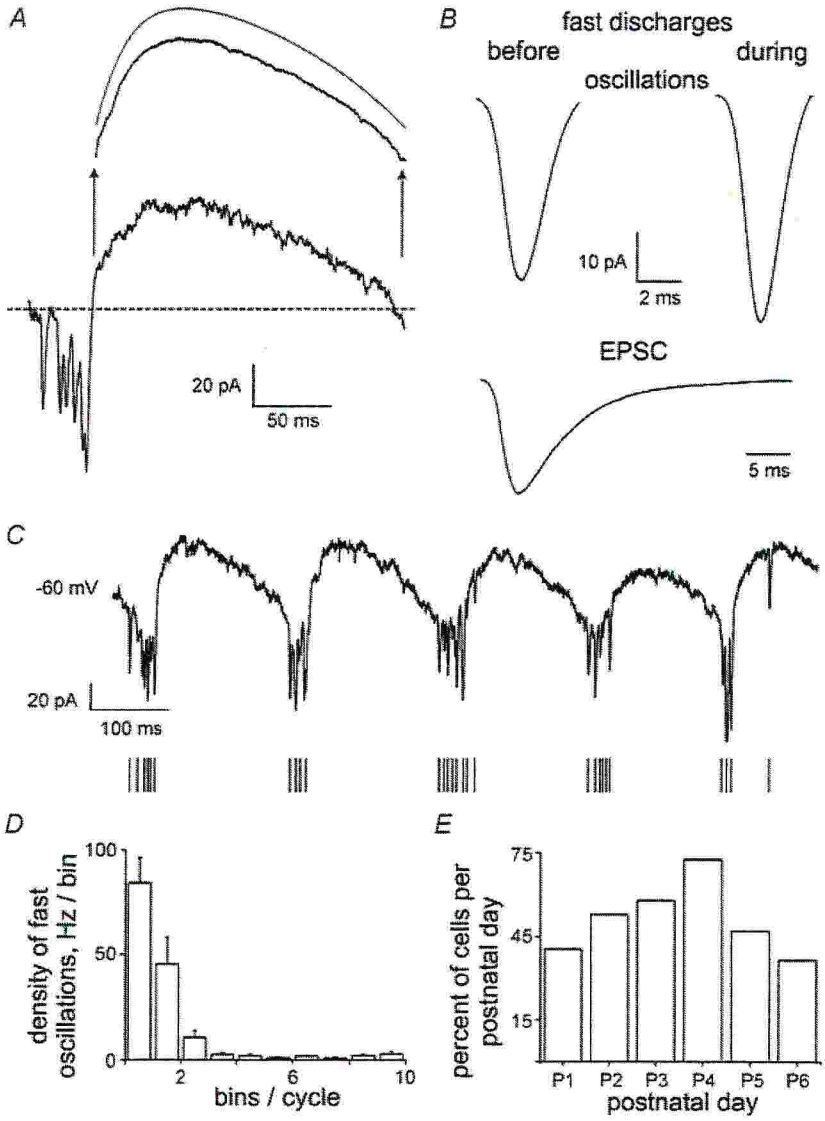

Figure 2. Characteristics of HM oscillations induced by DHPG
A, example of slow oscillation comprising repeated fast inward currents followed by a sustained outward current. The average outward component (216 events) is depicted above (see arrows) and can be well approximated by the sum of two exponents (top, grey). Note that synaptic events are superimposed on the outward currents Dashed line indicates baseline attained during application of 25 μM DHPG. *B*, average traces of fast inward discharges occurring before development of slow oscillations (left; see examples in Fig. 1*D*) or at the peak of each oscillations (see example in Fig. 1*E*). Their amplitude and time course are comparable; note, however, that these parameters are different from those of the average glutamatergic EPSC. All responses are from the same HM (further details in text); vertical bar applies to all three responses. *C*, tight relation between fast inward and slow outward currents during application of 25 μM DHPG. The occurrence of each fast inward current is indicated by a vertical bar below each cycle. *D*, plot of density of fast inward currents during the oscillatory cycle evoked by DHPG. For this purpose each cycle was divided into 10 bins (20.7 $\pm$ 2.7 ms bin time) and the number of fast inward current measured. Data are from 9 cells. Note clear clustering of fast inward currents at the start of each cycle. *E*, postnatal age-related occurrence of slow oscillations induced by DHPG. Maximum number of responsive HMs is at P4.

Table 1. Comparison of properties of oscillations and glutamatergic synaptic events of HMs in the presence of bicuculline and strychnine

	Amplitude (pA)	Rise time (ms)	Decay time (ms)	Periodicity	Period (CV, %)	*n*
Fast discharges	−47 ± 12	0.95 ± 0.08	2.06 ± 0.31	289 ± 78 ms	89 ± 39	9
Fast oscillations	−40 ± 4	0.98 ± 0.04	1.63 ± 0.11	15 ± 9 Hz	92 ± 50	13
EPSCs	−16 ± 2	1.38 ± 0.14†	5.62 ± 1.07*	2.6 ± 0.2 Hz	90 ± 18	8
Outward slow component	50 ± 3	18 ± 2	61 ± 8	154 ± 13 ms	24 ± 11	11

†$P = 0.01$ from fast discharges or fast oscillations; *$P = 0.0001$ from fast discharges or fast oscillations.

Inspection of the inward component (Fig. 2*A*) demonstrated multiple events of varying amplitude. Averaging 1255 such events from the same cell yielded a response of amplitude and time course very similar to those of the fast discharges ($n = 505$ events) preceding the slow oscillations. These events were therefore quite close in shape and amplitude (Table 1), suggesting that perhaps they had a common origin and could both be classified as fast discharges. Such discharges substantially differed from average spontaneous excitatory postsynaptic currents (EPSCs; Fig. 2*B*, $n = 1081$ events; Table 1).

We then examined, for slow oscillations, the temporal occurrence of fast oscillations within oscillatory cycles. This analysis is depicted in Fig. 2*C* and *D* in which, on the same HM, the number of fast oscillations was variable despite the regular periodicity of slow oscillations. It is, however, noteworthy that the number of fast oscillations in each event was always constrained between 2 and 10 for a very large sample of HMs ($n = 43$). Fast oscillations were usually clustered as shown by the histograms in Fig. 2*D* and typically occurred at 72 ± 8 ms ($n = 9$) before the peak of the slow outward component.

Conversely, when the temporal distribution of EPSCs was examined, it was apparent that the distribution of such events throughout the oscillation cycle was fitted by a simple Gaussian (not shown) with mean frequency of 2.6 ± 0.2 Hz ($n = 8$; Table 1), indicating that the probability of their occurrence was the same throughout the oscillation cycle.

Table 1 reports the basic properties of fast discharges and fast oscillations which were not significantly different in terms of amplitude, rise and decay times. These data thus strengthen the conclusions that these have a similar origin, and that they were clearly distinguishable from spontaneous EPSCs. The outward component of the slow oscillations was typically very regular in its periodicity (see low value of CV), unlike fast oscillations characterized by a very large CV value.

Predictors of slow oscillatory activity

Cells which generated slow oscillations had significantly larger cell capacitance (67 ± 4 pF, $n = 30$) than non-oscillatory cells (55 ± 3 pF, $n = 26$; $P < 0.009$).

Our previous observations about a significant input resistance increase evoked by DHPG (Sharifullina *et al.* 2004) were confirmed in the present study as long as HMs did not generate slow oscillations in the presence of DHPG (input resistance was augmented by 32 ± 9%; $n = 25$; $P < 0.05$). When slow oscillations appeared, cell input resistance returned close to control values (1 ± 6%; $n = 33$) despite the continuous presence of DHPG.

Once slow oscillations were generated, their properties (amplitude, periodicity) were not dependent on the actual concentration of DHPG (25–50 μM or even 5 μM that could evoke oscillations in a minority of cells only), and persisted as long as the mGluR agonist was applied (our longest test was about 1 h). As shown in Fig. 1*B*, once DHPG was washed out, slow oscillations gradually disappeared, were replaced by fast discharges and finally any repetitive activity was absent while the baseline control level was re-attained. However, fast discharges and slow oscillations could be reproduced by a further application of DHPG (not shown).

Figure 2*E* shows that the chance of detecting slow oscillations was dependent on the preparation postnatal age. The incidence was highest at P4, falling before and after this age.

Voltage sensitivity of oscillatory activities

The complex nature of oscillatory behaviour induced by DHPG raised questions concerning the identification of such activities, their origin and underlying mechanisms. First, we used changes in holding potential to find out if oscillations were generated by a network process or were intrinsic to the recorded HM. Once the steady inward current induced by DHPG was at plateau, we shifted the membrane potential to values ranging from −100 to +40 mV. One representative experiment is shown in Fig. 3*A* in which the period of the slow oscillations was essentially unchanged at three different levels of holding potential. Furthermore, slow oscillations could not be reversed even at very positive values of holding potential (+40 mV), although some slow, long outward responses were present (see example in Fig. 3*A*). Similar data were obtained by applying slow voltage ramps from −100 to +60 mV (not shown). Figure 3*B* shows that there was no

significant change in periodicity, amplitude of the slow oscillations and amplitude of the fast oscillations within the −100–0 mV range. Note that, in the absence of DHPG, analogous voltage shifts did not produce slow oscillations, although fast discharges could be observed between −40 and 20 mV in the presence of intracellular Cs^+ ($n = 25$; not shown).

We identified the slow, long outward currents intermittently appearing at +40 mV as reversed EPSCs as shown in Fig. 4 (see asterisks). In this cell that developed standard oscillations in the presence of 25 μM DHPG, we set the membrane potential at +40 mV and applied a combination of selective blockers for kainate receptors (10 μM UBP 301; More *et al.* 2003), NMDA receptors (50 μM APV) and $GABA_B$ receptors (10 μM CGP 55845; Towers *et al.* 2002) which did not block the generation of such slow, irregular outward currents (Fig. 4*A*). Full persistence of this activity was observed in seven cells. However, application of the selective AMPA receptor blocker SYM 2206 (10–30 μM; Behr *et al.* 2002) fully abolished the large outward currents while leaving the fast inward discharges. These data suggest the large, irregular outward currents were due to activation of AMPA-sensitive receptors by endogenously released glutamate (Fig. 4*B*; similar data were obtained from 4 cells).

The behaviour of the spontaneous reversed EPSCs was further explored in experiments like the one depicted in Fig. 5 which, for the sake of avoiding complications due to the concomitant occurrence of oscillations, shows responses from a HM not oscillating in DHPG solution (pipette filled with Cs^+ and QX-314). In this case, DHPG also produced a slowly developing inward current as exemplified in Fig. 5*A* associated with increased occurrence of spontaneous EPSCs. We then applied slow

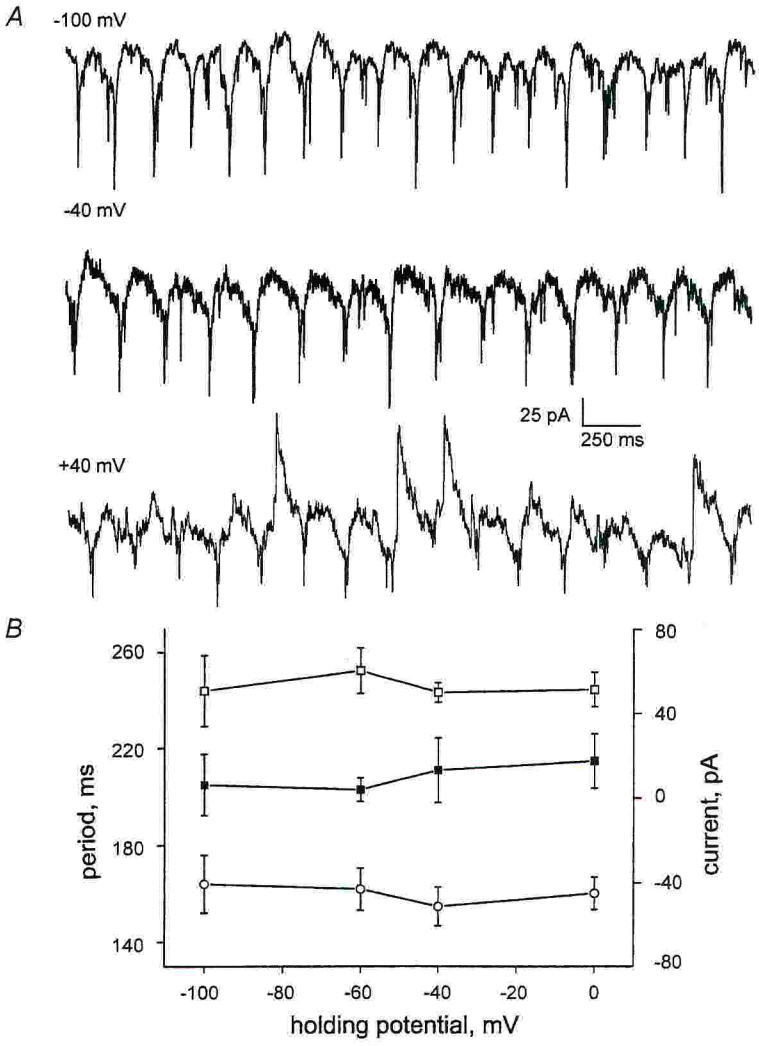

Figure 3. Voltage sensitivity of oscillations evoked by DHPG
A, sample records of oscillations recorded at three different levels of membrane potential (values indicated above each record) of the same HM. Patch pipette contained QX-314 (300 μM) to inhibit voltage-dependent Na^+ and I_h currents. Note relative insensitivity of oscillation period and amplitude to membrane potential. At +40 mV random outward events are reversed EPSCs. *B*, average plots of amplitude of oscillation outward currents (□; right vertical scale), oscillation period (■; left vertical scale), and amplitude of oscillation inward currents (○; right vertical scale). Values are from 9 cells recorded with QX-314-filled electrodes.

changes in the holding potential from −60 to +40 mV (see bottom trace in Fig. 5*A*) that fully reversed the irregular discharges which acquired a much slower decay phase (54 ± 7 *versus* 191 ± 13 ms time constant; see inset to Fig. 5*A*, comparing average currents at the two different holding potentials). Additional corroboration of the distinctive voltage sensitivity of AMPA receptor-mediated currents was obtained by examining the behaviour of currents elicited by puffer application of AMPA in a solution containing (in addition to strychnine and bicuculline) 10 μM UBP 301, 50 μM APV and 1 μM TTX. Figure 5*B* shows that both the peak amplitude as well as the area of the AMPA-evoked currents displayed outward rectification as their size grew at positive membrane potential.

Merely raising extracellular K^+ to 7.5–9 mM evoked a large inward current (−125 ± 15 pA; $n = 7$), enhanced EPSC frequency, yet failed to induce fast discharges and slow oscillations.

Pharmacology of oscillatory activity

A number of studies of brain slice neurones have shown that periodic oscillations can be generated (or modulated) by certain voltage-activated ionic channels, including those permeable to Na^+, or Ca^{2+}, or with Ca^{2+}-dependent K^+ permeability, as well as slow inward rectifiers (Traub *et al.* 2002, 2004).

Fast discharges and slow oscillations were routinely observed in DHPG solution when cells were recorded with an electrode containing the sodium current and I_h blocker QX-314 (Marchetti *et al.* 2003; $n = 56$ out of 92; 61%; see example in Fig. 3*A*). Likewise, the full range of oscillatory activity was detected in cells recorded with the Ca^{2+} buffer BAPTA (20 mM plus 5 mM EGTA; 11 out of 17 cells; 65%). Oscillatory activity induced by DHPG was not affected in the presence of extracellular Cs^+ (2–3 mM) and/or the I_h inhibitor ZD 7288 (20 μM; $n = 12$), Ba^{2+} (2 mM; $n = 5$) or apamin (100 nM; $n = 9$).

Omission of strychnine and bicuculline from the extracellular solution manifests large spontaneous postsynaptic inhibitory currents on HMs because the most conspicuous on-going activity is generated by network-dependent release of GABA and glycine (Donato & Nistri, 2000) rather than glutamate (Sharifullina *et al.* 2004). In the present experiments we could observe repeated oscillatory activity evoked by DHPG on nine HMs bathed in saline lacking bicuculline and strychnine. However, in three cells only, the oscillatory activity was not largely contaminated by intense inhibitory synaptic currents which are strongly facilitated by mGluR agonists (Donato & Nistri, 2000). On such cells, systematic analysis of their DHPG-evoked oscillatory activity showed it similar (Table 2) to the one recorded following pharmacological block of synaptic inhibition (see Table 1). Thus, inhibitory receptor antagonists were not a prerequisite to detect oscillations, rather they optimized the experimental conditions to analyse them.

In the presence of cholinergic antagonists (20 μM atropine, 50 μM dihydro-β-erythroidine; $n = 3$), or in the presence of APV (50 μM; $n = 5$), oscillatory activity was unaffected.

At standard holding potential, kynurenate (2 mM; $n = 14$), or CNQX (20 μM; $n = 6$) always blocked the DHPG (25 μM)-evoked slow oscillations as indicated in the example of Fig. 6*A* for a CNQX experiment. In the

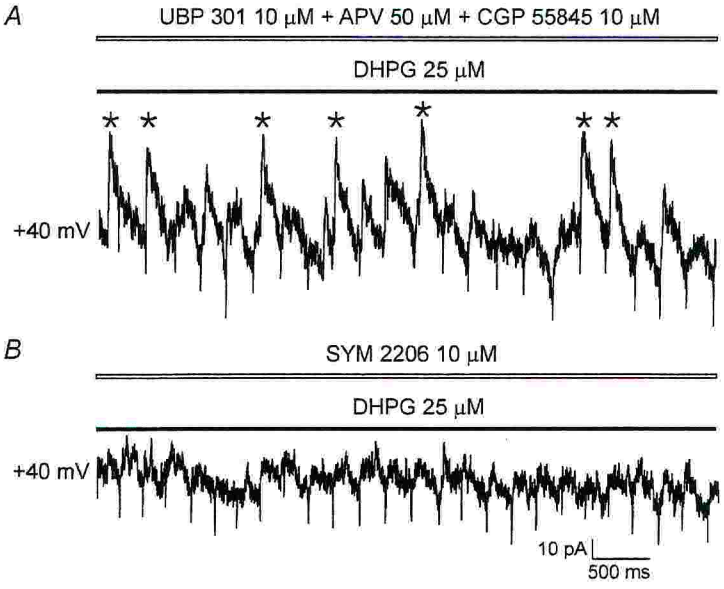

Figure 4. Slow, large outward currents during DHPG application to depolarized HMs are due to AMPA receptor activity
A, after initial application of DHPG (25 μM) that generated typical oscillations, the cell holding potential is shifted to +40 mV in the continuous presence of the kainate blocker UBP 301, the NMDA blocker APV and the $GABA_B$ antagonist CGP 55845. Note that large, slow currents (indicated by asterisks) persist. *B*, on the same cell shown in A, further application of the AMPA receptor antagonist SYM 2206 suppresses the slow, large outward currents.

continuous presence of CNQX or kynurenate plus DHPG, depolarizing the membrane potential by either holding it at a constant depolarized level (0 mV in the example of Fig. 6*A*) or applying a voltage ramp (not shown), could, however, evoke fast discharges. Slow oscillation recovery was attained after washout of CNQX (Fig. 6*A*). Analogous data were obtained with the selective AMPA receptor antagonist SYM 2206 (10 μM; $n = 4$; not shown). To confirm the involvement of ionotropic glutamate receptors in slow oscillations, puffer applications of AMPA were delivered in control conditions (Fig. 6*B*) and after applying a concentration of DHPG (5 μM) which was subthreshold to generate oscillations (Fig. 6*B*). In the presence of DHPG, the peak amplitude of the AMPA-induced inward current was increased ($21 \pm 6\%$; $n = 5$; Sharifullina *et al.* 2004), and was associated with strong oscillatory activity (4 out of 5 cells) reversible on washout. Figure 7 shows that the combined action by AMPA and DHPG in promoting oscillatory activity did not require activation of kainate receptors. In fact, in the continuous presence of the kainate antagonist UBP 301 (10 μM), DHPG generated an inward current (see downward shift in baseline) and enabled AMPA (applied by the puffer pipette) to elicit repeated oscillations after the peak inward current response (Fig. 7*A*). Similar data were obtained from four cells. It is noteworthy that 10 μM UBP 301 *per se* did not significantly affect the peak amplitude of AMPA-induced currents ($94 \pm 8\%$; $n = 4$) nor did it change the oscillatory pattern evoked by 25 μM DHPG ($n = 4$). On the other hand, in the presence of the selective AMPA receptor blocker SYM 2206 (10 μM), despite the inward current generation by DHPG, AMPA responses

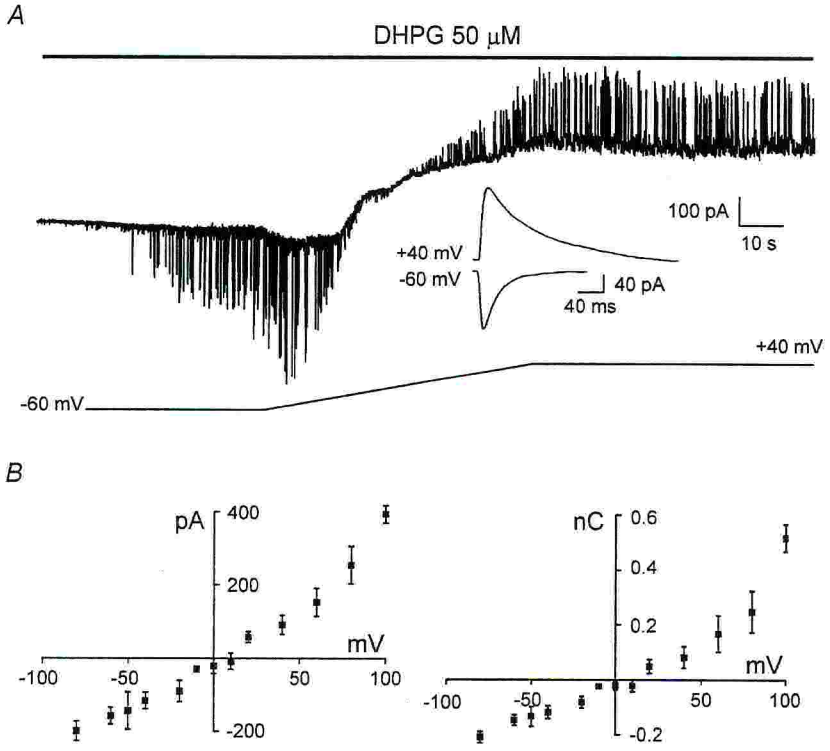

Figure 5. Rectification of AMPA receptor mediated responses of HMs
A, application of DHPG (50 μM) evokes a slowly developing inward current without associated oscillations on this cell, but it strongly facilitates spontaneous inward glutamatergic currents which reverse polarity once the cell is slowly depolarized to +40 mV (see scheme of the voltage change below the current trace). The inset shows that the average synaptic outward current (100 events) at +40 mV has different kinetics from the corresponding average current (112 events) recorded at −60 mV. Application of the slow voltage ramp protocol evokes a non-linear behaviour of whole membrane current probably due to activation of voltage-dependent conductances of the recorded HM. Bathing solution contained 10 μM bicuculline and 0.4 μM strychnine only. *B*, plots of mean peak amplitude and area of currents evoked by puffer application of AMPA to HMs in the presence of 1 μM TTX, 10 μM UBP 301 and 50 μM APV (plus bicuculline and strychnine) and recorded at different holding potentials. Note that the amplitude and, particularly, the area of the response grows non-linearly at positive potentials. Data are from 4 cells.

Table 2. Properties of DHPG induced oscillations of HMs recorded in the absence of bicuculline and strychnine

	Amplitude (pA)	Rise time (ms)	Decay time (ms)	Periodicity	Period (CV, %)	n
Fast discharges	−60 ± 12	1.12 ± 0.16	2.12 ± 0.45	250 ± 103 ms	97 ± 38	3
Fast oscillations	−33 ± 15	0.85 ± 0.14	1.71 ± 0.20	18 ± 8 Hz	72 ± 25	3
Outward slow component	40 ± 13	23 ± 5	76 ± 11	127 ± 15 ms	50 ± 2	3

were largely attenuated to 21 ± 4% of control ($n = 3$) and failed to be associated with oscillations (Fig. 7*B*; same cell as in Fig. 7*A*).

Application of TTX (1 μM) via the bathing solution always eliminated slow oscillations and prevented appearance of fast discharges upon membrane depolarization ($n = 10$). Likewise, adding the inorganic Ca^{2+} antagonist Mn^{2+} (2 mM; $n = 6$) rapidly blocked slow oscillations and fast discharges, an effect which was reversible within 15 min washout of this divalent cation. The action of DHPG was blocked by application of the selective mGluR1 antagonist CPCCOEt (100 μM; $n = 7$), and unaffected by the selective subtype 5 blocker MPEP (40 μM; $n = 6$) (data not shown).

Collectively, these data suggest that, at network level, combined activation of both mGluRs and AMPA receptors created the conditions to generate slow oscillations.

Electrical coupling amongst HMs is essential for oscillatory activity

Previous studies have identified electrical coupling between brainstem motoneurones under *in vivo* and *in vitro* conditions (Mazza *et al.* 1992; Rekling *et al.* 2000). Since electrical coupling can be responsible for oscillatory activity in other brain areas (Galarreta & Hestrin, 1999; Landisman *et al.* 2002; LeBeau *et al.* 2003), it was important to ascertain whether this process was influencing oscillations of HMs. For this purpose we performed simultaneous patch clamp recording from pairs of HMs (within the same nucleus hypoglossus). Fourteen pairs were thus recorded, of which six (43%) were electrically coupled with a coupling coefficient of 0.039 ± 0.008 for depolarizing current and 0.049 ± 0.012 for hyperpolarizing current, indicating lack of significant rectification ($P > 0.05$). An example of two electrically coupled HMs is shown for control conditions in Fig. 8*A* in which one cell was under voltage clamp (cell 1, top) and the other one under current clamp (cell 2, bottom). Application of a depolarizing (left) or hyperpolarizing (right) current pulse to cell 2 elicited in cell 1 an inward or an outward current, respectively (the latter followed by an off-response in either cell). Note that, during repeated firing of cell 2, cell 1 displayed fast inward discharges locked 1 : 1 with spikes as indicated by the cross-correlation plot. Thus, fast discharges could be identified as 'spikelets' (Perez Velazquez & Carlen, 2000; Hughes *et al.* 2002*a*; Long *et al.* 2004).

Figure 8*B* (same cell as in Fig. 8*A*) shows that, in the presence of DHPG (25–50 μM), cell 2 exhibited regular spiking activity associated (on a 1 : 1 basis) with slow oscillations resembling 'burstlets' (Long *et al.* 2004). The peak of each action potential of cell 2 coincided with the peak of spikelets in cell 1, while the interspike interval (ISI) was associated with burstlets. The strong association between spikes and spikelets as well as ISIs and burstlets is shown in the plot of Fig. 8*B*. Pooling data from all paired cells oscillating in the presence of DHPG gave a coupling coefficient of 0.028 ± 0.0005, that was not significantly different ($P = 0.33$) from control.

Confirmation of the dependence of oscillations on electronic coupling amongst HMs was obtained by applying the gap junction blocker carbenoxolone (100 μM; $n = 6$) as demonstrated in Fig. 8*C* (same pair of cells as in Fig. 8*A* and *B*). After 12 min application of this drug, full suppression of spiking in cell 2 and slow oscillations in cell 1 became apparent. Furthermore, in the continuous presence of DHPG and carbenoxolone, a large depolarizing pulse (0.6 nA) applied to cell 2 elicited spikes in the same cell, yet it failed to generate a current response in cell 1. Further evidence for electrotonic coupling between such cells was also demonstrated by applying a large hyperpolarizing current to cell 2 to suppress its spike activity during application of DHPG, although oscillations persisted even at −76 mV membrane potential (Fig. 8*D*). This manoeuvre was associated with a clear slowing down of slow oscillations in cell 1 and subsequent recovery after injection of current into cell 2 was terminated (Fig. 8*D*). In the presence of carbenoxolone the coupling coefficient amongst cells was severely reduced (0.0015 ± 0.00003; $n = 6$).

Figure 8*E* and *F* shows examples of other responses recorded from pairs of cells during application of DHPG. In Fig. 8*E* both cells were generated slow oscillations and regular spiking, although at different frequencies and thus uncorrelated as shown by the corresponding correlogram ($n = 2$ pairs). In Fig. 8*F*, one cell was not oscillating while the other one was spiking regularly ($n = 2$ pairs). In all these cases application of carbenoxolone disrupted bursting indicating that, although within these

pairs cells were not coupled, they were presumably coupled to other neurones to support their oscillatory activity.

Experiments with carbenoxolone were also carried out on single-recorded HMs ($n = 9$) in which full suppression of slow oscillations was observed despite the persistence of the inward current induced by DHPG (not shown).

K_{ATP} conductance as pacer of slow oscillations

Because various pharmacological blockers acting on disparate voltage-activated conductances failed to suppress the DHPG-induced slow oscillations, the question of the identity of the mechanisms responsible for the large outward currents inherent in each oscillatory cycle remained unanswered. Recent studies have suggested that some brainstem respiratory neurones possess a K_{ATP} conductance which controls their rhythmic bursting because their intracellular ATP is metabolically consumed and thus the block of the K^+ channels is transiently removed (Haller *et al.* 2001). The rapid cycle of ATP generation and consumption would then be a major contributor for setting the respiratory rhythm frequency (Haller *et al.* 2001).

We examined if an analogous mechanism might have been applicable to HMs oscillating in the presence of DHPG. To this end, we applied two known K_{ATP} blockers, namely glibenclamide (50 μM) and tolbutamide (500 μM). Figure 9*A* exemplifies one such experiment. Typical slow oscillations were evoked by bath-applied DHPG (25 μM; filled horizontal bar; see also left inset to Fig. 9*A* with expanded time scale). Subsequent application of tolbutamide (open horizontal bar) induced a further slow inward current and disruption of slow oscillatory activity, while less regular (CV = 36% *versus* 8% prior to tolbutamide) fast discharges survived (see middle inset to Fig. 9*A*). Washing out tolbutamide in the continuous presence of DHPG restored the baseline current to the level attained during the oscillatory activity and regenerated typical oscillations. Similar effects were observed on HMs bathed in glibenclamide ($n = 10$) or tolbutamide ($n = 7$) solution, although the blocking action by glibenclamide could not be reversed on washout, in accordance with its known irreversible block of K_{ATP} channels (Ashcroft, 1988). The steady inward current induced by glibenclamide or tolbutamide was essentially the same in amplitude so that data for the two treatments were pooled and gave an average magnitude of -57 ± 9 pA.

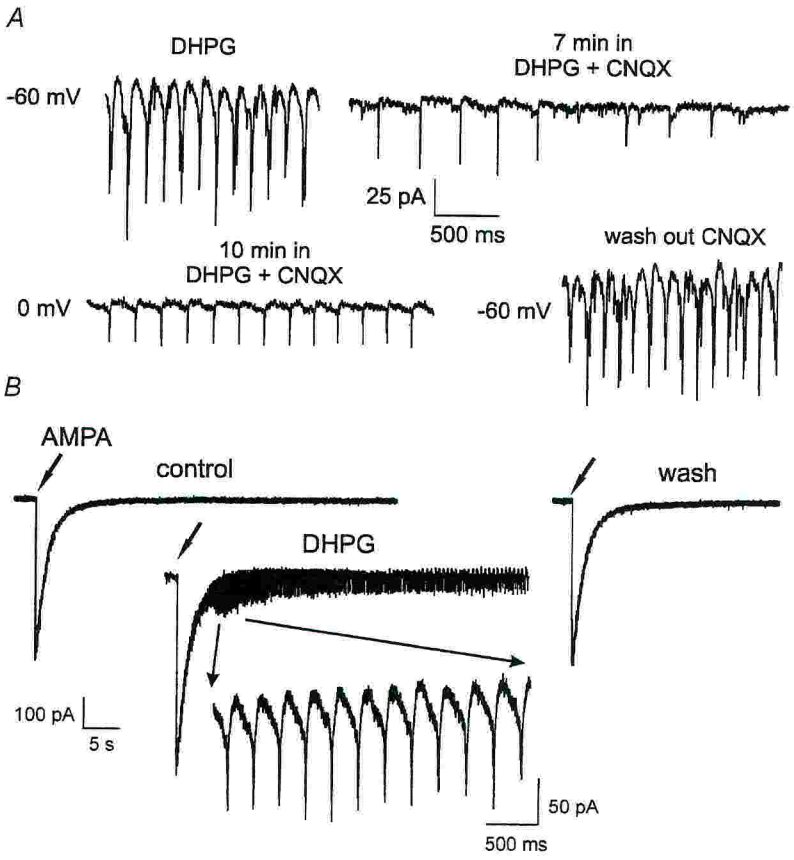

Figure 6. Block or activation of AMPA receptors depresses or facilitates oscillations evoked by DHPG
A, oscillations recorded at steady-state level in 25 μM DHPG solution (left, top) are disrupted by 20 μM CNQX, a blocker of AMPA/kainate receptors (right, top). This treatment leaves sporadic fast discharges only. Depolarization to 0 mV regenerates fast inward currents in the continuous presence of DHPG plus CNQX, although slow oscillations are absent (left, bottom). Washout of CNQX restores slow oscillations after 15 min at −60 mV (right, bottom). All records are from the same HM. *B*, puffer application of AMPA (see arrows) elicits inward current in control condition at −60 mV membrane potential (left). When the same application is repeated in the presence of a low concentration of DHPG (5 μM) subthreshold for oscillations, slow oscillations appear during the decay phase of the AMPA response (middle). This effect is reversible on washout of DHPG (right).

Figure 9*B* shows average *I–V* plots (achieved with voltage ramp protocols) obtained from cells ($n = 12$) during oscillations in the presence of DHPG (■) and their subsequent block by tolbutamide or glibenclamide (□). To aid comparison, the steady baseline current elicited by the sulphonylureas was subtracted from each curve. It is apparent that in the presence of sulphonylureas the average *I–V* relation was shifted downwards at all tested levels of membrane potential. Figure 9*C* (current scale larger than in Fig. 9*B*) shows that, in the range negative to the holding potential, the reduced slope of the plot in the presence of sulphonylureas led to an extrapolated crossover at −106 mV, namely close to the calculated K^+ reversal potential (−98 mV).

The effects of tolbutamide or glibenclamide on HMs were also investigated in current clamp experiments. Pre-incubation (20–60 min) in glibenclamide solution always prevented oscillatory activity by subsequent administration of DHPG, even if the DHPG-evoked depolarization had similar amplitude (12 ± 1 mV; $n = 5$ cells) as in control solution (14 ± 2 mV; $n = 35$; $P > 0.05$). On two HMs under current clamp, after full onset of slow oscillation in the presence of DHPG, subsequent application of tolbutamide (which induced an average 11 ± 2 mV depolarization) suppressed oscillations fully and reversibly. Collectively, these data therefore demonstrate that the ability of sulphonylureas to disrupt oscillations could be observed under voltage as well current clamp conditions.

HM firing characteristics during oscillations induced by DHPG

Experiments in current clamp conditions were performed to find out whether slow oscillations evoked by DHPG conferred certain properties to the cell's ability to fire action potentials. First, we compared cells which, in the presence of DHPG, did not oscillate with those that did (see example in Fig. 10*A*). At comparable level of membrane potential, a non-oscillating neurone (top

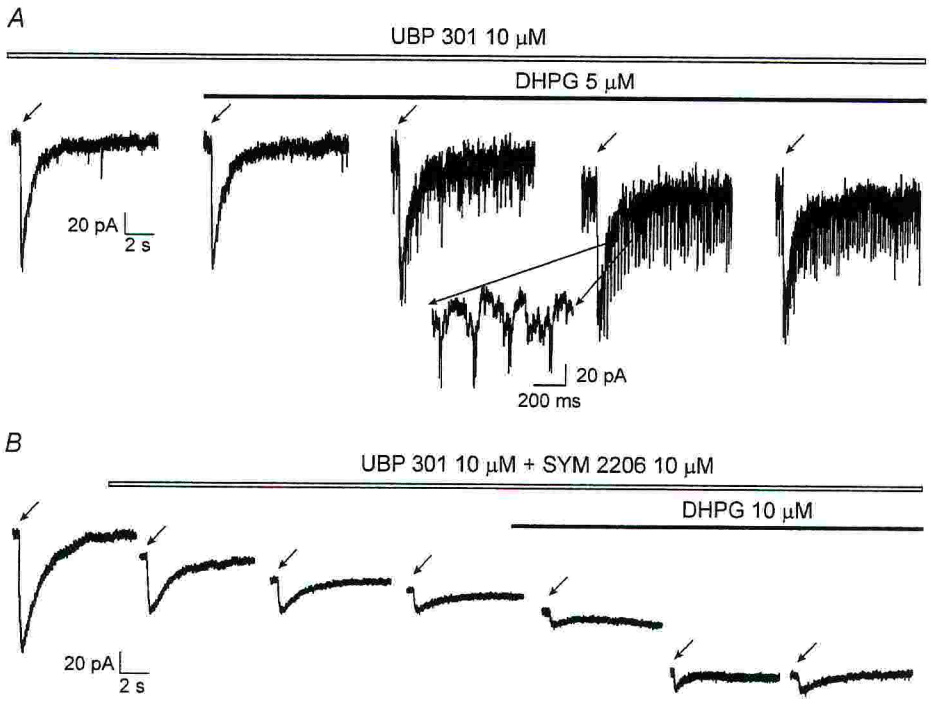

Figure 7. Synergic activation of oscillatory activity by AMPA and DHPG does not require kainate receptor activation

A, puffer application of AMPA to single HM generates inward currents which, when repeated in the presence of a concentration of DHPG (5 μM) subthreshold to induce oscillations, are followed by repeated oscillations (shown on faster time base in the inset) during the response decay despite the continuous presence of the kainate blocker UBP 301. *B*, on the same cell shown in *A*, after washout of DHPG and return to control conditions, further application of the AMPA receptor antagonist SYM 2206 largely blocks AMPA-evoked currents and prevents the generation of oscillations once DHPG is applied. Holding potential is −60 mV for all traces.

records in Fig. 10*A*) fired irregularly with individual spikes followed by a biphasic pause before the subsequent spike (see right inset for averaged spike from 256 events). Conversely, in an oscillating cell (bottom traces of Fig. 10*A*) spikes were always occurring at the peak of each oscillation, were very regular and followed by a longer pause (see inset on the right; average of 180 events).

On a sample of non-oscillating cells ($n = 9$) the CV for spike firing periodicity was $99 \pm 15\%$, indicating random spike occurrence. In comparison, on oscillating cells ($n = 7$) the CV for spike periodicity was $17 \pm 3\%$. Thus, oscillations determined very regular firing discharges.

An additional property was conferred by DHPG-evoked oscillations as exemplified in Fig. 10*B*. The random firing (CV = 54%) observed at −53 mV in standard saline solution (Fig. 10*B*, top left) was transformed into more regular high frequency firing (CV = 35%) at −40 mV (Fig. 10*B*, bottom left). Conversely, when a neurone was exposed to DHPG and generated oscillations and was kept at a membrane potential (−51 mV) comparable to control, spike generation was not present for each oscillation (Fig. 10*B*, top right), although when it did occur, it was always at the oscillation peak. Further membrane depolarization (−38 mV) increased the number of spikes per oscillation and evoked doublets (interspike interval = 46 ms). Further depolarization to −33 mV generated spike triplets at the peak of oscillations with unchanged frequency (not shown). Thus, cell spiking modality was altered by the DHPG-induced oscillations as spikes could occur only at the peak of oscillations. Furthermore, the average firing rate was constrained by oscillations that limited the incremental rise of firing

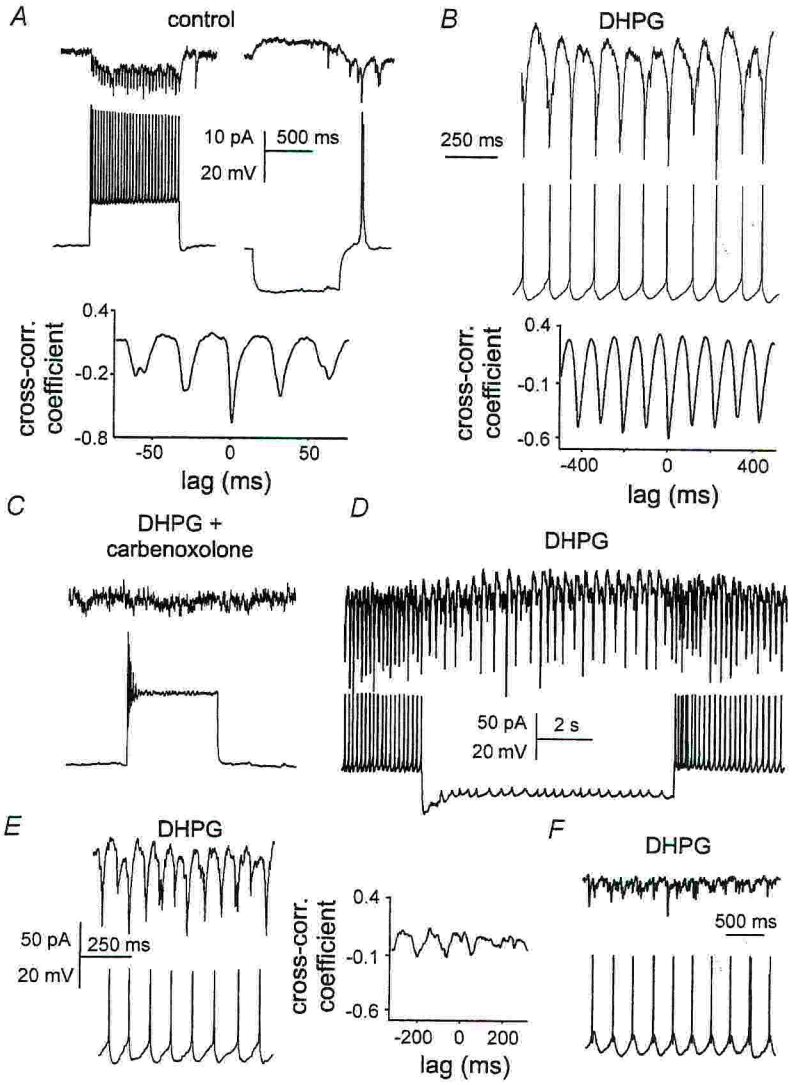

Figure 8. Simultaneous pair recording from HMs reveals their electrical coupling
A, cell 1 (top) under voltage clamp is electrically coupled to cell 2 under current clamp as demonstrated by currents responses elicited in cell 1 by depolarizing or hyperpolarizing changes in membrane potential of cell 2 (0.3 nA injected current of either polarity). As shown in the cross-correlogram (which also includes traces shown above it), responses in both cells were tightly associated (peak occurred near 0 ms) with a small lag between cell 1 and cell 2. *B*, simultaneous slow oscillations present in cell 1 and cell 2 during 25 μM DHPG application. Responses are strongly correlated as indicated by the corresponding plot (which also includes traces shown above it). Same cells as in *A* with the same current and voltage calibrations. *C*, carbenoxolone (100 μM) blocked oscillatory activity in both cells (same pair as in *A* and *B*). Injection of a large depolarizing current (0.6 nA) into cell 2 evoked transient firing in this neurone but no response in cell 1, demonstrating loss of electrical coupling. Calibrations as in *A*. *D*, on a pair of HMs oscillating in the presence of DHPG (25 μM), injection of −0.3 nA steady current into cell 2 slows down oscillatory activity in cell 1, a phenomenon reversible at the end of current injection. *E*, example of pair recording from two HMs oscillating in the presence of DHPG with different oscillatory period (see lack of correlation between such events in the cross-correlogram which also includes traces shown alongside it). *F*, example of pair of cells in which top HM does not oscillate in the presence of DHPG (25 μM) while the bottom one generates repeated slow oscillations. Current and voltage calibrations as in *E*.

versus membrane potential as demonstrated in the plots (Fig. 10*C*) for cells in control saline (■) or in the presence of DHPG-evoked oscillations (□).

Raising extracellular K^+ (7.5–9 mM) induced HM membrane depolarization (from −60 to −52 mV in the example of Fig. 7*D*; −12 ± 2 mV on average; $n = 5$) without oscillations, and it elicited repetitive irregular firing as indicated in the inset to Fig. 10*D*. On average the CV for spike discharges in high external K^+ was 63 ± 10%. Thus, current injection or high K^+ evoked a firing pattern clearly different from the one associated with oscillations.

Finally, we tested if the efficiency of the glutamatergic input to activate HM via the dorso-medullary reticular column (DMRC; Cunningham & Sawchenko, 2000) could be modulated in the presence of DHPG. For such tests we stimulated electrically the DMRC (Sharifullina *et al.* 2004) and used a small subthreshold concentration of DHPG to induce slow oscillations (and associated firing) to avoid them interfering with synaptic processes. Figure 10*E* shows an example in which, in the presence of 5 μM DHPG, after repolarizing the cell membrane potential to the initial resting level (−64 mV), the EPSP could now generate a spike followed (after 184 ± 4 ms delay) by cycles of oscillatory activity (see inset to Fig. 10*E*). Comparable data were observed on five HMs.

Discussion

The principal finding of the present study is the demonstration that, on brainstem motoneurones at early postnatal age, mGluR1s evoked a novel oscillatory (4–8 Hz) activity hitherto unreported on such cells. Oscillations required electrical coupling amongst HMs, and were apparently paced by rhythmic activation of K_{ATP} conductances. Because these oscillations constrained spike firing into a regular mode, they might represent a mechanism to coordinate motor discharges to tongue muscles at a critical stage of neonatal development.

Origin and characteristics of oscillations

Oscillations did not arise spontaneously (even when the network was depolarized by high K^+) and were not a consequence of synaptic inhibition block, as they were

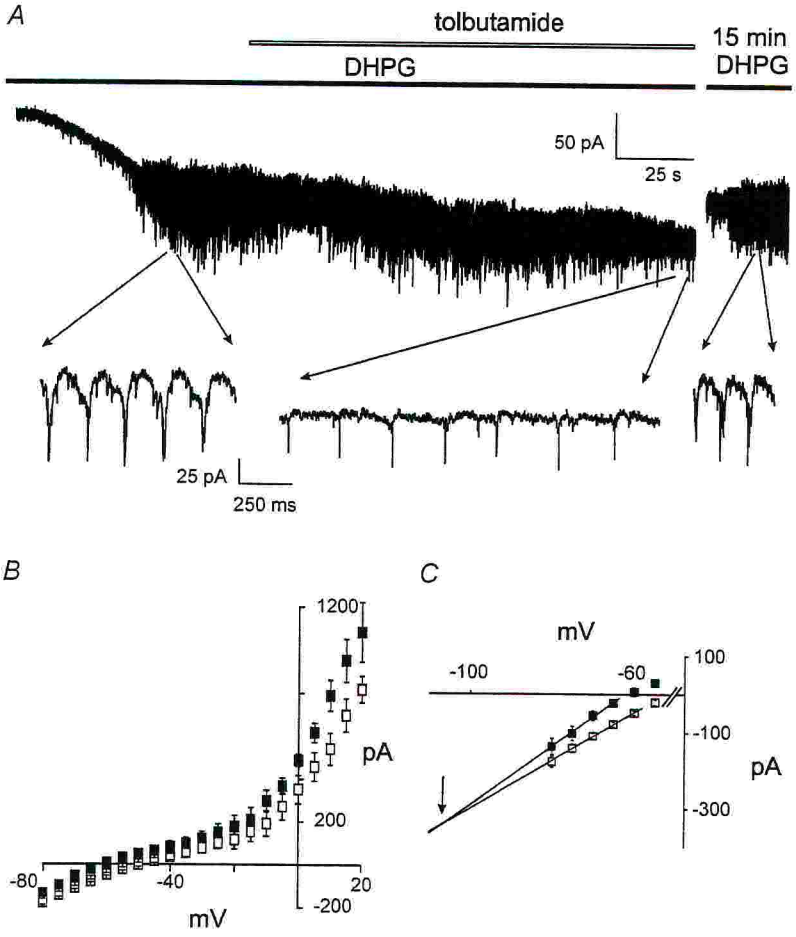

Figure 9. Sulphonylureas block slow oscillations evoked by DHPG
A, DHPG (25 μM) elicits inward current and slow oscillations (see inset with expanded time base). Further application of tolbutamide (500 μM) induces inward current and disrupts slow oscillations while leaving less regular (CV = 36% *versus* 8% prior to tolbutamide) fast discharges (inset, middle). Return of slow oscillations in the continuous presence of DHPG is observed after 15 min washout of tolbutamide (right). *B*, *I–V* plots (produced by 6 s voltage ramps from −80 to +20 mV) obtained during the oscillatory activity induced by DHPG (■) and after application (□) of either glibenclamide (50 μM) or tolbutamide (500 μM). Data with these agents were pooled together. Values are from 12 HMs. *C*, the *I–V* plot of *B* in the region negative to the holding potential is expanded to show decreased slope in the presence of sulphonylureas with extrapolated line crossover at −106 mV as indicated by the arrow.

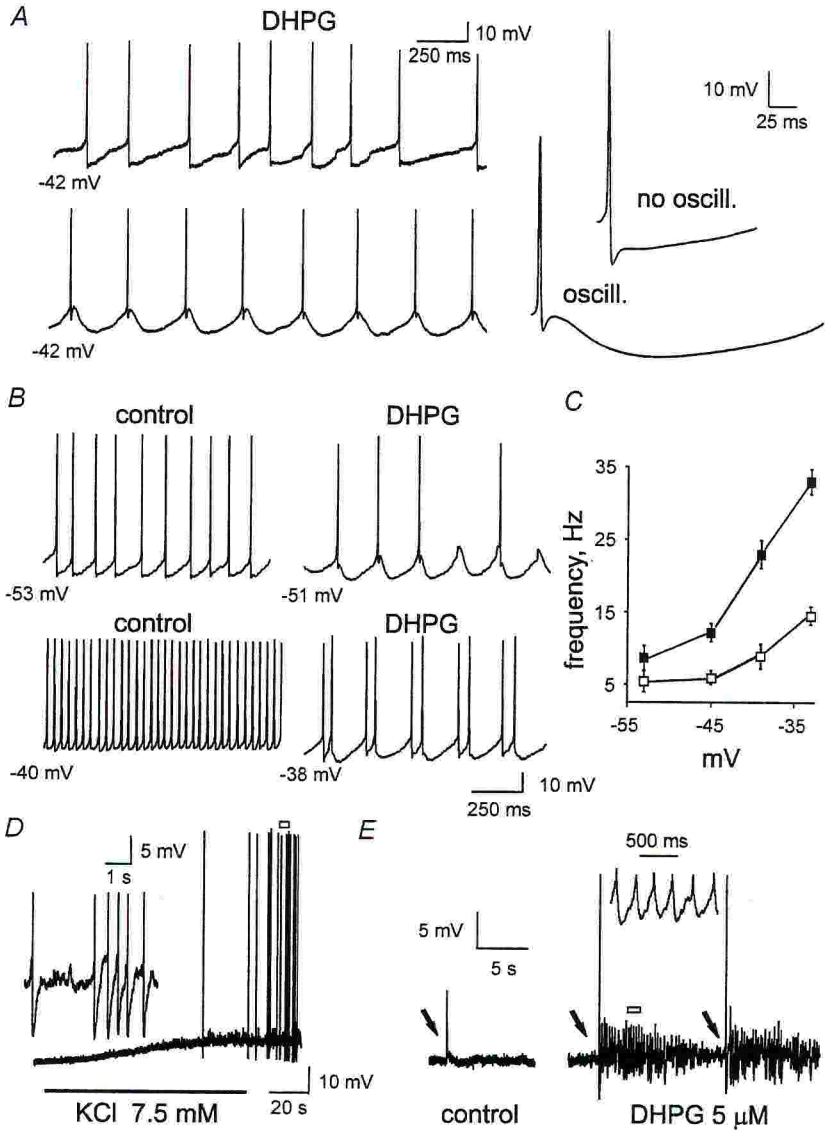

Figure 10. Firing properties of HMs during oscillatory activity evoked by DHPG
A, example of two HMs recorded in the presence of DHPG (25 μM) at the same membrane potential from two different slices. The cell at the top did not generate oscillations and fired randomly. Averaged spike is shown on the right. Bottom is an example of a cell oscillating in DHPG solution and regularly firing (average spike on the right). *B*, comparison of firing properties of a cell in control saline (left; firing irregularly at −53 mV, or at high frequency at −40 mV) with a cell oscillating in DHPG solution (right) with intermittent firing in coincidence with oscillations at −51 mV, or highly regular doublets at −38 mV. *C*, plots of average firing frequency *versus* membrane potential for a sample of 5 HMs in control saline (■) or in DHPG solution (□). Data for control cells were obtained by analysing 10-s-long records while data from DHPG-treated cells were averaged from 5- to 10-s-long records. *D*, application of 7.5 mM K^+ solution depolarizes HM from −61 to −52 mV, and induces irregular firing (see inset where spikes are truncated which corresponds to open horizontal bar). *E*, EPSPs induced by electrical stimulation (0.1 Hz; 0.1 ms; subthreshold for spiking as indicated by arrows) of the DMRC in control solution (left) or in the presence of 5 μM DHPG (middle and right), a concentration subthreshold for generating oscillations. Coincidence of EPSP and DHPG brings about spike generation and oscillations following the synaptic response (see inset for expanded trace corresponding to open horizontal bar). All responses are obtained at −64 mV after injection of steady current to repolarize the cell in the presence of DHPG.

present even in the absence of strychnine and bicuculline. Note that application of the selective $GABA_B$ receptor blocker CGP 55845 did not change oscillations induced by DHPG, suggesting that $GABA_B$ receptors were not involved in oscillations. This result accords with the previous demonstration that, at least at this developmental age, there is no contribution by $GABA_B$ receptors to inhibitory synaptic transmission on rat HMs even during repeated neuronal activity (Donato & Nistri, 2001).

The triggering factor was activation of mGluR1s by DHPG, a selective mGluR1 agonist (Schoepp *et al.* 1999) that generates neuronal depolarization with increased input resistance and enhances glutamatergic transmission (Sharifullina *et al.* 2004) through stimulation of intracellular IP_3 synthesis and Ca^{2+} release (Schoepp *et al.* 1999). These combined effects of DHPG presumably activated premotoneurones at network level to trigger oscillations as demonstrated by the requirement for efficient glutamatergic transmission (via AMPA receptors sensitive to the selective blocker SYM 2206). Oscillations could also arise after activating network neurones with focal pulses of AMPA in the presence of DHPG. Thus, the origin of HM oscillations was based on spike-dependent, Ca^{2+}-mediated release of endogenous glutamate in accordance with the observed block by TTX or Mn^{2+}. Note, however, that once oscillations were developed, there was no rhythmic discharge of glutamatergic premotoneurones because synaptic currents were equally distributed throughout the oscillation cycle, ruling out concerted periodic firing of premotoneurones as the mechanism generating and maintaining oscillations. Thus, enhanced glutamatergic input was necessary to constrain HMs into an oscillatory mode; however, once established, oscillations were crucially dependent on HM collective behaviour.

Although endogenous glutamate can activate different classes of ionotropic receptors, it seems unlikely that NMDA receptors contributed to the recorded oscillations because these responses were insensitive to the selective receptor blocker APV. Furthermore, synaptically released glutamate may also activate kainate receptors which, on cortical neurones, mediate EPSCs characterized by rather slow kinetics (Kidd & Isaac, 2001; Ali, 2003). In the present experiments on DHPG-evoked oscillations, the emergence of slow, large synaptic responses, especially at positive holding potential, may have suggested underlying activation of kainate receptors. Nevertheless, application of the selective kainate receptor antagonist UBP 301 failed to block oscillations as well as the slow, large outward synaptic currents, making it unlikely that kainate receptor activity took part in such oscillations. The predominant role of AMPA receptors activated by endogenous glutamate was further corroborated by the observation that the selective AMPA antagonist SYM 2206 (Behr *et al.* 2002) blocked HM currents induced by puffer-applied AMPA as well as any oscillatory activity evoked by DHPG.

The large, slow outward currents intermingled with oscillations at positive potentials were thus likely to be summated synaptic events due to AMPA receptors because of their SYM 2206 sensitivity. Their slow kinetics at positive potential were shared by AMPA-elicited currents, which exhibited clear outward rectification, probably because they reflected the relative lack of GluR2 subunits in AMPA receptors of HMs (Essin *et al.* 2002), a fact that confers them rectification properties.

It would be inappropriate to consider oscillations as an intrinsic property of individual motoneurones due to cyclic interactions among certain voltage-activated conductances. In fact, on HMs strong buffering of intracellular Ca^{2+} or intracellular application of QX-314 to block Na^+ and I_h currents, or a range of channel inhibitors (Ba^{2+}, apamin, Cs^+, ZD 7288) failed to affect either the amplitude or the period of oscillations, in keeping with the notion that intrinsic membrane conductances of HMs had little effect on the genesis of oscillations. In this sense oscillations of HMs were therefore different from those recorded from other brain neurones in which a role for a variety of voltage-activated ion channels can be demonstrated (Traub *et al.* 2002, 2004). Hence, activation of mGluR1 receptors of brainstem neurones represents a novel and very efficient mechanism to up-regulate cell excitability without interference with major voltage-activated conductances. The amplitude and period of oscillations were also insensitive to membrane potential, suggesting that oscillations recorded from HMs were not just large excitatory synaptic currents.

Electrical coupling amongst HMs is necessary for oscillatory activity and unveils concerted rhythmic behaviour of HMs

In other brain areas, like for example the hippocampus or the thalamus, electrical coupling amongst neurones is an essential process to produce oscillatory activity (Skinner *et al.* 1999; Hughes *et al.* 2002*b*; LeBeau *et al.* 2003; Long *et al.* 2004). Manifestations of such coupling are fast inward currents ('spikelets') and slow bursts ('burstlets') passively propagated from one cell to the next via specialized gap junctions made up of carbenoxolone-sensitive membrane proteins termed connexins (Honma *et al.* 2004) and pannexins (Bruzzone *et al.* 2003). Since early discharges and fast inward currents during slow oscillations of HMs had similar kinetics and pharmacology, it seems likely that they were all spikelets due to repeated firing of HM action potentials.

In accordance with previous studies indicating that a substantial number of rat HMs are electrically coupled (Mazza *et al.* 1992; Rekling *et al.* 2000),

the present investigation, using simultaneous patch recording from HMs, found significant electrical coupling (without rectification) readily blocked by carbenoxolone. Regardless of whether pairs of cells were coupled or not, and on all single-recorded cells, carbenoxolone always suppressed oscillations. These data suggest that spikelets and burstlets making up oscillations were electrically propagated responses generated by cells close to the recorded one, in analogy to the phenomenon described for thalamic neurones (Long *et al.* 2004). Although DHPG application was therefore responsible to spark off HM depolarization, activation of mGluR1s was not apparently accompanied by changes in gap junction efficiency as demonstrated by the preserved value of the electrical coupling coefficient. Since this coupling normally involves a few HMs (Mazza *et al.* 1992), injection of current into one HM could slow down oscillations in the paired recorded cell without fully suppressing oscillations probably still driven by other coupled neurones.

The insensitivity of the oscillation period to membrane potential in a *single* HMs could be explained by the fact that blocking just one HM (and/or its immediate neighbour) could not suppress oscillations propagated by nearby HMs. Likewise, intracellular application of channel blockers to a single cell could not disrupt oscillations as these drugs did not apparently cross to adjacent HMs. In fact, neurobiotin-injected HMs did not show dye coupling despite the presence of oscillations presumably because gap junctions are ill-suited to transport chemical substances (Arabshahi *et al.* 1997; Devor & Yarom, 2002). As far as the locus for electrical coupling among HMs is concerned, the insensitivity of the oscillatory period to active membrane properties of the recorded HM plus the block of oscillations by AMPA antagonists (or the triggering of oscillations by focal pulses of AMPA) all make unlikely an axo-axonic coupling source and rather point to a somato-dendritic location (Honma *et al.* 2004) of gap junctions (Traub *et al.* 2003, 2004). In fact, in hippocampal slice neurones, axo-axonic coupling responsible for spikelets is typically suppressed by somatic membrane hyperpolarization (Schmitz *et al.* 2001), contrary to the findings of the present study. In conclusion, within the nucleus hypoglossus, gap junctions are unlikely to be axo-axonic and appear to tighten the organization of the rhythm rather than generate network oscillations, as in the case of the hippocampus (Draguhn *et al.* 1998; Traub *et al.* 2002).

A mechanism to pace oscillations

A distinguishing feature of HM oscillations was that, in the presence of DHPG, they could last indefinitely as long as recording was possible. While this property rules out mGluR1 desensitization or rundown, it also implies a mechanism to ensure periodicity of oscillations, especially because oscillations could be routinely observed in the presence of synaptic inhibition blockers.

The slow inward current evoked by DHPG was initially associated with a resistance increase presumably due to block of an outward K^+ conductance (Sharifullina *et al.* 2004). Nevertheless, this resistance rise rapidly dissipated once slow oscillations emerged. The simplest interpretation is that emergence of the oscillatory activity coincided not only with depolarization spread via gap junctions but also with activation of a conductance mechanism functionally opposite to the closure of leak channels. Although we cannot exclude the additional contribution by activation of certain voltage-dependent conductances due to current flow from nearby unclamped cells, this hypothesis is made unlikely by the insensitivity of input resistance to large depolarization or hyperpolarization (−80 to +20 mV). Pharmacological data on the blocking effect of sulphonylureas instead suggested a different explanation, namely co-activation of an outward K^+ current mediated by K_{ATP} channels to contrast the resistance increase evoked by DHPG, and to arrest oscillations. Because the K_{ATP} conductance targeted by sulphonylureas has relatively modest voltage dependence (Aguilar-Bryan & Bryan, 1999), its sulphonylurea-dependent inhibition during the oscillatory phase is expected to be accompanied by a quasi-parallel downward shift of the cell I–V relation, as was indeed found in the present study. Furthermore, in the presence of sulphonylureas slow oscillations were severely disrupted, leaving irregular spikelets. This observation indicates that gap junctions were not blocked by sulphonylureas, even though their synchronizing mechanism had been lost.

On cerebellar granule (D'Angelo *et al.* 2001) or thalamic (Fuentealba *et al.* 2004) neurones, oscillations in the frequency range found on HMs were demonstrated to be paced by cyclic activation of a slow K^+ conductance with kinetics comparable to the slow outward current of HM oscillations. While the precise identification of such a K^+ conductance remains to be established, previous studies have shown that on brainstem respiratory neurones rhythmic changes in K_{ATP} channel activity take place during oscillations presumably because of cyclic variations in the intracellular ATP concentration in the immediate vicinity of the K_{ATP} channels (Haller *et al.* 2001). We suspect that the excitation of HMs set off by DHPG might have been associated with analogous changes in intracellular ATP so that a periodic block/unblock of K_{ATP} channels could occur depending on the energy metabolism of HMs during application of DHPG.

Developmental characteristics of oscillatory mechanisms

In view of the strong developmental regulation of connexins (Honma *et al.* 2004), it seems likely that the

extent of their expression, which is particularly high after birth, was an important element to determine whether HMs could oscillate. In addition, the postnatal period is also associated with major changes in the expression of mGluR1s (Shigemoto *et al.* 1992; Catania *et al.* 1994) and K_{ATP} channels (Mourre *et al.* 1990). Thus, concurrent expression of mGluR1s, connexins and K_{ATP} channels may explain why optimization of HM oscillatory activity had a narrow time window relying on the synergy between these phenomena. It is currently unknown if activation of mGluR1 receptors in the brainstem of the adult rat can generate analogous oscillations. Although HMs gradually change some of their electrical properties during postnatal maturation (Berger *et al.* 1996), it is clear that certain characteristics such as those of gap junctions (Ramirez *et al.* 1997; Simbürger *et al.* 1997) and responsiveness to K_{ATP} channel blockers are retained (Pierrefiche *et al.* 1997), suggesting that at least in principle activation of mGluR1 receptors might generate fast oscillations which might participate in certain fast discharges normally recorded from the adult hypoglossal nerve *in vivo* (O'Neal III *et al.* 2004). This issue will, however, require future experiments to investigate the role of mGluR1 receptors in the adult brainstem.

Oscillations are due to the interplay amongst HM conductances

mGluR-dependent theta (4–12 Hz) oscillations of hippocampal pyramidal cells possess distinctive properties like dependence on GABA-mediated inhibition, requirement of AMPA receptor block, and out of phase discharge of inhibitory interneurones (Traub *et al.* 2004), indicating cellular mechanisms distinct from those of HM oscillations.

On certain reticulothalamic neurones theta oscillations are induced by mGluR1 activation with characteristics similar to those of HMs, including strong dependence on gap junctions (Hughes *et al.* 2004). There are, however, a few properties which make such theta oscillations different from those of HMs: for instance, thalamic oscillations persist in the presence of TTX and require intact GABAergic transmission (Hughes *et al.* 2004).

We might envisage the following scenario for the 4–8 Hz oscillations recorded from HMs: even in the absence of synaptic inhibition, oscillations started because of DHPG-enhanced glutamatergic transmission at network level, and were amplified by the associated resistance increase in premotoneurones and HMs. Network glutamatergic activity (evoked by DHPG) could lead to repeated HM firing sensitive to TTX and manifested as spikelets which are believed to be individual spikes electrotonically spread via gap junctions (Hughes *et al.* 2002*a*, 2004; Long *et al.* 2004).

HMs possess comparatively large intracellular levels of free Ca^{2+} (Ladewig & Keller, 2000) and generate long lasting increases in intracellular Ca^{2+} even after a single action potential (Donato *et al.* 2003). Intracellular Ca^{2+} homeostasis in brain neurones is largely dependent on the operation of the Ca^{2+}-ATPase pump expected to consume a significant concentration of intracellular ATP (Watson *et al.* 2003). Release of intracellular Ca^{2+} from organelle stores after application of DHPG (Schoepp *et al.* 1999) plus lingering intracellular Ca^{2+} due to repeated spikes might have therefore cooperated to induce strong operation of the Ca^{2+} pump and depleted ATP with consequent activation of K_{ATP} channels to hyperpolarize HMs (burstlets). The interplay among these mechanisms might have presumably established the conditions necessary for the cyclic waxing and waning of the depolarization cycle propagated and synchronized across gap junctions.

Firing characteristics during oscillations

Current clamp experiments demonstrated that the emergence of oscillations conferred important properties to the firing characteristics of HMs. While rhythmic oscillations of respiratory neurones are believed to facilitate spike firing (Parkis *et al.* 2003), for HMs the main consequence was transformation of irregular firing, often at high rate, into a regular, lower frequency discharge. Because the oscillatory period was little dependent on membrane voltage, the overall spike output of the cell was constrained to the number of oscillatory cycles. Even if, at more depolarized level of membrane potential, oscillations could generate doublets or triplets of action potentials, the remarkable consequence of oscillations was the emergence of low rhythmic firing. This phenomenon might even represent a braking system to avoid excessive excitation of HMs which are particularly vulnerable to large elevations in intracellular Ca^{2+} and excitotoxic damage (Ladewig *et al.* 2003).

A brain slice preparation is ill suited to investigate the role of projection pathways because many connections are inevitably severed. Nevertheless, in the brainstem slice preparation it is possible to preserve a strong glutamatergic input from the DMRC to HMs (Cunningham & Sawchenko, 2000). In the present experiments electrical stimulation of this pathway in association with a DHPG concentration subthreshold for oscillations, facilitated EPSP–spike coupling and elicited a set of oscillations for each synaptic stimulus. These data suggest that it was not necessary to apply DHPG in very large concentrations to enhance firing and generate oscillations.

Functional implications

HMs receive rhythmic synaptic inputs from a variety of brainstem networks which include oscillators for respiration, swallowing, mastication, etc. (Nakamura *et al.* 1999; Jean, 2001; Ballanyi, 2004). As far as respiratory rhythms transmitted to the hypoglossal nucleus are

concerned, in the adult as well as neonate rat *in vivo*, inspiratory discharges occur at about 1–2 Hz (Thomas & Marshall, 1997) with superimposed much faster oscillations, whose frequency increases during development (Kocsis *et al.* 1999; Marchenko *et al.* 2002). Pioneer work by Suzue (1984) has demonstrated that isolated brainstem preparations retain rhythmic activities although at lower frequency probably because of the different experimental conditions (including the use of ambient temperature and severance of peripheral afferents). The spontaneous inspiratory rhythm of the isolated brainstem preparation recorded from the rat hypoglossus nerve *in vitro* has about 0.1 Hz frequency (Morin *et al.* 1992), but it can be readily accelerated by serotonin (Morin *et al.* 1992) or high K^+, or largely slowed down by hypoxia (Ballanyi, 2004). While HMs within the thin brainstem slice preparation showed no spontaneous rhythmic activity, application of DHPG persistently increases their synaptic inputs in a dose-dependent fashion (Sharifullina *et al.* 2004), showing that the effect of DHPG goes in the opposite direction of the anoxic response (Ballanyi, 2004). Thus, there is no evidence that the oscillations induced by DHPG on *in vitro* HMs were the expression of a pathophysiological effect. On the contrary, the fast oscillations evoked by DHPG at room temperature were approaching the frequency range (22–43 Hz) normally found for medium frequency oscillations superimposed on the inspiratory discharges of the newborn rat *in vivo* (Kocsis *et al.* 1999). Although pattern similarity cannot indicate equivalence of function, these data suggest that oscillations as fast as those evoked by DHPG might also be expressed by *in vivo* brainstem neurones. The frequency of slow oscillations (about 6 Hz) induced by DHPG would be too fast for the normal inspiratory rhythm of *in vivo* normoxic animals, but it could correspond to reflex-enhanced respiratory rhythmicity especially because mGluRs are believed to increase the respiratory frequency even if they are not usually active in eupnoea (Li & Nattie, 1995). Furthermore, since application of DHPG facilitated synaptic inputs from the DMRC, a structure regarded as particularly important for swallowing (Cunningham & Sawchenko, 2000), it is feasible that activation of mGluR1s on brainstem neurones might represent a global strategy to facilitate HM rhythmic firing to tongue muscles under high demand-led conditions set by brainstem networks like, for instance, during suckling behaviour (Berger *et al.* 1996). *In vivo* experiments will, however, be necessary to clarify the role of mGluRs in the complex functions mediated by HMs.

References

Aguilar-Bryan L & Bryan J (1999). Molecular biology of adenosine triphosphate-sensitive potassium channels. *Endocr Rev* **20**, 101–135.

Ali A (2003). Involvement of post-synaptic kainate receptors during synaptic transmission between unitary connections in rat neocortex. *Eur J Neurosci* **17**, 2344–2350.

Arabshahi A, Giaume C & Peusner KD (1997). Lack of biocytin transfer at gap junctions in the chicken vestibular nuclei. *Int J Dev Neurosci* **15**, 343–352.

Ashcroft FM (1988). Adenosine 5′-triphosphate-sensitive potassium channels. *Annu Rev Neurosci* **11**, 97–118.

Ballanyi K (2004). Protective role of neuronal K_{ATP} channels in brain hypoxia. *J Exp Biol* **207**, 3201–3212.

Behr J, Gebhardt C, Heinemann U & Mody I (2002). Kindling enhances kainate receptor-mediated depression of GABAergic inhibition in rat granule cells. *Eur J Neurosci* **16**, 861–867.

Beierlein M, Gibson JR & Connors BW (2000). A network of electrically coupled interneurons drives synchronized inhibition in neocortex. *Nat Neurosci* **3**, 904–910.

Berger AJ, Bayliss DA & Viana F (1996). Development of hypoglossal motoneurons. *J Appl Physiol* **81**, 1039–1048.

Bruzzone R, Hormuzdi SG, Barbe MT, Herb A & Monyer H (2003). Pannexins, a family of gap junction proteins expressed in brain. *Proc Natl Acad Sci U S A* **100**, 13644–13649.

Catania MV, Landwehrmeyer GB, Testa CM, Standaert DG, Penney JB Jr & Young AB (1994). Metabotropic glutamate receptors are differentially regulated during development. *Neuroscience* **61**, 481–495.

Cobb SR, Bulters DO & Davies CH (2000). Coincident activation of mGluRs and mAChRs imposes theta frequency patterning on synchronised network activity in the hippocampal CA3 region. *Neuropharmacology* **39**, 1933–1942.

Cunningham ET Jr & Sawchenko PE (2000). Dorsal medullary pathways subserving oromotor reflexes in the rat: implications for the central neural control of swallowing. *J Comp Neurol* **417**, 448–466.

D'Angelo E, Nieus T, Maffei A, Armano S, Rossi P, Taglietti V, Fontana A & Naldi G (2001). Theta-frequency bursting and resonance in cerebellar granule cells: experimental evidence and modeling of a slow K^+-dependent mechanism. *J Neurosci* **21**, 759–770.

Devor A & Yarom Y (2002). Electrotonic coupling in the inferior olivary nucleus revealed by simultaneous double patch recordings. *J Neurophysiol* **87**, 3048–3058.

Donato R, Canepari M, Lape R & Nistri A (2003). Effects of caffeine on the excitability and intracellular Ca^{2+} transients of neonatal rat hypoglossal motoneurons in vitro. *Neurosci Lett* **346**, 177–181.

Donato R & Nistri A (2000). Relative contribution by GABA or glycine to Cl^--mediated synaptic transmission on rat hypoglossal motoneurons in vitro. *J Neurophysiol* **84**, 2715–2724.

Donato R & Nistri A (2001). Differential short-term changes in GABAergic or glycinergic synaptic efficacy on rat hypoglossal motoneurons. *J Neurophysiol* **86**, 565–574.

Draguhn A, Traub RD, Schmitz D & Jefferys JG (1998). Electrical coupling underlies high-frequency oscillations in the hippocampus in vitro. *Nature* **394**, 189–192.

Essin K, Nistri A & Magazanik L (2002). Evaluation of GluR2 subunit involvement in AMPA receptor function of neonatal rat hypoglossal motoneurons. *Eur J Neurosci* **15**, 1899–1906.

Fuentealba P, Timofeev I & Steriade M (2004). Prolonged hyperpolarizing potentials precede spindle oscillations in the thalamic reticular nucleus. *Proc Natl Acad Sci U S A* **101**, 9816–9821.

Galarreta M & Hestrin S (1999). A network of fast-spiking cells in the neocortex connected by electrical synapses. *Nature* **402**, 72–75.

Grillner S, Ekeberg El Manira A, Lansner A, Parker D, Tegner J & Wallen P (1998). Intrinsic function of a neuronal network – a vertebrate central pattern generator. *Brain Res Rev* **26**, 184–197.

Haller M, Mironov SL, Karschin A & Richter DW (2001). Dynamic activation of K_{ATP} channels in rhythmically active neurons. *J Physiol* **537**, 69–81.

Hay M, McKenzie H, Lindsley K, Dietz N, Bradley SR, Conn PJ & Hasser EM (1999). Heterogeneity of metabotropic glutamate receptors in autonomic cell groups of the medulla oblongata of the rat. *J Comp Neurol* **403**, 486–501.

Honma S, De S, Li D, Shuler CF & Turman JE Jr (2004). Developmental regulation of connexins 26, 32, 36, and 43 in trigeminal neurons. *Synapse* **52**, 258–271.

Hughes SW, Blethyn KL, Cope DW & Crunelli V (2002*a*). Properties and origin of spikelets in thalamocortical neurones in vitro. *Neuroscience* **110**, 395–401.

Hughes SW, Cope DW, Blethyn KL & Crunelli V (2002*b*). Cellular mechanisms of the slow (<1 Hz) oscillation in thalamocortical neurons in vitro. *Neuron* **33**, 947–958.

Hughes SW, Lorincz M, Cope DW, Blethyn KL, Kekesi KA, Parri HR, Juhasz G & Crunelli V (2004). Synchronized oscillations at alpha and theta frequencies in the lateral geniculate nucleus. *Neuron* **42**, 253–268.

Jean A (2001). Brain stem control of swallowing: neuronal network and cellular mechanisms. *Physiol Rev* **81**, 929–969.

Kidd F & Isaac J (2001). Kinetics and activation of postsynaptic kainate receptors at thalamocortical synapses: role of glutamate clearance. *J Neurophysiol* **86**, 1139–1148.

Kiehn O, Kjaerulff O, Tresch MC & Harris-Warrick RM (2000). Contributions of intrinsic motor neuron properties to the production of rhythmic motor output in the mammalian spinal cord. *Brain Res Bull* **53**, 649–659.

Kirk IJ & Mackay JC (2003). The role of theta-range oscillations in synchronising and integrating activity in distributed mnemonic networks. *Cortex* **39**, 993–1008.

Kocsis B, Gyimesi-Pelczer K & Vertes RP (1999). Medium-frequency oscillations dominate the inspiratory nerve discharge of anesthetized newborn rats. *Brain Res* **818**, 180–183.

Ladewig T & Keller BU (2000). Simultaneous patch-clamp recording and calcium imaging in a rhythmically active neuronal network in the brainstem slice preparation from mouse. *Pflugers Arch* **440**, 322–332.

Ladewig T, Kloppenburg P, Lalley PM, Zipfel WR, Webb WW & Keller BU (2003). Spatial profiles of store-dependent calcium release in motoneurones of the nucleus hypoglossus from newborn mouse. *J Physiol* **547**, 775–787.

Landisman CE, Long MA, Beierlein M, Deans MR, Paul DL & Connors BW (2002). Electrical synapses in the thalamic reticular nucleus. *J Neurosci* **22**, 1002–1009.

Lape R & Nistri A (2001). Characteristics of fast Na^+ current of hypoglossal motoneurons in a rat brainstem slice preparation. *Eur J Neurosci* **13**, 763–772.

LeBeau FE, Traub RD, Monyer H, Whittington MA & Buhl EH (2003). The role of electrical signaling via gap junctions in the generation of fast network oscillations. *Brain Res Bull* **62**, 3–13.

Leznik E, Makarenko V & Llinas R (2002). Electrotonically mediated oscillatory patterns in neuronal ensembles: an in vitro voltage-dependent dye-imaging study in the inferior olive. *J Neurosci* **22**, 2804–2815.

Li A & Nattie EE (1995). Prolonged stimulation of respiration by brain stem metabotropic glutamate receptors. *J Appl Physiol* **79**, 1650–1656.

Long MA, Landisman CE & Connors BW (2004). Small clusters of electrically coupled neurons generate synchronous rhythms in the thalamic reticular nucleus. *J Neurosci* **24**, 341–349.

Marchenko V, Granata AR & Cohen MI (2002). Respiratory cycle timing and fast inspiratory discharge rhythms in the adult decerebrate rat. *Am J Physiol Regul Integr Comp Physiol* **283**, R931–940.

Marchetti C, Pagnotta S, Donato R & Nistri A (2002). Inhibition of spinal or hypoglossal motoneurons of the newborn rat by glycine or GABA. *Eur J Neurosci* **15**, 975–983.

Marchetti C, Taccola G & Nistri A (2003). Distinct subtypes of group I metabotropic glutamate receptors on rat spinal neurons mediate complex facilitatory and inhibitory effects. *Eur J Neurosci* **18**, 1873–1883.

Mazza E, Nunez-Abades PA, Spielmann JM & Cameron WE (1992). Anatomical and electrotonic coupling in developing genioglossal motoneurons of the rat. *Brain Res* **598**, 127–137.

More J, Troop H, Dolman N & Jane D (2003). Structural requirements for novel willardiine derivatives acting as AMPA and kainate receptor antagonists. *Br J Pharmacol* **138**, 1093–1100.

Morin D, Monteau R & Hilaire G (1992). Compared effects of serotonin on cervical and hypoglossal inspiratory activities: an in vitro study in the newborn rat. *J Physiol* **451**, 605–629.

Mourre C, Widmann C & Lazdunski M (1990). Sulfonylurea binding sites associated with ATP-regulated K^+ channels in the central nervous system: autoradiographic analysis of their distribution and ontogenesis, and of their localization in mutant mice cerebellum. *Brain Res* **519**, 29–43.

Nakamura Y, Katakura N & Nakajima M (1999). Generation of rhythmical ingestive activities of the trigeminal, facial, and hypoglossal motoneurons in in vitro CNS preparations isolated from rats and mice. *J Med Dent Sci* **46**, 63–73.

O'Neal MH III, Spiegel ET, Chon KH & Solomon IC (2004). Time-frequency representation of inspiratory motor output in anesthetized C57BL/6 mice in vivo. *J Neurophysiol*; DOI:10.1152/jn.00646.2004.

Oyamada Y, Andrzejewski M, Muckenhoff K, Scheid P & Ballantyne D (1999). Locus coeruleus neurones in vitro: pH-sensitive oscillations of membrane potential in an electrically coupled network. *Respir Physiol* **118**, 131–147.

Parkis MA, Feldman JL, Robinson DM & Funk GD (2003). Oscillations in endogenous inputs to neurons affect excitability and signal processing. *J Neurosci* **23**, 8152–8158.

Perez Velazquez JL & Carlen PL (2000). Gap junctions, synchrony and seizures. *Trends Neurosci* **23**, 68–74.

Pierrefiche O, Bischoff AM, Richter DW & Spyer KM (1997). Hypoxic response of hypoglossal motoneurones in the in vivo cat. *J Physiol* **15**, 785–795.

Ramirez JM, Quellmalz UJ & Wilken B (1997). Developmental changes in the hypoxic response of the hypoglossus respiratory motor output in vitro. *J Neurophysiol* **78**, 383–392.

Rekling JC, Shao XM & Feldman JL (2000). Electrical coupling and excitatory synaptic transmission between rhythmogenic respiratory neurons in the preBotzinger complex. *J Neurosci* **20**, RC113.

Rybak IA, Shevtsova NA, St John WM, Paton JF & Pierrefiche O (2003). Endogenous rhythm generation in the pre-Botzinger complex and ionic currents: modelling and in vitro studies. *Eur J Neurosci* **18**, 239–257.

Schmidt BJ, Hochman S & MacLean JN (1998). NMDA receptor-mediated oscillatory properties: potential role in rhythm generation in the mammalian spinal cord. *Ann N Y Acad Sci* **860**, 189–202.

Schmitz D, Schuchmann S, Fisahn A, Draguhn A, Buhl EH, Petrasch-Parwez E, Dermietzel R, Heinemann U & Traub RD (2001). Axo-axonal coupling a novel mechanism for ultrafast neuronal communication. *Neuron* **31**, 831–840.

Schoepp DD, Jane DE & Monn JA (1999). Pharmacological agents acting at subtypes of metabotropic glutamate receptors. *Neuropharmacology* **38**, 1431–1476.

Sharifullina E, Ostroumov K & Nistri A (2004). Activation of group I metabotropic glutamate receptors enhances efficacy of glutamatergic inputs to neonatal rat hypoglossal motoneurons in vitro. *Eur J Neurosci* **20**, 1245–1254.

Shigemoto R, Nakanishi S & Mizuno N (1992). Distribution of the mRNA for a metabotropic glutamate receptor (mGluR1) in the central nervous system: an in situ hybridization study in adult and developing rat. *J Comp Neurol* **322**, 121–135.

Simbürger E, Stang A, Kremer M & Dermietzel R (1997). Expression of connexin43 mRNA in adult rodent brain. *Histochem Cell Biol* **107**, 127–137.

Skinner FK, Zhang L, Velazquez JL & Carlen PL (1999). Bursting in inhibitory interneuronal networks: a role for gap-junctional coupling. *J Neurophysiol* **81**, 1274–1283.

Steriade M & Timofeev I (2003). Neuronal plasticity in thalamocortical networks during sleep and waking oscillations. *Neuron* **37**, 563–576.

Suzue T (1984). Respiratory rhythm generation in the in vitro brain stem–spinal cord preparation of the neonatal rat. *J Physiol* **354**, 173–183.

Thomas T & Marshall JM (1997). The roles of adenosine in regulating the respiratory and cardiovascular systems in chronically hypoxic, adult rats. *J Physiol* **501**, 439–447.

Towers S, LeBeau F, Gloveli T, Traub RD, Whittington MA & Buhl EH (2002). Fast network oscillations in the rat dentate gyrus in vitro. *J Neurophysiol* **87**, 1165–1168.

Traub RD, Bibbig A, LeBeau FE, Buhl EH & Whittington MA (2004). Cellular mechanisms of neuronal population oscillations in the hippocampus in vitro. *Annu Rev Neurosci* **27**, 247–278.

Traub RD, Draguhn A, Whittington MA, Baldeweg T, Bibbig A, Buhl EH & Schmitz D (2002). Axonal gap junctions between principal neurons: a novel source of network oscillations, and perhaps epileptogenesis. *Rev Neurosci* **13**, 1–30.

Traub RD, Pais I, Bibbig A, LeBeau FE, Buhl EH, Hormuzdi SG, Monyer H & Whittington MA (2003). Contrasting roles of axonal (pyramidal cell) and dendritic (interneuron) electrical coupling in the generation of neuronal network oscillations. *Proc Natl Acad Sci U S A* **100**, 1370–1374.

Watson WD, Facchina SL, Grimaldi M & Verma A (2003). Sarco-endoplasmic reticulum Ca^{2+} ATPase (SERCA) inhibitors identify a novel calcium pool in the central nervous system. *J Neurochem* **87**, 30–43.

Whittington MA, Traub RD & Jefferys JG (1995). Synchronized oscillations in interneuron networks driven by metabotropic glutamate receptor activation. *Nature* **373**, 612–615.

Wu N, Hsiao CF & Chandler SH (2001). Membrane resonance and subthreshold membrane oscillations in mesencephalic V neurons: participants in burst generation. *J Neurosci* **21**, 3729–3739.

Acknowledgements

This work was supported by a FIRB grant.

Glutamate uptake block triggers deadly rhythmic bursting of neonatal rat hypoglossal motoneurons

Elina Sharifullina and Andrea Nistri

Neurobiology Sector and CNR-INFM Democritos National Simulation Center, International School for Advanced Studies (SISSA), 34014 Trieste, Italy

In the brain the extracellular concentration of glutamate is controlled by glial transporters that restrict the neurotransmitter action to synaptic sites and avoid excitotoxicity. Impaired transport of glutamate occurs in many cases of amyotrophic lateral sclerosis, a devastating motoneuron disease. Motoneurons of the brainstem nucleus hypoglossus are among the most vulnerable, giving early symptoms like slurred speech and dysphagia. However, the direct consequences of extracellular glutamate build-up, due to uptake block, on synaptic transmission and survival of hypoglossal motoneurons remain unclear and have been studied using the neonatal rat brainstem slice preparation as a model. Patch clamp recording from hypoglossal motoneurons showed that, in about one-third of these cells, inhibition of glutamate transport with the selective blocker DL-threo-β-benzyloxyaspartate (TBOA; 50 μM) unexpectedly led to the emergence of rhythmic bursting consisting of inward currents of long duration with superimposed fast oscillations and synaptic events. Synaptic inhibition block facilitated bursting. Bursts had a reversal potential near 0 mV, and were blocked by tetrodotoxin, the gap junction blocker carbenoxolone, or antagonists of AMPA, NMDA or mGluR1 glutamate receptors. Intracellular Ca^{2+} imaging showed bursts as synchronous discharges among motoneurons. Synergy of activation of distinct classes of glutamate receptor plus gap junctions were therefore essential for bursting. Ablating the lateral reticular formation preserved bursting, suggesting independence from propagated network activity within the brainstem. TBOA significantly increased the number of dead motoneurons, an effect prevented by the same agents that suppressed bursting. Bursting thus represents a novel hallmark of motoneuron dysfunction triggered by glutamate uptake block.

(Resubmitted 19 October 2005; accepted after revision 1 February 2006; first published online 2 February 2006)
Corresponding author A. Nistri: Neurobiology Sector and CNR-INFM Center, International School for Advanced Studies (SISSA), 34014 Trieste, Italy. Email: nistri@sissa.it

Amyotrophic lateral sclerosis (ALS) is a devastating neurodegenerative disease primarily affecting motoneurons (Bruijn *et al.* 2004). A large number of ALS patients show a deficit in the transport process of the excitatory transmitter glutamate that builds up extracellularly to produce excitotoxic damage to motor cells (Rothstein *et al.* 1992; Cleveland & Rothstein, 2001; Rao & Weiss, 2004). Because in the vast majority of cases the disease is sporadic and associated with normal synthesis of the transporter proteins (Rao & Weiss, 2004), various environmental factors are suspected to generate this condition by inhibiting glutamate transport in vulnerable brain regions (Bruijn *et al.* 2004).

One important form of ALS (termed bulbar) is clinically manifested as severe degeneration of brainstem motoneurons, although some motor nuclei are more vulnerable than others (Rowland & Shneider, 2001). In particular, the nucleus hypoglossus, that exclusively innervates tongue muscles, is among the most strongly involved in ALS (Krieger *et al.* 1994; Lips & Keller, 1999; Laslo *et al.* 2001), producing slurred speech, difficulty in mastication, swallowing and breathing. While the early damage of hypoglossal motoneurons (HMs) may be related to their characteristic intracellular Ca^{2+} homeostasis (Ladewig *et al.* 2003) and expression of Ca^{2+}-permeable AMPA receptors (Del Cano *et al.* 1999; Laslo *et al.* 2001; Essin *et al.* 2002), it is also suggested that vulnerable motor nuclei normally possess distinctive properties of glutamate uptake to protect them against the risk factor of excitoxocity (Medina *et al.* 1996).

Previous studies have indicated that excitatory transmission on HMs is mediated by glutamate via AMPA-sensitive receptors (Rekling *et al.* 2000*a*; Essin *et al.* 2002), while glycine and GABA act as inhibitory transmitters (Donato & Nistri, 2000; Marchetti *et al.* 2002). Pharmacological block of glutamate uptake potentiates

DOI: 10.1113/jphysiol.2005.100412

glutamatergic transmission and has been used as a model to investigate excitotoxicity and to devise prevention treatments (Danbolt, 2001; Huang & Bergles, 2004; Shigeri *et al.* 2004).

However, little is known about the functional consequences of glutamate uptake block and build-up of extracellular glutamate on HMs and their surrounding network. For instance, AMPA receptors may become inactive in the continuous presence of their agonist (Mayer & Armstrong, 2004). It might then be predicted that lingering glutamate (Cavelier *et al.* 2005) should rather activate NMDA receptors (Campbell & Hablitz, 2004; Huang & Bordey, 2004) and glutamate metabotropic receptors (mGluRs, Brasnjo & Otis, 2001; Huang *et al.* 2004) to stimulate firing of HMs.

In the present study, based on electrophysiological recording, and intracellular Ca^{2+} imaging from HMs of the rat brainstem slice preparation, we used the very selective glutamate transport inhibitor DL-threo-β-benzyloxyaspartate (TBOA; Shigeri *et al.* 2004) to explore how it may change synaptic transmission, and its consequences on HM survival estimated with histochemical methods. Even after a short period of uptake block, we discovered the emergence of a novel type of bursting with significant neurotoxic damage to HMs.

Methods

Ethical standards

In accordance with the regulations of the Italian Animal Welfare Act following the European Community directives and approved by the local authority veterinary service, neonatal Wistar rats (1–5 days old; P1–5) used for this study were anaesthetized with I.P. urethane (2 g (kg body weight)$^{-1}$) and quickly decapitated.

Slice preparation

The brainstem was removed and transverse slices were cut, as recently described (Sharifullina *et al.* 2004, 2005; Pagnotta *et al.* 2005). For this purpose, the brainstem was horizontally fixed to an agar block and sectioned with a vibroslicer (starting from the caudal end) while submerged in Krebs solution (see below) at 4°C. Slices (usually five) containing the nucleus hypoglossus were cut at 200 μm intervals. The presence of this nucleus in each slice was immediately confirmed by viewing it under light microscopy. Thereafter, slices were continuously superfused (2–3 ml min^{-1}) at room temperature (24–25°C) with Krebs solution (gassed with 95% O_2–5% CO_2) containing (mM): NaCl 130, KCl 3, NaH_2PO_4 1.5, $CaCl_2$ 1.5, $MgCl_2$ 1, $NaHCO_3$ 25, glucose 15 (pH 7.4; 300–320 mosmol). For further details see Sharifullina *et al.* (2005).

Ablation of the reticular formation

To remove the reticular formation adjacent to each nucleus hypoglossus, slightly thicker (300 μm) slices ($n = 14$) were cut due to the frailty of the tissue. Before patching, the lateral areas of slices were sectioned off under microscopic control as shown in the scheme of Fig. 2*E*. The ablation boundary was the lateral margin of the hypoglossus nucleus to remove a major excitatory input to this nucleus (Sharifullina *et al.* 2004, 2005). After this procedure, slices were used as for standard electrophysiological experiments. As indicated in the results, their bursting characteristics were identical to those of 200 μm slices.

Electrophysiology

Whole-cell patch clamping was used to record HM responses under voltage- or current-clamp conditions. HMs were visually identified with infrared microscopy (Ladewig *et al.* 2003). Patch pipettes were filled with intracellular solution containing (mM): CsCl 130, NaCl 5, $MgCl_2$ 2, $CaCl_2$ 1, Hepes 10, BAPTA 10, ATP–Mg 2, sucrose 2 (pH 7.2 with CsOH; 280–300 mosmol). This pipette solution was used for 67 HMs, 50 of which were recorded after adding QX-314 (300 μM) to the patch solution to block voltage-activated Na^+ currents and the hyperpolarization-activated current I_h (Marchetti *et al.* 2002). This drug preserved recording stability that allowed TBOA-induced bursting to be observed for at least 35 min. Ninety-four HMs were recorded with a patch solution in which 130 mM KCl had replaced CsCl; within this group, 33 HMs were recorded with QX-314 added to the solution. Since there was no difference in TBOA-evoked bursting characteristics between KCl- and CsCl-recorded HMs, these data were pooled together for statistical analysis. For 16 HMs recorded with CsCl and QX-314 we added 20 mM BAPTA (tetrapotassium salt) to the patch pipette, to enhance intracellular Ca^{2+} buffering. Cells were clamped at −60 or −65 mV holding potential, while series resistance (5–25 MΩ) was routinely monitored. All recorded currents were filtered at 3 kHz and sampled at 5–10 kHz. Postsynaptic currents, electrical oscillations and bursts were quantified as previously reported (Sharifullina *et al.* 2005) using a template search protocol (pClamp 9.0; Axon Instruments, Molecular Devices, Union City, CA, USA) applied to at least 5 min-long consecutive records.

Intracellular Ca^{2+} imaging

Ca^{2+} imaging was carried out according to the method recently described (Fabbro *et al.* 2004). In brief, slices were loaded with the fluorescent Ca^{2+} dye Fluo-3 AM (20 μM; Molecular Probes, Eugene, OR, USA) for 40 min in oxygenated standard saline solution. After a 20 min

wash, slices were transferred to the recording chamber and Ca^{2+} transients were visualized with a fast CCD camera (Coolsnap HQ; Roper Scientific, USA). Because of the need for continuous, long-lasting (about 1 h) recording, Ca^{2+} transients (usually 30 s long) from single cells within the nucleus hypoglossus were acquired at 1 Hz to minimize photobleaching as indicated by a stable baseline. In each slice, 10 randomly distributed motoneurons were identified as such because their somatic diameter was $> 20\ \mu$m, and were analysed by placing a small region of interest over the cell body using the Metafluor software (Metafluor Imaging Series 6.0, Universal Imaging Corporation, USA). Ca^{2+} transients were expressed as amplitude fractional increase ($\Delta F/F_0$, where F_0 is the baseline fluorescence level and ΔF is the rise over baseline). Cells with very bright baseline Ca^{2+} fluorescence were not analysed on the assumption they were already damaged. To maximize the detection of TBOA-induced rhythmic Ca^{2+} transients, 0.4 μM strychnine and 10 μM bicuculline were pre-applied to slices for 10 min prior to the start of 50 μM TBOA application, and maintained thereafter. Data were obtained from 16 slices from P4–6 rats ($n = 6$). In each slice 10 motoneurons were analysed; synchronicity of Ca^{2+} signals (within the temporal resolution of 1 s) was determined by cross-correlation analysis (Sharifullina *et al.* 2005) using the cross-correlation function (CCF) of Clampfit software (9.2 version; Axon Instruments, Molecular Devices, Union City, CA, USA). The same software was also used for analysing responses obtained with double patch recordings.

Drugs

Drugs were applied via the bathing solution with the exception of AMPA delivered by focal pressure pulses (10 ms; 6 p.s.i.; Pagnotta *et al.* 2005; Sharifullina *et al.* 2005) via a pipette. In this case the puffer pipette was filled with AMPA (0.1 mM) dissolved in standard Krebs solution and positioned approximately 20–50 μm away from the soma of the recorded cell. AMPA was applied once every 45 s to minimize desensitization. A number of experiments ($n = 112$ HMs) were performed in the continuous presence of bicuculline (10 μM) and strychnine (0.4 μM) in the bathing solution to block GABA- and glycine-mediated transmission (Donato & Nistri, 2000; Marchetti *et al.* 2002; Sharifullina *et al.* 2004) so that glutamatergic transmission could be studied in isolation. The following drugs were used: DL-threo-β-benzyloxyaspartate (TBOA), L-*trans*-pyrrolidine-2,4-dicarboxylic acid (PDC), 6-cyano-7-nitroquinoxaline-2,3-dione (CNQX), D-amino-phosphonovalerate (APV), 7-(hydroxyimino) cyclopropan[b]chromen-1a-carboxylate ethyl ester (CPCCOEt; selective antagonist for mGlu1 receptors), (*RS*)-α-amino-3-hydroxy-5-methyl-4-isoxazolepropionic acid (AMPA), *N*-2,6-dimethylphenylcarbamoylmethyl triethylammonium bromide (QX-314), ($\pm$)-4-(4-aminophenyl)-1,2-dihydro-1-methyl-2-propylcarbamoyl-6,7-methylenedioxyphthalazine (SYM 2206; selective antagonist for AMPA receptors), and the high-threshold Ca^{2+} channel blocker nifedipine were purchased from Tocris (Bristol, UK); bicuculline methiodide (bicuculline), strychnine hydrochloride (strychnine), 1,2-bis(2-aminophenoxy)ethane-*N*,*N*,*N*′,*N*′-tetraacetic acid tetrakis(acetoxymethyl ester) (BAPTA AM), and carbenoxolone (disodium salt) were from Sigma (Milan, Italy). Tetrodotoxin (TTX) was obtained from Latoxan (Valence, France).

HM identification and estimate of their excitotoxic damage

In the neonatal as well as in the adult rat (Nunez-Abades & Cameron, 1995), HMs comprise the largest population (about 90%; Viana *et al.* 1990) of neurons within the XII nucleus, are large cells (25–50 μm), multipolar in shape and distributed throughout this nucleus (Kitamura *et al.* 1983; Boone & Aldes, 1984). Conversely, interneurons (10–18 μm somatic diamater) are round- to oval-shaped neurons and are much less numerous (Boone & Aldes, 1984). Thus, within the hypoglossus nucleus, in control as well as in drug-treated slices, we counted only cells with somatic diameter $> 20\ \mu$m, to make sure that we analysed HMs. Control experiments were done to obtain further confirmation of the identification of large cells as motoneurons via immunocytochemical staining of brainstem slices with an antibody against the acetylcholine synthetic enzyme (ChAT; see also Donato & Nistri, 2000), and by the use of the monoclonal antibody against the non-phosphorylated form of neurofilament H (SMI32; a motoneuron marker; see Jacob *et al.* 2005; Raoul *et al.* 2005). For these experiments the brainstem was quickly removed from P3–5 rats, fixed in 4% paraformaldehyde containing 30% sucrose in phosphate buffer pH 7.4 (PBS) for 24 h at 4°C. Microtome sections (40 μm thick) were used for free-floating immunostaining as previously described (Pagnotta *et al.* 2005). Briefly, slices were treated with a blocking solution (5% bovine serum albumin, 4% fetal calf serum, 0.1% Triton X100 in phosphate-buffered saline, pH 7.4) for 60 min at room temperature. Slices were incubated overnight at 4°C with mouse monoclonal antibodies against ChAT (1 : 100; kindly provided by Dr L. Domenici, SISSA, Trieste; Umbriaco *et al.* 1994), or against SMI32 (1 : 1000; Sternberger monoclonals, Covance Research Products Inc., Berkeley, CA, USA) in the same blocking buffer at 4°C. The secondary antibodies used were AlexaFluor 488 (1 : 500 dilution; Molecular Probes, Invitrogen, San Giuliano Milanese, Italy) for 2 h at room temperature. Slices

stained with secondary antibody only showed no immunostaining. Measurements were obtained with ImagePro software (Hamamatsu srl, Arese, Italy).

Intracellular markers such as the cytosolic enzyme ChAT may be lost when cell membranes are damaged as a result of toxicity and death. Moreover, since ChAT is also present in a number of interneurons and afferent terminals to HMs (Ichikawa & Hirata, 1990; Ichikawa & Shimizu, 1998) and many HMs only show moderate ChAT staining (Ichikawa & Hirata, 1990), counting motoneurons killed by a certain drug treatment on the basis of ChAT staining may produce confusing results. Hence, to evaluate the number of HMs surviving after pharmacological treatment, we counted only cells (within the nucleus hypoglossus) with somatic diameter $> 20\,\mu$m after applying the cell-permeable dye Hoechst 33342 (10 mg ml^{-1} stock from Molecular Probes, Invitrogen; final dilution was 1 : 500 in standard Krebs solution) that, once bound to DNA, emits blue fluorescence. Only cell profiles with a clearly outlined nucleus at the same focal plane were analysed. This method provided the global number of motoneurons (surviving plus damaged) in each tissue section. To investigate the number of HMs killed by glutamate excitotoxicity, in analogy with previous studies (Kristensen *et al.* 2001; Babot *et al.* 2005; Bosel *et al.* 2005) including those with TBOA (Bonde *et al.* 2003), we then stained dead cells with propidium iodide (PI) solution (1.0 mg ml^{-1} stock from Sigma, Milan, Italy; 1 : 3000 in Krebs solution), a cell-impermeable DNA dye which can bind DNA and emits red fluorescence exclusively when cell and nuclear membranes have been severely damaged. For each experiment on excitotoxicity, brainstem slices were separated into various groups: control, TBOA (50 μM), and TBOA plus an antagonist. Slices were incubated at room temperature in the corresponding solution, continuously oxygenated for 1 h, then rinsed with Krebs solution, and placed in Krebs containing Hoechst (1 : 500) and PI (1 : 3000) for at least 45 min. Thereafter, slices were transferred to glass coverslips (without any fixation) and examined under a fluorescence microscope (×5). An 18-square grid was applied over each hypoglossal nucleus (see scheme in Fig. 7*D*). For each protocol at least six brainstem slices (from 24 rats) were used. Cells were counted at the same level in each slice.

Statistics

The electrophysiological database of the present study comprises 193 HMs. Results were expressed as means ± S.E.M. where n refers to the number of cells. For immunohistochemical analysis, data with PI staining were expressed as a percentage of those labelled with Hoechst 33342 (taken as 100%). Statistical significance was assessed with Student's paired t test applied to parametric raw data only, or for non-parametric values with ANOVA followed by the Tukey test. Two groups of data were considered statistically different if $P < 0.05$.

Results

Bursting induced by glutamate uptake blocker

As shown in Fig. 1*A*, bath-application of TBOA (50 μM) induced a slowly developing inward current (−44 pA) which stabilized at a plateau after approximately 4 min. In 33/103 HMs (32%) bathed in standard Krebs solution, the TBOA-induced inward current was accompanied by the emergence of bursting activity (Fig. 1*A*) characterized by large inward episodes (open arrow points to expanded trace of a single burst) with superimposed fast (9.5 Hz) stereotypic discharges intermingled with much slower, composite spontaneous postsynaptic currents (sPSCs; see expanded timebase averages during one burst shown in Fig. 1*A*). Since the fast discharges possessed all the characteristics of action potentials generated in nearby HMs and transmitted to the voltage-clamped HM via gap junctions (Sharifullina *et al.* 2005), they were referred to as spikelets (Long *et al.* 2004, 2005). During the interburst interval, sPSCs had higher frequency (2.3 ± 0.3 Hz *versus* 1.2 ± 0.2 Hz; $n = 33$; $P < 0.005$) and larger amplitude (−69 ± 11 pA *versus* −40 ± 4 pA; $n = 33$; $P < 0.05$) than in control, although the cell input resistance did not change significantly (150 ± 14 MΩ *versus* 177 ± 21 MΩ in control; $n = 33$; $P > 0.05$).

The TBOA-evoked bursts had −319 ± 36 pA average amplitude, 136 ± 14 s period (with 25 ± 6% coefficient of variation; CV) and average burst duration of 35 ± 2 s ($n = 29$). The scatter plots of Fig. 1*B* show that burst period or duration had no relation to burst amplitude. Bursts could be recorded with either current or voltage clamp configuration at the same membrane potential (Fig. 1*C*). Current clamp records (top record in Fig. 1*C*) showed that bursts appeared as large depolarizing waves with spike activity and time course analogous to the burst currents (bottom trace in Fig. 1*C*). Washout with Krebs solution after application of TBOA lasting < 20 min blocked bursting in approximately 10 min (not shown).

Bursts induced by TBOA were sensitive to changes in cell membrane potential between −100 and +40 mV (Fig. 1*D*). They reversed near 0 mV and became outward currents at positive values (Fig. 1*D*), suggesting that burst suppression near 0 mV was not due to deactivation of HM voltage-dependent conductances. Figure 1*D* (bottom) presents the average current–voltage relation for bursts which had a null potential at +10 mV.

Since certain glutamate uptake blockers can have agonist action on glutamate receptors (Danbolt, 2001), we explored whether TBOA could alter currents elicited by brief puffer applications of the non-transportable

glutamate agonist AMPA. As shown in Fig. 1*E*, the amplitude of the AMPA-induced currents was not changed in the presence of TBOA, thus indicating that the uptake blocker did not bind to AMPA-sensitive receptors.

In 70 HMs, despite the fact that TBOA elicited an inward current (-47 ± 6 pA) and increased the frequency (2.9 ± 0.2 *versus* 1.7 ± 0.2 Hz; $P < 0.005$) and amplitude (-98 ± 9 *versus* -47 ± 3 pA; $P < 0.005$) of sPSCs, no bursting was apparent for at least 20 min continuous application of this agent. These cells were therefore regarded as non-bursters. Unlike bursters, non-bursters showed a significant fall in input resistance in the presence of TBOA (132 ± 9 *versus* 169 ± 10 MΩ in control, $n = 34$; $P < 0.002$). Seven of these cells did, however, generate burstlets similar to those evoked by application of an mGluR agonist (Sharifullina *et al.* 2005).

Bursting was facilitated by synaptic inhibition block

Because bursting due to glutamate uptake block was present in a minority of HMs only, it seemed possible that synaptic inhibition mediated by glycine and GABA might have curtailed the onset of this activity. When synaptic inhibition was suppressed by strychnine and bicuculline (Donato & Nistri, 2000; Marchetti *et al.* 2002), subsequent application of TBOA produced bursts in 47% of tested cells (23/49), as exemplified in Fig. 2*A*. In this condition, it was possible to observe pharmacologically isolated glutamatergic currents (see example of averaged events in the inset to Fig. 2*A*) which exhibited larger amplitude and slower decay in the presence of TBOA (full details about the properties of these events are in Table 1). Note that pharmacologically isolated synaptic events had much slower kinetics than spikelets and displayed variable

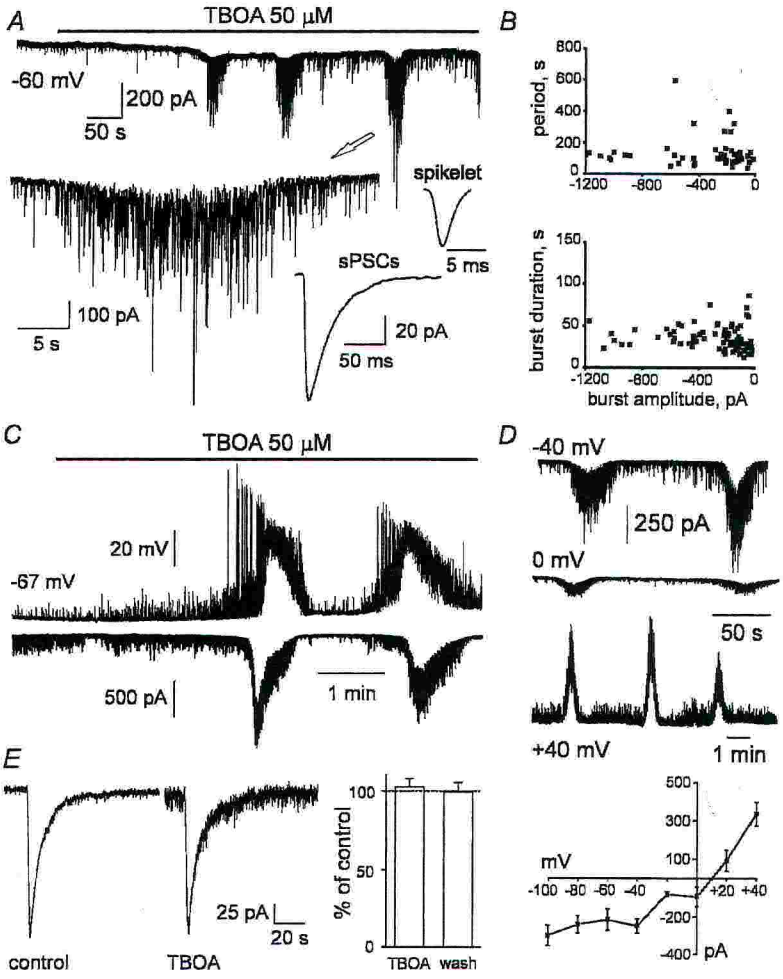

Figure 1. Bursting induced by TBOA (50 μM) application
A, sample record of HM voltage clamped at −60 mV (patch pipette containing Cs and QX-314), demonstrating emergence of bursts over a slow inward current. One burst (open arrow) is shown at higher gain and faster speed to depict its components that include averaged spikelets and composite sPSCs. Vertical calibration for sPSCs applies also to spikelets. *B*, scatter plots of burst period (top) and duration (bottom) for varying burst amplitudes. Note lack of correlation between these parameters. *C*, TBOA-induced bursting has a similar time course under current- (top) or voltage- (bottom) clamp conditions at the same membrane potential (two different cells both recorded with KCl-filled electrodes). *D*, voltage dependence of TBOA-evoked bursts (same cell as in *A*), indicating that burst currents became outwards at positive potentials. The inset shows average current amplitude–voltage plots for bursts recorded from 11 HMs. *E*, example of five averaged inward currents induced by puffer application (10 ms) of AMPA to HMs in control solution or in the presence of TBOA in the interval between bursts. The histograms summarize the AMPA response amplitude in TBOA solution as percentage of control (in Krebs solution containing strychnine and bicuculline to avoid AMPA-mediated release of glycine and GABA) and after washout of TBOA. No significant difference was found ($n = 6$ HMs). Error bars are the standard error of the means.

Table 1. Characteristics of glutamatergic spontaneous postsysnaptic currents (sPSCs) in the presence of strychnine and bicuculline

		Control	DL-TBOA	DL-TBOA+ D-APV	DL-TBOA + SYM 2206
Amplitude (pA)		−12.9 ± 0.7 ($n = 42$)	−16.1 ± 1.1* ($n = 30$)	−12.4 ± 1.3 ($n = 7$)	−12.7 ± 0.5 ($n = 5$)
Frequency (Hz)		0.55 ± 0.11 ($n = 42$)	1.71 ± 0.20** ($n = 30$)	0.727 ± 0.2 ($n = 7$)	1.38 ± 0.57* ($n = 5$)
Decay time constant (monoexponential) (ms)	τ	8.7 ± 0.7 ($n = 14$)	16.8 ± 5.7 ($n = 3$)	16.0 ± 3.2* ($n = 1$)	—
Decay time constants (biexponential) (ms)	τ_1	9.1 ± 1.8	17.7 ± 0.9*	8.3 ± 2.2	12.5 ± 2.2
	τ_2	64.4 ± 14 ($n = 11$)	69 ± 18.7 ($n = 22$)	42.8 ± 27.2 ($n = 6$)	38.2 ± 8.5 ($n = 5$)

n = number of cells. *$P < 0.05$, **$P < 0.005$.

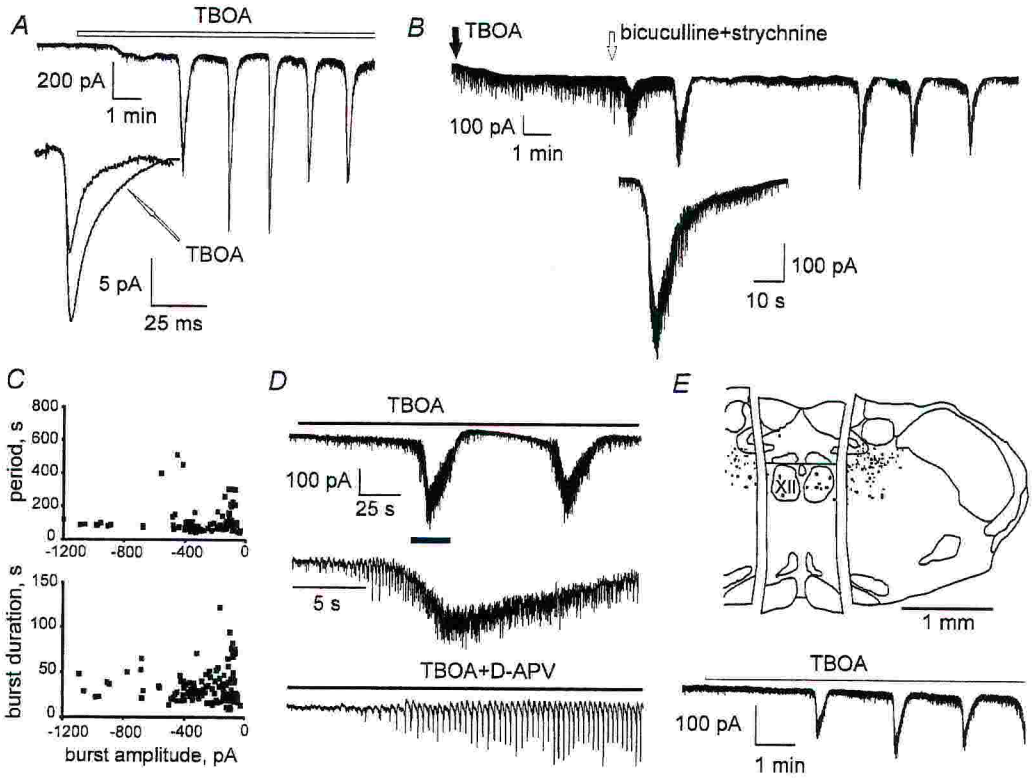

Figure 2. Characteristics of TBOA-evoked bursts in strychnine and bicuculline solution
A, in the continuous presence of strychnine (0.4 μM) and bicuculline (10 μM), TBOA produces a slow inward current and repeated bursts (−60 mV holding potential). In the interburst intervals composite glutamatergic sPSCs (see inset for averaged responses before ($n = 214$ events) and after adding TBOA ($n = 600$ events)) are largely increased and prolonged. *B*, example of a non-bursting HM after TBOA application (filled arrow) that generates bursts after adding strychnine and bicuculline (open arrow). One burst is shown at higher gain. *C*, scatter plots of burst period or durations *versus* burst amplitude. Note lack of correlation. *D*, in the presence of strychnine and bicuculline (−60 mV holding potential), TBOA induced bursting (top trace) with repeated oscillations (middle record shows, at faster speed, one burst indicated by horizontal bar) that are more evident after application of D-APV (50 μM; bottom trace). *E*, the example shows that removal of the lateral regions of the brainstem slice (see scheme) does not prevent TBOA-induced bursting in strychnine and bicuculline solution (holding potential = −60 mV). All records were obtained with CsCl- and QX-314-filled electrodes.

amplitude in contrast with the stereotypic size of spikelets (Sharifullina *et al.* 2005). In the presence of strychnine and bicuculline, the baseline inward current evoked by TBOA on bursting HMs was -57 ± 9 pA ($n = 23$).

In 13/70 HMs that did not burst in the presence of TBOA alone, subsequent application of strychnine plus bicuculline brought about bursting. Hence, although strychnine and bicuculline facilitated the incidence of TBOA bursting, there was still a group of HMs which did not burst despite block of synaptic inhibition (in such cells the steady inward current induced by TBOA was -32 ± 7 pA). In general, the TBOA-evoked bursting during synaptic inhibition block was similar to the one in control solution (-308 ± 33 pA amplitude, 122 ± 11 s period with $21 \pm 4\%$ CV, and 34 ± 2 s duration; $n = 39$). Neither burst period nor duration bore a relation to burst amplitude (Fig. 2*C*). In seven HMs, burstlets, comprising fast inward oscillations followed by a slower outward component were present (Fig. 2*D*, middle trace) and were more clearly detectable after blocking bursts with D-APV (Fig. 2*D*, bottom record).

On seven HMs we also tested the glutamate uptake inhibitor PDC (100 μM; a concentration fully inhibiting glutamate transporters; Shigeri *et al.* 2004) that evoked a slow inward current (-49 ± 8 pA) without triggering burst activity.

Ablation of the reticular formation

To establish if bursting required an extensive circuitry comprising the reticular formation, we resected regions of the slice immediately lateral to the nucleus hypoglossus (scheme in Fig. 2*E*). On 14 HMs (one in each reduced slice), TBOA did not evoke bursting activity. Subsequent application of bicuculline and strychnine turned six cells into bursters (43% of all tested cells; see Fig. 2*E*, lower panel). Bursts had -160 ± 22 pA amplitude, 120 ± 17 s period ($22 \pm 8\%$ CV) and 23 ± 1 s duration that was significantly shorter than in intact slices ($P = 0.017$).

Role of Ca^{2+} in TBOA-evoked bursting

It seemed useful to explore the spatiotemporal distribution of bursting HMs within the TBOA-treated slices. For this purpose we studied changes in intracellular Ca^{2+} ($[Ca^{2+}]_i$) after loading slices with the membrane-permeable fluorescent Ca^{2+} indicator Fluo-3 AM and maximizing bursting occurrence with application of strychnine and bicuculline. Figure 3*A* shows an example of these experiments in which $[Ca^{2+}]_i$ changes were recorded from 10 bursting HMs, the distribution of which in the slice is shown in Fig. 3*B*. TBOA induced a gradual rise in HM baseline $[Ca^{2+}]_i$, and triggered the onset of repetitive Ca^{2+} signals. Despite their widespread topography within the slice (Fig. 3*B*), bursting HMs generated transients strongly correlated as indicated by the cross-correlation plot (Fig. 3*C*) for the 10 HMs of Fig. 3*A*. For example, the cell labelled as '1' (Fig. 3*A*) was 287 μm apart from cell 2, yet they both generated synchronous $[Ca^{2+}]_i$ transients. In each cell, bursting developed after the baseline rise had reached an apparent plateau. While the amplitude of $[Ca^{2+}]_i$ transients was variable because of dissimilar dye loading among HMs, their period was 52 ± 3 s ($CV = 13 \pm 2\%$) with average duration of 29 ± 1 s ($CV = 18 \pm 1\%$; $n = 6$ slices; 60 HMs in total). Hence,

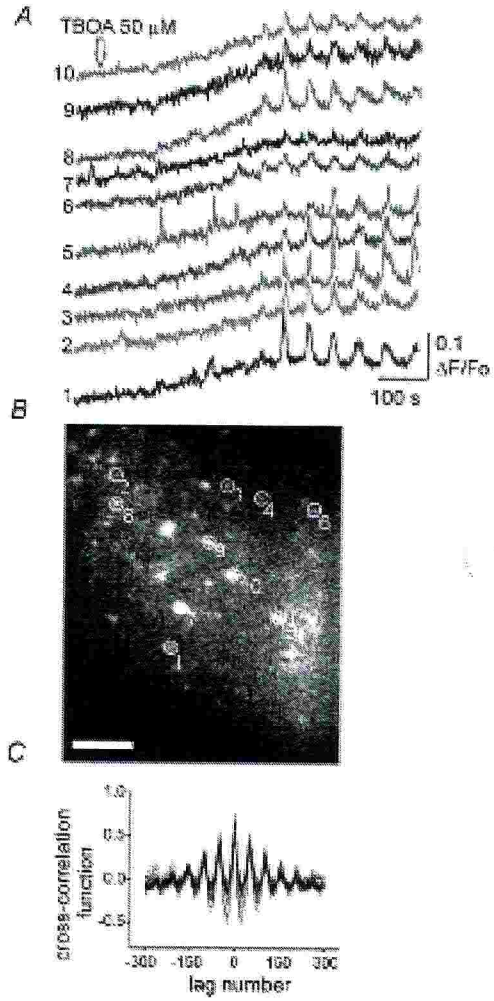

Figure 3. Rhythmic changes in $[Ca^{2+}]_i$ evoked by application of TBOA

A, example of records of $[Ca^{2+}]_i$ changes taken from 10 HMs distributed within the same slice preparation (*B*, where each circle indicates a different cell). Note that, after a slow rise in baseline, all 10 motoneurons developed rhythmic changes in $[Ca^{2+}]_i$ Bar = 100 μm. *C*, plot of superimposed cross-correlation functions for the 10 HMs shown in *A* and *B*. Note strong synchrony of $[Ca^{2+}]_i$ signals. Recording made in the continuous presence of bicuculline and strychnine.

TBOA application induced rhythmic changes in $[Ca^{2+}]_i$, which occurred synchronously.

We further explored the role of Ca^{2+} in TBOA-evoked bursting by applying the Ca^{2+} chelator BAPTA (20 mM) to single HMs via the patch pipette: in this case bursting could still occur (4/16 cells). Bursts were attenuated by the Ca^{2+} channel antagonist nifedipine (20 μM; $n = 4$) that decreased burst amplitude ($59 \pm 6\%$) without changing period or duration (regardless of the presence of strychnine and bicuculline). Finally, we tested the effect of the cell-permeable BAPTA AM (50 μM) using the following protocol: we first established that at least two motoneurons in each slice exposed to TBOA (50 μM; 7 min; strychnine and bicuculline solution) could generate bursting, then TBOA was washed out for 10 min and BAPTA AM applied for 30 or 60 min, and then washed out for 10 min. HMs were again patch clamped and TBOA re-applied for up to 25 min. In four HMs treated with BAPTA AM for 30 min, only one generated delayed bursts in the presence of TBOA (see BAPTA AM figure in Supplemental material). On five HMs treated with BAPTA AM for 60 min, no bursting could be observed.

Pharmacology of bursting

Once bursting was established, it was always fully suppressed by TTX (1 μM; $n = 17$; Fig. 4*A*) while the steady inward current persisted (-31 ± 7 pA). Table 2 shows that miniature glutamatergic currents (mPSCs) in TBOA solution had slower decay with otherwise unchanged characteristics. Figure 4*B* indicates that the gap junction blocker carbenoxolone (100 μM) completely

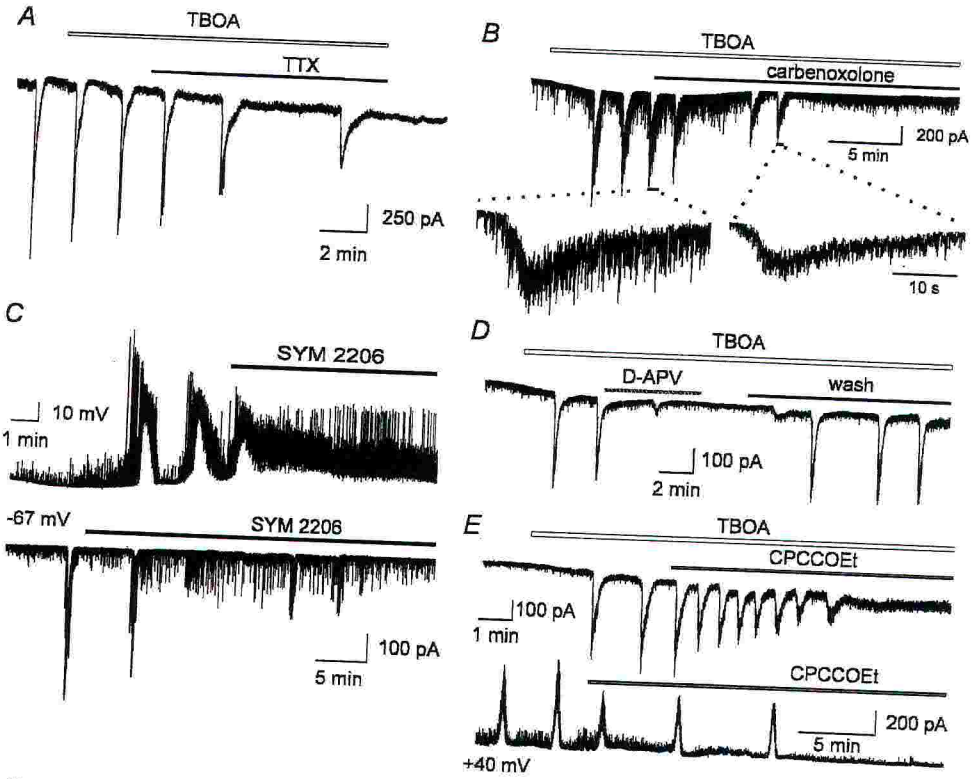

Figure 4. Pharmacology of TBOA-induced bursting
A, in the presence of strychnine and bicuculline, TBOA induces bursts that are suppressed by TTX (1 μM). KCl-filled patch pipette. *B*, in Krebs solution TBOA-evoked bursts are blocked by carbenoxolone (100 μM). The two horizontal bars show one single burst before carbenoxolone with fast discharges (spikelets) and the last burst during carbenoxolone when fast discharges are absent. CsCl-filled patch pipette. *C*, in Krebs solution (KCl-filled electrodes), TBOA-dependent bursts are blocked by the AMPA antagonist SYM 2206 (20 μM) leaving a background of high-frequency activity either in current (top trace) or in voltage (bottom trace) clamp (same membrane potential; −67 mV). *D*, in the presence of strychnine and bicucculline, TBOA-elicited bursts are reversibly suppressed by applying the NMDA receptor antagonist D-APV (50 μM). KCl-filled patch pipette. *E*, top, in the presence of strychnine and bicuculline TBOA-induced bursts are blocked by the selective mGluR1 antagonist CPCCOEt (100 μM). Bottom, in a different cell bathed in standard solution, CPCCOEt (100 μM) blocks TBOA bursting even when the cell is held at +40 mV, and displays outward burst currents. CsCl and QX-314-filled patch pipette.

Table 2. Effect of TBOA on glutamatergic mPSCs

		Control	dl-TBOA
Amplitude (pA)		−10.9 ± 1.3 (n = 17)	−11.2 ± 1.0 (n = 17)
Frequency (Hz)		0.28 ± 0.1 (n = 17)	0.18 ± 0.03 (n = 17)
Decay time constant (monoexponential) (ms)	τ	7.2 ± 0.7* (n = 16)	11.2 ± 0.8* (n = 14)
Decay time constants (biexponential) (ms)	τ_1	4.9	8.6 ± 2.1
	τ_2	32.2 (n = 1)	45.4 ± 29.0 (n = 3)

All data were obtained in the presence of strychnine, bicuculline and TTX. n = number of cells. *$P < 0.05$.

abolished bursting activity and associated spikelets (compare responses in the inset to Fig. 4*B*). However, on average the baseline inward current evoked by TBOA was not significantly changed (−5 ± 11 pA; n = 9) by carbenoxolone, the action of which was present even when outward burst currents were observed at +40 mV membrane potential, or in the presence of strychnine and bicuculline (n = 4). Further support for the role of electrical coupling in bursting was obtained by simultaneous double patch recording from two HMs as exemplified in Fig. 5*A*, in which, in the presence of TBOA (in strychnine plus bicuculline solution), one cell was recorded under voltage clamp at −61 mV (top) and the neighbouring one under current clamp at −48 mV (bottom). The inward currents (−40 pA) were associated with depolarizing bursts in the nearby motoneuron which generated repeated firing. Taking the records during bursts and analysing them for their cross-correlation (Fig. 5*B*) demonstrated event synchronicity.

Glutamate antagonists were found to be effective in blocking bursting, regardless of the presence of strychnine and bicuculline. In particular, the selective AMPA receptor antagonist SYM 2206 (10–20 μM; n = 6) suppressed bursting (Fig. 4*C*, top voltage clamp, bottom current clamp), although excitation with high-frequency sPSCs and spikes persisted in standard solution. The blocking action with residual high level of sPSCs was also observed with CNQX (20 μM; n = 4). In the presence of SYM 2206 or CNQX the baseline inward current caused by TBOA remained virtually unchanged (3 ± 5 pA change; n = 15). The NMDA receptor antagonist APV (50 μM; n = 7) completely (and reversibly) eliminated TBOA-evoked bursting as shown in Fig. 4*D*, although it did not change the inward current induced by TBOA (1 ± 10 pA; n = 7). Table 1 lists changes in sPSC kinetics in the presence of SYM 2206 or D-APV. CPCCOEt is a selective antagonist for the mGluR1 subtype of group I mGluRs (Schoepp *et al.* 1999). While application of CPCCOEt (100 μM) did not change the slow current evoked by TBOA (−11 ± 13 pA; n = 7), it consistently blocked bursting in seven HMs (Fig. 4*E*) even when cells were clamped at +40 mV (bottom trace of Fig. 4*E*).

Time course of bursting

Although the effect of TBOA was reversible if applied for less than 20 min, longer exposure to this agent was

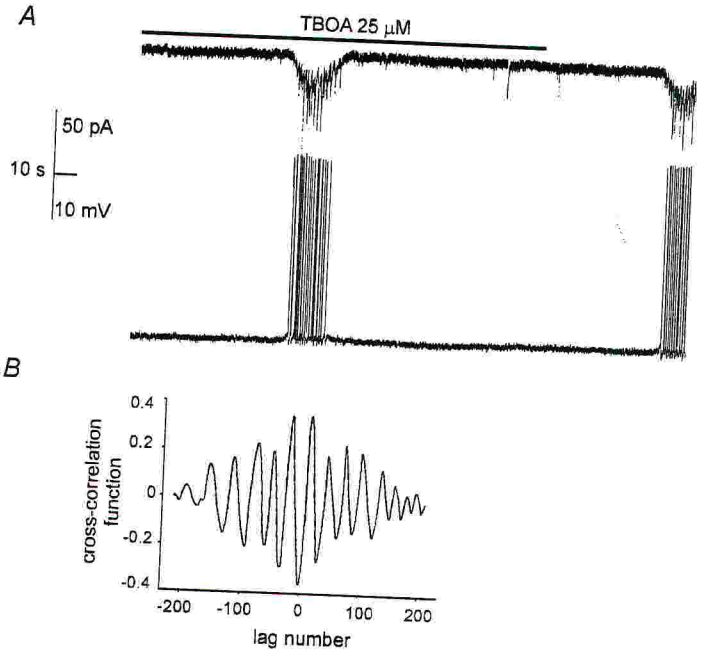

Figure 5. Double recording from HMs of TBOA-evoked bursting
A, sample traces in the presence of TBOA (in strychnine and bicuculline solution) showing recording from two adjacent HMs in the same slice. One cell (top) is under voltage clamp (−61 mV), while the other one is under current clamp (−48 mV). Bursting is observed to occur concomitantly as large burst currents (top) in association with depolarizing bursts with superimposed repeated firing of action potentials (bottom). *B*, cross-correlogram analysis of records taken during each burst event to demonstrate synchronicity between these two cells.

deleterious for HMs as shown in the example of Fig. 6*A* depicting the temporal evolution of the action of TBOA in strychnine and bicuculline solution. After 35 min application, the HM expressed a large inward current and became leaky, indicating cell deterioration without recovery. Monitoring the time profile of $[Ca^{2+}]_i$ changes simultaneously in several HMs allowed us to discover whether any sign of cellular damage, like an irreversible large rise in $[Ca^{2+}]_i$, was a common phenomenon. To this end, we performed continuous, long-lasting imaging (60 min) as exemplified in Fig. 6*B*, in which 10 HMs were recorded during sustained application of TBOA plus strychnine and bicuculline (their location in the slice is shown in Fig. 6*C*). HMs labelled 1–3 had minimal $[Ca^{2+}]_i$ rise and minimal bursting after applying TBOA, while HMs 4–6 displayed a short cycle of low-amplitude bursts. HMs 7–10 showed a large, irreversible increment of $[Ca^{2+}]_i$ baseline together with bursting activity. We analysed the cross-correlation of $[Ca^{2+}]_i$ transients at the early (8–14 min) and late (26–32 min) stages of TBOA application. The early transients had good cross-correlation for HMs 4–10 (CCF = 0.59 ± 0.08), although the CCF later fell to 0.25 ± 0.03, indicating disorganized discharges within the slice. The implication that sustained application of TBOA caused excitotoxic damage to HMs was then quantitatively evaluated with histochemical techniques.

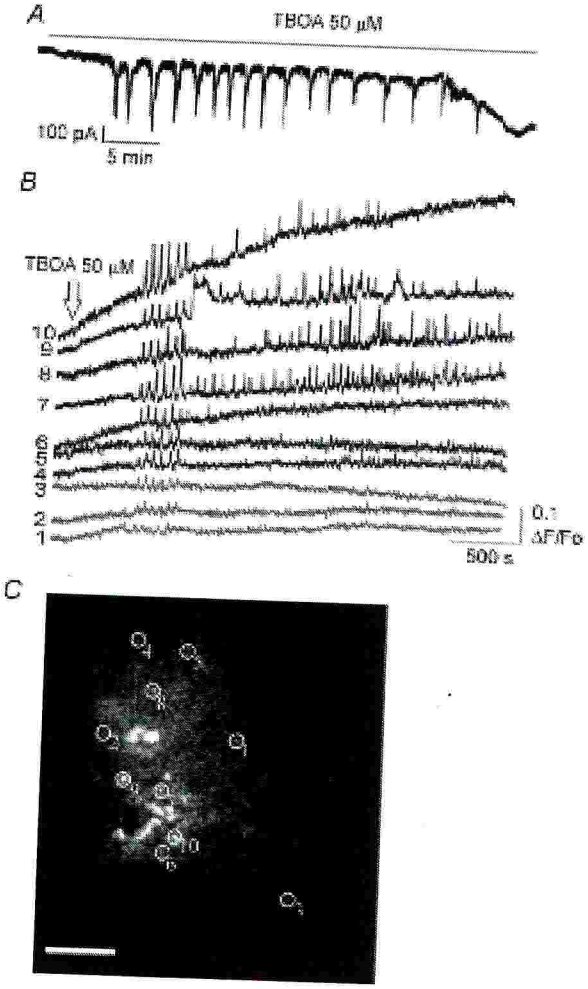

Figure 6. Time course of TBOA-induced bursting
A, example of HM (recorded with CsCl and QX-314-filled pipette; bathing solution contains strychnine and bicuculline) under voltage clamp showing the action of TBOA with early inward current, bursting and final deterioration of the cell (35 min later) with onset of very large inward current and loss of membrane resistance. *B*, simultaneous Ca^{2+} imaging from 10 HMs (indicated in *C* with corresponding numbers) following TBOA application in strychnine and bicuculline solution to show evolution and topography of bursting over 68 min of continuous recording. Bar = 100 μm.

Histochemical observations

For quantitative analysis of motoneuron survival after TBOA application, we first wished to validate that, within the nucleus hypoglossus, large (> 20 μm cell body diameter) cells were indeed HMs. Hence, we used an antibody against ChAT to map HMs, as these are prototypical cholinergic neurons. In accordance with previous studies, as shown in Fig. 7*A* (middle), ChAT-positive neurons were large cells (with a large nucleus of 108 ± 20 μm^2 area; $n = 50$) densely packed within the nucleus hypoglossus. The identification of large cells as motoneurons was confirmed by staining them with the motoneuron marker SMI32 (Fig. 7*A*, left). However, both histochemical methods relied on fixed tissue and permeabilized cells to enable intracellular antibody-based staining. We wished to quantify motoneuron excitotoxicity in unfixed specimens using a standard method based on staining of dead cells with the nuclear dye PI, which penetrates inside cells only after their membrane disruption (Kristensen *et al.* 2001; Bonde *et al.* 2003; Babot *et al.* 2005; Bosel *et al.* 2005). Figure 7*A* (right) shows cells stained with PI within the nucleus hypoglossus. By counting just cells > 20 μm diameter within the area indicated in Fig. 7*D*, we therefore restricted our measurements to damaged HMs. The global number of cells (intact as well as damaged) within each section was estimated with the cell-permeable dye Hoechst 33342. As depicted in Fig. 7*B* (top left), after incubation in Krebs solution a few HMs were PI(+), in keeping with the inevitable consequence of tissue slicing. After 1 h exposure to TBOA the number of PI(+) cells was larger (top middle), an effect minimized when TBOA was applied in the presence of SYM 2206 (top right). Figure 7*C* quantifies these observations: whereas in Krebs solution about one-third of HMs were PI(+) (34 ± 1% of the Hoechst 33342-stained neurons within selected area, $n = 6$ slices), there was a significant increase in the number (46 ± 2%; $n = 6$) of PI(+) HMs with

TBOA application, an effect absent when D-APV (50 μM; $33 \pm 1\%$, $n = 7$), SYM 2206 (20 μM; $37 \pm 1\%$, $n = 5$), carbenoxolone (100 μM; $36 \pm 2\%$, $n = 6$) or CPCCOEt (100 μM; $30 \pm 1\%$, $n = 6$) were incubated in the presence of TBOA.

Discussion

One unexpected finding of the present study was that the glutamate uptake blocker TBOA triggered a novel type of electrical bursting of HMs due to the complex interplay of various classes of glutamate receptor, and apparently supported by gap junctions. TBOA also produced excitotoxicity in HMs which was prevented by the same drugs that blocked bursting. Our data thus suggest that this form of bursting was the hallmark of runaway excitation leading to motoneuron death.

Glutamate transporters: excitation and excitotoxicity

In the brain the extracellular concentration of the excitatory neurotransmitter glutamate is tightly controlled

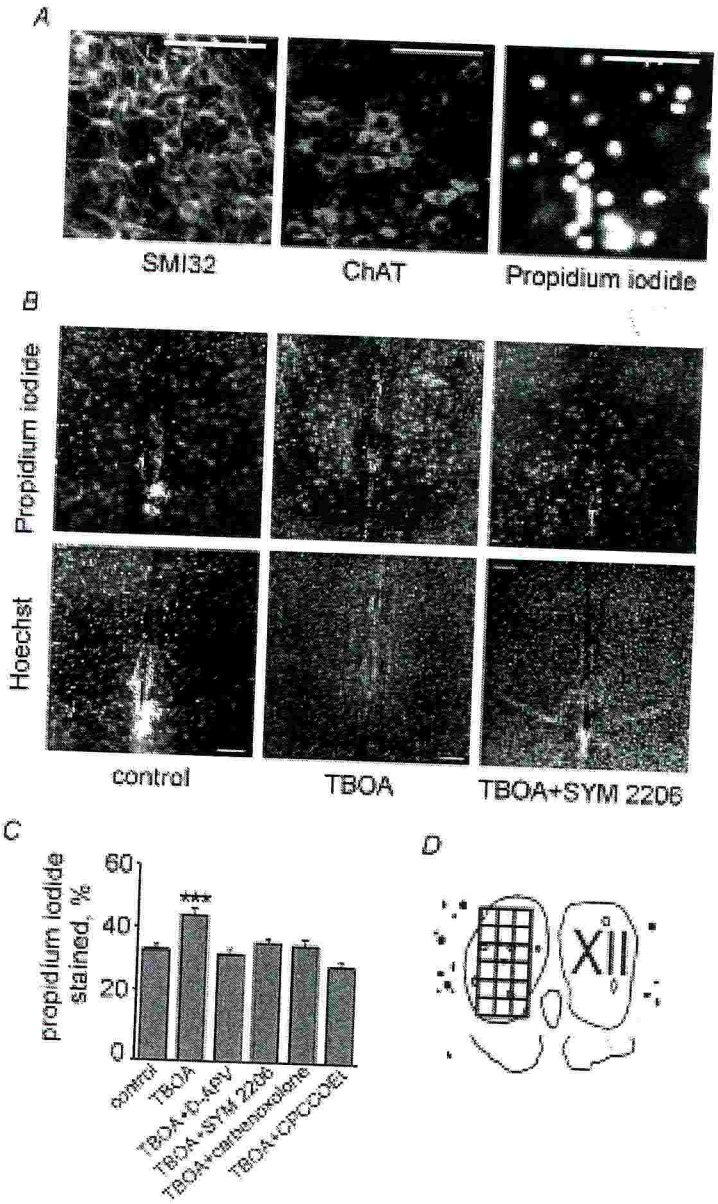

Figure 7. Excitotoxic damage by TBOA application
A, example of immunocytochemical identification of HMs with the SMI32 motoneuron marker (left) and the ChAT immunopositivity (middle). PI(+) HMs are shown on the right after 1 h TBOA application. In each panel the calibration bar is 100 μm. *B*, examples of fluorescent cell counts after staining with PI (top row) or Hoechst 33342 (bottom row) in various experimental protocols ranging from control Krebs (left) to TBOA (middle), and TBOA + SYM 2206 (right). In each panel PI(+) cells indicate dead motoneurons. Calibration bars are 100 μm (bottom rows) and apply to top panels as well. *C*, histograms quantifying the number of dead neurons (PI(+)) in various experimental protocols. TBOA significantly increases the number of PI(+) HMs, an effect absent when it is incubated together with D-APV, SYM 2206, carbenoxolone, or CPCCOEt, as the values are not different from control values that reflect cells damaged by the brain-slicing preparation. For each histogram the range of counted neurons was 239–388. Data are expressed as percentage of PI(+) cells with respect to those stained with Hoechst 33342. $^{***}P < 0.0005$ *D*, schematic diagram of the grid arrangement positioned over the nucleus hypoglossus to count HMs for histological purposes. Error bars are the standard error of the means.

by a family of membrane transporters predominantly expressed by glia and generating electrogenic signals due to cotransport of ions (Danbolt, 2001; Huang & Bergles, 2004; Shigeri *et al.* 2004). Their role is to regulate the large amount of glutamate released at synapses and to prevent its spillover activating extrasynaptic receptors (Cavelier *et al.* 2005). Because excessive activation of glutamate receptors is excitotoxic to neurons, change in the function and expression of transporters can have important pathogenetic roles in neurodegenerative diseases like ALS (Cleveland & Rothstein, 2001; Rao & Weiss, 2004).

While the full cycle of the transporter operation is usually slower that the duration of glutamatergic synaptic events (Danbolt, 2001), it appears that rapid glutamate binding to the transporter sites is already sufficient to buffer the transmitter synaptic concentration (Bergles *et al.* 1999). To prevent glutamate binding to the transporter and to investigate the impact of glutamate uptake systems on neuronal network functions, it is thus useful to apply a non-transportable, broad-spectrum blocker like TBOA (Danbolt, 2001; Shigeri *et al.* 2004). Conversely, transportable inhibitors like PDC can release endogenous glutamate from neuronal and glial pools (Danbolt, 2001), thus generating complex effects that are quite different from those observed with selective uptake blockers (like TBOA) which are non-competitive as well as non-transportable inhibitors (Danbolt, 2001). It is therefore not unexpected that, unlike TBOA, application of PDC could not evoke rhythmic bursting even though it generated an inward current comparable to the one observed with TBOA administration. It seems likely that widespread release of glutamate at network level was incompatible with burst generation. In support of this notion, we found that bath-applied 100 μM glutamate did not evoke bursting (Marchetti *et al.* 2002; authors' unpublished observation).

The nucleus hypoglossus as an *in vitro* model for studying the role of glutamate uptake

The brainstem nucleus hypoglossus is a compact region in which HMs make up at least 90% of its cell population (Viana *et al.* 1990). HMs are at special risk of glutamate-evoked Ca^{2+}-dependent excitotoxicity because of their expression of Ca^{2+}-permeable AMPA receptors (Del Cano *et al.* 1999; Laslo *et al.* 2001; Essin *et al.* 2002) and because of the large amount of intracellular free Ca^{2+} (Ladewig *et al.* 2003). While the nucleus hypoglossus expresses a higher level of glutamate transporter than any other brainstem nucleus (Medina *et al.* 1996), presumably to reduce these risk factors, it is important to note that deficit in glutamate uptake has been demonstrated in many cases of ALS (Rothstein *et al.* 1992; Cleveland & Rothstein, 2001; Rao & Weiss, 2004), and that the bulbar form of this insidious disease usually starts with early symptoms of tongue muscle impairment (slurred speech, dysphagia, tongue biting, etc.). For these reasons it seemed helpful to study the impact of glutamate transporters on HMs using a brainstem slice preparation as a model, bearing in mind that experimental conditions (motoneuron viability and stability *in vitro*) required the use of a neonatal preparation with intrinsic properties due to the developmental characteristics. With the present model it was unnecessary to seek long-range interaction among various circuits to explain bursting activity, because this phenomenon could be observed even with a reduced slice preparation from which most reticular formation inputs had been removed. This realization prompted us to focus our attention on local mechanisms underlying bursting.

Network origin of TBOA-induced bursting

In our conditions TBOA elicited a novel type of bursting from a number of HMs even when, on all recorded cells, there was an early, steady inward current and changes in synaptic event kinetics. In general, neuronal bursting is by no means a necessary result of uptake block because in other brain areas either synaptic depression (Iserhot *et al.* 2004) or massive depolarization shift (Tsukada *et al.* 2005) develops.

Several features of the TBOA-evoked bursts were analogous to those of the mGluR-dependent bursting we have recently reported following activation of group I mGluRs (Sharifullina *et al.* 2005). Hence, under voltage clamp, each burst was the expression of the depolarization (mainly due to glutamate receptor activity) affecting multiple, interconnected HMs (via gap junctions), and was accompanied by superimposed spikelets and synaptic events. The burst reversal potential near 0 mV, the burst period insensitivity to membrane voltage, and the observation that, under voltage clamp, bursts became outward currents, all indicate that these responses were summated currents mediated by the activation of glutamate receptors on premotoneurons and motoneurons (cf. pharmacological antagonism) rather than of voltage-dependent conductances intrinsic to HMs. These characteristics closely resemble those of disinhibited bursting of rat spinal motoneurons which has a clear network origin (Bracci *et al.* 1996), and are in accordance with the properties of rhythmogenic motor networks (Marder & Calabrese, 1996), to which the nucleus hypoglossus belongs. Burst suppression by TTX also suggests dependence on network-propagated activity. Further support for the network origin of these bursts is supplied by the fact that these phenomena were present even when HMs were recorded with a patch solution containing the Na^+ (and I_h) channel blocker QX-314. Since a large concentration of BAPTA in the

recording pipette could not inhibit bursting, it appears that bursts indeed originated from extensive network excitation which this Ca^{2+} chelator (applied to a single HM) could not switch off. Validation of the network origin of the TBOA-evoked bursts came from imaging $[Ca^{2+}]_i$. HMs generated synchronous, rhythmic changes in $[Ca^{2+}]_i$ riding on a slowly rising basal Ca^{2+}. Nevertheless, because imaging was restricted to superficial HMs in each slice, we could not use this method to quantify the number of bursting HMs.

The origin of Ca^{2+} waves recorded from motoneurons presumably comprised rhythmic intracellular release from internal stores subsequent to persistent activation of mGluRs (Schoepp *et al.* 1999), plus depolarization-dependent Ca^{2+} influx of an oscillatory nature due to the particular properties of HM bursts mediated by gap junctions and recurrent activation of certain K^+ conductances (Sharifullina *et al.* 2005). Of course, transmembrane influx of Ca^{2+} via activated AMPA and NMDA receptors is likely to have contributed to the intracellular Ca^{2+} rises. The heterogeneous origin of $[Ca^{2+}]_i$ signals might explain why rhythmic changes in $[Ca^{2+}]_i$ had a shorter period than electrical bursts, because the dynamics of $[Ca^{2+}]_i$ rise and buffering were possibly controlled by processes different from electrical oscillations, and actually contributed to the composite shape of electrical bursts. Confirmation of the network origin of bursting and its Ca^{2+} dependence was obtained with experiments based on the application of the cell-permeable BAPTA AM to the slice preparation. In this case, after long exposure to this agent to enable intracellular loading and Ca^{2+} buffering, bursting was, in fact, suppressed. Furthermore, simultaneous patch clamp recording from two adjacent HMs showed synchronicity of bursting in keeping with a network origin of this phenomenon.

Gap junctions and synaptic inhibition have opposite effects on TBOA-induced bursting

A process probably required for bursting (and indeed excitotoxicity) was the presence of gap junctions among HMs. These have been demonstrated *in vivo* (Mazza *et al.* 1992) and *in vitro* (Rekling *et al.* 2000*b*; Sharifullina *et al.* 2005) to involve about 40% HMs, approximately the same proportion of cells showing TBOA-dependent bursting. Although the incidence of gap junctions decreases with developmental maturation (Mazza *et al.* 1992), certain connexins responsible for electrical coupling among motoneurons are strongly expressed even in adult brainstem motoneurons (Rekling *et al.* 2000*b*; Honma *et al.* 2004), suggesting that motoneuron coupling can occur even after development is complete. Further studies will be necessary to understand if TBOA-induced bursting occurs in adult HMs with properties analogous to those found in neonatal motoneurons, and whether gap junctions contribute to it.

This type of bursting displayed certain features of gap junction-dependent activity such as appearance of spikelets, and block by carbenoxolone. In the neonatal rat spinal cord, gap junctions among motoneurons have been recently shown to mediate synchronicity of motor discharges (Tresch & Kiehn, 2000). It seems likely that gap junctions among HMs not only had a similar action, but were also responsible for spreading glutamate-dependent excitation once its uptake was inhibited. In fact, Ca^{2+} imaging showed that synchronous bursting could develop between HMs at distant locations within the same slice preparation. It is feasible that in such cases, synchronicity was due to coactivation of local circuits rather than direct electrical coupling between remote HMs. Nevertheless, gap junctions played a major role because their pharmacological block suppressed bursting. Bursting was partly suppressed also by GABA- and glycine-mediated synaptic inhibition because blocking glycinergic and GABAergic transmission increased the likelihood of observing bursting, though the majority of HMs remained non-bursters.

Mechanisms underlying TBOA-induced bursting

Gap junctions were not the only contributors to bursting. AMPA, NMDA and mGluR1 receptors also played an important role because blocking any one of these systems suppressed bursting and excitotoxicity. Previous studies have shown how glutamate uptake block enables activation, by ambient glutamate, of NMDA receptors (Campbell & Hablitz, 2004; Huang & Bordey, 2004) and mGluRs (Brasnjo & Otis, 2001; Huang *et al.* 2004) not normally accessible to synaptic glutamate. We suggest that, through HM gap junctions that allow spread and synchronization of excitation (Sharifullina *et al.* 2005), each glutamate receptor class brought its distinctive, yet complementary contribution. The coincidence of all of them (plus the presence of gap junctions) was the condition necessary for the onset of bursting. A mechanistic hypothesis to account for bursting is provided in Fig. 8 with a schematic diagram to summarize the role of various types of glutamate receptors. Electrical coupling among HMs is proposed to be important for recruiting these cells to bursting and to synchronize their discharges. AMPA receptors were probably responsible for supporting glutamatergic transmission to mediate depolarization of HMs and local network neurons. Although the actual concentration of free glutamate after application of TBOA was unknown, it is likely that it was insufficient to largely desensitize AMPA receptors that have lower affinity than NMDA receptors for glutamate (Danbolt, 2001). When

AMPA-mediated depolarization was pharmacologically inhibited by SYM 2206 or CNQX, high-frequency synaptic events presumably caused by activation of glycine and GABA receptors (Donato & Nistri, 2000; Marchetti *et al.* 2002) persisted, although they were apparently inadequate to activate Mg^{2+}-blocked NMDA receptors. Likewise, mGluRs could not relieve blocked NMDA receptors because they mediate a relatively small inward current even when saturating agonist concentrations are used (Sharifullina *et al.* 2004).

NMDA receptors, that have a high affinity for glutamate and may be activated by its spillover (Cavelier *et al.* 2005), were also necessary to support bursting, presumably via widespread membrane depolarization. It has been previously reported that, after application of TBOA, the neonatal rat cerebral cortex generates NMDA receptor-dependent bursting (Demarque *et al.* 2004). In that case though, the consequence of uptake block is shorter bursting activity unrelated to mGluRs and apparently without neuronal death. It seems likely that the sensitivity of brain regions to TBOA bursting may differ depending on their receptor distribution, uptake efficiency and wiring arrangements.

The third major contributor to busting in the nucleus hypoglossus was the mGluR1 receptor class. Our previous work has demonstrated that activation of such receptors triggers sustained oscillations of rat HMs via a combination of effects including increased release of glutamate, enhanced neuronal resistance and membrane depolarization (Sharifullina *et al.* 2004, 2005). Mere activation of such receptors by an exogenous agonist in Krebs solution is, however, insufficient for this type of bursting, possibly because they generate moderate membrane depolarization only and glutamate uptake protects the network from widespread excitation. When uptake was blocked by TBOA, glutamate acting on these receptors not only facilitated further glutamate release, but it also increased membrane resistance to render neurons electrotonically more compact and thus more sensitive to excitatory inputs. Since strong bursting of rat spinal motoneurons is controlled by processes like cyclic operation of the electrogenic Na^+–K^+ pump and synaptic fatigue (Rozzo *et al.* 2002), it seems feasible that analogous mechanisms were responsible for the termination of single bursts in HMs. A further contributor might be pulsatile release of glutamate during uptake block as suggested for bursts generated in the cerebral cortex (Demarque *et al.* 2004).

Correlation between bursting and excitotoxicity

Continuous electrical recording or Ca^{2+} imaging showed that, after a period of bursting, an irreversible large inward current or baseline $[Ca^{2+}]_i$ rise developed. $[Ca^{2+}]_i$ imaging indicated that bursting became disorganized and asynchronous among HMs. These data thus suggested HM damage. Not all imaged HMs displayed these

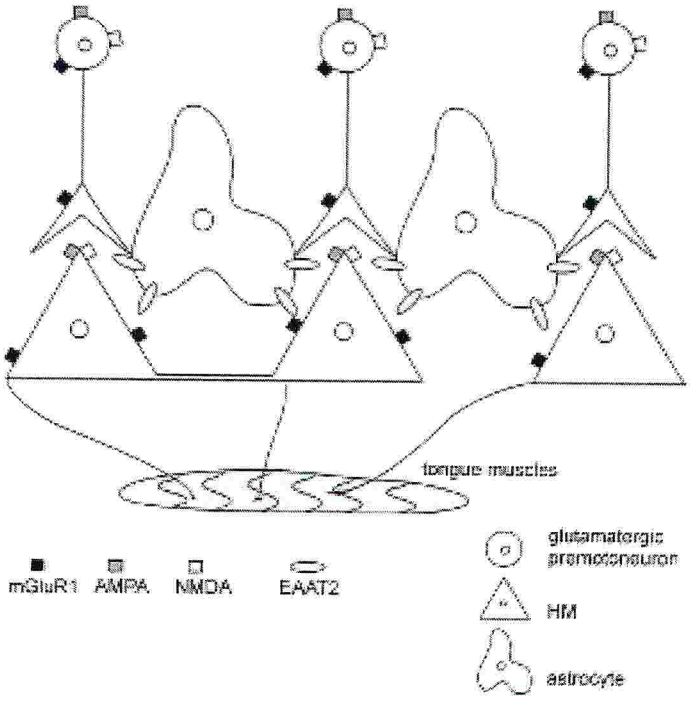

Figure 8. Idealized diagram to account for the mechanism of HM bursting evoked by TBOA
Network premotoneurons (expressing receptors for AMPA, NMDA and mGluR1s) release glutamate onto motoneurons to activate AMPA and NMDA receptors. Astrocytes in close proximity to synapses mop up released glutamate, minimizing its spillover to extrasynaptic mGluR1s. Some HMs are electrically coupled via gap junctions. When astrocyte uptake is blocked by TBOA, build-up of extracellular glutamate activates premotoneurons and motoneurons, an effect amplified by mGluR1 activation, which increases cell input resistance and thus excitability. Gap junctions enhance excitation among coupled HMs and facilitate synchronous bursting. Coincidence of strong glutamate receptor activity with gap junctions therefore enables rhythmic bursting. Non-coupled HMs are much less prone to bursting. The scheme is highly simplified and omits inhibitory interneurons. EAAT2; excitatory amino acid transporter 2.

effects, indicating that, at least within the framework of the present study, there was no generalized excitotoxic death of HMs. Previous experiments with purified cultures of motoneurons have also shown that glutamate excitotoxicity is not a universal phenomenon despite a rise in $[Ca^{2+}]_i$, and that some subsets of motoneurons are more sensitive than others (Fryer *et al.* 1999). It is also interesting that, in ALS, motoneuron degeneration shows patchy disease progression (Rowland & Shneider, 2001; Bruijn *et al.* 2004). While a long exposure to glutamate uptake blockers has been used to generate excitotoxicity in cell cultures (Bonde *et al.* 2003), our report shows significant excitotoxic damage to HMs after applying an uptake blocker for 1 h only.

Using vital staining of HMs to quantify their excitotoxic damage, it was apparent that the number of PI(+) HMs (thus with severe membrane lesion) reached nearly half of the counted ones. On average, this amounted to a significant 43% increase. We propose that the strong, repeated excitation due to bursting was the functional substrate promoting the intracellular metabolic dysfunction leading to the excitotoxic lesion (Rao & Weiss, 2004). In accordance with our model (Fig. 8), we observed that each one of the pharmacological antagonists that blocked bursting also prevented excitotoxicity. Hence, the early inward current of relatively small amplitude induced by TBOA on all HMs was *per se* inadequate to produce HM damage during the time protocol of the present study, because drugs that prevented HM excitotoxicity did not abolish this current. Such a current was probably due to ambient glutamate directly affecting receptors on the HM membrane and did not differ among bursting and non-bursting HMs.

Since the present model was obtained from data collected using neonatal brain slices, it remains to be established whether analogous mechanisms might be applicable to adult brainstem neurons. In principle, this seems likely because glutamate uptake is already expressed in the neonatal brain and readily demonstrated even in primary cultures (Danbolt, 2001). In addition, TBOA neurotoxicity is reported to occur when this agent is bath-applied to neuronal cultures from neonatal animals as much as when it is microinjected into the rat adult brain *in vivo* (Selkirk *et al.* 2005), indicating a widespread potential for neurotoxicity when glutamate uptake is blocked.

A recent theory (Cleveland & Rothstein, 2001) to account for the timing and selectivity of motoneuron killing in neurodegenerative diseases proposes that this process arises from the unfortunate convergence of a series of factors (genetic, environmental, metabolic), all of which are necessary to place motoneurons at risk, whereas each one in isolation is insufficient (the 'convergence model'). Our results suggest that, in the case of vulnerable HMs, there might be additional convergence of molecular (glutamate receptors) and histological (gap junctions) factors that amplify the likelihood of motoneuron death when the uptake of glutamate is impaired.

References

Babot Z, Cristofol R & Sunol C (2005). Excitotoxic death induced by released glutamate in depolarized primary cultures of mouse cerebellar granule cells is dependent on $GABA_A$ receptors and niflumic acid-sensitive chloride channels. *Eur J Neurosci* **21**, 103–112.

Bergles DE, Diamond JS & Jahr CE (1999). Clearance of glutamate inside the synapse and beyond. *Curr Opin Neurobiol* **9**, 293–298.

Bonde C, Sarup A, Schousboe A, Gegelashvili G, Zimmer J & Noraberg J (2003). Neurotoxic and neuroprotective effects of the glutamate transporter inhibitor DL-threo-beta-benzyloxyaspartate (DL-TBOA) during physiological and ischemia-like conditions. *Neurochem Int* **43**, 371–380.

Boone TB & Aldes LD (1984). The ultrastructure of two distinct neuron populations in the hypoglossal nucleus of the rat. *Exp Brain Res* **54**, 321–326.

Bosel J, Gandor F, Harms C, Synowitz M, Harms U, Djoufack PC *et al.* (2005). Neuroprotective effects of atorvastatin against glutamate-induced excitotoxicity in primary cortical neurones. *J Neurochem* **92**, 1386–1398.

Bracci E, Ballerini L & Nistri A (1996). Spontaneous rhythmic bursts induced by pharmacological block of inhibition in lumbar motoneurons of the neonatal rat spinal cord. *J Neurophysiol* **75**, 640–647.

Brasnjo G & Otis TS (2001). Neuronal glutamate transporters control activation of postsynaptic metabotropic glutamate receptors and influence cerebellar long-term depression. *Neuron* **31**, 607–616.

Bruijn LI, Miller TM & Cleveland DW (2004). Unraveling the mechanisms involved in motor neuron degeneration in ALS. *Annu Rev Neurosci* **27**, 723–749.

Campbell SL & Hablitz JJ (2004). Glutamate transporters regulate excitability in local networks in rat neocortex. *Neuroscience* **127**, 625–635.

Cavelier P, Hamann M, Rossi D, Mobbs P & Attwell D (2005). Tonic excitation and inhibition of neurons: ambient transmitter sources and computational consequences. *Prog Biophys Mol Biol* **87**, 3–16.

Cleveland DW & Rothstein JD (2001). From Charcot to Lou Gehrig: deciphering selective motor neuron death in ALS. *Nat Rev Neurosci* **2**, 806–819.

Danbolt NC (2001). Glutamate uptake. *Prog Neurobiol* **65**, 1–105.

Del Cano GG, Millan LM, Gerrikagoitia I, Sarasa M & Matute C (1999). Ionotropic glutamate receptor subunit distribution on hypoglossal motoneuronal pools in the rat. *J Neurocytol* **28**, 455–468.

Demarque M, Villeneuve N, Manent JB, Becq H, Represa A, Ben Ari Y & Aniksztejn L (2004). Glutamate transporters prevent the generation of seizures in the developing rat neocortex. *J Neurosci* **24**, 3289–3294.

Donato R & Nistri A (2000). Relative contribution by GABA or glycine to Cl^--mediated synaptic transmission on rat hypoglossal motoneurons *in vitro*. *J Neurophysiol* **84**, 2715–2724.

Essin K, Nistri A & Magazanik L (2002). Evaluation of GluR2 subunit involvement in AMPA receptor function of neonatal rat hypoglossal motoneurons. *Eur J Neurosci* **15**, 1899–1906.

Fabbro A, Skorinkin A, Grandolfo M, Nistri A & Giniatullin R (2004). Quantal release of ATP from clusters of PC12 cells. *J Physiol* **560**, 505–517.

Fryer HJ, Knox RJ, Strittmatter SM & Kalb RG (1999). Excitotoxic death of a subset of embryonic rat motor neurons *in vitro*. *J Neurochem* **72**, 500–513.

Honma S, De S, Li D, Shuler CF & Turman JE Jr (2004). Developmental regulation of connexins 26, 32, 36, and 43 in trigeminal neurons. *Synapse* **52**, 258–271.

Huang YH & Bergles DE (2004). Glutamate transporters bring competition to the synapse. *Curr Opin Neurobiol* **14**, 346–352.

Huang H & Bordey A (2004). Glial glutamate transporters limit spillover activation of presynaptic NMDA receptors and influence synaptic inhibition of Purkinje neurons. *J Neurosci* **24**, 5659–5669.

Huang YH, Sinha SR, Tanaka K, Rothstein JD & Bergles DE (2004). Astrocyte glutamate transporters regulate metabotropic glutamate receptor-mediated excitation of hippocampal interneurons. *J Neurosci* **24**, 4551–4559.

Ichikawa T & Hirata Y (1990). Organization of choline acetyltransferase-containing structures in the cranial nerve motor nuclei and lamina IX of the cervical spinal cord of the rat. *J Hirnforsch* **31**, 251–257.

Ichikawa T & Shimizu T (1998). Organization of choline acetyltransferase-containing structures in the cranial nerve motor nuclei and spinal cord of the monkey. *Brain Res* **779**, 96–103.

Iserhot C, Gebhardt C, Schmitz D & Heinemann U (2004). Glutamate transporters and metabotropic receptors regulate excitatory neurotransmission in the medial entorhinal cortex of the rat. *Brain Res* **1027**, 151–160.

Jacob DA, Bengston CL & Forger NG (2005). Effects of *Bax* gene deletion on muscle and motoneuron degeneration in a sexually dimorphic neuromuscular system. *J Neurosci* **25**, 5638–5644.

Kitamura S, Nishiguchi T & Sakai A (1983). Location of cell somata and the peripheral course of axons of the geniohyoid and thyrohyoid motoneurons: a horseradish peroxidase study in the rat. *Exp Neurol* **79**, 87–96.

Krieger C, Jones K, Kim SU & Eisen AA (1994). The role of intracellular free calcium in motor neuron disease. *J Neurol Sci* **124**, 27–32.

Kristensen BW, Noraberg J & Zimmer J (2001). Comparison of excitotoxic profiles of ATPA, AMPA, KA and NMDA in organotypic hippocampal slice cultures. *Brain Res* **917**, 21–44.

Ladewig T, Kloppenburg P, Lalley PM, Zipfel WR, Webb WW & Keller BU (2003). Spatial profiles of store-dependent calcium release in motoneurones of the nucleus hypoglossus from newborn mouse. *J Physiol* **547**, 775–787.

Laslo P, Lipski J, Nicholson LF, Miles GB & Funk GD (2001). GluR2 AMPA receptor subunit expression in motoneurons at low and high risk for degeneration in amyotrophic lateral sclerosis. *Exp Neurol* **169**, 461–471.

Lips MB & Keller BU (1999). Activity-related calcium dynamics in motoneurons of the nucleus hypoglossus from mouse. *J Neurophysiol* **82**, 2936–2946.

Long MA, Jutras MJ, Connors BW & Burwell RD (2005). Electrical synapses coordinate activity in the suprachiasmatic nucleus. *Nat Neurosci* **8**, 61–66.

Long MA, Landisman CE & Connors BW (2004). Small clusters of electrically coupled neurons generate synchronous rhythms in the thalamic reticular nucleus. *J Neurosci* **24**, 341–349.

Marchetti C, Pagnotta S, Donato R & Nistri A (2002). Inhibition of spinal or hypoglossal motoneurons of the newborn rat by glycine or GABA. *Eur J Neurosci* **15**, 975–983.

Marder E & Calabrese RL (1996). Principles of rhythmic motor pattern generation. *Physiol Rev* **76**, 687–717.

Mayer ML & Armstrong N (2004). Structure and function of glutamate receptor ion channels. *Annu Rev Physiol* **66**, 161–181.

Mazza E, Nunez-Abades PA, Spielmann JM & Cameron WE (1992). Anatomical and electrotonic coupling in developing genioglossal motoneurons of the rat. *Brain Res* **598**, 127–137.

Medina L, Figueredo-Cardenas G, Rothstein JD & Reiner A (1996). Differential abundance of glutamate transporter subtypes in amyotrophic lateral sclerosis (ALS)-vulnerable versus ALS-resistant brain stem motor cell groups. *Exp Neurol* **142**, 287–295.

Nunez-Abades PA & Cameron WE (1995). Morphology of developing rat genioglossal motoneurons studied *in vitro*: relative changes in diameter and surface area of somata and dendrites. *J Comp Neurol* **353**, 129–142.

Pagnotta SE, Lape R, Quitadamo C & Nistri A (2005). Pre- and postsynaptic modulation of glycinergic and gabaergic transmission by muscarinic receptors on rat hypoglossal motoneurons *in vitro*. *Neuroscience* **130**, 783–795.

Rao SD & Weiss JH (2004). Excitotoxic and oxidative cross-talk between motor neurons and glia in ALS pathogenesis. *Trends Neurosci* **27**, 17–23.

Raoul C, Abbas-Terki T, Bensadoun JC, Guillot S, Haase G, Szulc J, Henderson CE & Aebischer P (2005). Lentiviral-mediated silencing of SOD1 through RNA interference retards disease onset and progression in a mouse model of ALS. *Nat Med* **11**, 423–428.

Rekling JC, Funk GD, Bayliss DA, Dong XW & Feldman JL (2000a). Synaptic control of motoneuronal excitability. *Physiol Rev* **80**, 767–852.

Rekling JC, Shao XM & Feldman JL (2000b). Electrical coupling and excitatory synaptic transmission between rhythmogenic respiratory neurons in the preBotzinger complex. *J Neurosci* **20**, RC113.

Rothstein JD, Martin LJ & Kuncl RW (1992). Decreased glutamate transport by the brain and spinal cord in amyotrophic lateral sclerosis. *N Engl J Med* **326**, 1464–1468.

Rowland LP & Shneider NA (2001). Amyotrophic lateral sclerosis. *N Engl J Med* **344**, 1688–1700.

Rozzo A, Ballerini L, Abbate G & Nistri A (2002). Experimental and modeling studies of novel bursts induced by blocking Na^+ pump and synaptic inhibition in the rat spinal cord. *J Neurophysiol* **88**, 676–691.

Schoepp DD, Jane DE & Monn JA (1999). Pharmacological agents acting at subtypes of metabotropic glutamate receptors. *Neuropharmacology* **38**, 1431–1476.

Selkirk JV, Nottebaum LM, Vana AM, Verge GM, Mackay KB, Stiefel TH, Naeve GS, Pomeroy JE, Petroski RE, Moyer J, Dunlop J & Foster AC (2005). Role of the GLT-1 subtype of glutamate transporter in glutamate homeostasis: the GLT-1-preferring inhibitor WAY-855 produces marginal neurotoxicity in the rat hippocampus. *Eur J Neurosci* **21**, 3217–3228.

Sharifullina E, Ostroumov K & Nistri A (2004). Activation of group I metabotropic glutamate receptors enhances efficacy of glutamatergic inputs to neonatal rat hypoglossal motoneurons in vitro. *Eur J Neurosci* **20**, 1245–1254.

Sharifullina E, Ostroumov K & Nistri A (2005). Metabotropic glutamate receptor activity induces a novel oscillatory pattern in neonatal rat hypoglossal motoneurones. *J Physiol* **563**, 139–159.

Shigeri Y, Seal RP & Shimamoto K (2004). Molecular pharmacology of glutamate transporters, EAATs and VGLUTs. *Brain Res Brain Res Rev* **45**, 250–265.

Tresch MC & Kiehn O (2000). Motor coordination without action potentials in the mammalian spinal cord. *Nat Neurosci* **3**, 593–599.

Tsukada S, Iino M, Takayasu Y, Shimamoto K & Ozawa S (2005). Effects of a novel glutamate transporter blocker, (2S,3S)-3-[3-[4-(trifluoromethyl) benzoylamino] benzyloxy]aspartate (TFB-TBOA), on activities of hippocampal neurons. *Neuropharmacology* **48**, 479–491.

Umbriaco D, Watkins KC, Descarries L, Cozzari C & Hartman BK (1994). Ultrastructural and morphometric features of the acetylcholine innervation in adult rat parietal cortex: an electron microscopic study in serial sections. *J Comp Neurol* **348**, 351–373.

Viana F, Gibbs L & Berger AJ (1990). Double- and triple-labeling of functionally characterized central neurons projecting to peripheral targets studied *in vitro*. *Neuroscience* **38**, 829–841.

Acknowledgements

We are most grateful to Dr Elsa Fabbretti for her collaboration with immunohistochemistry experiments. We also thank Drs Massimo Righi and Micaela Grandolfo for their help with histology, and Dr Sergio Graziosi for software support. This work was supported by a FIRB grant to A.N.

Supplemental material

The online version of this paper can be accessed at:
DOI: 10.1113/jphysiol.2005.100412
http://jp.physoc.org/cgi/content/full/jphysiol.2005.100412/DC1
and contains supplemental material consisting of a figure and legend entitled: Patch clamp recording (under voltage clamp at −65 mV) from HMs in the presence of TBOA (50 μM) in strychnine and bicuculline solution.

This material can also be found as part of the full-text HTML version available from http://www.blackwell-synergy.com

J Physiol 572.2 (2006) pp 323–334

Topical Review

Tuning and playing a motor rhythm: how metabotropic glutamate receptors orchestrate generation of motor patterns in the mammalian central nervous system

Andrea Nistri, Konstantin Ostroumov, Elina Sharifullina and Giuliano Taccola

Neurobiology Sector, CNR-INFM DEMOCRITOS National Simulation Center, and S.P.I.N.A.L. Laboratory, International School for Advanced Studies (SISSA), Via Beirut 4, 34014 Trieste, Italy

Repeated motor activities like locomotion, mastication and respiration need rhythmic discharges of functionally connected neurons termed central pattern generators (CPGs) that cyclically activate motoneurons even in the absence of descending commands from higher centres. For motor pattern generation, CPGs require integration of multiple processes including activation of ion channels and transmitter receptors at strategic locations within motor networks. One emerging mechanism is activation of glutamate metabotropic receptors (mGluRs) belonging to group I, while group II and III mGluRs appear to play an inhibitory function on sensory inputs. Group I mGluRs generate neuronal membrane depolarization with input resistance increase and rapid fluctuations in intracellular Ca^{2+}, leading to enhanced excitability and rhythmicity. While synchronicity is probably due to modulation of inhibitory synaptic transmission, these oscillations occurring in coincidence with strong afferent stimuli or application of excitatory agents can trigger locomotor-like patterns. Hence, mGluR-sensitive spinal oscillators play a role in accessory networks for locomotor CPG activation. In brainstem networks supplying tongue muscle motoneurons, group I receptors facilitate excitatory synaptic inputs and evoke synchronous oscillations which stabilize motoneuron firing at regular, low frequency necessary for rhythmic tongue contractions. In this case, synchronicity depends on the strong electrical coupling amongst motoneurons rather than inhibitory transmission, while cyclic activation of K_{ATP} conductances sets its periodicity. Activation of mGluRs is therefore a powerful strategy to trigger and recruit patterned discharges of motoneurons.

(Received 24 October 2005; accepted after revision 9 February 2006; first published online 9 February 2006)
Corresponding author A. Nistri: SISSA, via Beirut 4, 34014 Trieste, Italy. Email: nistri@sissa.it

The making of a motor rhythm: concerted neuronal interactions produced by a central pattern generator network

Most motor activities (like locomotion, respiration, swallowing, suckling, etc.) require rapid, repeated contractions of selected groups of skeletal muscles. Rather than being simply driven by descending inputs or triggered by peripheral afferents, such motor rhythms are the expression of oscillatory discharges from an ensemble of neurons wired together to generate a coherent motor output. In analogy with networks amply studied in invertebrates, these circuits are collectively termed central pattern generators (CPG).

As far as the locomotor programme is concerned, the identification of the CPG neurons responsible for it and their precise connectivity remain unclear. Nonetheless, various models of CPG operation as well as available experimental evidence assume the existence of a class of interneurons (located ventrally to the spinal central canal) using commissural interneurons to distribute synaptic inputs to left and right motor pools of the leg muscles (Kiehn *et al.* 2000; Grillner & Wallen, 2002; Kiehn & Kullander, 2004). A recent model obtained from the feline spinal cord further distinguishes between rhythm-generating interneurons (the 'clock') which set the pace of locomotion, and the pattern-generating interneurons whose task is to distribute motor commands (of excitatory or inhibitory nature) to various motor pools (Lafreniere-Roula & McCrea, 2005). These motor signals would then be transmitted to motoneurons via

Authors are in alphabetical order since they all contributed equally to this work.

DOI: 10.1113/jphysiol.2005.100610

premotoneurons. Within such a scheme, the role of motoneurons would not be the one of rhythm generation, but of pattern refinement obtained through the activation of certain intrinsic membrane conductances (Kiehn *et al.* 2000; Grillner & Wallen, 2002; Kiehn & Kullander, 2004). Although the topography of the spinal CPG remains elusive, there is broad interest in elucidating the cellular processes which can modulate CPG activity (Grillner *et al.* 2000; Fetz *et al.* 2000).

In the case of respiration, recent studies have highlighted the crucial role of distinct areas of the brainstem like the pre-Bötzinger complex and the parafacial respiratory nucleus as rhythm generators via a complex interaction between local neurons releasing glutamate, GABA or glycine (Greer *et al.* 2006). Such an activity would represent a potent inspiratory drive to accelerate the rapid maturation of motoneurons involved in diaphragm muscle contractions, though motoneurons themselves are not rhythmogenic. Recent investigations using fast Ca^{2+} imaging have shown that, at least in the case of the fetal mouse brain, the central pattern generator for respiration may be more distributed than hitherto supposed as firing of neurons in immature respiratory circuits is a stochastic process, suggesting that the rhythm does not depend on a single pacemaker (Eugenin *et al.* 2006).

The cyclic output of most motor circuits in the spinal cord or brainstem depends on the interplay between the excitation mediated by glutamate acting on ionotropic receptors, the GABA- and glycine-mediated inhibition, and the activity of voltage-sensitive channels (Grillner & Wallen, 2002; Alford *et al.* 2003; Kudo *et al.* 2004; Greer *et al.* 2006). Glutamate also activates metabotropic glutamate receptors (mGluRs) producing long lasting changes in neuronal excitability (Anwyl, 1999) and modulating rhythmic motor patterns generation (Krieger *et al.* 1998; El Manira *et al.* 2002). To illustrate the role of mGluRs as triggers and gain-setters of rhythmic oscillations, we shall discuss as examples the circuits within the lumbar spinal cord and the brainstem nucleus hypoglossus. Thus, spinal motoneurons send rhythmic signals to extensor and flexor muscles of the lower (hind) limbs (during locomotion) while hypoglossal motoneurons (HMs) cyclically contract tongue muscles during respiration, swallowing, chewing, etc. In the latter case rhythmic activity emerges from a single set of motoneurons supplying the tongue muscles, while in the case of the spinal cord alternating activity appears in two distinct sets of motoneuron pools. We shall examine whether mGluRs have a role in both networks to switch on rhythmogenesis that is usually silent.

Central pattern generators: localization

A combination of molecular, genetic and imaging studies has been employed to investigate the distribution of CPG neurons in lumbar spinal cord (Demir *et al.* 2002; Kiehn & Butt, 2003; Kiehn & Kullander, 2004; Hinckley *et al.* 2005; Kullander, 2005). Briefly, networks organizing locomotor activity are distributed throughout the lower thoracic and lumbar regions of the spinal cord. On each spinal side, the ventro-medial part of laminae VII, VIII and X contains the elements responsible for generation of rhythmicity.

Swallowing, sucking and respiration involve rhythmic movements of the tongue driven by synchronously active hypoglossal nuclei. Cunningham & Sawchenko (2000) showed that the main excitatory inputs to the hypoglossal nucleus come from the dorsal medullary reticular column (DMRC) and the nucleus of the tractus solitarius (NTS). The CPG for swallowing includes neurons localized in the NTS (responsible for timing, triggering and shaping the rhythm) and neurons localized in the ventrolateral medulla which sends swallowing commands to different orofaringeal motoneurons including hypoglossal ones (Jean, 2001). Lesion studies have shown that the neuronal networks responsible for NMDA-induced fictive sucking are located in the medulla oblongata (Nakamura & Katakura, 1995). For each inspiratory phase, the hypoglossus nucleus receives a rhythmic excitatory input from brainstem respiratory neurons within the pre-Bötzinger complex which appears to play an important role in the origin of respiration rhythmogenesis (Rekling & Feldman, 1998; Feldman *et al.* 2003).

Different groups of mGluRs

mGluRs are G-protein-coupled receptors that trigger intracellular signalling cascades to modulate neuronal signalling. mGluRs are divided into three groups, depending on sequence homology, transduction mechanisms and pharmacological profiles. The group I comprises mGluR1 and mGluR5, while group II consists of mGluR2 and mGluR3, and group III is made up by mGluR4, mGluR6, mGluR7 and mGluR8.

The group I mGluRs increase intracellular Ca^{2+} levels to activate protein kinase C. Both group II and group III mGluRs are coupled to inhibition of adenylyl cyclase. For reviews of mGluR electrophysiology, pharmacology, structure and second messengers mechanisms see Anwyl (1999), Pin *et al.* (1999), Schoepp *et al.* (1999) and Cartmell & Schoepp (2000). Figure 1 shows the distribution of group I mGluRs in the spinal cord and brainstem as these receptors are the largest group in terms of local expression.

Possible scenarios of mGluR action on synaptic transmission

Approaches to understand the function of mGluRs during motor activity comprise studying either the effects of selective receptor agonists/antagonists on physiological

responses or the phenotype of genetic models with receptor deletion (Aiba *et al.* 1994; Conquet *et al.* 1994; Li & Nattie, 1995; Fundytus *et al.* 2001; Mao *et al.* 2001; Shutoh *et al.* 2002). Another approach is to investigate *in vitro* spinal models which preserve CPG networks and generate rhythmic activities (for example El Manira *et al.* 2002; Whelan, 2003).

One important question is the origin of endogenous glutamate to activate mGluRs. In several brain areas glutamatergic neurons, firing at sufficiently high frequency, release an amount of glutamate that can temporarily overwhelm the normal amino acid uptake systems so that mGluRs are activated by overspill (Min *et al.* 1998; Gegelashvili *et al.* 2000; Reichelt & Knopfel, 2002). In general, even in relatively simple networks *in vitro*, the slow time course of the mGluR-mediated response (~2 s) may reflect the prolonged rise in the concentration of intracellular signalling molecules, which in turn would

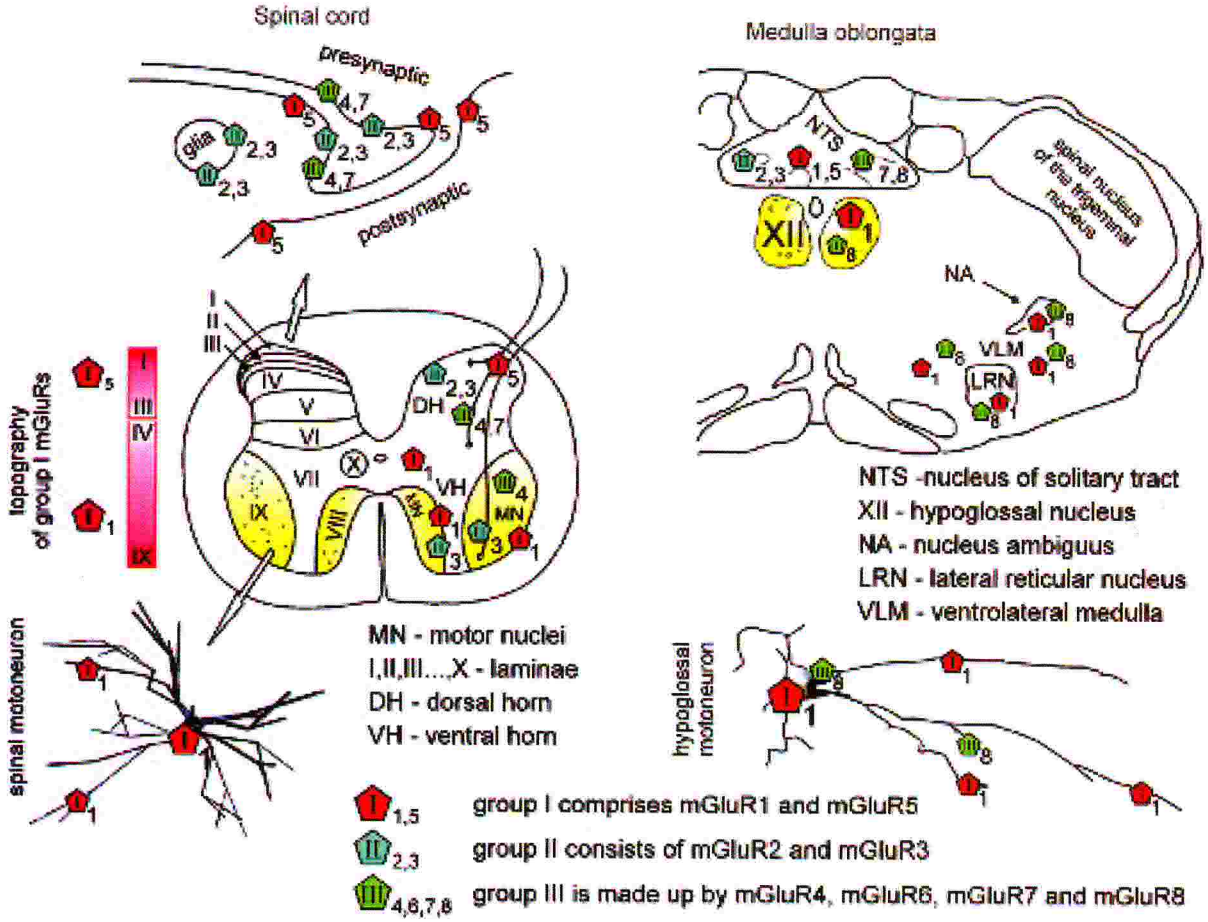

Figure 1. Topography of mGluRs in the spinal cord and brainstem
Left, top scheme shows that the majority of mGluR immunoreactivity is found on the perisynaptic and extrasynaptic plasma membrane of neurons, and partly on glia. Middle, schematic section of the adult rat spinal cord indicates that mGluR5s are densely expressed in laminae I–III of the dorsal horn (DH) with gradual decrease in deeper laminae. About half of vesicle-containing profiles stained for mGluR5 are also positively stained for GABA (Jia *et al.* 1999). mGluR1s are mostly distributed throughout laminae III–X (Berthele *et al.* 1999; Alvarez *et al.* 2000) with patchy immunoreactivity of varying intensity in somata and dendrites of spinal motor nuclei (MN) including motoneurons and interneurons (see inset marked by open arrow) of the ventral horn (VH), and in presynaptic axon terminals (Alvarez *et al.* 1997, 2000). Group II and III are scattered throughout the spinal cord with predominance in the DH (Berthele *et al.* 1999) and even some glial labelling (Ohishi *et al.* 1995; Jia *et al.* 1999; Azkue *et al.* 2000, 2001). In addition, group II mGluR3 mRNA is expressed in the small cells surrounding motoneurons, while group III mGluR4 mRNA is present in the spinal motoneurons (Berthele *et al.* 1999). Right, in the medulla oblongata group I (mGluR1a/5), group II (mGluR2/3) and group III (mGluR7/8) mGluRs (Hay *et al.* 1999; Pamidimukkala *et al.* 2002) show different distribution throughout subnuclei of NTS and of the ventrolateral medulla. Only mGluR1 and mGluR8 subtypes are expressed by hypoglossal motoneurons (XII; Hay *et al.* 1999; Pamidimukkala *et al.* 2002).

promote pooling to activate common ion channel effectors (Mori & Gerber, 2002). It is therefore difficult to suppose that mGluR activity can induce a cycle-by-cycle modulation of relatively faster patterns in motor networks. It seems more likely that such a slow response due to mGluRs modulates neuronal excitability and thus constrains the network ability to generate patterned inputs at a certain frequency. The ability of endogenous glutamate to activate mGluRs may be enhanced by certain experimental *in vitro* conditions like the use of ambient temperature, which reduces the efficiency of glutamate uptake and slows down its diffusion to facilitate interaction with mGluRs (Asztely *et al.* 1997; Kullmann & Asztely, 1998). Nevertheless, since mGluR1 antagonists administered *in vivo* block hyperalgesia (Dolan & Nolan, 2002) or the stimulatory role of glutamate on respiration (Li & Nattie, 1995), it is clear that, even at physiological temperature, endogenous glutamate can activate mGluR1 receptors during intense network activity.

Group I mGluR antagonists do not block glutamatergic transmission evoked by single or low frequency afferent stimulation. Only when repeated network discharges evoke strong release of glutamate, blocking these receptors inhibits electrically induced synaptic transmission (Marchetti *et al.* 2003; Sharifullina *et al.* 2004). These data can suggest two possibilities not mutually exclusive: a fraction of the population of mGluRs is synaptically located (Alvarez *et al.* 2000; Hubert *et al.* 2001; Kuwajima *et al.* 2004), yet because of the intrinsically slow activation process, their contribution to synaptic events comes into action only with sustained neurotransmitter delivery occurs. A second possibility is that group I mGluRs are predominantly extrasynaptic and thus activated by glutamate spillover (Batchelor *et al.* 1994; Alford *et al.* 1995; Scanziani *et al.* 1997; Cochilla & Alford, 1998; Min *et al.* 1998; Huang & Bergles, 2004). While cumulative depolarization of spinal motoneurons evoked by trains of dorsal root stimuli is insensitive to selective blockers of group II or III mGluRs (Taccola *et al.* 2004*a*), the presynaptic location of group III receptors would make them suitable to control nociceptive inputs to the spinal cord dorsal horn (Azkue *et al.* 2001), in analogy with their role in glutamatergic transmission on brainstem auditory neurons (Billups *et al.* 2005). In the case of group II receptors (Azkue *et al.* 2000), their location appears to be mainly extrasynaptic.

Decreased spontaneous locomotor activity occurs in mGluR1$^{-/-}$ mice (Conquet *et al.* 1994), indicating an important role of such receptors in the control of motor patterns. Conversely, genetic models of mGluR2$^{-/-}$ (Yokoi *et al.* 1996), mGluR4$^{-/-}$ (Pekhletski *et al.* 1996), or mGluR6$^{-/-}$ (Takao *et al.* 2000) do not show changes in normal motor activity, indicating that these receptors are not activated by glutamate released during physiological activity in motor circuits. Nevertheless, such receptors may be a target for pharmacological modulation of network activity during pathological conditions (e.g. chronic inflammation and pain; Fisher *et al.* 2002) or after spinal lesion (Mills *et al.* 2002). On the basis of these considerations, the present review is focused on the role of mGluRs in motor networks.

Modulation of the lamprey respiratory and spinal locomotor networks by mGluRs

The lamprey spinal cord preparation is a useful model to study locomotor systems which, like in mammals, are activated by ionotropic glutamate receptors and modulated by mGluRs. Fictive swimming is typically induced by bath-applied NMDA because activation of NMDA receptors gives rise to plateau-like depolarizations suitable for CPG operation (see review by Grillner *et al.* 2000).

It was suggested by Cochilla & Alford (1998) that, in the larval lamprey, presynaptically localized group I mGluRs (activated by sustained release of glutamate) stimulate liberation of Ca^{2+} from ryanodine-sensitive intracellular stores. The enhanced presynaptic intracellular Ca^{2+} plus Ca^{2+} accumulation during repeated neuronal activity might facilitate further glutamate release essential for continuous fictive locomotion (Takahashi & Alford, 2002). In the adult lamprey, activation of group I mGluR1s speeds up locomotor frequency and increases NMDA-induced depolarization (Krieger *et al.* 1998, 2000) by increasing NMDA-induced influx of Ca^{2+} (Krieger *et al.* 2000). Since block of this subtype of mGluRs reduces locomotor frequency (Krieger *et al.* 1998; Kettunen *et al.* 2002), it seems that there is on-going activation of group I mGluR1 during fictive locomotion.

Unlike group I mGluR1s, mGluR5 activity decreases the frequency of NMDA-induced locomotor rhythm, suggesting mGluR5s as contributors to slowing down locomotor activity (Kettunen *et al.* 2002). The precise reason for the discrepancy between the effects of group I mGluR subtype activity remains unclear (El Manira *et al.* 2002). One possibility may reside in the fact that mGluR1 receptors depolarize spinal neurons by inhibiting a leak current to boost membrane depolarization and increase excitability of locomotor networks (Kettunen *et al.* 2003) including facilitation of NMDA receptors. mGluR5 receptors do not alter neuronal membrane potential or resistance, as their action is mainly linked to increasing intracellular Ca^{2+} and generating Ca^{2+} waves (Kettunen *et al.* 2002) which could reduce neuronal excitability via activation of Ca^{2+}-dependent K^+ conductances.

A physiological role for group II and III mGluRs in adult lamprey remains uncertain because such a receptor activity is limited to slight retardation of locomotor frequency and amplitude, possibly by direct depression of the release machinery for glutamate (Krieger *et al.* 1998).

On respiratory networks, block of group I mGluRs reversibly decreases respiratory frequency, while antagonism of group II mGluRs leads to frequency increase; both findings reveal endogenous activation of group I and II during respiration in the adult lamprey (Bongianni *et al.* 2002).

Role of mGluRs in rhythmic activity of the turtle

In vitro brainstem or spinal cord preparations of the turtle can generate rhythmic motor oscillations (Douse & Mitchell, 1990; Guertin & Hounsgaard, 1998*a*; Delgado-Lezama *et al.* 1999). To produce this pattern, it is possible to use either NMDA or cholinergic muscarinic agonists that induce intrinsic oscillations by independent cellular mechanisms (Guertin & Hounsgaard, 1998*b*, 1999). While oscillations ultimately need L-type calcium channel activation, only the oscillations evoked by NMDA/5-HT depend on voltage-sensitive NMDA-activated channels.

Since activation of mGluRs evokes plateau potentials of motoneurons and interneurons by facilitating voltage-activated Ca^{2+} channels (Delgado-Lezama *et al.* 1997; Svirskis & Hounsgaard, 1998; Perrier *et al.* 2002), it seems likely that mGluRs contribute to rhythm generation, though the precise identification of their subtypes remains a matter for future studies. Moreover, group I mGluR1 block suppresses the characteristic hyper-excitability induced by motor network activity (Alaburda & Hounsgaard, 2003).

Cellular mechanisms responsible for group I mGluR effects on excitability of rat spinal and brainstem motor networks

Figure 2 compares and contrasts the effects of group I mGluR activation by the selective agonist 3,5-dihydroxyphenyl-glycine (DHPG) on spinal (top left) or hypoglossal (top right) motoneurons and networks of *in vitro* rat preparations. Figure 2*A* and *B* shows intracellular (I, green) records from spinal motoneurons demonstrating onset of slow rhythmic oscillations (0.2–0.3 Hz) over a background of membrane depolarization, raised input resistance and increased synaptic activity (Marchetti *et al.* 2003). On top of slow oscillations, faster (4–11 Hz) oscillations with frequent spike firing are also apparent (Fig. 2*B* is a faster record of the trace indicated with a horizontal bar in *A*). This phenomenon is accompanied by a larger monosynaptic component of the DR-evoked response and by depression of the slower, polysynaptic phase probably due to facilitation of glycinergic inhibition (Marchetti *et al.* 2003). Recurrent inhibitory postsynaptic potentials (IPSP) due to Renshaw cell activity are, however, depressed (Marchetti *et al.* 2005). Oscillations have a network origin, are not intrinsic to motoneurons, and, because of their synchronicity, cannot evoke fictive standard locomotor patterns. Note that oscillations require mGluR5 activity, while membrane depolarization and resistance increase depend on mGluR1 activation (Marchetti *et al.* 2003).

Also on HMs (under voltage clamp; V, blue) DHPG induces rhythmic oscillations which initially comprise fast discharges (3–5 Hz) evolving into bursts (4–8 Hz) with superimposed fast oscillations (Fig. 2*C*, top trace; Sharifullina *et al.* 2005). The bottom record of Fig. 2*C* (faster timebase) shows the distinct features of fast oscillations and bursts. Bursts induce regular spontaneous firing with no change in input resistance. Approximately 50% of the recorded cells show rhythmic activity after DHPG application. Fast oscillations and bursts are mediated by gap junctions that functionally couple HMs (Sharifullina *et al.* 2005). Likewise, in the rat spinal cord, synchronous oscillations induced by DHPG are also inhibited by the gap junction blocker carbenoxolone, which does not affect fictive locomotor patterns (G. Taccola, unpublished observation).

In the nucleus hypoglossus, bursting depends on mGluR1 rather than mGluR5 receptors and it is paced by cyclic activation of ATP-sensitive K^+ channels (K_{ATP}) (Sharifullina *et al.* 2005). Figure 2*D* shows tight burst coupling between two electrically connected motoneurons under voltage (V, blue, top) or current (C, green, bottom) clamp. Evoked excitatory responses are also enhanced by DHPG. Since on HMs bursting can take place with or without intact synaptic inhibition, it is clear that, in the brainstem, the rhythmogenic network does not involve changes in synaptic inhibition as observed in the spinal cord.

mGluRs tune motor networks in the brainstem and spinal cord

The functional consequences of mGluR1 activation on motor output are exemplified in Fig. 3.

On spinal networks, the spontaneous rhythmic bursts which arise after block of synaptic inhibition ('disinhibited bursting') are shortened and accelerated by 5 μM DHPG to demonstrate that CPG elements express group I mGluR receptors with excitatory function (Fig. 3*A*; Taccola *et al.* 2004*b*). Disinhibited bursting occurs spontaneously via activation of network glutamatergic ionotropic receptors predominantly of the AMPA type, while NMDA receptors simply modulate this pattern (Bracci *et al.* 1996). While disinhibited bursting cannot support locomotion in view of its slow frequency and lack of alternation, the current view is that it originates from the same CPG responsible for locomotion whenever the network brake on excitability is

removed by application of glycine and GABA antagonists (Beato & Nistri, 1999).

Fictive locomotion can be induced by applying excitatory substances like NMDA and serotonin (5-HT) which generate sustained, rhythmic discharges alternating at various segmental levels, with locomotor-like frequency, to activate hindlimb flexors and extensor muscles (Kiehn *et al.* 2000; Kiehn & Butt, 2003; Kiehn & Kullander, 2004). As 5-HT operates via activation of multiple receptor classes with inhibitory and excitatory function on spinal networks (Bracci *et al.* 1998), it can *per se* trigger fictive locomotion *in vivo* (Kiehn & Butt, 2003) or *in vitro* (Beato *et al.* 1997) probably via coordinating left–right movements during this pattern (Zhong *et al.* 2006).

The complexity of simultaneous activation of distinct receptor subgroups and/or uneven distribution

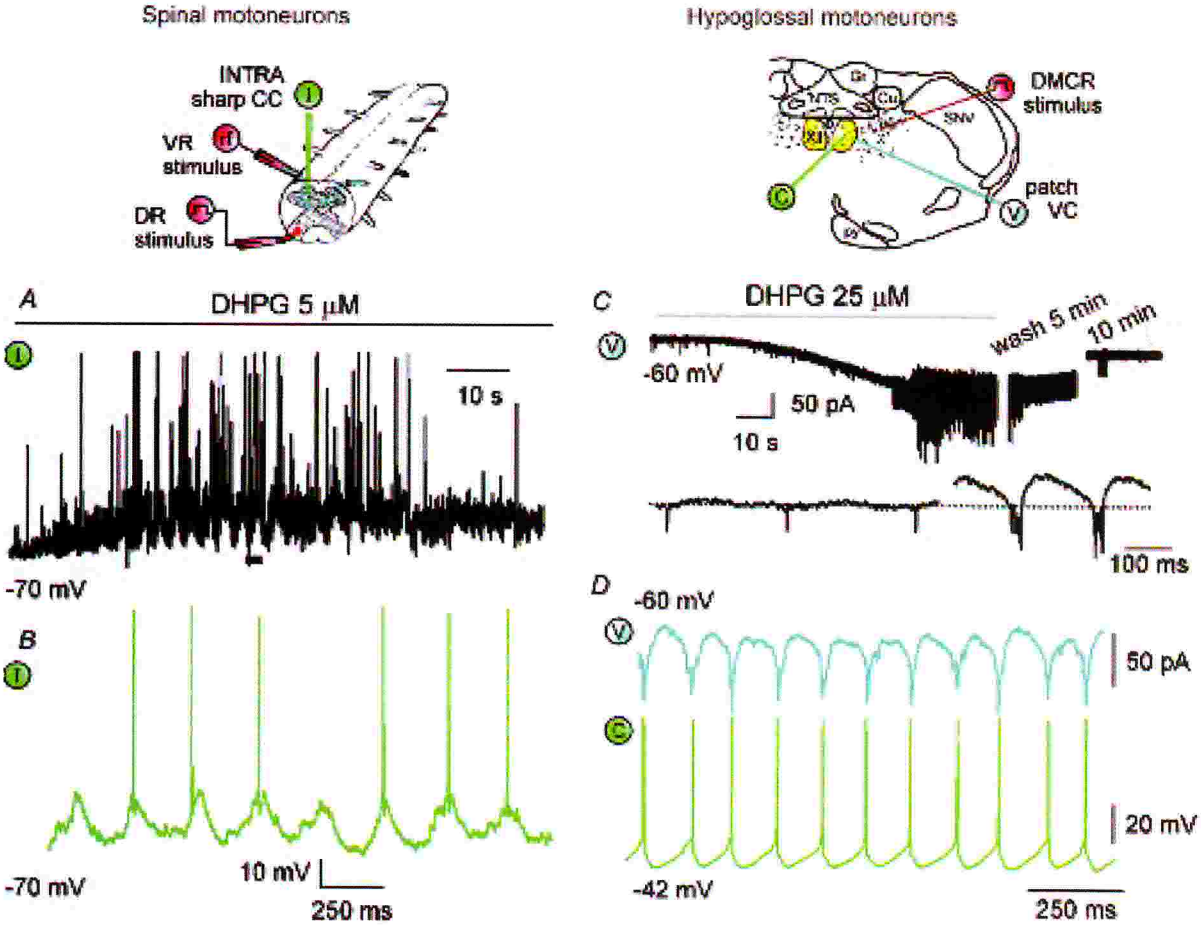

Figure 2. Cellular actions of group I mGluR activation
Left (top), schematic diagram showing the electrophysiological arrangements used for the rat isolated spinal cord preparation with sharp electrode intracellular recording (I; green) from lumbar motoneurons, DR electrical stimulation (step symbol; red) and ventral root (VR) antidromic stimuli to elicit recurrent IPSP (rI; red). *A*, application of DHPG induces membrane depolarization (with associated input resistance rise), membrane oscillations and enhancement in synaptic activity (large deflections are truncated spikes). *B* shows faster time base record of motoneuron oscillations with spikes taken from the trace marked by filled bar (voltage calibration in *B* applies also to *A*). Data are reproduced with permission from Marchetti *et al*. (2003, 2005). Right (top), schematic coronal section of the brainstem to show location of patch clamp electrode (under voltage clamp, VC, blue; current clamp, CC, green) for recording from HMs. The stimulating electrode is placed in the DMRC as shown (step symbol, red). *C*, under VC conditions application of DHPG induces inward current with emergence of fast oscillations and subsequent bursts; 10 min washout restores control conditions. Faster time base record taken from the trace depicts fast oscillations subsequently followed by bursts. *D*, paired recording from adjacent HMs shows strong phase coincidence of DHPG-evoked oscillatory patterns under voltage (top) and current (bottom) clamp. Data are reproduced, with permission, from Sharifullina *et al*. (2004, 2005).

of analogous receptors within non-homogeneous populations of neurons, is demonstrated by the use of the group I mGluR agonist DHPG. In fact, high concentrations (20 μM) of DHPG arrest the fictive locomotor pattern (Fig. 3*B*, middle) probably via over-activity of local inhibitory glycinergic pathways, an effect reversed by further network stimulation with a larger dose (9 μM) of NMDA (Fig. 3*B*, right). Conversely, low concentrations (5 μM) of DHPG actually trigger fictive locomotion when the concentration of excitatory agents is just below threshold (Fig. 3*C*) because CPG neurons contain DHPG-sensitive receptors as

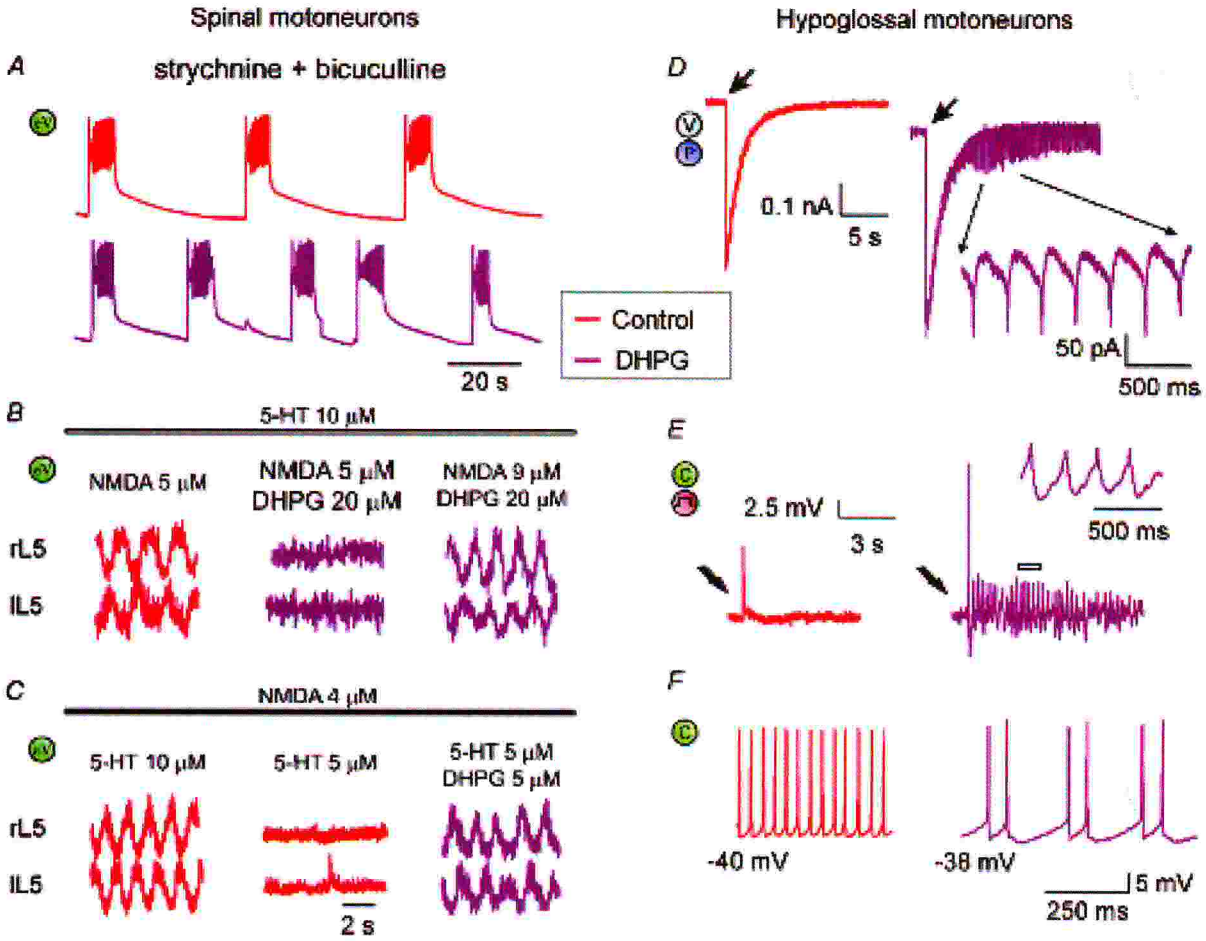

Figure 3. Network actions of group I mGluR activation
A, disinhibited bursting evoked by block of synaptic inhibition (red trace; 1 μM strychnine plus 20 μM bicuculline application) is accelerated by DHPG (5 μM; crimson trace) which significantly reduces burst duration and periodicity. Because disinhibited bursting is believed to originate from the rhythmic discharges by CPG, this effect suggests activation of CPG interneurons by DHPG. eV (green), extracellular DC recording from VR. *B*, fictive locomotor patterns induced by co-application of NMDA and 5-HT is depressed by 20 μM DHPG and restored by increasing the NMDA concentration to 9 μM. *C*, conversely, fictive locomotor patterns brought below threshold by decreasing the 5-HT concentration are restored by adding a small (5 μM) dose of DHPG. Data are reproduced, with permission, from Taccola *et al.* (2004*b*). *D*, fast inward current recorded (under voltage clamp, V) from single HM induced by puffer application (P) of AMPA is followed by rhythmic oscillations when occurring in coincidence with a concentration of DHPG (5 μM) subthreshold for oscillations. *E*, electrically evoked EPSP (by stimulating the DMRC, see step symbol in red) recorded under current clamp (C, green) in control solution (red trace) generates spike and oscillations (crimson trace; see also inset at faster time scale for record corresponding to the open bar) when repeated in the presence of DHPG (5 μM). *F*, comparison of two HMs (left and right) at similar membrane potential in the presence of DHPG (20 μM). The one on the left (red) produces high-frequency firing without oscillations, while the one on the right (crimson) generates oscillations with lower firing rate. Data reproduced with permission from Sharifullina *et al*. (2005).

indicated by the action of this substance on disinhibited rhythmicity (see Fig. 3*A*). Furthermore, DHPG facilitates the alternating locomotor patterns associated with the network depolarization evoked by repeated DR stimuli (Taccola *et al.* 2004*b*). Activation of group I mGluRs by endogenous glutamate during fictive locomotion is shown by lengthening of the locomotor cycle period by group I antagonists (Taccola *et al.* 2004*b*).

On HMs (Fig. 3, right; Sharifullina *et al.* 2005), a low concentration of DHPG, subthreshold for oscillations (5 μM), triggers them when applied in coincidence with a brief pulse application of AMPA (Fig. 3*D*). Likewise, the same concentration of DHPG unmasks rhythmic oscillations (Fig. 3*E*) during electrical stimulation of the DMRC input to motoneurons (see scheme at the top right of Fig. 2). The standard non-linear increment in the spike frequency with membrane depolarization is converted, in the presence of DHPG, into low frequency, regular firing (Fig. 3*F*) in which an oscillatory motoneuron (right) is compared with a non-oscillatory one (left) at similar membrane potential.

The similar oscillatory patterns produced by group I mGluR activity in rat spinal and brainstem circuits indicate that these mGluRs produce analogous electrical responses, though mediated by distinct receptor subtypes and with dissimilar functional consequence. In the rat brainstem, mGluR1-dependent oscillations stabilize HM firing at a steady level so as they might coordinate bilateral motor output for optimal recruitment of tongue muscles (Fig. 3*F*). Scant expression of mGluR5 receptors within this area (Hay *et al.* 1999) means that oscillatory activity is supported by mGluR1 receptors. The latter evoke membrane depolarization plus raised input resistance which are the two key factors to trigger motoneuron oscillations largely dependent on their gap junction connections and intrinsic conductances.

Conversely, while in the spinal cord, group I mGluRs are present within the locomotor CPG as shown by their acceleration of the disinhibited rhythm (Fig. 3*A*), they appear to be insufficiently expressed in this area to trigger locomotor activity. Furthermore, spinal motoneurons probably do not express electrical coupling as strong as the one found in the nucleus hypoglossus nor identical conductances. In view of this condition, the oscillatory activity of spinal motoneurons arises from distant sites within the dorsal horns where mGluR5s are strongly expressed. Such regions can therefore be seen as accessory spinal networks, the operation of which facilitates the onset of CPG activity and is then inhibited when alternating locomotor patterns emerge. Spinal topographic segregation of mGluR1 and mGluR5 receptors therefore ensures separation between neurons (including motoneurons) generating depolarization, and neurons inducing oscillations.

It is interesting that the role of mGluRs in the control of locomotor circuits appears to be evolution dependent. In fact, although mGluR1 receptors consistently accelerate the rhythmic oscillatory output of motor networks in the lamprey and rat spinal cord, mGluR5 receptors possess an inhibitory influence on fictive swimming as discussed earlier, while in the rat spinal cord they might contribute (via accessory motor circuits) to rhythmicity.

A scheme describing mGluR-dependent rhythmic operation of mammalian motor networks

Figure 4 shows an idealized diagram to account for the action of mGluRs on synaptic pathways and oscillatory activity of spinal (left) and hypoglossal (right) motoneurons.

In the spinal cord (for the sake of simplicity one side only of the segmental network is shown here) the mGluR5 oscillators are suggested to be premotoneurons driving synchronous discharges to motoneurons. Rhythm synchronicity may arise because the activity of Renshaw cell interneurons is concomitantly depressed (Marchetti *et al.* 2005), and may be aided by a degree of motoneuron electrical coupling (Tresch & Kiehn, 2000). Such oscillations do not evolve into runaway excitation as there is concomitant facilitation (via mGluR1 receptor activation) of glycinergic transmission from premotoneurons to motoneurons. The duration of the oscillatory cycle might be controlled by periodic fluctuations in input resistance of premotoneurons and motoneurons due the strong increment of synaptic inputs and subsequent membrane shunting in analogy with the phenomenon recently reported for turtle motor networks (Alaburda *et al.* 2005).

In the brainstem, oscillations crucially depend on electrical coupling between motoneurons (Fig. 4, right) as mGluR1 activity functionally blends together clusters of motoneurons. Indeed, synchronous oscillations can be generated when synaptic inhibition is blocked (even though glycinergic transmission is facilitated by mGluRs; Donato & Nistri, 2000). However, for large neurons like HMs intense, rhythmic oscillations must be metabolically demanding because of the need to preserve the correct ionic homeostasis via the Na^+–K^+ and Ca^{2+}-ATPase pumps. Since the latter are the main consumers of ATP (Ainscow *et al.* 2002; Watson *et al.* 2003), this phenomenon may cyclically deplete intracellular ATP to ensure activation of K_{ATP} channels that set burst frequency and duration. Normally K_{ATP} channels play a role in the rhythmic electrical discharges of brainstem respiratory neurons (Haller *et al.* 2001; Mironov & Richter, 2001) including HMs which fire in synchrony with inspiratory commands. Thus, activation of mGluR1 receptors

amplifies a self-regulatory mechanism already operational under physiological conditions. Nevertheless, excessive concentrations of extracellular glutamate achieved, for example, via block of glutamate transporters can trigger rhythmic slow bursting which leads to motoneuron death due to excitotoxicity in which mGluR1 receptors appear to play an important role (Sharifullina & Nistri, 2006).

Conclusions

The hallmark of group I mGluR activation in spinal and brainstem networks is the onset of rhythmic oscillations. *In vitro* experiments cannot disclose the precise contribution of such oscillations to motor behaviour, but they do reveal a common strategy to synchronize and recruit motor circuits. The hypoglossal motor output triggered by mGluRs appears to be tightly controlled by the special properties (gap junctions and K_{ATP} channels) of its motoneurons as phase-locked motor commands are necessary for synchronous contraction of tongue bilateral muscles. The spinal locomotor output is a complex process of functional interaction amongst discrete motor modules, in which activation of widely distributed mGluRs can provide the synergy for generation of full motor patterns. Future studies with novel agents targeted at certain mGluR subtypes or isoforms specifically expressed by motor systems should further refine our understanding of the role of group I mGluRs on motor output and their interaction with group II and III mGluRs.

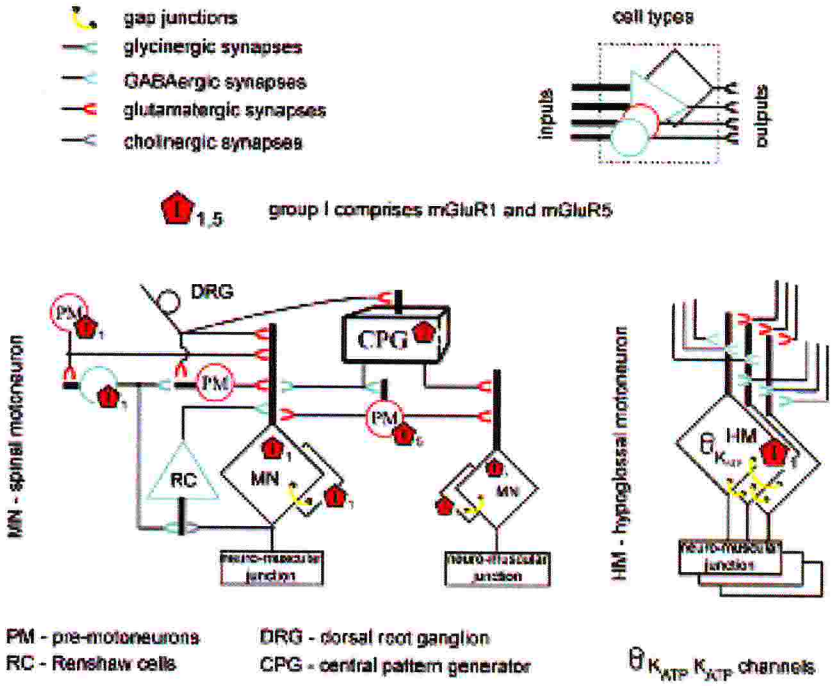

Figure 4. Idealized diagram of motor networks activated by group I mGluRs
Different types of neuron are indicated by dissimilar cell body shapes: their inputs are compacted into a single dendritic shaft, while their output is indicated by a horseshoe symbol colour-coded according to the released transmitter. Group I mGluRs (mainly found at extrasynaptic sites) are assigned on the basis of cell type rather than specific cell compartments. Left, schematic representation of spinal networks (one side only of the segmental circuit is shown) with excitatory (glutamatergic, red; cholinergic, grey), inhibitory (GABAergic, light blue; glycinergic, dark blue) and electrical (yellow) synapses. CPG interneurons are collectively lumped into a black box with inputs from DRs, and output to premotoneurons and motoneurons. mGluR1 and mGluR5 receptors (red pentagons) are expressed by various cell types. While mGluR5 activity is believed to generate motoneuron oscillations, mGluR1 activity is thought responsible for network depolarization (including CPG elements and motoneurons). Gap junctions and depression of Renshaw cell activity probably concur to produce oscillation synchronicity. Note that facilitation of glycinergic interneuron (blue circle)-bearing mGluR1 receptors contributes to restrain network excitation. Right, network of HMs bearing mGluR1 receptors and coupled via gap junctions. HM expression of K_{ATP} channels enables pacing of bursting at low frequency. Network synaptic inputs important for oscillatory activity are also shown. Note apparent lack of mGluR5 receptors.

References

Aiba A, Kano M, Chen C, Stanton ME, Fox GD, Herrup K, Zwingman TA & Tonegawa S (1994). Deficient cerebellar long-term depression and impaired motor learning in mGluR1 mutant mice. *Cell* **79**, 377–388.

Ainscow EK, Mirshamsi S, Tang T, Ashford ML & Rutter GA (2002). Dynamic imaging of free cytosolic ATP concentration during fuel sensing by rat hypothalamic neurones: evidence for ATP-independent control of ATP-sensitive K^+ channels. *J Physiol* **544**, 429–445.

Alaburda A & Hounsgaard J (2003). Metabotropic modulation of motoneurons by scratch-like spinal network activity. *J Neurosci* **23**, 8625–8629.

Alaburda A, Russo R, MacAulay N & Hounsgaard J (2005). Periodic high-conductance states in spinal neurons during scratch-like network activity in adult turtles. *J Neurosci* **25**, 6316–6321.

Alford S, Schwartz E & Di Prisco GV (2003). The pharmacology of vertebrate spinal central pattern generators. *Neuroscientist* **9**, 217–228.

Alford S, Zompa I & Dubuc R (1995). Long-term potentiation of glutamatergic pathways in the lamprey brainstem. *J Neurosci* **15**, 7528–7538.

Alvarez FJ, Dewey DE, Carr PA, Cope TC & Fyffe RE (1997). Downregulation of metabotropic glutamate receptor 1a in motoneurons after axotomy. *Neuroreport* **8**, 1711–1716.

Alvarez FJ, Villalba RM, Carr PA, Grandes P & Somohano PM (2000). Differential distribution of metabotropic glutamate receptors 1a, 1b, and 5 in the rat spinal cord. *J Comp Neurol* **422**, 464–487.

Anwyl R (1999). Metabotropic glutamate receptors: electrophysiological properties and role in plasticity. *Brain Res Brain Res Rev* **29**, 83–120.

Asztely F, Erdemli G & Kullmann DM (1997). Extrasynaptic glutamate spillover in the hippocampus: dependence on temperature and the role of active glutamate uptake. *Neuron* **18**, 281–293.

Azkue JJ, Mateos JM, Elezgarai I, Benitez R, Osorio A, Diez J, Bilbao A, Bidaurrazaga A & Grandes P (2000). The metabotropic glutamate receptor subtype mGluR 2/3 is located at extrasynaptic loci in rat spinal dorsal horn synapses. *Neurosci Lett* **287**, 236–238.

Azkue JJ, Murga M, Fernandez-Capetillo O, Mateos JM, Elezgarai I, Benitez R, Osorio A, Diez J, Puente N, Bilbao A, Bidaurrazaga A, Kuhn R & Grandes P (2001). Immunoreactivity for the group III metabotropic glutamate receptor subtype mGluR4a in the superficial laminae of the rat spinal dorsal horn. *J Comp Neurol* **430**, 448–457.

Batchelor AM, Madge DJ & Garthwaite J (1994). Synaptic activation of metabotropic glutamate receptors in the parallel fibre-Purkinje cell pathway in rat cerebellar slices. *Neuroscience* **63**, 911–915.

Beato M, Bracci E & Nistri A (1997). Contribution of NMDA and non-NMDA glutamate receptors to locomotor pattern generation in the neonatal rat spinal cord. *Proc Roy Soc London B* **264**, 877–884.

Beato M & Nistri A (1999). Interaction between disinhibited bursting and fictive locomotor patterns in the rat isolated spinal cord. *J Neurophysiol* **82**, 2029–2038.

Berthele A, Boxall SJ, Urban A, Anneser JM, Zieglgansberger W, Urban L & Tolle TR (1999). Distribution and developmental changes in metabotropic glutamate receptor messenger RNA expression in the rat lumbar spinal cord. *Brain Res Dev Brain Res* **112**, 39–53.

Billups B, Graham BP, Wong AY & Forsythe ID (2005). Unmasking group III metabotropic glutamate autoreceptor function at excitatory synapses in the rat CNS. *J Physiol* **565**, 885–896.

Bongianni F, Mutolo D, Carfi M & Pantaleo T (2002). Group I and II metabotropic glutamate receptors modulate respiratory activity in the lamprey. *Eur J Neurosci* **16**, 454–460.

Bracci E, Ballerini L & Nistri A (1996). Spontaneous rhythmic bursts induced by pharmacological block of inhibition in lumbar motoneurons of the neonatal rat spinal cord. *J Neurophysiol* **75**, 640–647.

Bracci E, Beato M & Nistri A (1998). Extracellular K^+ induces locomotor-like patterns in the rat spinal cord in vitro: comparison with NMDA or 5-HT induced activity. *J Neurophysiol* **79**, 2643–2652.

Cartmell J & Schoepp DD (2000). Regulation of neurotransmitter release by metabotropic glutamate receptors. *J Neurochem* **75**, 889–907.

Cochilla AJ & Alford S (1998). Metabotropic glutamate receptor-mediated control of neurotransmitter release. *Neuron* **20**, 1007–1016.

Conquet F, Bashir ZI, Davies CH, Daniel H, Ferraguti F, Bordi F, Franz-Bacon K, Reggiani A, Matarese V, Conde F, Collingridge GL & Crépel F (1994). Motor deficit and impairment of synaptic plasticity in mice lacking mGluR1. *Nature* **372**, 237–243.

Cunningham ET Jr & Sawchenko PE (2000). Dorsal medullary pathways subserving oromotor reflexes in the rat: implications for the central neural control of swallowing. *J Comp Neurol* **417**, 448–466.

Delgado-Lezama R, Perrier JF & Hounsgaard J (1999). Oscillatory interaction between dorsal root excitability and dorsal root potentials in the spinal cord of the turtle. *Neuroscience* **93**, 731–739.

Delgado-Lezama R, Perrier JF, Nedergaard S, Svirskis G & Hounsgaard J (1997). Metabotropic synaptic regulation of intrinsic response properties of turtle spinal motoneurones. *J Physiol* **504**, 97–102.

Demir R, Gao BX, Jackson MB & Ziskind-Conhaim L (2002). Interactions between multiple rhythm generators produce complex patterns of oscillation in the developing rat spinal cord. *J Neurophysiol* **87**, 1094–1105.

Dolan S & Nolan AM (2002). Behavioral evidence supporting a differential role for spinal group I and II metabotropic glutamate receptors in inflammatory hyperalgesia in sheep. *Neuropharmacology* **43**, 319–326.

Donato R & Nistri A (2000). Relative contribution by GABA or glycine to Cl^--mediated synaptic transmission on rat hypoglossal motoneurons in vitro. *J Neurophysiol* **84**, 2715–2724.

Douse MA & Mitchell GS (1990). Episodic respiratory related discharge in turtle cranial motoneurons: in vivo and in vitro studies. *Brain Res* **536**, 297–300.

El Manira A, Kettunen P, Hess D & Krieger P (2002). Metabotropic glutamate receptors provide intrinsic modulation of the lamprey locomotor network. *Brain Res Brain Res Rev* **40**, 9–18.

Eugenin J, Nicholls JG, Cohen LB & Muller KJ (2006). Optical recording from respiratory pattern generator of fetal mouse brainstem reveals a distributed network. *Neuroscience* **137**, 1221–1227.

Feldman JL, Mitchell GS & Nattie EE (2003). Breathing: rhythmicity, plasticity, chemosensitivity. *Annu Rev Neurosci* **26**, 239–266.

Fetz EE, Perlmutter SI & Prut Y (2000). Functions of mammalian spinal interneurons during movement. *Curr Opin Neurobiol* **10**, 699–707.

Fisher K, Lefebvre C & Coderre TJ (2002). Antinociceptive effects following intrathecal pretreatment with selective metabotropic glutamate receptor compounds in a rat model of neuropathic pain. *Pharmacol Biochem Behav* **73**, 411–418.

Fundytus ME, Yashpal K, Chabot JG, Osborne MG, Lefebvre CD, Dray A, Henry JL & Coderre TJ (2001). Knockdown of spinal metabotropic glutamate receptor 1 (mGluR1) alleviates pain and restores opioid efficacy after nerve injury in rats. *Br J Pharmacol* **132**, 354–367.

Gegelashvili G, Dehnes Y, Danbolt NC & Schousboe A (2000). The high-affinity glutamate transporters GLT1, GLAST, and EAAT4 are regulated via different signalling mechanisms. *Neurochem Int* **37**, 163–170.

Greer JJ, Funk GD & Ballanyi K (2006). Preparing for the first breath: prenatal maturation of respiratory neural control. *J Physiol* **570**, 437–444.

Grillner S, Cangiano L, Hu G, Thompson R, Hill R & Wallen P (2000). The intrinsic function of a motor system – from ion channels to networks and behavior. *Brain Res* **886**, 224–236.

Grillner S & Wallen P (2002). Cellular bases of a vertebrate locomotor system-steering, intersegmental and segmental co-ordination and sensory control. *Brain Res Rev* **40**, 92–106.

Guertin PA & Hounsgaard J (1998*a*). Chemical and electrical stimulation induce rhythmic motor activity in an in vitro preparation of the spinal cord from adult turtles. *Neurosci Lett* **245**, 5–8.

Guertin PA & Hounsgaard J (1998*b*). NMDA-induced intrinsic voltage oscillations depend on L-type calcium channels in spinal motoneurons of adult turtles. *J Neurophysiol* **80**, 3380–3382.

Guertin PA & Hounsgaard J (1999). L-type calcium channels but not N-methyl-D-aspartate receptor channels mediate rhythmic activity induced by cholinergic agonist in motoneurons from turtle spinal cord slices. *Neurosci Lett* **261**, 81–84.

Haller M, Mironov SL, Karschin A & Richter DW (2001). Dynamic activation of K_{ATP} channels in rhythmically active neurons. *J Physiol* **537**, 69–81.

Hay M, McKenzie H, Lindsley K, Dietz N, Bradley SR, Conn PJ & Hasser EM (1999). Heterogeneity of metabotropic glutamate receptors in autonomic cell groups of the medulla oblongata of the rat. *J Comp Neurol* **403**, 486–501.

Hinckley CA, Hartley R, Wu L, Todd A & Ziskind-Conhaim L (2005). Locomotor-like rhythms in a genetically distinct cluster of interneurons in the mammalian spinal cord. *J Neurophysiol* **93**, 1439–1449.

Huang YH & Bergles DE (2004). Glutamate transporters bring competition to the synapse. *Curr Opin Neurobiol* **14**, 346–352.

Hubert GW, Paquet M & Smith Y (2001). Differential subcellular localization of mGluR1a and mGluR5 in the rat and monkey Substantia nigra. *J Neurosci* **21**, 1838–1847.

Jean A (2001). Brain stem control of swallowing: neuronal network and cellular mechanisms. *Physiol Rev* **81**, 929–969.

Jia H, Rustioni A & Valtschanoff JG (1999). Metabotropic glutamate receptors in superficial laminae of the rat dorsal horn. *J Comp Neurol* **410**, 627–642.

Kettunen P, Hess D & El Manira A (2003). mGluR1, but not mGluR5, mediates depolarization of spinal cord neurons by blocking a leak current. *J Neurophysiol* **90**, 2341–2348.

Kettunen P, Krieger P, Hess D & El Manira A (2002). Signaling mechanisms of metabotropic glutamate receptor 5 subtype and its endogenous role in a locomotor network. *J Neurosci* **22**, 1868–1873.

Kiehn O & Butt SJ (2003). Physiological, anatomical and genetic identification of CPG neurons in the developing mammalian spinal cord. *Prog Neurobiol* **70**, 347–361.

Kiehn O, Kjaerulff O, Tresch MC & Harris-Warrick RM (2000). Contributions of intrinsic motor neuron properties to the production of rhythmic motor output in the mammalian spinal cord. *Brain Res Bull* **53**, 649–659.

Kiehn O & Kullander K (2004). Central pattern generators deciphered by molecular genetics. *Neuron* **41**, 317–321.

Krieger P, Grillner S & El Manira A (1998). Endogenous activation of metabotropic glutamate receptors contributes to burst frequency regulation in the lamprey locomotor network. *Eur J Neurosci* **10**, 3333–3342.

Krieger P, Hellgren-Kotaleski J, Kettunen P & El Manira AJ (2000). Interaction between metabotropic and ionotropic glutamate receptors regulates neuronal network activity. *J Neurosci* **20**, 5382–5391.

Kudo N, Nishimaru H & Nakayama K (2004). Developmental changes in rhythmic spinal neuronal activity in the rat fetus. *Prog Brain Res* **143**, 49–55.

Kullander K (2005). Genetics moving to neuronal networks. *Trends Neurosci* **28**, 239–247.

Kullmann DM & Asztely F (1998). Extrasynaptic glutamate spillover in the hippocampus: evidence and implications. *Trends Neurosci* **21**, 8–14.

Kuwajima M, Hall RA, Aiba A & Smith Y (2004). Subcellular and subsynaptic localization of group I metabotropic glutamate receptors in the monkey subthalamic nucleus. *J Comp Neurol* **474**, 589–602.

Lafreniere-Roula M & McCrea DA (2005). Deletions of rhythmic motoneuron activity during fictive locomotion and scratch provide clues to the organization of the mammalian central pattern generator. *J Neurophysiol* **94**, 1120–1132.

Li A & Nattie EE (1995). Prolonged stimulation of respiration by brain stem metabotropic glutamate receptors. *J Appl Physiol* **79**, 1650–1656.

Mao L, Conquet F & Wang JQ (2001). Augmented motor activity and reduced striatal preprodynorphin mRNA induction in response to acute amphetamine administration in metabotropic glutamate receptor 1 knockout mice. *Neuroscience* **106**, 303–312.

Marchetti C, Taccola G & Nistri A (2003). Distinct subtypes of group I metabotropic glutamate receptors on rat spinal neurons mediate complex facilitatory and inhibitory effects. *Eur J Neurosci* **18**, 1873–1883.

Marchetti C, Taccola G & Nistri A (2005). Activation of group I metabotropic glutamate receptors depresses recurrent inhibition of motoneurons in the neonatal rat spinal cord in vitro. *Exp Brain Res* **164**, 406–410.

Mills CD, Johnson KM & Hulsebosch CE (2002). Role of group II and group III metabotropic glutamate receptors in spinal cord injury. *Exp Neurol* **173**, 153–167.

Min MY, Rusakov DA & Kullmann DM (1998). Activation of AMPA, kainate, and metabotropic receptors at hippocampal mossy fiber synapses: role of glutamate diffusion. *Neuron* **21**, 561–570.

Mironov SL & Richter DW (2001). Oscillations and hypoxic changes of mitochondrial variables in neurons of the brainstem respiratory centre of mice. *J Physiol* **533**, 227–236.

Mori M & Gerber U (2002). Slow feedback inhibition in the CA3 area of the rat hippocampus by synergistic synaptic activation of mGluR1 and mGluR5. *J Physiol* **544**, 793–799.

Nakamura Y & Katakura N (1995). Generation of masticatory rhythm in the brainstem. *Neurosci Res* **23**, 1–19.

Ohishi H, Nomura S, Ding YQ, Shigemoto R, Wada E, Kinoshita A, Li JL, Neki A, Nakanishi S & Mizuno N (1995). Presynaptic localization of a metabotropic glutamate receptor, mGluR7, in the primary afferent neurons: an immunohistochemical study in the rat. *Neurosci Lett* **202**, 85–88.

Pamidimukkala J, Hoang CJ & Hay M (2002). Expression of metabotropic glutamate receptor 8 in autonomic cell groups of the medulla oblongata of the rat. *Brain Res* **957**, 162–173.

Pekhletski R, Gerlai R, Overstreet LS, Huang XP, Agopyan N, Slater NT, Abramow-Newerly W, Roder JC & Hampson DR (1996). Impaired cerebellar synaptic plasticity and motor performance in mice lacking the mGluR4 subtype of metabotropic glutamate receptor. *J Neurosci* **16**, 6364–6373.

Perrier JF, Alaburda A & Hounsgaard J (2002). Spinal plasticity mediated by postsynaptic L-type Ca^{2+} channels. *Brain Res Brain Res Rev* **40**, 223–229.

Pin JP, De Colle C, Bessis AS & Acher F (1999). New perspectives for the development of selective metabotropic glutamate receptor ligands. *Eur J Pharmacol* **375**, 277–294.

Reichelt W & Knopfel T (2002). Glutamate uptake controls expression of a slow postsynaptic current mediated by mGluRs in cerebellar Purkinje cells. *J Neurophysiol* **87**, 1974–1980.

Rekling JC & Feldman JL (1998). PreBotzinger complex and pacemaker neurons: hypothesized site and kernel for respiratory rhythm generation. *Annu Rev Physiol* **60**, 385–405.

Scanziani M, Salin PA, Vogt KE, Malenka RC & Nicoll RA (1997). Use-dependent increases in glutamate concentration activate presynaptic metabotropic glutamate receptors. *Nature* **385**, 630–634.

Schoepp DD, Jane DE & Monn JA (1999). Pharmacological agents acting at subtypes of metabotropic glutamate receptors. *Neuropharmacology* **38**, 1431–1476.

Sharifullina E & Nistri A (2006). Glutamate uptake block triggers deadly rhythmic bursting of neonatal rat hypoglossal motoneurons. *J Physiol*; DOI: 10.1113/jphysiol.2005.100412.

Sharifullina E, Ostroumov K & Nistri A (2004). Activation of group I metabotropic glutamate receptors enhances efficacy of glutamatergic inputs to neonatal rat hypoglossal motoneurons in vitro. *Eur J Neurosci* **20**, 1245–1254.

Sharifullina E, Ostroumov K & Nistri A (2005). Metabotropic glutamate receptor activity induces a novel oscillatory pattern in neonatal rat hypoglossal motoneurones. *J Physiol* **563**, 139–159.

Shutoh F, Katoh A, Kitazawa H, Aiba A, Itohara S & Nagao S (2002). Loss of adaptability of horizontal optokinetic response eye movements in mGluR1 knockout mice. *Neurosci Res* **42**, 141–145.

Svirskis G & Hounsgaard J (1998). Transmitter regulation of plateau properties in turtle motoneurons. *J Neurophysiol* **79**, 45–50.

Taccola G, Marchetti C & Nistri A (2004*a*). Role of group II and III metabotropic glutamate receptors in rhythmic patterns of the neonatal rat spinal cord in vitro. *Exp Brain Res* **156**, 495–504.

Taccola G, Marchetti C & Nistri A (2004*b*). Modulation of rhythmic patterns and cumulative depolarization by group I metabotropic glutamate receptors in the neonatal rat spinal cord in vitro. *Eur J Neurosci* **19**, 533–541.

Takahashi M & Alford S (2002). The requirement of presynaptic metabotropic glutamate receptors for the maintenance of locomotion. *J Neurosci* **22**, 3692–3699.

Takao M, Morigiwa K, Sasaki H, Miyoshi T, Shima T, Nakanishi S, Nagai K & Fukuda Y (2000). Impaired behavioral suppression by light in metabotropic glutamate receptor subtype 6-deficient mice. *Neuroscience* **97**, 779–787.

Tresch MC & Kiehn O (2000). Motor coordination without action potentials in the mammalian spinal cord. *Nat Neurosci* **3**, 593–599.

Watson WD, Facchina SL, Grimaldi M & Verma A (2003). Sarco-endoplasmic reticulum Ca^{2+} ATPase (SERCA) inhibitors identify a novel calcium pool in the central nervous system. *J Neurochem* **87**, 30–43.

Whelan PJ (2003). Developmental aspects of spinal locomotor function: insights from using the *in vitro* mouse spinal cord preparation. *J Physiol* **553**, 695–706.

Yokoi M, Kobayashi K, Manabe T, Takahashi T, Sakaguchi I, Katsuura G, Shigemoto R, Ohishi H, Nomura S, Nakamura K, Nakao K, Katsuki M & Nakanishi S (1996). Impairment of hippocampal mossy fiber LTD in mice lacking mGluR2. *Science* **273**, 645–647.

Zhong G, Diaz-Rios ME & Harris-Warrick RM (2006). Serotonin modulates the properties of ascending commissural interneurons in the neonatal mouse spinal cord. *J Neurophysiol* **95**, 1545–1555.

Acknowledgements

This work was supported by grants from MIUR (FIRB; PRIN), Fondazione Casali (Trieste), and FVG Region.

DISCUSSION

The present study was able to obtain the following results:

1. Activation of group I mGluRs directly excited hypoglossal motoneurons without facilitating the AMPA receptors, normally mediating excitatory neurotransmission. Spontaneous glutamatergic activity was enhanced via presynaptic network mechanisms, as miniature events were not affected, but the frequency of minis was increased. mGluR-evoked excitation was apparently due to block of a leak K^+-conductance. Evoked glutamatergic events were inhibited via subgroup 1 receptors, likely because such receptors were coupled to presynaptic reduction of Ca^{2+}-influx in the restricted group of electrically stimulated afferents. Despite the reduction of evoked excitatory postsynaptic currents, activation of I group of mGluRs globally produced more efficient firing of hypoglossal motoneurons.

2. The barrage of network synaptic inputs evoked by mGluR activity triggered persistent, synchronous oscillations (4-8 Hz theta frequency) in HMs. Oscillations were supported by strong electrical coupling and depended on the cyclic operation of K_{ATP} channels in view of their block by tolbutamide or glibenclamide. Theta-oscillations required intact glutamatergic transmission via AMPA receptors independent of synaptic inhibition. Under current clamp, oscillations generated more regular spike firing of motoneurones and facilitated glutamatergic excitatory inputs.

3. Build-up of endogenous glutamate within brainstem hypoglossus nuclei caused by blocking the glutamate transporter system strongly increased network excitability, activated ionotropic (AMPA and NMDA) and metabotropic receptors, and evoked irregular, slow bursts. Bursts were blocked by tetrodotoxin, the gap junction blocker carbenoxolone, or antagonists of AMPA, NMDA or mGluR1 glutamate receptors. Bursts developed in half of the HM population only. Blocking synaptic inhibition facilitated the occurrence of bursting. Intracellular Ca^{2+} imaging showed bursts as synchronous discharges among motoneurons. Ablating the lateral reticular formation preserved bursting, suggesting independence from long range propagated network activity within the brainstem.

4. Histochemical studies demonstrated that TBOA-induced bursting significantly increased the number of dead motoneurons, an effect prevented by the same agents, which suppressed bursts.

These results were systematically discussed in the 'discussion' section of the enclosed papers. Here I will summarize the obtained results and discussed them accordingly with the questions on page 33.

1. ACTIVATION OF GROUP I METABOTROPIC GLUTAMATE RECEPTORS ENHANCED THE EFFICACY OF GLUTAMATERGIC INPUTS TO NEONATAL RAT HYPOGLOSSAL MOTONEURONS IN VITRO

The most important finding of the first part of this study was the demonstration of functional consequences of I group mGluR activation in the HM network. In particular, activation of group I mGluRs generated complex actions in the brainstem hypoglossal nucleus, comprising direct action on HMs (postsynaptic level) and at network (presynaptic) level. Application of DHPG, a selective agonist of group I mGluRs, to HMs elicited an inward current with increased input resistance and excited HMs without facilitating AMPA receptors. At the network level DHPG strongly enhanced spontaneous glutamatergic transmission and increased the frequency of the miniature glutamatergic events. Electrically evoked excitatory responses were, however, depressed, suggesting that mGluRs of premotoneurons in DMRC were negatively coupled to presynaptic Ca^{2+} currents, responsible for transmitter release (Meir *et al*, 1999). Both actions of DHPG (pre- and postsynaptic) were mediated via subtype 1 mGluRs, in view of the antagonism by the selective antagonist CPCCOEt, but not by the subtype 5 mGluR antagonist MPEP. These observations are consistent with the immunolabeling study performed by Hay *et al*, (1999) (see 4.1, Introduction). Neither antagonist *per se* could significantly change glutamatergic transmission, hinting that ambient level glutamate was usually insufficient to activate group I mGluRs, evidently located far away from active zones of synaptic release. Nevertheless, pharmacological activation of subtype 1 mGluRs was an important tool to facilitate motoneuron firing. This might suggest new approaches to the treatment of respiratory diseases like sleep apnea or for controlling

dysphagia associated with a variety of brain disorders like Parkinsons's disease, stroke, amyotrophic lateral sclerosis (ALS) and cervical spinal injury.

2. METABOTROPIC GLUTAMATE RECEPTOR ACTIVITY INDUCED A NOVEL OSCILLATORY PATTERN IN NEONATAL RAT HYPOGLOSSAL MOTONEURONS

In approximately 60% of HMs DHPG elicited 4-8 Hz frequency oscillatory activity. Each oscillation cycle was biphasic, including a slow outward and a fast inward component, kinetically different from the average spontaneous excitatory postsynaptic currents. Both components were propagated from one cell to the next via specialized gap junctions, and observed as burstlets and spikelets. The presence of gap junctions was confirmed by simultaneous recordings from two neighboring HMs within the same hypoglossal nucleus. Furthermore, electrical oscillations were blocked by the gap junction blocker carbenoxolone. Oscillations were mediated by subtype 1 receptors of group I mGluRs (mGluR1s) in view of their sensitivity to the selective antagonists CPCCOEt. These electrical oscillations required intact glutamatergic transmission via AMPA receptors and were normally observed during pharmacological block of glycinergic and GABAergic inhibition, although they could also be recorded in standard saline. Theta-oscillations started because of DHPG-enhanced glutamatergic transmission at network level, and were amplified by the associated resistance increase presumably occurring in premotoneurones and HMs. Network glutamatergic activity (evoked by DHPG) led to repeated HM firing sensitive to TTX and manifested as spikelets. HMs possess comparatively large intracellular levels of free Ca^{2+} (Ladewig & Keller, 2000) and slow Ca^{2+} buffering capacity (for review see von Lewinski & Keller, 2005). Intracellular Ca^{2+} homeostasis in brain neurons is largely dependent on the operation of the Ca^{2+}-ATPase pump, which is expected to consume a significant amount of intracellular ATP (Watson *et al*, 2003). Release of intracellular Ca^{2+} from organelle stores after application of DHPG (Schoepp *et al*, 1999) plus lingering intracellular Ca^{2+} due to repeated spikes might have therefore cooperated to induce strong operation of the Ca^{2+} pump and depleted ATP with consequent activation of K_{ATP} channels to hyperpolarize HMs and terminate each burstlet. Recent studies have suggested that some brainstem respiratory neurons possess a K_{ATP} conductance which controls their rhythmic bursting because their intracellular ATP is

metabolically consumed during each respiratory cycle and thus the block of K^+ channels transiently removed (Haller *et al*, 2001). The rapid cycle of ATP generation and consumption would then be a major contributor for setting the respiratory rhythm frequency. K_{ATP} channels are generally known for their ability to convert metabolic signals into changes in electrical activity in excitable cells such as neurons, cardiac muscle cells, and some endocrine cells – including the insulin-producing beta-cells of the pancreas (for review see Rendell, 2004). The channels close when bound by ATP or sulphonylureas (a class of drugs used for the treatment of type 2 diabetes), and are opened by ADP (a metabolic product of ATP), by certain lipids and insulin. K_{ATP} channels regulate both the resting membrane potential and cell excitability. Opening the channels by, for example, decreasing the relative amount of ATP in response to falling glucose levels, increases potassium permeability, resulting in membrane hyperpolarization and reduced membrane excitability, which dampens its electrical activity (for review see Ashcroft & Ashcroft, 1990). As it has been reported by Wind *et al*, (1997), activation of ATP-sensitive potassium channels decreases neuronal injury caused by chemical hypoxia, because opening of these channels limits neuronal excitability and Ca^{2+} influx and thus can block the subsequent neurotoxic biochemical cascade (Seino & Miki, 2003). Pacing of slow oscillations, induced by DHPG, apparently depends on the operation of K_{ATP} channels in view of the block by tolbutamide or glibenclamide.

Hence, oscillations were due to the modulatory role of mGluR activity on CPG function as well as to the special properties of hypoglossal motoneurons.

These data demonstrate a powerful mechanism intrinsic to motoneurons which acts to synchronize oscillations to oscillate synchronously. Current clamp experiments demonstrated how previously random, high frequency firing of HMs was transformed into regular, lower frequency spike activity by the emergence of these oscillations. Hence, theta-like oscillatory activity is a very efficient mechanism to regulate the HMs excitability. This phenomenon could represent a braking system to avoid excessive excitation of HMs which are particularly vulnerable to large elevations in intracellular Ca^{2+} and excitotoxic damage (Ladewig *et al*, 2003). These results have, however, been obtained following activation of metabotropic glutamate receptors by an exogenous agonist.

Alongside its physiological function, glutamate receptors can have an important role in the metabolic pathways to neuronal death caused by excessive stimulation of glutamate receptors (excitotoxicity). Excitotoxicity can be defined as "a phenomenon whereby the excitatory

action of glutamate and related excitatory amino acids becomes transformed into a neuropathological process that can rapidly kill CNS cells" (Olney, 1969). Impaired transport of glutamate occurs in many cases of ALS, a devastating motoneuron disease (Rothstein *et al*, 1992; Cleveland & Rothstein, 2001; Rao & Weiss, 2004). Because, in the vast majority of cases, the disease is sporadic and associated with normal synthesis of the transporter proteins (Rao & Weiss, 2004), various environmental factors are suspected to generate this condition by inhibiting glutamate transport in vulnerable brain regions (Bruijn *et al*, 2004), like brainstem hypoglossal motoneurons. In the subsequent study we investigated the consequences of raising endogenous glutamate concentrations on rhythmic patterns of hypoglossal motoneurons.

3. GLUTAMATE UPTAKE BLOCK TRIGGERS DEADLY RHYTHMIC BURSTING OF NEONATAL RAT HYPOGLOSSAL MOTONEURONS

Because of the high rates of glutamate release, inhibition of glutamate uptake quickly led to high extracellular levels of glutamate within brainstem hypoglossus nuclei (Jabaudon *et al*, 1999). This phenomenon could potently activate ionotropic (AMPA and NMDA) and metabotropic receptors to increase network excitability and long-lasting bursts. In fact, glutamate antagonists (of AMPA or NMDA receptors, and of subtype 1 of mGluRs I) were found to be effective blockers of bursting. The incidence of bursts was limited by synaptic inhibition (mediated by GABA and glycine). Bursts developed in half of the HM population only. In our previous work we showed, by using simultaneous patch recording from pairs of HMs in strychnine and bicuculline solution, that more than 40% of hypoglossal motoneurons are electrically coupled (Sharifullina *et al*, 2005). Over the background of HM gap junctions that allow spread and synchronization of excitation, each glutamate receptor class brought its distinctive, yet complementary contribution. Our lesion study demonstrated that bursting did not need an extensive brainstem circuitry. Although the effect of TBOA was reversible if applied for the less than 20 min, after longer exposure ($\geq$35 min), HMs expressed large inward currents and became leaky, showing cell deterioration without recovery. Monitoring the time profile of simultaneous Ca^{2+} changes in several HMs, allowed us to understand how widespread the cellular damage (indicated by the irreversible large rise in Ca^{2+}) was. In fact, some HMs showed a large irreversible increment of Ca^{2+} baseline, coincident with bursting

activity. To quantify how many cells were actually damaged, we performed a histochemical analysis. For this we compared, the number of HMs stained by the cell-permeable dye Hoechst 33342, which stains all HMs, with those labelled with propidium iodide (PI), which stains dead cells only. After 1 h exposure to TBOA, the number of PI(+) cells was larger, an effect prevented by the same antagonists which prevented cell bursts. Bursting thus represents a novel hallmark of motoneuron dysfunction, which is triggered by glutamate uptake block and serves as an early sign of impending motoneuron death.

The use of the slice preparation as a model to study a local network and its rhythmic activity has its advantages and limitations. On the one hand, the dendritic trees of hypoglossal motoneurons are oriented primarily in the transverse plane, so that most of such trees are preserved in transverse brain stem slices (Nunez-Abades *et al*, 1994). This allows preservation of a local motor network sufficient for expressing tongue movement commands, as observed by recording rhythmic discharges from the XII nerve rootlets (Sharifullina E, unpublished). On the other hand, in none of our experiments did we find spontaneous oscillatory activity after pharmacological block of synaptic inhibition. This observation differs from previous findings using the isolated spinal cord (Bracci *et al*, 1996), which contains a much larger neuronal network. In fact, disinhibited bursting in the spinal cord, observed after applying GABA and glycinergic transmitter blockers (Bracci *et al*, 1996), relies on the presence of recurrent excitatory collaterals (Streit , 1993) and/or bistable behavior (Schwindt & Crill 1984; Hultborn & Kiehn 1992).

We could generate oscillatory activity in HMs by pharmacological agents like the agonist of group I mGluRs DHPG, the blocker of glutamate uptake TBOA or NMDA (see preliminary report in Introduction). Our data suggest that, in a brainstem slice preparation, motoneuron and local networks were functionally viable and susceptible generating rhythmic bursting of various patterns as long as pharmacological agents boosted glutamatergic activity. The limited size of the brainstem network after slicing, however, removed rhythmic inputs from other nuclei like the pre-Bötzinger complex. Furthermore, slicing presumably severed the recurrent collaterals necessary to propagate excitation when synaptic inhibition was suppressed. Our results indicate that in the slice preparation single HMs had no intrinsic rhythmogenic properties. They could burst only when triggered to do so. Hence, HMs could be considered as 'conditional bursters' (Marder & Eisen 1984; Smith *et al*, 1991).

ANALOGIES AND DIFFERENCES BETWEEN DHPG AND TBOA EVOKED OSCILLATORY ACTIVITIES

DHPG-induced theta-frequency oscillations represented a network phenomenon due to local glutamate release, activation of AMPA receptors and electrical coupling among HMs. As mentioned above, by transforming the HM firing into a lower frequency activity, mGluRs, probably, restrained an excessive Ca^{2+}influx into HMs, which may otherwise cause disruption of intracellular Ca^{2+} homeostasis as proposed for neurodegenerative disorders (Alexianu *et al*, 1994; Palecek *et al*, 1999). Another role of mGluRs was played during impaired glutamate uptake. We previously demonstrated that activation of group I of mGluRs produced a complex action on HMs (Sharifullina *et al*, 2004), leading to an increase in motoneuronal excitability, via a combination of effects including augmented release of glutamate, enhanced neuronal resistance and membrane depolarization. Under condition of glutamate uptake block this effect of mGluRs activation coincided with activation of AMPA and also NMDA receptors. The latter, due to their remote localization from the glutamate release zone, should have been activated by glutamate spillover (Cavelier *et al*, 2005). The synergy of activation of mGluRs and ionotropic glutamate receptors after administration of TBOA thus transformed the main functional property of group mGluRs from improved efficacy of glutamatergic transmission, to a pathological component of excitotoxicity.

A few features of the TBOA-evoked bursts were analogous to these induced by group I mGluRs. For example, under voltage clamp, each burst was the expression of the depolarization affecting multiple, interconnected HMs (via gap junctions), and was accompanied by superimposed spikelets and synaptic events. Three burst properties, namely 0 mV reversal potential, period insensitivity to membrane voltage, and actual current reversal at positive potentials, indicate that bursts were summated currents mediated by the activation of glutamate receptors on premotoneurons and motoneurons.

HMs AS A FUNCTIONAL MOTOR SYNCYTIUM

Insights into how HMs may supply fast repetitive, rhythmical commands to tongue muscles has been achieved by our recent demonstration of strong electrical coupling amongst HMs.

Gap junctions of HMs represent an important mechanism to bind together a large motoneuronal population. Evidently, because of electrical coupling between HMs, it would be difficult to obtain their adequate voltage clamp (unless the input resistance had been raised with mGluR activation). Several studies have demonstrated the presence of gap junctions between neurons at many levels of the motor system, in both motoneuronal and in premotoneuronal pattern generating circuits in the spinal cord (for review see Kiehn & Tresch, 2002). Although gap junctions are prominent in early development, there is also considerable evidence that, gap junctions are present in adults as well (Ramirez *et al*, 1997; Simbürger *et al*, 1997; Chang & Balice-Gordon, 2000). Recent data, however, demonstrate that commissural interneurons play the major role of binding synergies across the spinal cord (for review see Kiehn, 2006). Hence, unlike for HMs the role of electrical gap junctions for spinal CPG is, perhaps, diminished.

DIFFERENT EFFECT OF K_{ATP} CHANNEL BLOCKERS ON HMs AND SPINAL NEURONS

Involvement of a K_{ATP} conductance was previously demonstrated for rhythmic bursting in some brainstem respiratory neurons (Haller *et al*, 2001). In our study the maintenance of theta frequency was apparently dependent on the cyclic operation of K_{ATP}-channels. Rapid ATP consumption during the excitation of HMs set off by DHPG likely was associated with a periodic block/unblock of K_{ATP} channels which depended on the energy metabolism of HMs. In the spinal cord, application of the K_{ATP} channel blockers glibenclamide and tolbutamide hyperpolarized motoneurons, increased their input resistance and action potential amplitude, decreased Renshaw cell-mediated recurrent inhibition, and raised network excitability by depressing GABA and glycine mediated transmission (Ostroumov *et al*, 2006). This dual action of sulphonylureas might be explained by the fact that glibenclamide, apart from blocking K_{ATP} channels, can block the cystic fibrosis transmembrane conductance regulator (CFTR) (Schultz *et al*, 1999), expressed in the spinal cord, to regulate Cl^- conductance. Hence, sulphonylureas may increase excitability of HMs or spinal motoneurons through a different mechanism of action. However, there is no evidence for an electrophysiological effect of glibenclamide on HMs that could be explained via CFTR inhibition.

MODEL OF EXCITOTOXIC HM DEATH AND ITS RELEVANCE TO ALS

Increased extracellular glutamate level results from reduced glutamate uptake, which can be caused by oxidative damage to the glutamate transporter $EAAT_2$ or by aberrant RNA processing (Maragakis & Rothstein, 2001). Damage to motoneurons by increased glutamate-mediated stimulation seems to involve disregulation of Ca^{2+} homeostasis (for review see Arundine & Tymianski, 2003). Glutamate activates postsynaptic receptors which allow influx of Ca^{2+} and Na^{+}. Although physiological elevations in intracellular Ca^{2+} ($[Ca^{2+}]_i$) occur during normal cell function, excessive influx of Ca^{2+} together with extensive Ca^{2+} release from intracellular compartments can overwhelm Ca^{2+}-regulatory mechanisms and lead to cell death. Certain features of HMs, such as cell size, mitochondrial activity, neurofilament content, relative lack of certain calcium-binding proteins and molecular chaperones, relatively low expression of $GluR_2$ AMPA receptor subunits (Essin *et al*, 2002) and low Ca^{2+} buffering properties (for review see von Lewinski & Keller, 2005), may predispose HMs to the neurodegenerative process of ALS. This susceptibility may be enhanced by high AMPA receptor density, mediating much larger elevations in intracellular Ca^{2+} concentrations than in other ALS-resistant brainstem motoneurons (Carriedo *et al*, 1996). These properties TBOA-induced bursting as an early sign of metabolic stress of HMs and their subsequent death may represent one model of motoneuron degeneration in ALS (for earlier models based on organotypic spinal cord cultures see Rothstein *et al*, 1992, 1993). Unfortunately, our model has some limitations, which need to be discussed.

Firstly, since the present model was based on neonatal brain slices, it remains to be established whether analogous mechanisms might be applicable to adult brainstem neurons. In principle, this seems likely because glutamate uptake is already expressed in the neonatal brain and readily demonstrated even in primary cultures (Danbolt, 2001). In addition, TBOA neurotoxicity is reported to occur when this agent is bath-applied to neuronal cultures from neonatal animals as much as when it is microinjected into the rat adult brain in vivo (Selkirk *et al*, 2005), indicating a widespread potential for neurotoxicity when glutamate uptake is blocked.

Secondly, by using the broad-spectrum blocker of glutamate uptake TBOA, we largely sped up the onset of cell death: already one hour after the block of glutamate uptake a large number of damaged cells was observed in brainstem slice, a phenomenon, which does not

occur so rapidly in vivo. In fact, in ALS, there is a gradual progression of motoneuronal damage, leading to extensive paralysis, with death from respiratory weakness or aspiration pneumonia (Danbolt, 2001; Rowland & Shneider, 2001; Grosskreutz *et al*, 2006). Nevertheless, the aim of our model was not to produce wide-spread cell excitotoxicity, using pharmacological agents like L-glutamate, AMPA and kainate, but to demonstrate how an excessive amount of endogenous glutamate could produce patchy motoneuron damage. Although $[Ca^{2+}]_i$ disregulation is paramount to neurodegeneration (Arundine & Tymianski, 2003), the exact cellular mechanisms by which $[Ca^{2+}]_i$ actually mediates excitotoxicity are less clear. One theory (for review see Verkhratsky & Toescu, 2003) suggests that Ca^{2+}-dependent neurotoxicity occurs following the activation of distinct signaling cascades downstream from key points of Ca^{2+} entry at synapses. The triggers of these cascades maybe co-localized with specific glutamate receptors. Several pathways contributing to the toxic effects include activation of calpain, protein kinase C, lipases, phospholipases, endonucleases, the arachidonic acid cascade, xanthine oxidase, and nitric oxide synthase (for review see Heath & Shaw, 2002).

To account for the timing and selectivity of motoneuron killing in neurodegenerative diseases, the recent theory by Cleveland & Rothstein, (2001) proposes that this process arises from the unfortunate convergence of a series of factors (genetic, environmental, metabolic), all of which are necessary to place motoneurons at risk, whereas each one in isolation is insufficient (the 'convergence model'). Our results suggest that, in the case of vulnerable HMs, there might be convergence of molecular (glutamate receptors) and histological (gap junctions) factors that amplify the likelihood of motoneuron death when the uptake of glutamate is impaired. Furthermore, abnormalities in many cellular cascades (e.g., calcium homeostasis, inositol phospholipid metabolism, mitochondrial disfunction, etc.) could act in series with ongoing glutamate-mediated toxicity to produce motorneuron degeneration. Thus, our model might provide a convenient way to test some of these hypotheses.

Future developments of the present project should investigate the intracellular signaling cascade underlying HM responses in high glutamate concentrations, and the role of apoptosis in delayed motorneuron degeneration.

The use of a brainstem slice preparation provides an interesting model to study HM integration, dynamic output and survival. These concepts were developed by applying a

synthetic glutamate agonist like DHPG or by full block of glutamate uptake (with TBOA). It would be desirable to test the possibility of triggering rhythmic motor patterns by more subtle modulatory tools, such as, for example, facilitation of endogenous glutamate release. Very recent data, demonstrating that application of nicotine facilitated glutamate release and synchronized HM output into rhythmic electrical discharges (Lamanauskas & Nistri, 2006), providing a basis to explore different levels of enhancement of glutamatergic transmission. Future work must consider the wide range of rhythmic activities expressed by HMs from low frequency oscillations, probably associated with breathing, to higher frequency ones, more typical of sucking, chewing or other type of oro-motor activity (Nakamura & Katakura, 1995; Nakamura *et al*, 1999).

REFERENCES

1. Agar J& Durham H (2003). Relevance of oxidative injury in the pathogenesis of motor neuron diseases. *Amyotroph. Lateral Scler. Other Motor Neuron Disord.* **4**, 232–242
2. Alberts B (2002). Molecular biology of the cell, 4th edition, New York: Garland Science.
3. Aldes LD (1995). Subcompartmental organization of the ventral (protrusor) compartment in the hypoglossal nucleus of the rat. *J Comp Neurol* **353,** 89-108
4. Alexianu ME, Ho BK, Mohamed AH, La Bella V, Smith RG, Appel SH (1994) The role of calcium-binding proteins in selective motoneuron vulnerability in amyotrophic lateral sclerosis. *Ann. Neurol.* **36**, 846–858
5. Alford S, Schwartz E & Di Prisco GV (2003). The pharmacology of vertebrate spinal central pattern generators. *Neuroscientist* **9**, 217–228
6. Altevogt BM & Paul DL (2004). Four classes of intercellular channels between glial cells in the CNS. *J Neurosci* **24**, 4313-4323
7. Amaral DG & Dent JA (1981). Development of the mossy fibers of the dentate gyrus: I. A light and electron microscopic study of the mossy fibers and their expansions. *J Comp Neurol* **195**, 51–86
8. Amri M & Car A (1988). Projections from the medullary swallowing center to the hypoglossal motor nucleus: a neuroanatomical and electrophysiological study in sheep. *Brain Res* **441**, 119-126
9. Anwyl R (1999). Metabotropic glutamate receptors: electrophysiological properties and role in plasticity. *Brain Res Brain Res Rev* **29**, 83–120

10. Arriza JL, Eliasof S, Kavanaugh MP, Amara SG (1997). Excitatory amino acid transporter 5, a retinal glutamate transporter coupled to a chloride conductance. *Proc Natl Acad Sci USA* **94**, 4155–4160

11. Arundine M & Tymianski M (2003). Molecular mechanisms of calcium-dependent neurodegeneration in excitotoxicity. *Cell Calcium* **34**, 325-337

12. Ashcroft SJ & Ashcroft FM (1990). Properties and functions of ATP-sensitive K-channels *Cell Signal* **2**, 197-214

13. Balcar VJ & Johnston GAR (1972). The structural specificity of the high affinity uptake of L-glutamate and L-aspartate by rat brain slices. *J Neurochem* **19**, 2657–2666

14. Ballanyi K, Onimaru H, Homma I. (1999) Respiratory network function in the isolated brainstem-spinal cord of newborn rats. *Prog Neurobiol.* **59**, 583-634

15. Barnard EA, Sutherland M, Zaman S, Matsumoto M, Nayeem N, Green T, Darlison MG, and Bateson AN (1993). Multiplicity, structure, and function in GABAA receptors. *Ann NY Acad Sci* **707**, 116-125

16. Barrett JN & Crill WE (1980). Voltage clamp of cat motoneurone somata: properties of the fast inward current. *J Physiol* **304**, 231-49

17. Baude A, Nusser Z, Roberts JD, Mulvihill E, McIlhinney RA, Somogyi P (1993). The metabotropic glutamate receptor (mGluR1 alpha) is concentrated at perisynaptic membrane of neuronal subpopulations as detected by immunogold reaction. *Neuron* **11**, 771-787

18. Bayliss DA, Viana F, Bellingham MC, Berger AJ (1994). Characteristics and postnatal development of a hyperpolarization-activated inward current in rat hypoglossal motoneurons in vitro. *J Neurophysiol* **71**, 119-128

19. Beierlein M, Gibson JR & Connors BW (2000). A network of electrically coupled interneurons drives synchronized inhibition in neocortex. *Nat Neurosci* **3**, 904–910

20. Bennett DJ, Hultborn H, Fedirchuk B, Gorassini M (1998). Synaptic activation of plateaus in hindlimb motoneurons of decerebrate cats. *J Neurophysiol* **80**, 2023-2037

21. Bennett MV & Zukin RS (2004). Electrical coupling and neuronal synchronization in the Mammalian brain. *Neuron* **41**, 495-511

22. Bennett, M.V.L. (1977). Electrical transmission: a functional analysis and comparison with chemical transmission. In Cellular Biology of Neurons, vol. I, sec. I, Handbook of Physiology. The Nervous System, E.R. Kandel, ed. (Baltimore, MD: Williams and Wilkins), pp. 357–416.

23. Berger AJ & Huynh P (2002). Activation of 5HT1B receptors inhibits glycinergic synaptic inputs to mammalian motoneurons during postnatal development. *Brain Res* **956**, 380-384

24. Berger H (1929). Uber das Elektroenkephalogram des Menschen. *Arch. Psychiatr. Nervenkrankh*

25. Bergles DE & Jahr CE (1998). Glial contribution to glutamate uptake at Schaffer collateral-commissural synapses in the hippocampus. *J Neurosci* **18**, 7709-7716.

26. Blackstad TW & Kjaerheim A (1961). Special axo-dendritic synapses in the hippocampal cortex: electron and light microscopic studies of the layer of mossy fibers. *J Comp Neurol* **117**, 133–159

27. Bocchiaro CM & Feldman JL (2004). Synaptic activity-independent persistent plasticity in endogenously active mammalian motoneurons. *Proc Natl Acad Sci U S A* **101,** 4292-4295

28. Boone TB & Aldes LD (1984). The ultrastructure of two distinct neuron populations in the hypoglossal nucleus of the rat. *Exp Brain Res* **54**, 321–326

29. Booth V, Rinzel J & Kiehn O (1997). Compartmental model of vertebrate motoneurons for Ca2+-dependent spiking and plateau potentials under pharmacological treatment. *J Neurophysiol* **78**, 3371-3385

30. Bracci E, Ballerini L & Nistri A (1996). Spontaneous rhythmic bursts induced by pharmacological block of inhibition in lumbar motoneurons of the neonatal rat spinal cord. *J Neurophysiol* **75**, 640–647

31. Brasnjo G & Otis TS (2001). Neuronal glutamate transporters control activation of postsynaptic metabotropic glutamate receptors and influence cerebellar long-term depression. *Neuron* **31**, 607-616.

32. Bruijn LI, Miller TM & Cleveland DW (2004). Unraveling the mechanisms involved in motor neuron degeneration in ALS. *Annu Rev Neurosci* **27**, 723–749

33. Buzsaki G (2002). Theta oscillations in the hippocampus. *Neuron* **33,** 325-340

34. Carlin KP, Jones KE, Jiang Z, Jordan LM, Brownstone RM (2000). Dendritic L-type calcium currents in mouse spinal motoneurons: implications for bistability. *Eur J Neurosci* **12**, 1635-1646

35. Carriedo SG, Yin HZ, Weiss JH (1996). Motor neurons are selectively vulnerable to AMPA/kainate receptor-mediated injury in vitro. *J Neurosci* **16**, 4069–4079

36. Cartmell J & Schoepp DD (2000). Regulation of neurotransmitter release by metabotropic glutamate receptors. *J Neurochem* **75**, 889–907

37. Cavelier P, Hamann M, Rossi D, Mobbs P & Attwell D (2005). Tonic excitation and inhibition of neurons: ambient transmitter sources and computational consequences. *Prog Biophys Mol Biol* **87**, 3–16

38. Chamberlin NL & Saper CB (1998). A brainstem network mediating apneic reflexes in the rat. *J Neurosci* **18**, 6048-6056

39. Chang, Q & Balice-Gordon RJ (2000). Gapjunctional communication among developing andinjured motor-neurons. *Brain Res. Rev* **32**, 242–249

40. Chang Q, Gonzalez M, Pinter MJ, Balice-Gordon RJ (1999). Gap junctional coupling and patterns of connexin expression among neonatal rat lumbar spinal motor neurons. *J Neurosci* **19**, 10813-10828

41. Chang Q, Pereda A, Pinter MJ, Balice-Gordon RJ (2000). Nerve injury induces gap junctional coupling among axotomized adult motor neurons. *J Neurosci* **20**, 674-684

42. Chicurel ME & Harris KM (1992). Three-dimensional analysis of the structure and composition of CA3 branched dendritic spines and their synaptic relationships with mossy fiber boutons in the rat hippocampus. *J Comp Neurol* **325**, 169–182

43. Cleveland DW, Rothstein JD (2001). From Charcot to Lou Gehrig: deciphering selective motor neuron death in ALS. *Nat Rev Neurosci* **2,** 806-819

44. Cobb SR, Bulters DO & Davies CH (2000). Coincident activation of mGluRs and mAChRs imposes theta frequency patterning on synchronised network activity in the hippocampal CA3 region. *Neuropharmacology* **39**, 1933–1942

45. Cochilla AJ, Alford S (1998). Metabotropic glutamate receptor-mediated control of neurotransmitter release. *Neuron* **20**, 1007-1016

46. Collingridge GL & Lester RA (1989). Excitatory amino acid receptors in the vertebrate central nervous system. *Pharmacol Rev* **41**, 143-210

47. Conn PJ & Pin JP (1997). Pharmacology and functions of metabotropic glutamate receptors. *Annu Rev Pharmacol Toxicol* **37**, 205-237

48. Conn PJ (2003). Physiological roles and therapeutic potential of metabotropic glutamate receptors. *Ann NY Acad Sci* **1003**, 12-21

49. Cope DW, Hughes SW, Crunelli V (2005). $GABA_A$ receptor-mediated tonic inhibition in thalamic neurons. *J Neurosci* **25**, 11553-11563

50. Couratier P, Hugon J, Sindou P, Vallat JM, Dumas M (1993). Cell culture evidence for neuronal degeneration in amyotrophic lateral sclerosis being linked to glutamate AMPA/kainate receptors. *Lancet* **341**, 265-268

51. Crunelli V, Toth TI, Cope DW, Blethyn K, Hughes SW (2005). The 'window' T-type calcium current in brain dynamics of different behavioural states. *J Physiol.* **562**, 121-129.

52. Cunningham ET Jr & Sawchenko PE (2000). Dorsal medullary pathways subserving oromotor reflexes in the rat: implications for the central neural control of swallowing. *J Comp Neurol* **417**, 448–466

53. Danbolt NC (2001). Glutamate uptake. *Prog Neurobiol* **65**, 1–105

54. Del Cano GG, Millan LM, Gerrikagoitia I, Sarasa M & Matute C (1999). Ionotropic glutamate receptor subunit distribution on hypoglossal motoneuronal pools in the rat. *J Neurocytol* **28**, 455–468

55. Del Negro CA & Chandler SH (1998). Regulation of intrinsic and synaptic properties of neonatal rat trigeminal motoneurons by metabotropic glutamate receptors. *J Neurosci* **18**, 9216-9226

56. Delgado-Lezama R, Perrier JF, Hounsgaard J (1999). Local facilitation of plateau potentials in dendrites of turtle motoneurones by synaptic activation of metabotropic receptors. *J Physiol* **515**, 203-207

57. Deschenes M, Paradis M, Roy JP, Steriade M (1984). Electrophysiology of neurons of lateral thalamic nuclei in cat: resting properties and burst discharges. *J Neurophysiol* **51**, 1196-1219

58. Dingledine R, Borges K, Bowie D, Traynelis SF (1999). The glutamate receptor ion channels. *Pharmacol Rev* **51**, 7-61

59. Dobbins EG & Feldman JL (1994). Brainstem network controlling descending drive to phrenic motoneurons in rat. *J Comp Neurol* **347**, 64-86

60. Dobbins EG & Feldman JL (1995). Differential innervation of protruder and retractor muscles of the tongue in rat. *J Comp Neurol* **357**, 376-394

61. Donato R & Nistri A (2000). Relative contribution by GABA or glycine to Cl–-mediated synaptic transmission on rat hypoglossal motoneurons in vitro. *J Neurophysiol* **84**, 2715–2724

62. Donato R, Canepari M, Lape R & Nistri A (2003). Effects of caffeine on the excitability and intracellular Ca2+ transients of neonatal rat hypoglossal motoneurons in vitro. *Neurosci Lett* **346**, 177–181

63. Dong XW & Feldman JL (1999). Distinct subtypes of metabotropic glutamate receptors mediate differential actions on excitability of spinal respiratory motoneurons. *J Neurosci* **19**, 5173-5184

64. Doty RW, Richmond WH & Storey AT (1967). Effect of medullary lesions on coordination of deglutition. *Exp Neurol* **17**, 91-106

65. Douse MA & Mitchell GS (1990). Episodic respiratory related discharge in turtle cranial motoneurons: in vivo and in vitro studies. *Brain Res* **536**, 297–300

66. Dragoi G & Buzsaki G (2006). Temporal encoding of place sequences by hippocampal cell assemblies *Neuron* **50**, 145-157

67. Durand J (1991). NMDA Actions on Rat Abducens Motoneurons. *Eur J Neurosci* **3**, 621-633

68. El Manira A, Kettunen P, Hess D & Krieger P (2002). Metabotropic glutamate receptors provide intrinsic modulation of the lamprey locomotor network. *Brain Res Brain Res Rev* **40**, 9–18

69. Essin K, Nistri A & Magazanik L (2002). Evaluation of GluR2 subunit involvement in AMPA receptor function of neonatal rat hypoglossal motoneurons. *Eur J Neurosci* **15**, 1899–1906

70. Eugenin J, Nicholls JG, Cohen LB & Muller KJ (2006). Optical recording from respiratory pattern generator of fetal mouse brainstem reveals a distributed network. *Neuroscience* **137**, 1221–1227

71. Fairman WA, Vandenberg RJ, Arriza JL, Kavanaugh MP, Amara SG (1995). An excitatory amino-acid transporter with properties of a ligand-gated chloride channel. *Nature* **375**, 599–603

72. Fay RA & Norgren R (1997a). Identification of rat brainstem multisynaptic connections to the oral motor nuclei in the rat using pseudorabies virus I. Masticatory muscle motor systems. *Brain Res Rev* **25**, 255–275

73. Fay RA & Norgren R (1997b). Identification of rat brainstem multisynaptic connections to the oral motor nuclei in the rat using pseudorabies virus II. Facial muscle motor systems. *Brain Res Rev* **25**, 276–290

74. Fay RA & Norgren R (1997c). Identification of rat brainstem multisynaptic connections to the oral motor nuclei in the rat using pseudorabies virus III. Lingual muscle motor systems. *Brain Res Rev* **25**, 291–311

75. Fitzsimonds RM & Dichter MA (1996). Heterologous modulation of inhibitory synaptic transmission by metabotropic glutamate receptors in cultured hippocampal neurons. *J Neurophysiol* **75**, 885-893

76. Freeman WJ (1968). Analog simulation of prepiriform cortex in the cat. *Math BioSci* **2**, 181-190

77. Freeman WJ (1972). Measurement of oscillatory responses to electrical stimulation in olfactory bulb of cat. *J Neurophysiol* **35**, 762-779

78. French LB, Lanning CC, Matly M, Harris-Warrick RM (2004). Cellular localization of Shab and Shaw potassium channels in the lobster stomatogastric ganglion. *Neuroscience* **123**, 919-930

79. Friedman, L.K (1998). Selective reduction of GluR2 protein in adult hippocampal CA3 neurons following status epilepticus but prior to cell loss. *Hippocampus* **8**, 511–525

80. Gereau RW 4th & Conn PJ (1995). Multiple presynaptic metabotropic glutamate receptors modulate excitatory and inhibitory synaptic transmission in hippocampal area CA1. *J Neurosci* **15**, 6879-6889

81. Gibson JR, Beierlein M, Connors BW (1999). Two networks of electrically coupled inhibitory neurons in neocortex. *Nature* **402**, 75-79

82. Gillies MJ, Traub RD, LeBeau FE, Davies CH, Gloveli T, Buhl EH, Whittington MA (2002). A model of atropine-resistant theta oscillations in rat hippocampal area CA1. *J Physiol* **543**, 779-793

83. Golomb D, Yue C, Yaari Y (2006). Contribution of persistent Na+current and M-type K+ current to somatic bursting in CA1 pyramidal cells: combined experimental and modeling study. *J Neurophysiol* Jun 28; [Epub ahead of print]

84. Granit R, Kernell D, Shortess GK (1963). Quantitative aspects of repetitive firing of mammalian motoneurones, caused by injected currents. *J Physiol* **168**, 911-931

85. Gray CM (1994) Synchronous oscillations in neuronal systems: mechanisms and functions. *J Comput Neurosci.* **1**, 11-38

86. Gray CM, Konig P, Engel AK, Singer W (1989) Oscillatory responses in cat visual cortex exhibit inter-columnar synchronization which reflects global stimulus properties. *Nature* **338**, 334-337

87. Greer JJ, Funk GD & Ballanyi K (2006). Preparing for the first breath: prenatal maturation of respiratory neural control. *J Physiol* **570**, 437–444

88. Grenier F, Timofeev I, Steriade M (2001). Focal synchronization of ripples (80-200 Hz) in neocortex and their neuronal correlates. *J Neurophysiol* **86**, 1884-1898

89. Grenier F, Timofeev I, Steriade M (2003). Neocortical very fast oscillations (ripples, 80-200 Hz) during seizures: intracellular correlates. *J Neurophysiol* **89**, 841-852

90. Grillner S & Wallen P (2002). Cellular bases of a vertebrate locomotor system-steering, intersegmental and segmental co-ordination and sensory control. *Brain Res Rev* **40**, 92–106

91. Grillner S (1981). Control of locomotion in bipeds, tetrapods and fish. In *Handbook of Physiology. The Nervous System. Motor Control.* Bethesda, MD: Am. Physiol. Sot., sect. 1, vol. 2, p. 1179-1236.

92. Grillner S, Ekeberg, El Manira A, Lansner A, Parker D, Tegner J, Wallen P (1998). Intrinsic function of a neuronal network - a vertebrate central pattern generator. *Brain Res Brain Res Rev* **26**, 184-197

93. Grosskreutz J, Kaufmann J, Fradrich J, Dengler R, Heinze HJ, Peschel T (2006). Widespread sensorimotor and frontal cortical atrophy in Amyotrophic Lateral Sclerosis. *BMC Neurol* **6**, 17

94. Guertin PA, Hounsgaard J (1998a). NMDA-Induced intrinsic voltage oscillations depend on L-type calcium channels in spinal motoneurons of adult turtles. *J Neurophysiol* **80**, 3380-3382

95. Guertin PA & Hounsgaard J (1998b). Chemical and electrical stimulation induce rhythmic motor activity in an in vitro preparation of the spinal cord from adult turtles. *Neurosci Lett* **245**, 5–8

96. Gundersen, V., Danbolt, N.C., Ottersen, O.P., Storm-Mathisen, J (1993). Demonstration of glutamate/aspartate uptake activity in nerve endings by use of antibodies recognizing exogenous D-aspartate. *Neuroscience* **57**, 97–111

97. Gundersen, V., Ottersen, O.P., Storm-Mathisen, J (1996). Selective excitatory amino acid uptake in glutamatergic nerve terminals and in glia in the rat striatum: quantitative electron microscopic immunocytochemistry of exogenous D-aspartate and endogenous glutamate and GABA. *Eur J Neurosci* **8**, 758–765

98. Haddad GG, Donnelly DF, Getting PA (1990). Biophysical properties of hypoglossal neurons in vitro: intracellular studies in adult and neonatal rats. *J Appl Physiol* **69**, 1509-1517

99. Haller M, Mironov SL, Karschin A & Richter DW (2001). Dynamic activation of K_{ATP} channels in rhythmically active neurons. *J Physiol* **537**, 69–81

100. Harris K & Sultan P (1995). Variation in the number, location and size of synaptic vesicles provides an anatomical basis for the nonuniform probability of release at hippocampal CA1 synapses. *Neuropharmacology* **34**, 1387–1395

101. Hartline DK, Russell DF, Raper JA, Graubard K (1988). Special cellular and synaptic mechanisms in motor pattern generation. *Comp Biochem Physiol C* **91**, 115-131

102. Hay M, McKenzie H, Lindsley K, Dietz N, Bradley SR, Conn PJ & Hasser EM (1999). Heterogeneity of metabotropic glutamate receptors in autonomic cell groups of the medulla oblongata of the rat. *J Comp Neurol* **403**, 486–501

103. Heath PR & Shaw PJ (2002). Update on the glutamatergic neurotransmitter system and the role of excitotoxicity in amyotrophic lateral sclerosis. *Muscle Nerve* **26**, 438-458

104. Hochman S, Jordan LM & MacDonald JF (1994). N-methyl-D-aspartate receptor-mediated voltage oscillations in neurons surrounding the central canal in slices of rat spinal cord. *J Neurophysiol* **72**, 565-577

105. Hounsgaard J & Kiehn O (1989). Serotonin-induced bistability of turtle motoneurones caused by a nifedipine-sensitive calcium plateau potential. *J Physiol* **414**, 265-282

106. Hounsgaard J & Kiehn O (1993). Calcium spikes and calcium plateaux evoked by differential polarization in dendrites of turtle motoneurones in vitro. *J Physiol* **468**, 245-259

107. Hounsgaard J, Hultborn H, Jespersen B, Kiehn O (1984). Intrinsic membrane properties causing a bistable behavior of -motoneurones. *Exp Brain Res* **55**, 391-394

108. Hounsgaard J, Hultborn H, Jespersen B, Kiehn O (1988). Bistability of alpha-motoneurones in the decerebrate cat and in the acute spinal cat after intravenous 5-hydroxytryptophan. *J Physiol* **405**, 345-367

109. Hsiao CF, DelNegro CA, Trueblood PR, Chandler SH (1998). Ionic basis for serotonin-induced bistable membrane properties in guinea pig trigeminal motoneurons. *J Neurophysiol* **79**, 2847-2856

110. Huang YH & Bergles DE (2004). Glutamate transporters bring competition to the synapse. *Curr Opin Neurobiol* **14**, 346–352

111. Hughes SW, Cope DW, Blethyn KL & Crunelli V (2002). Cellular mechanisms of the slow (<1 Hz) oscillation in thalamocortical neurons in vitro. *Neuron* **33**, 947-958

112. Hultborn H & Kiehn O (1992). Neuromodulation of vertebrate motor neuron membrane properties. *Curr Opin Neurobiol* **2**, 770-775

113. Jabaudon D, Shimamoto K, Yasuda-Kamatani Y, Scanziani M, Gähwiler BH & Gerber U (1999). Inhibition of uptake unmasks rapid extracellular turnover of glutamate of nonvesicular origin. *Proc. Natl. Acad. Sci. USA* **96**, 8733–8738

114. Jablonka S, Wiese S, Sendtner M (2004). Axonal defects in mouse models of motoneuron disease. *J Neurobiol* **58**, 272-286

115. Jahr CE & Yoshioka K (1986). Ia afferent excitation of motoneurones in the in vitro new-born rat spinal cord is selectively antagonized by kynurenate. *J Physiol* **370**, 515-530

116. Jean A (2001). Brain stem control of swallowing: neuronal network and cellular mechanisms. *Physiol Rev* **81**, 929–969

117. Johnston, GAR (1981). Glutamate uptake and its possible role in neurotransmitter inactivation. In: Roberts, PJ, Storm-Mathisen, J, Johnston, GAR (Eds.), *Glutamate: Transmitter in the Central Nervous System* Wiley, Chichester, UK, pp. 77–87

118. Kamondi A, Acsády L, Wang XJ, Buzsáki G (1998). Theta oscillations in somata and dendrites of hippocampal pyramidal cells in vivo: activity-dependent phase-precession of action potentials. *Hippocampus* **8**, 244–261

119. Kanai Y, Hediger MA (1992). Primary structure and functional characterization of a high-affinity glutamate transporter. *Nature* **360**, 467–471

120. Kandel ER, Schwartz JH, Jessell TM (2000). Principles of Neural Science, 4th ed, pp.178-180. McGraw-Hill, New York

121. Katakura N, Jia L, Nakamura Y (1995). NMDA-induced rhythmical activity in XII nerve of isolated CNS from newborn rats. *Neuroreport* **6**, 601-604

122. Kawahara Y, Ito K, Sun H, Aizawa H, Kanazawa I, Kwak S (2004). Glutamate receptors: RNA editing and death of motor neurons. *Nature* **427**, 801

123. Kernell D (1965a). The adaptation and the relation between discharge frequency and current strength of cat lumbosacral motoneurons stimulated by long-lasting injected currents. *Acta Physiol Scand* **65**, 65-73

124. Kernell D (1965b). High-frequency repetitive firing of cat lumbosacral motoneurons stimulated by long-lasting injected currents. *Acta Physiol Scand* **65**, 74-86

125. Kew JN & Kemp JA (2005). Ionotropic and metabotropic glutamate receptor structure and pharmacology. *Psychopharmacology (Berl)* **179**, 4-29

126. Kiehn O & Kjaerulff O (1996). Spatiotemporal characteristics of 5-HT and dopamine-induced rhythmic hindlimb activity in the in vitro neonatal rat. *J Neurophysiol.* **75**, 1472-1482

127. Kiehn O & Tresch MC (2002). Gap junctions and motor behavior. *Trends Neurosci* **25**, 108-115

128. Kiehn O (2006) Locomotor circuits in the Mammalian spinal cord. *Annu Rev Neurosci* **29**, 279-306

129. Kiehn O, Kjaerulff O, Tresch MC, Harris-Warrick RM (2000). Contributions of intrinsic motor neuron properties to the production of rhythmic motor output in the mammalian spinal cord. *Brain Res Bull* **53**, 649-659

130. Kim YI & Chandler SH (1995). NMDA-induced burst discharge in guinea pig trigeminal motoneurons in vitro. *J Neurophysiol* **74,** 334-346

131. Kirk IJ & Mackay JC (2003). The role of theta-range oscillations in synchronising and integrating activity in distributed mnemonic networks. *Cortex* **39**, 993-1008

132. Krieger P, Grillner S, El Manira A (1998) Endogenous activation of metabotropic glutamate receptors contributes to burst frequency regulation in the lamprey locomotor network. *Eur J Neurosci* **10**, 3333-3342

133. Krieger, C., Jones, K., Kim, S.U. & Eisen, A.A (1994). The role of intracellular free calcium in motor neuron disease. *J Neurol. Sci* **124**, 27–32

134. Kudo N, Nishimaru H & Nakayama K (2004). Developmental changes in rhythmic spinal neuronal activity in the rat fetus. *Prog Brain Res* **143**, 49–55

135. Kuhse J, Betz H, Kirsch J (1995). The inhibitory glycine receptor: architecture, synaptic localization and molecular pathology of a postsynaptic ion-channel complex. *Curr Opin Neurobiol* **5**, 318-23

136. Kullmann DM, Min MY, Asztely F, Rusakov DA. (1999) Extracellular glutamate diffusion determines the occupancy of glutamate receptors at CA1 synapses in the hippocampus. *Philos Trans R Soc Lond B Biol Sci* **354**, 395-402

137. Ladewig T & Keller BU (2000) Simultaneous patch-clamp recording and calcium imaging in a rhythmically active neuronal network in the brainstem slice preparation from mouse *Pflugers Arch* **440**, 322-332

138. Ladewig T, Kloppenburg P, Lalley PM, Zipfel WR, Webb WW, Keller BU. (2003). Spatial profiles of store-dependent calcium release in motoneurones of the nucleus hypoglossus from newborn mouse. *J Physiol.* **547**, 775-787

139. Lafreniere-Roula M & McCrea DA (2005). Deletions of rhythmic motoneuron activity during fictive locomotion and scratch provide clues to the organization of the mammalian central pattern generator. *J Neurophysiol* **94**, 1120-1132

140. Lamanauskas N & Nistri A (2006). Nicotine induces sustained rhythmic oscillations of hypoglossal motoneurons. FENS Forum Abstracts, vol. 3, A012.13

141. Lape R & Nistri A (1999). Voltage-activated K+ currents of hypoglossal motoneurons in a brain stem slice preparation from the neonatal rat. *J Neurophysiol* **81**, 140-148

142. Lape R & Nistri A (2000). Current and voltage clamp studies of the spike medium afterhyperpolarization of hypoglossal motoneurons in a rat brain stem slice preparation *J Neurophysiol* **83**, 2987-2995

143. Lape R & Nistri A (2001). Characteristics of fast Na(+) current of hypoglossal motoneurons in a rat brainstem slice preparation. *Eur J Neurosci* **13**, 763-772

144. Larson CR, Yajima Y, Ko P (1994). Modification in activity of medullary respiratory-related neurons for vocalization and swallowing. *J Neurophysiol* **71**, 2294-2304

145. Larson J & Lynch G (1988). Role of N-methyl-D-aspartate receptors in the induction of synaptic potentiation by burst stimulation patterned after the hippocampal theta-rhythm. *Brain Res* **441**, 111-118

146. Laslo P, Lipski J, Nicholson LF, Miles GB & Funk GD (2001). GluR2 AMPA receptor subunit expression in motoneurons at low and high risk for degeneration in amyotrophic lateral sclerosis. *Exp Neurol* **169**, 461–471

147. Launey T, Ivanov A, Kapus G, Ferrand N, Tarnawa I, Gueritaud JP (1999). Excitatory amino acids and synaptic transmission in embryonic rat brainstem motoneurons in organotypic culture *Eur J Neurosci* **11**, 1324-1334

148. Laurent G, Wehr M, Davidowitz H (1996). Temporal representations of odors in an olfactory network. *J Neurosci* **16**, 3837-3847

149. Lee RH & Heckman CJ (1998a). Bistability in spinal motoneurons in vivo: systematic variations in rhythmic firing patterns. *J Neurophysiol* **80**, 572-582

150. Lee RH & Heckman CJ (1998b). Bistability in spinal motoneurons in vivo: systematic variations in persistent inward currents. *J Neurophysiol* **80**, 583-593

151. Lee RH & Heckman CJ (2000). Adjustable amplification of synaptic input in the dendrites of spinal motoneurons in vivo. *J Neurosci* **20**, 6734-6740

152. Lehre KP & Danbolt NC (1998). The number of glutamate transporter subtype molecules at glutamatergic synapses: chemical and stereological quantification in young adult rat brain. *J Neurosci* **18**, 8751–8757

153. Leinekugel X, Khazipov R, Cannon R, Hirase H, Ben-Ari Y, Buzsaki G (2002). Correlated bursts of activity in the neonatal hippocampus in vivo. *Science* **296**, 2049-2052

154. Leung LW & Yim CY (1991). Intrinsic membrane potential oscillations in hippocampal neurons in vitro. *Brain Res* **553**, 261-274

155. Levi R, Samoilova M, Selverston AI (2003). Calcium signaling components of oscillating invertebrate neurons in vitro. *Neuroscience* **118**, 283-296

156. Li Z & Hatton GI (1996). Oscillatory bursting of phasically firing rat supraoptic neurones in low-Ca^{2+} medium: Na^{+} influx, cytosolic Ca^{2+} and gap junctions. *J Physiol* **496**, 379-394

157. Lips MB & Keller BU (1998). Endogenous calcium buffering in motoneurones of the nucleus hypoglossus from mouse. *J Physiol* **511**, 105–117

158. Lips MB & Keller BU (1999). Activity-related calcium dynamics in motoneurons of the nucleus hypoglossus from mouse. *J Neurophysiol* **82**, 2936-2946

159. Liu, S.J. & Cull-Candy, S.G (2000). Synaptic activity at calcium-permeable AMPA receptors induced a switch in receptor subtype. *Nature* **405**, 454–458

160. Liu, S.J. & Cull-Candy, S.G (2002). Activity-dependent change in AMPA receptor properties in cerebellar stellate cells. *J Neurosci* **22**, 3881–3889

161. Llinas R & Yarom Y (1986) Oscillatory properties of guinea-pig inferior olivary neurones and their pharmacological modulation: an in vitro study. *J Physiol* **376**, 163-182

162. Llinas RR, Grace AA, Yarom Y (1991). In vitro neurons in mammalian cortical layer 4 exhibit intrinsic oscillatory activity in the 10- to 50-Hz frequency range. *Proc Natl Acad Sci U S A* **88**, 897-901

163. Logan WJ & Snyder SH (1972). High affinity uptake systems for glycine, glutamic and aspaspartic acids in synaptosomes of rat central nervous tissues. *Brain Res* **42**, 413-431

164. Ludolph AC & Munch C (1999). Neurotoxic mechanisms of degeneration in motor neuron diseases. *Drug Metab* **31**, 619-634

165. Lujan R, Nusser Z, Roberts JD, Shigemoto R, Somogyi P (1996). Perisynaptic location of metabotropic glutamate receptors mGluR1 and mGluR5 on dendrites and dendritic spines in the rat hippocampus. *Eur J Neurosci* **8**, 1488-1500

166. Maki R, Robinson MB, Dichter MA (1994). The glutamate uptake inhibitor L-trans-pyrrolidine-2,4-dicarboxylate depresses excitatory synaptic transmission via a presynaptic mechanism in cultured hippocampal neurons. *J Neurosci* **14**, 6754-6762

167. Mannaioni G, Marino MJ, Valenti O, Traynelis SF, Conn PJ (2001). Metabotropic glutamate receptors 1 and 5 differentially regulate CA1 pyramidal cell function. *J Neurosci* **21**, 5925-5934

168. Maragakis N.J & Rothstein J.D (2001). Glutamate transporters in neurologic disease. *Arch. Neurol.* **58**, 365–370

169. Marchetti C, Taccola G & Nistri A (2003). Distinct subtypes of group I metabotropic glutamate receptors on rat spinal neurons mediate complex facilitatory and inhibitory effects. *Eur J Neurosci* **18**, 1873–1883

170. Marchetti C, Taccola G, Nistri A (2005). Activation of group I metabotropic glutamate receptors depresses recurrent inhibition of motoneurons in the neonatal rat spinal cord in vitro. *Exp Brain Res* **164**, 406-410

171. Marder E & Calabrese RL (1996). Principles of rhythmic motor pattern generation *Physiol Rev* **76**, 687-717

172. Marder E & Eisen JS (1984). Electrically coupled pacemaker neurons respond differently to same physiological inputs and neurotransmitters. *J Neurophysiol* **51**, 1362-1374

173. Marshall SP & Lang EJ (2004). Inferior olive oscillations gate transmission of motor cortical activity to the cerebellum. *J Neurosci* **24**, 11356-11367

174. Martina M, Vida I, Jonas P (2000). Distal initiation and active propagation of action potentials in interneuron dendrites. *Science* **287**, 295–300

175. McClung JR, Goldberg SJ (1999). Organization of motoneurons in the dorsal hypoglossal nucleus that innervate the retrusor muscles of the tongue in the rat. *Anat Rec* **254,** 222-230

176. McClung JR, Goldberg SJ (2000). Functional anatomy of the hypoglossal innervated muscles of the rat tongue: a model for elongation and protrusion of the mammalian tongue. *Anat Rec* **260**, 378-386

177. McCormick DA & Pape HC (1990). Properties of a hyperpolarization-activated cation current and its role in rhythmic oscillation in thalamic relay neurones. *J Physiol* **431**, 291-318

178. Medina L, Figueredo-Cardenas G, Rothstein JD & Reiner A (1996). Differential abundance of glutamate transporter subtypes in amyotrophic lateral sclerosis (ALS)-vulnerable versus ALS-resistant brain stem motor cell groups. *Exp Neurol* **142**, 287–295

179. Meir A, Ginsburg S, Butkevich A, Kachalsky SG, Kaiserman I, Ahdut R, Demirgoren S, Rahamimoff R. (1999). Ion channels in presynaptic nerve terminals and control of transmitter release. *Physiol Rev* **79**, 1019-1088

180. Meyrand P, Simmers J, Moulins M (1991). Construction of a pattern-generating circuit with neurons of different networks. *Nature* **351**, 60-63

181. Meyrand P, Simmers J, Moulins M (1994). Dynamic construction of a neural network from multiple pattern generators in the lobster stomatogastric nervous system. *J Neurosci* **14**, 630-644

182. Miltner WH, Braun C, Arnold M, Witte H, Taub E (1999). Coherence of gamma-band EEG activity as a basis for associative learning. *Nature* **397**, 434-436

183. Moghaddam B (2004). Targeting metabotropic glutamate receptors for treatment of the cognitive symptoms of schizophrenia. *Psychopharmacology (Berl)* **174**, 39-44

184. Mosfeldt Laursen A & Rekling JC (1989). Electrophysiological properties of hypoglossal motoneurons of guinea-pigs studied in vitro. *Neuroscience* **30**, 619-637

185. Mugnaini E, Dino MR & Jaarsma D (1997). The unipolar brush cells of the mammalian cerebellum and cochlear nucleus: cytology and microcircuitry. *Prog Brain Res* **114**, 131–150

186. Murthy VN & Fetz EE (1996). Oscillatory activity in sensorimotor cortex of awake monkeys: synchronization of local field potentials and relation to behavior. *J Neurophysiol* **76**, 3949-3967

187. Nakamura Y & Katakura N (1995). Generation of masticatory rhythm in the brainstem. *Neurosci Res* **23**, 1–19

188. Nakamura Y, Katakura N, Nakajima M (1999). Generation of rhythmical ingestive activities of the trigeminal, facial, and hypoglossal motoneurons in in vitro CNS preparations isolated from rats and mice. *J Med Dent Sci* **46**, 63-73

189. Nicholls D & Attwell D. (1990). The release and uptake of excitatory amino acids. *Trends Pharmacol Sci* **11**, 462-468

190. Nishimura Y, Schwindt PC, Crill WE (1989). Electrical properties of facial motoneurons in brainstem slices from guinea pig. *Brain Res* **502**, 127-142

191. Nistri A (1983). Spinal cord pharmacology of GABA and chemically related amino acids. In: Handbook of the Spinal Cord, edited by Davidoff RA. New York: Dekker, , vol. 1, p. 45-105

192. Nistri A, Ostroumov K, Sharifullina E, Taccola G. (2006) Tuning and playing a motor rhythm: how metabotropic glutamate receptors orchestrate generation of motor patterns in the mammalian central nervous system. *J Physiol* **572**, 323-334

193. Nunez-Abades PA & Cameron WE (1995). Morphology of developing rat genioglossal motoneurons studied in vitro: relative changes in diameter and surface area of somata and dendrites. *J Comp Neurol* **353**, 129–142

194. Nunez-Abades PA, He F, Barrionuevo G, Cameron WE (1994). Morphology of developing rat genioglossal motoneurons studied in vitro: changes in length, branching pattern, and spatial distribution of dendrites. *J Comp Neurol* **339**, 401-420

195. Nunez-Abades PA, Spielmann JM, Barrionuevo G, Cameron WE (1993). In vitro electrophysiology of developing genioglossal motoneurons in the rat. *J Neurophysiol* **70**, 1401-1411

196. O'Brien JA, Isaacson JS, Berger AJ (1997). NMDA and non-NMDA receptors are co-localized at excitatory synapses of rat hypoglossal motoneurons. *Neurosci Lett* **227**, 5-8

197. Ohishi H, Shigemoto R, Nakanishi S, Mizuno N (1993). Distribution of the messenger RNA for a metabotropic glutamate receptor, mGluR2, in the central nervous system of the rat. *Neuroscience* **53**, 1009-1018

198. Olney, J.W (1969). Brain lesions, obesity, and other disturbances in mice treated with monosodium glutamate. *Science* **164**, 719–721

199. Ostroumov K, Grandolfo M, Nistri A (2006). Cystic fibrosis transmembrane conductance regulator controls neuronal excitability and inhibitory neurotransmission in the neonatal spinal cord. FENS Forum Abstracts, vol. 3, A007.13

200. Ouardouz M & Durand J (1994). Involvement of AMPA receptors in trigeminal post-synaptic potentials recorded in rat abducens motoneurons in vivo. *Eur J Neurosci* **6**, 1662-1668

201. Pagnotta SE, Lape R, Quitadamo C, Nistri A (2005). Pre- and postsynaptic modulation of glycinergic and gabaergic transmission by muscarinic receptors on rat hypoglossal motoneurons in vitro. *Neuroscience* **130**, 783-795

202. Palay SL & Chan-Palay V (1974). Cerebellar Cortex — Cytology and Organization. *Springer*, Berlin.

203. Palecek J, Lips MB, Keller BU. (1999) Calcium dynamics and buffering in motoneurones of the mouse spinal cord. *J Physiol.* **520**,485-502

204. Pamidimukkala J, Hoang CJ & Hay M (2002). Expression of metabotropic glutamate receptor 8 in autonomic cell groups of the medulla oblongata of the rat. *Brain Res* **957**, 162–173

205. Pape HC, Munsch T, Budde T (2004). Novel vistas of calcium-mediated signalling in the thalamus. *Pflugers Arch* **448**, 131-138

206. Parri HR, Gould TM, Crunelli V (2001) Spontaneous astrocytic Ca2+ oscillations in situ drive NMDAR-mediated neuronal excitation. *Nat Neurosci* **4**, 803-812

207. Pellegrini-Giampietro DE, Gorter JA, Bennett MV, Zukin RS (1997). The $GluR_2$ (GluR-B) hypothesis: Ca^{2+}-permeable AMPA receptors in neurological disorders. *Trends Neurosci* **20**, 464-470

208. Penttonen M, Kamondi A, Acsády L, Buzsáki G (1998). Gamma frequency oscillation in the hippocampus: intracellular analysis in vivo. *Eur J Neurosci* **10**, 718–728

209. Perl TM, Bedard L, Kosatsky T, Hockin JC, Todd EC, Remis RS (1990). An outbreak of toxic encephalopathy caused by eating mussels contaminated with domoic acid. *N Engl J Med.* **322**, 1775-1780

210. Petralia RS, Wang YX, Zhao HM, Wenthold RJ (1996). Ionotropic and metabotropic glutamate receptors show unique postsynaptic, presynaptic, and glial localizations in the dorsal cochlear nucleus. *J Comp Neurol* **372**, 356-383

211. Pines G, Danbolt NC, Bjøras M, Zhang Y, Bendahan A, Eide L, Koepsell H, Storm-Mathisen J, Seeberg E, Kanner BI (1992). Cloning and expression of a rat brain L-glutamate transporter. *Nature* **360**, 464–467

212. Plant TD, Schirra C, Katz E, Uchitel D, Konnerth A (1998). Single-cell RT-PCR and functional characterization of Ca2+ channels in motoneurons of the rat facial nucleus. *J Neurosci* **18**, 9573-9584

213. Powers RK & Binder MD (2000). Summation of effective synaptic currents and firing rate modulation in cat spinal motoneurons. *J Neurophysiol* **83**, 483-500

214. Powers RK & Binder MD (2003). Persistent sodium and calcium currents in rat hypoglossal motoneurons. *J Neurophysiol* **89**, 615-624

215. Prather JF, Powers RK, Cope TC (2001). Amplification and linear summation of synaptic effects on motoneuron firing rate. *J Neurophysiol* **85**, 43-53

216. Prinz AA, Billimoria CP, Marder E (2003). Alternative to hand-tuning conductance-based models: construction and analysis of databases of model neurons. *J Neurophysiol* **90**, 3998-4015

217. Przedborski S (2004). Molecular targets for neuroprotection. *Amyotroph Lateral Scler Other Motor Neuron Disord.* **5**, 14-18

218. Rajendra S, Lynch JW, and Schofield PR (1997). The glycine receptor. *Pharmacol Ther* **73**, 121-146

219. Ramirez JM, Quellmalz UJ & Wilken B (1997). Developmental changes in the hypoxic response of the hypoglossus respiratory motor output in vitro. *J Neurophysiol* **78**, 383–392

220. Ramirez JM, Tryba AK, Pena F (2004) Pacemaker neurons and neuronal networks: an integrative view. *Curr Opin Neurobiol* **14**, 665-674

221. Rao SD & Weiss JH (2004). Excitotoxic and oxidative cross-talk between motor neurons and glia in ALS pathogenesis. *Trends Neurosci* **27**, 17-23

222. Reid ME, Toms NJ, Bedingfield JS, Roberts PJ (1999). Group I mGlu receptors potentiate synaptosomal [3H] glutamate release independently of exogenously applied arachidonic acid. *Neuropharmacology* **38**, 477-485

223. Reiner, A., Medina, L., Figueredo-Cardenas, G. & Anfinson, S (1995). Brainstem motoneuron pools that are selectively resistant in amyotrophic lateral sclerosis are preferentially enriched in parvalbumin: evidence from monkey brainstem for a calcium-mediated mechanism in sporadic ALS. *Exp. Neurol* **131**, 239–250

224. Rekling JC & Laursen AM (1989). Evidence for a persistent sodium conductance in neurons from the nucleus prepositus hypoglossi. *Brain Res.* **500**,276-286

225. Rekling JC, Funk GD, Bayliss DA, Dong XW & Feldman JL (2000). Synaptic control of motoneuron excitability. *Physiol. Rev.* **80**, 767-852

226. Rendell M (2004). The role of sulphonylureas in the management of type 2 diabetes mellitus. *Drugs* **64**, 1339-1358

227. Rioult-Pedotti MS (1997). Intrinsic NMDA-induced oscillations in motoneurons of an adult vertebrate spinal cord are masked by inhibition. *J Neurophysiol* **77**, 717-730

228. Rodriguez E, George N, Lachaux JP, Martinerie J, Renault B, Varela FJ (1999). Perception's shadow: long-distance synchronization of human brain activity. *Nature* **397**, 430-433

229. Rodriguez-Moreno A, Sistiaga A, Lerma J, Sanchez-Prieto J (1998). Switch from facilitation to inhibition of excitatory synaptic transmission by group I mGluR desensitization. *Neuron* **21**, 1477-1486

230. Roelfsema PR, Konig P, Engel AK, Sireteanu R, Singer W 1(994). Reduced synchronization in the visual cortex of cats with strabismic amblyopia. *Eur J Neurosci* **6**, 1645-1655

231. Romano C, Sesma MA, McDonald CT, O'Malley K, Van den Pol AN, Olney JW (1995). Distribution of metabotropic glutamate receptor mGluR5 immunoreactivity in rat brain. *J Comp Neurol* **355**, 455-469

232. Ross SM, Roy DN, Spencer PS (1989). Beta-N-oxalylamino-L-alanine action on glutamate receptors. *J Neurochem* **53**, 710-715

233. Rossi DJ, Alford S, Mugnaini E & Slater NT (1995). Properties of transmission at a giant glutamatergic synapse in cerebellum: the mossy fiber-unipolar brush cell synapse. *J Neurophysiol* **74**, 24–42

234. Rothstein JD (1995-1996). Excitotoxicity and neurodegeneration in amyotrophic lateral sclerosis. *Clin Neurosci* **3**, 348-359

235. Rothstein JD, Jin L, Dykes-Hoberg M, Kuncl RW (1993). Chronic inhibition of glutamate uptake produces a model of slow neurotoxicity. *Proc Natl Acad Sci U S A* **90**, 6591-6595

236. Rothstein, J.D., Martin, L.J., Kuncl, R.W (1992). Decreased glutamate transport by the brain and spinal cord in amyotrophic lateral sclerosis. *N. Engl. J. Med.* **326**, 1464–1468

237. Rowland LP & Shneider NA (2001). Amyotrophic lateral sclerosis. *N Engl J Med* **344**, 1688–1700

238. Sah P & McLachlan EM (1992). Potassium currents contributing to action potential repolarization and the afterhyperpolarization in rat vagal motoneurons *J Neurophysiol* **68**, 1834-1841

239. Saier MH (1999). Eukaryotic transmembrane solute transport systems. *Int Rev Cytol* **190**, 61–136

240. Sawczuk A, Powers RK, Binder MD (1995). Spike frequency adaptation studied in hypoglossal motoneurons of the rat. *J Neurophysiol* **73**, 1799-1810

241. Sawczuk A, Powers RK, Binder MD (1997). Contribution of outward currents to spike-frequency adaptation in hypoglossal motoneurons of the rat. *J Neurophysiol* **78**, 2246-2253

242. Scanziani M, Gahwiler BH, Thompson SM (1995). Presynaptic inhibition of excitatory synaptic transmission by muscarinic and metabotropic glutamate receptor activation in the hippocampus: are Ca2+ channels involved? *Neuropharmacology* **34**, 1549-1557

243. Scanziani M, Salin PA, Vogt KE, Malenka RC & Nicoll RA (1997). Use-dependent increases in glutamate concentration activate presynaptic metabotropic glutamate receptors. *Nature* **385**, 630–634

244. Schmidt BJ, Hochman S, MacLean JN (1998). NMDA receptor-mediated oscillatory properties: potential role in rhythm generation in the mammalian spinal cord. *Ann N Y Acad Sci* **860**, 189-202

245. Schoepp DD (2001). Unveiling the functions of presynaptic metabotropic glutamate receptors in the central nervous system. *J Pharmacol Exp Ther*. **299**, 12-20

246. Schoepp DD, Jane DE & Monn JA (1999). Pharmacological agents acting at subtypes of metabotropic glutamate receptors. *Neuropharmacology* **38**, 1431–1476

247. Schools GP, Zhou M, Kimelberg HK (2006). Development of gap junctions in hippocampal astrocytes: evidence that whole cell electrophysiological phenotype is an intrinsic property of the individual cell. *J Neurophysiol* **96**, 1383-1392

248. Schultz BD, Singh AK, Devor DC, Bridges RJ (1999). Pharmacology of CFTR chloride channel activity. *Physiol Rev* **79**, 109-144

249. Schwindt PC & Crill WE (1982). Factors influencing motoneuron rhythmic firing: results from a voltage-clamp study. *J Neurophysiol* **48**: 875-890

250. Schwindt PC & Crill WE (1984). The spinal cord model of experimental epilepsy. In: *Electrophysiology of Epilepsy*, edited by P. A. Schwartzkroin and H. V. Wheal. London: Academic, pp. 219-251

251. Seino S & Miki T (2003). Physiological and pathophysiological roles of ATP-sensitive K^+ channels. *Prog Biophys Mol Biol* **81**, 133–176

252. Selkirk JV, Nottebaum LM, Vana AM, Verge GM, Mackay KB, Stiefel TH, Naeve GS, Pomeroy JE, Petroski RE, Moyer J, Dunlop J & Foster AC (2005). Role of the GLT-1 subtype of glutamate transporter in glutamate homeostasis: the GLT-1-preferring inhibitor WAY-855 produces marginal neurotoxicity in the rat hippocampus. *Eur J Neurosci* **21**, 3217–3228

253. Selverston AI (1985). Model neural networks and behavior. New York: Plenum.

254. Semyanov A & Kullmann DM (2001). Kainate receptor-dependent axonal depolarization and action potential initiation in interneurons. *Nat Neurosci* **4**, 718-723

255. Sharifullina E & Nistri A (2006). Glutamate uptake block triggers deadly rhythmic bursting of neonatal rat hypoglossal motoneurons. *J Physiol* **572**, 407-423

256. Sharifullina E, Ostroumov K & Nistri A (2005). Metabotropic glutamate receptor activity induces a novel oscillatory pattern in neonatal rat hypoglossal motoneurones. *J Physiol* **563**, 139–159

257. Sharifullina E, Ostroumov K, Nistri A (2004) Activation of group I metabotropic glutamate receptors enhances efficacy of glutamatergic inputs to neonatal rat hypoglossal motoneurons in vitro *Eur J Neurosci,* **20**, 1245-1254

258. Shaw PJ (1999). Calcium, glutamate, and amyotrophic lateral sclerosis: more evidence but no certainties. *Ann Neurol* **46**, 803-805

259. Shiba K, Satoh I, Kobayashi N, and Hayashi F. (1999) Multifunctional laryngeal motoneurons: an intracellular study in the cat. *J Neurosci* **19**, 2717-2727

260. Shigemoto R, Kinoshita A, Wada E, Nomura S, Ohishi H, Takada M, Flor PJ, Neki A, Abe T, Nakanishi S, Mizuno N (1997). Differential presynaptic localization of metabotropic glutamate receptor subtypes in the rat hippocampus. *J Neurosci* **17**, 7503-7522

261. Simbürger E, Stang A, Kremer M & Dermietzel R (1997). Expression of connexin43 mRNA in adult rodent brain. *Histochem Cell Biol* **107**, 127–137

262. Singer W & Gray CM (1995). Visual feature integration and the temporal correlation hypothesis. *Annu Rev Neurosci* **18**, 555-586

263. Sladeczek F, Pin JP, Recasens M, Bockaert J, Weiss S (1985). Glutamate stimulates inositol phosphate formation in striatal neurones. *Nature* **317**, 717-719

264. Slotboom DJ, Konings WN, Lolkema JS (1999). Structural features of the glutamate transporter family. *Microbiol Mol Biol Rev* **63**, 293–307

265. Smith JC, Ellenberger HH, Ballanyi K, Richter DW, Feldman JL (1991). Pre-Botzinger complex: a brainstem region that may generate respiratory rhythm in mammals. *Science* **254**, 726-729

266. Sohal VS, Pangratz-Fuehrer S, Rudolph U, Huguenard JR (2006). Intrinsic and synaptic dynamics interact to generate emergent patterns of rhythmic bursting in thalamocortical neurons. *J Neurosci* **26**, 4247-4255

267. Sokoloff AJ (2000). Localization and contractile properties of intrinsic longitudinal motor units of the rat tongue. *J Neurophysiol* **84**, 827-835

268. Sotelo C & Korn H (1978). Morphological correlates of electrical and other interactions through low-resistance pathways between neurons of the vertebrate central nervous system. *Int Rev Cytol* **55**, 67-107

269. Soteropoulos DS & Baker SN (2006). Cortico-cerebellar coherence during a precision grip task in the monkey. *J Neurophysiol* **95**, 1194-1206

270. Spacek, J (1985). Three-dimensional analysis of dendritic spines. III. Glial sheath. *Anat. Embryol* **171**, 245–252

271. Spencer PS (1999). Food toxins, ampa receptors, and motor neuron diseases. *Drug Metab Rev* **31**, 561-587

272. Staton PC & Bristow DR (1997). The dietary excitotoxins beta-N-methylamino-L-alanine and beta-N-oxalylamino-L-alanine induce necrotic- and apoptotic-like death of rat cerebellar granule cells. *J Neurochem* **69**, 1508-1518

273. Steriade M & Timofeev I (2003). Neuronal plasticity in thalamocortical networks during sleep and waking oscillations. *Neuron* **37**, 563-576

274. Steriade M (2001). Impact of network activities on neuronal properties in corticothalamic systems. *J Neurophysiol* **86,** 1-39

275. Steriade M (2006). Grouping of brain rhythms in corticothalamic systems. *Neuroscience* **137**, 1087-1106

276. Steriade M, McCormick DA, Sejnowski TJ (1993). Thalamocortical oscillations in the sleeping and aroused brain. *Science* **262**, 679-685

277. Stewart GR, Zorumski CF, Price MT, Olney JW (1990). Domoic acid: a dementia-inducing excitotoxic food poison with kainic acid receptor specificity *Exp Neurol* **110**, 127-138

278. Storck T, Schulte S, Hofmann K, Stoffel W (1992). Structure, expression, and functional analysis of a Na+-dependent glutamate/aspartate transporter from rat brain. *Proc Natl Acad Sci USA* **89**, 10955–10959

279. Streit J (1993). Regular oscillations of synaptic activity in spinal networks in vitro. *J Neurophysiol* **70**, 871-878

280. Sugiyama H, Ito I, Hirono C (1987). A new type of glutamate receptor linked to inositol phospholipid metabolism. *Nature* **325,** 531-533

281. Sumi T. (1963). The activity of brainstem respiratory neurons and spinal respiratory motoneurons during swallowing. *J Neurophysiol* **26**, 466-477

282. Sumi T. (1969) Synaptic potentials of hypoglossal motoneurons and their relation to reflex deglutition. *Jpn J Physiol* **19**, 68-79

283. Sumi T. (1977). Interrelation between rhythmic mastication and reflex deglutition as studied on the unitary activity of trigeminal motoneurons in rabbits. *Jpn J Physiol* **27**, 687-699

284. Sumi T. (1970). Activity in single hypoglossal fibers during cortically induced swallowing and chewing in rabbits. *Pflügers Arch* **314**, 329-346

285. Svirskis G & Hounsgaard J (1997). Depolarization-induced facilitation of a plateau-generating current in ventral horn neurons in the turtle spinal cord. *J Neurophysiol* **78**, 1740-1742

286. Taccola G, Marchetti C, Nistri A (2003). Effect of metabotropic glutamate receptor activity on rhythmic discharges of the neonatal rat spinal cord in vitro. *Exp Brain Res* **153,** 388-393

287. Taccola G, Marchetti C, Nistri A (2004). Modulation of rhythmic patterns and cumulative depolarization by group I metabotropic glutamate receptors in the neonatal rat spinal cord in vitro. *Eur J Neurosci* **19**, 533-541

288. Takahashi M & Alford S (2002). The requirement of presynaptic metabotropic glutamate receptors for the maintenance of locomotion. *J Neurosci* **22**, 3692–3699

289. Takahashi M, Sarantis M, Attwell D (1996). Postsynaptic glutamate uptake in rat cerebellar Purkinje cells. *J Physiol* **497,** 523-530

290. Takayasu Y, Iino M, Kakegawa W, Maeno H, Watase K, Wada K, Yanagihara D, Miyazaki T, Komine O, Watanabe M, Tanaka K, Ozawa S (2005). Differential roles of glial and neuronal glutamate transporters in Purkinje cell synapses. *J Neurosci* **25**, 8788-8793

291. Takayasu Y, Iino M, Shimamoto K, Tanaka K, Ozawa S (2006). Glial glutamate transporters maintain one-to-one relationship at the climbing fiber-Purkinje cell synapse by preventing glutamate spillover. *J Neurosci* **26**, 6563-6572

292. Talley EM, Lei Q, Sirois JE, Bayliss DA (2000). TASK-1, a two-pore domain K+ channel, is modulated by multiple neurotransmitters in motoneurons. *Neuron* **25**, 399-410

293. Tanabe Y, Masu M, Ishii T, Shigemoto R, Nakanishi S (1992). A family of metabotropic glutamate receptors. *Neuron* **8**, 169-179

294. Tanaka K (1993). Expression cloning of a rat glutamate transporter. *Neurosci Res* **16**, 149–153

295. Tateno M, Sadakata H, Tanaka M, Itohara S, Shin RM, Miura M, Masuda M, Aosaki T, Urushitani M, Misawa H, Takahashi R (2004). Calcium-permeable AMPA receptors promote misfolding of mutant SOD1 protein and development of amyotrophic lateral sclerosis in a transgenic mouse model. *Hum Mol Genet* **13**, 2183-2196

296. Teitelbaum J, Zatorre RJ, Carpenter S, Gendron D, Cashman NR (1990). Neurological sequelae of domoic acid intoxication. *Can Dis Wkly Rep* **16**, 9-12

297. Toth TI, Hughes SW & Crunelli V (1998). Analysis and biophysical interpretation of bistable behaviour in thalamocortical neurons. *Neuroscience* **87**, 519–523

298. Traub RD & Miles R (1995) Pyramidal cell-to-inhibitory cell spike transduction explicable by active dendritic conductances in inhibitory cell. *J Comput Neurosci.* **2**, 291-298

299. Traub RD, Bibbig A, LeBeau FE, Buhl EH, Whittington MA (2004). Cellular mechanisms of neuronal population oscillations in the hippocampus in vitro. *Annu Rev Neurosci* **27**, 247-278

300. Traub RD, Whittington MA, Buhl EH, LeBeau FE, Bibbig A, Boyd S, Cross H, Baldeweg T (2001). A possible role for gap junctions in generation of very fast EEG oscillations preceding the onset of, and perhaps initiating, seizures. *Epilepsia* **42**, 153-170

301. Traub RD, Whittington MA, Stanford IM, Jefferys JG (1996). A mechanism for generation of long-range synchronous fast oscillations in the cortex. *Nature* **383**, 621-624

302. Travers JB & Norgren R (1983). Afferent projections of the oral motor nuclei in the rat. *J Comp Neurol* **220**, 280–298

303. Tresch MC & Kiehn O (2000). Motor coordination without action potentials in the mammalian spinal cord. *Nat Neurosci* **3**, 593–599

304. Trotti D, Peng JB, Dunlop J, Hediger MA (2001). Inhibition of the glutamate transporter EAAC1 expressed in Xenopus oocytes by phorbol esters. *Brain Res.* **914**, 196-203

305. Trueblood PR, Levine MS, Chandler SH (1996). Dual-component excitatory amino acid-mediated responses in trigeminal motoneurons and their modulation by serotonin in vitro. *J Neurophysiol* **76**, 2461-2473

306. Ugolini G (1995). Specificity of rabies virus as a transneuronal tracer of motor networks: transfer from hypoglossal motoneurons to connected second-order and higher order central nervous system cell groups. *J Comp Neurol* **356**, 457–480

307. Umemiya M & Berger AJ (1994). Properties and function of low- and high-voltage-activated Ca2+ channels in hypoglossal motoneurons. *J Neurosci* **14**, 5652-5660

308. Umezaki T, Nakasawa K, and Miller AD (1998b).Behaviors of hypoglossal hyoid motoneurons in laryngeal and vestibular reflexes and in deglutition and emesis. *Am J Physiol Regulatory Integrative Comp Physiol* **274**, 950-955

309. van den Pol AN, Romano C, Ghosh P (1995). Metabotropic glutamate receptor mGluR5 subcellular distribution and developmental expression in hypothalamus. *J Comp Neurol* **362**, 134-150

310. Vandenberghe, W., Ihle, E.C., Patneau, D.K., Robberecht, W. & Brorson, D.R (2000). AMPA receptor current density, not desensitization, predicts selective motoneuron vulnerability. *J Neurosci* **20**, 7158–7166

311. Ventura R & Harris KM (1999). Three-dimensional relationships between hippocampal synapses and astrocytes. *J Neurosci* **19**, 6897–6906

312. Verkhratsky A & Toescu EC (2003). Endoplasmic reticulum Ca(2+) homeostasis and neuronal death. *J Cell Mol Med* **7**, 351-361

313. Viana F, Bayliss DA, Berger AJ (1993b). Multiple potassium conductances and their role in action potential repolarization and repetitive firing behavior of neonatal rat hypoglossal motoneurons. *J Neurophysiol* **69**, 2150-2163

314. Viana F, Bayliss DA, Berger AJ (1995). Repetitive firing properties of developing rat brainstem motoneurones. *J Physiol* **486**, 745-761

315. Viana F, Bayliss DA, Berger AJ. (1993a). Calcium conductances and their role in the firing behavior of neonatal rat hypoglossal motoneurons. *J Neurophysiol* **69**, 2137-2149

316. Viana F, Gibbs L & Berger AJ (1990). Double- and triple-labeling of functionally characterized central neurons projecting to peripheral targets studied in vitro. *Neuroscience* **38**, 829–841

317. von Lewinski F & Keller BU (2005). Ca2+, mitochondria and selective motoneuron vulnerability: implications for ALS. *Trends Neurosci* **28**, 494-500

318. Walmsley B & Bolton PS (1994). An in vivo pharmacological study of single group Ia fibre contacts with motoneurones in the cat spinal cord. *J Physiol* **481**, 731-741

319. Watson WD, Facchina SL, Grimaldi M & Verma A (2003). Sarco-endoplasmic reticulum Ca2+ ATPase (SERCA) inhibitors identify a novel calcium pool in the central nervous system. *J Neurochem* **87**, 30–43

320. Whiting MG (1964). Food practices in ALS. Foci in Japan, the Marianas, and New Guinea. *Fed Proc* **23,** 1343-1345

321. Whittington MA & Traub RD. (2003). Interneuron diversity series: inhibitory interneurons and network oscillations in vitro. *Trends Neurosci.* **26**, 676-682

322. Whittington MA, Traub RD & Jefferys JG (1995). Synchronized oscillations in interneuron network driven by metabotropic glutamate receptor activation. *Nature* **373**, 612-615

323. Williams SR, Toth TI, Turner JP, Hughes SW & Crunelli V (1997). The 'window' component of the low threshold Ca2+ current produces input signal amplification and bistability in cat and rat thalamocortical neurones. *J Physiol* **505**, 689–705

324. Wilson M & Bower JM. (1992). Cortical oscillations and temporal interactions in a computer simulation of piriform cortex. *J Neurophysiol* **67**, 981-995

325. Wind T, Prehn JH, Peruche B, and Krieglstein J (1997). Activation of ATP-sensitive potassium channels decreases neuronal injury caused by chemical hypoxia. *Brain Res* **751**, 295-299

326. Wittmann M, Hubert GW, Smith Y, Conn PJ (2001). Activation of metabotropic glutamate receptor 1 inhibits glutamatergic transmission in the substantia nigra pars reticulata. *Neuroscience* **105**, 881-889

327. Wu N, Enomoto A, Tanaka S, Hsiao CF, Nykamp DQ, Izhikevich E, Chandler SH (2005). Persistent sodium currents in mesencephalic v neurons participate in burst generation and control of membrane excitability. *J Neurophysiol* **93**, 2710-2722

328. Yokoi M, Kobayashi K, Manabe T, Takahashi T, Sakaguchi I, Katsuura G Shigemoto R, Ohishi H, Nomura S, Nakamura K, Nakao K, Katsuki M, Nakanishi S (1996). Impairment of hippocampal mossy fiber LTD in mice lacking mGluR2. *Science* **273**, 645-647

ACKNOWLEDGEMENTS

I would like to thank people, whose patience, supervision, help and love supported me during my PhD study.

I thank Professor Rashid Giniatullin for his opening to me the door to the magic world of science, for his absolute talent in giving outstanding lectures to students, among whom I feel privileged to have been one of them, and for being always available to discuss with me all my doubts and steps during the ten years I have pleasure to know him.

I thank Doctor Andrey Skorinkin for being brave enough to name me among his friends and going through all the consequences of this decision.

I thank Konstantin Ostroumov for his brilliant brain and wisdom, love and patience to be by my side for all these years; for taking a huge part in my research and for his smart ideas to transform the sometimes boring process of studying into a thrilling and challenging philosophical crossword.

I thank Professor John Nicholls for his sympathy and sense of humor, for being ready to listen to me and discuss with me all my questions, for his fountain of energy, which never ceases to amaze me.

I thank my sister Inna, my guardian angel, for being diligent and strong in a constant process of waiting for me at home.

I thank my family whose love makes me strong, stronger, the strongest.

And my hearty thanks go to my supervisor, Professor Andrea Nistri for his responsibility for growing me up in the world of neuroscience, for encouraging me from the beginning, for the all things transmitted from teacher to student, and for making all this happen.